Role of TILRR in modulating inflammatory responses relevant to vaginal HIV-1 acquisition

By

Mohammad Abul Kashem

A Thesis Submitted to the Faculty of Graduate Studies of

The University of Manitoba

In partial fulfillment of the requirements of the degree of

DOCTOR OF PHILOSOPHY

Department of Medical Microbiology and Infectious Diseases

University of Manitoba

Winnipeg, Manitoba, Canada

SUMMARY

Background: TILRR (**T**oll-like **I**nter**l**eukin 1 **R**eceptor **R**egulator) is a transcript variant of FREM1 (Fras-related extracellular matrix 1) and the expression of TILRR is observed in a broad range of human cells including cervicovaginal epithelial cells and PBMCs (Peripheral blood mononuclear cells). TILRR is reported as a co-receptor of IL-1R1 (Interleukin-1 receptor type 1) and potentiates NF-κB activation and inflammatory responses. Because TILRR expresses in cervicovaginal epithelial cells and modulates inflammatory response, it may play a role in enhancing the risk of vaginal HIV-1 infection. To investigate the potential role of TILRR on vaginal HIV transmission, I used two cervicovaginal epithelial cell lines and investigated the influence of TILRR on the expression of genes in the NF-κB inflammatory pathway, including the downstream signaling molecules, and the production of inflammatory cytokines/chemokines, as well as the effect on the migration of immune cells. I also investigated whether TILRR exists in human blood and whether the blood TILRR level is correlated with blood inflammatory cytokines/chemokines and susceptibility to HIV-1 infection.

Methods: TILRR was overexpressed in HeLa and VK2/E6E7 cells by introducing plasmid encoding TILRR with Endofectin Max transfection reagent (GeneCopoeia). Overexpression of TILRR was confirmed by Confocal microscopy, Western blot analysis, qRT-PCR, and flow cytometry analysis. The mRNA expression of 84 genes associated with the NF-κB signaling pathway was examined by RT^2 qPCR primer assay and RT^2 profiler PCR array. The production of cytokines/chemokines in cell culture supernatants was examined by an in-house developed Bio-Plex multiplex magnetic bead array system. The influence of TILRR overexpression on the migration of immune cells was evaluated by Transwell assay and with a novel microfluidic device. In addition, the existence of soluble TILRR (sTILRR) protein in human blood plasma

was examined by an in-house developed Bio-Plex method, affinity purification, and Western blot analysis. TILRR protein was quantified in human plasma samples collected from women of the Pumwani cohort with different HIV-1 status (HIV seroconverters [HIV SCON], HIV resistant or HIV-exposed seronegative [HESN], and newly enrolled HIV negative). Enzyme immunoassays (EIA), immunoblot testing, and PCR (polymerase chain reaction) assay were used to confirm HIV status. Women who were HIV-1 negative at the time of enrolment, but later identified as positive by EIA, immunoblot testing, and PCR were defined as HIV SCON. Besides, women who were actively engaged in the sex work, but persistently remained HIV-1 seronegative and PCR negative for three or more years before 2000 were defined as HESN. The data were analyzed using gene globe data analysis center (Qiagen), GraphPad Prism (version 7.0 and later), ImageJ (NIH, USA), Image Studio Lite (LI-COR, USA), Quantity One (Bio-Rad), OriginPro (USA), and SPSS software (IBM).

Results: Overexpression of TILRR in cervicovaginal epithelial cell lines significantly upregulated the mRNA expression of many inflammation-responsive genes in the NF-κB signal transduction pathway. TILRR overexpression increased the production of several pro-inflammatory cytokines/chemokines in cervicovaginal epithelial cell culture supernatants. The increased cytokine/chemokine production from epithelial cells significantly influenced the migration of monocytes (THP-1) and lymphocytes (MOLT-4), the CD4+ HIV-1 target cells. I also found that TILRR protein is circulating in human blood, and the level of plasma TILRR is significantly correlated with FREM1 SNP rs1552896 genotypes, plasma inflammatory cytokines/chemokines, and HIV seroconversion.

Conclusion: TILRR overexpression in cervicovaginal cell lines increased the expression of many genes involved in inflammatory responses in the NF-κB signaling pathway, and increased

the production of pro-inflammatory mediators. The increased production of pro-inflammatory mediators attracts immune cells. TILRR also exists as a soluble protein in human blood, and high plasma TILRR level is correlated with high plasma inflammatory cytokines/chemokines and is associated with FREM1 SNP rs1552896 genotypes and HIV seroconversion. Because systemic and mucosal inflammation increases susceptibility to HIV-1 infection, TILRR could be a novel target to reduce inflammation and HIV-1 infection.

ACKNOWLEDGEMENT

I would like to take this opportunity to convey my sincere thanks to my supervisor Dr. Ma Luo for her incredible support, guidance, and mentorship and for always being there ready to help whenever I needed her in any situation. In my humble opinion, Dr. Luo is one of the best supervisors any student can ever dream of. Needless to emphasize, the research excellence of her lab has benefited me tremendously and I feel so proud and lucky to be part of Dr. Luo's research team. With this great opportunity, I would like to directly say to her: I would forever remain grateful to you Dr. Luo for your unforgettable support and the opportunity you provided me to develop my career as a scientist under your mentorship. You are such an amazing and excellent supervisor/mentor I have ever seen. I would also like to thank and commemorate Dr. Francis Plummer for his suggestions and important words to conduct my research works successfully.

I would like to thank my committee members, Drs. Joanne Embree, Stephanie Booth, Brian Fristensky, and Kevin Coombs, for providing their insightful comments, and criticism to improve my research work along with their excellent guidance and encouragement to develop my research career as a scientist. I would forever remain grateful to you all.

I would like to extend my thanks to everyone in the lab for their continued support and friendship. To Dr. Binhua Liang for his excellent encourage and support to stay strong throughout the PhD program especially during a hard time. I will never forget the time that we had together during the office and lunch hours. I would like to thank Dr. Lin Li for her tremendous support during my research work with the guidance of purchasing all necessary research materials. You were the one who made part of my protein biology work simple and easy to understand. I would like to thank Dr. Hongzhao Li for his extraordinary love, friendship, and advice that guided me how to think positively during a critical moment, how to revive from a true disaster of a life, and how to become a good scientist. You were incredible Dr. Hongzhao! I would like to thank Dr. Robert Omange for his valuable advice to improve my research. Besides, I am truly indebted to Drs. Luo, Liang, and Li for their tireless assistance to sign in and sign out from the JC Wilt facilities despite their busy schedule and for providing longer than usual time to finish up my daily research work. All of you will forever remain in my heart with love and respect. Thank you all!

Thank you to all of my fellow students for your warm welcome, support, friendship, and for providing a good work environment to pursue my PhD program. I would like to thank Dr. Elnaz Shadhabi for her valuable suggestions and guidance to familiarize myself with the policies of the University of Manitoba and the National Microbiology Laboratory at the beginning of my program. I want to thank Lewis Liu, my fellow PhD student, for his continuous support in every moment of the program. You are an excellent friend and I will never forget your support and friendship. I want to thank Nikki Toledo for her support, valuable time, and efforts to help in

conducting experiments and sharing technical knowledge to overcome difficulties in Bio-Plex experiments.

I would like to thank Dr. Matthew Gilmour, former scientific director general (DG), National Microbiology Laboratory (NML), for his tremendous support and advice to pursue my PhD program. Your guidance meant a lot to think positively to overcome a hard time in the program. I would like to thank Dr. Guillaume Poliquin, acting scientific DG, NML, for his support of my research. I would also like to thank Drs. Paul Sandstrom, Terry Ball, Adrienne Meyers, John Kim, Paul McLaren, Ruey-Chyi Su, Catherine Card, Hezhao Ji, and Sandra Kiazyk for their smiley greetings, and a short chat on the way to the lab, Cafeteria, and wherever we met each other. I would like to thank Drs. Keith Fowke, Grant McClarty, Denice Bay, Jason Kindrachuk, Xiaojian Yao, Yoav Keynan, and Lyle McKinnon for their support and advice on academic information and help to build up a good scientific career. You all are doing a fantastic job in the Department. I feel proud to be a member of the MMID community.

I want to thank our entire past lab technicians, Philip Lacap, Jeffrey Tuff, David La, David Tang, Thomas Bielawny, Mikaela Nykoluk, Chris Chernecki, Rupert Capina, Christina Daniuk, and Lukas Schroeder for their valuable support to perform my research work in a friendly environment. Especially, I would like to thank Philip Lacap for his incredible mentorship and teaching on how to conduct cell culture works successfully, real-time RT-qPCR technique, and data analysis at the beginning of my project. I also thank all Co-op students who attended our lab during my PhD program for their understanding and cooperation to manage the work environment smoothly.

I want to thank Bernard Abrenica, Xuefen Yang, Abu Siddik, and Christine Mesa for their help in doing Confocal Microscopy imaging and Flow cytometry analysis. I want to thank Jasmine frost for her help in conducting Western blot analysis using the Odyssey CLx imaging system (LI-COR). I also thank Andrew Plesniarski and Xin-Yong Yuan for providing VK2/E6E7 cell line and anti-FREM1 antibodies, respectively. My sincere thanks also go to Rachelle Wiebe, Florence Matua, Winnie Apidi, Zipporah Machuki, Francois Cholette, and Max Abou for their friendship and supportive attitudes. I want to thank all security personnel and supportive staff at JC Wilt Infectious Diseases Research Center.

I am very grateful for the excellent support staff Angela Nelson, Jude Zieske, and Sue Ramdahin in the Department of Medical Microbiology and Infectious Diseases. These people, especially Angela, made my academic work much easier to continue without any hassle. Thank you all! I would like to thank funding agencies, including the Canadian Institute of Health Research (CIHR), GETS funding, Department of Medical Microbiology, Faculty of Graduate Studies, National Microbiology Laboratory (NML), and Children's Hospital Research Institute of Manitoba for their financial help to conduct this study. I would also like to thank all women in

the Pumwani sex worker cohort (PSWC) whose participation made it possible to conduct part of my research work using plasma samples.

Finally, I would like to thank my lovely wife for her invaluable love, and sacrifice, for her understanding, believing, and taking care of me. My sincere thanks also go to my all family members. Without their love and support, writing this thesis was simply impossible.

DEDICATION

I dedicate this thesis to **Almighty Creator** who gave me good health, patience, and energy to conduct this work successfully. My dedication goes to my beloved mom, **late Ayesha Begum**, who consistently encouraged me to work hard to achieve the goal.

I dedicate this work to my wonderful wife, **Mrs. Sayda Kamrun Nahar**, who is always beside me with her love, support, and great patience. Without her understanding and support, I could not be able to fight a hard time and continue my PhD program. My dedication also goes to my cute daughter, **Fatematuj Shimaz Sohaila,** and my newly born son, **Faizaan Saheel Kashem**, who energized me with their innocent love whenever I needed to revive myself.

PUBLICATIONS ARISING FROM THIS THESIS

1 **Kashem, M.A.,** H. Li, N.P. Toledo, R.W. Omange, B. Liang, L.R. Liu, L. Li, X. Yang, X.-Y. Yuan, J. Kindrachuk, F.A. Plummer, and M. Luo, *Toll-like Interleukin 1 Receptor Regulator Is an Important Modulator of Inflammation Responsive Genes.* Frontiers in Immunology, 2019. **10**(272): p. 1-16.

2 **Kashem, M.A.,** X. Ren, H. Li, B. Liang, L. Li, F. Lin, F.A. Plummer, and M. Luo, *TILRR promotes the migration of HIV-1 target cells through modulation of soluble inflammatory mediators' production.* Frontiers in Cell and Developmental Biology, 2020. **8**(563): p. 1-13.

3 **Kashem, M.A.,** H. Li, L.R. Liu, B. Liang, R.W. Omange, F.A. Plummer, and M. Luo, *The potential role of FREM1 and its isoform TILRR in HIV acquisition through mediating inflammation.* International Journal of Molecular Sciences, 2021. 22(15): p.7825.

4 **Kashem, M.A.,** X.-Y. Yuan, L. Li, J. Kimani, F.A. Plummer, and M. Luo, *TILRR (Toll-like interleukin-1 receptor regulator), an important modulator of inflammation responsive genes, is circulating in the blood.* Submitted to "Journal of Inflammation Research" (in revision).

5 **Kashem, M.A.,** J. Lischynski, L. Li, B. Stojak, X.-Y. Yuan, B. Liang, J. Kimani, F.A. Plummer, and M. Luo, *Plasma TILRR is correlated with HIV seroconversion.* The manuscript is in preparation and will be submitted to "Lancet HIV".

6 **Kashem, M.A.,** and M. Luo, *TILRR (Toll-like interleukin-1 receptor regulator) protein is predominantly expressed in different cells and tissues.* The manuscript is in preparation and will be submitted to "Frontiers in immunology".

OTHER PUBLICATIONS ARISING FROM PhD PROGRAM

7 Li, H., R.W. Omange, B. Liang, N. Toledo, Y. Hai, L.R. Liu, D. Schalk, J. Crecente-Campo, T.G. Dacoba, A.B. Lambe, S.Y. Lim, L. Li, **M.A. Kashem,** Y. Wan, J.F. Correia-Pinto, X.Q. Liu, R.F. Balshaw, Q. Li, N. Schultz-Darken, M.J. Alonso, F.A. Plummer, J. Whitney, and M. Luo, *Vaccine targeting SIVmac251 protease cleavage sites protects macaques against vaginal infection*. Journal of Clinical Investigation, 2020.

8 Toledo, NP., H. Li, R.W. Omange, T.G. Dacoba, J. Crecente-Campo, D. Schalk, **M.A. Kashem**, E. Rakasz, N. Schultz-Darken, Q. Li, J.B. Whitney, M.J. Alonso, F.A. Plummer, and M. Luo, *Cervico-vaginal inflammatory cytokine and chemokine responses to two different SIV immunogens,* Frontiers in Immunology, 2020.

9 Li, H., Y. Hai, S.Y. Lim, N. Toledo, J. Crecente-Campo, D. Schalk, L. Li, R.W. Omange, T.G. Dacoba, L.R. Liu, **M.A. Kashem,** Y. Wan, B. Liang, Q. Li, E. Rakasz, N. Schultz-Darken, M.J. Alonso, F.A. Plummer, J.B. Whitney, and M. Luo, *Mucosal antibody responses to vaccines targeting SIV protease cleavage sites or full-length Gag and Env proteins in Mauritian cynomolgus macaques.* PLoS One, 2018. **13**(8): p. e0202997.

10 Li, H., L. Li, L.R. Liu, R.W. Omange, N. Toledo, **M.A. Kashem,** Y. Hai, B. Liang, F.A. Plummer, and M. Luo, *Hypothetical endogenous SIV-like antigens in Mauritian cynomolgus macaques.* Bioinformation, 2018. **14**(2): p. 48-52.

11 Li, H., M. Nykoluk, L. Li, L.R. Liu, R.W. Omange, G. Soule, L.T. Schroeder, N. Toledo, **M.A. Kashem,** J.F. Correia-Pinto, B. Liang, N. Schultz-Darken, M.J. Alonso, J.B. Whitney, F.A. Plummer, and M. Luo, *Natural and cross-inducible anti-SIV antibodies in Mauritian cynomolgus macaques.* PLoS One, 2017. **12**(10): p. e0186079.

12 Omange, R.W., Z. Yuan, A. Tjernlund, X.Y. Yuan, **M.A. Kashem,** J. Sainsbury, H. Li, J. Zhang, L.R. Liu, B. Liang, L. Li, M. Kimani, C. Wachihi, J. Kimani, K. Broliden, Q. Li, F.A. Plummer, and M. Luo, *FREM1 modulates proinflammatory responses during HIV/SIV vaginal infection via association with TLR4.* Submitted to PlosOne (in revision).

Table of Contents

LIST OF FIGURES

LIST OF TABLES

LIST OF COPYRIGHTED MATERIALS WITH PERMISSION

Chapter 1

Figure 1.1 and Figure 1.3: Reprinted with permission from *Molecules*, 2015. **20**(9): 17511-32; Licensed under Creative Commons Attribution 4.0 International [CC BY 4.0].

Figure 1.2: Adapted with permission from Frontiers in Cellular and Infection Microbiology, 2019. **9**: 69; Licensed under Creative Commons Attribution [CC BY 4.0].

Figure 1.4: Reprinted with permission from *Frontiers in Immunology* 2019, **10**: 272; Licensed under Creative Commons Attribution [CC BY 4.0].

Figure 1.5: Reprinted with permission from *Monoclonal antibodies in immunodiagnosis and immunotherapy* 2014, **33(2):**129-40. Permission was obtained by email communication (© by Mary Ann Liebert, Inc.).

Figure 1.6: Adapted with permission from *Journal of Biological Chemistry* 2010, **282 (10)**: 7222-7232. Licensed under Creative Commons Attribution Non-Commercial 3.0 [CC BY-NC 3.0].

Figure 1.7: Reprinted with permission from *JACC Basic Translational Science* 2017, **2 (4)**: 415-417. Licensed under Creative Commons Attribution-NonCommercial-NoDerivatives 4.0 International [CC BY-NC-ND 4.0].

Chapter 2

Figure 2.2: Adapted with permission from GeneCopoeia. Permission was obtained by email communication.

Figure 2.4 and Figure 2.5: Adapted with permission from Bio-Rad. Permission was obtained by email communication.

Figure 2.7 and Figure 2.8: Reprinted with permission from *Frontiers in Cell and Developmental Biology* 2020, **8**: 563; Licensed under Creative Commons Attribution [CC BY 4.0].

Figure 2.10: Adapted with permission from *Frontiers in Immunology* 2019, **10**: 272; Licensed under Creative Commons Attribution [CC BY 4.0].

Chapter 3

All data and figures: Reprinted with permission from *Frontiers in Immunology* 2019, **10**: 272; and *Frontiers in Cell and Developmental Biology* 2020, **8**: 563; Licensed under Creative Commons Attribution [CC BY 4.0].

Chapter 5

Figure 5.1: Reprinted with permission from *International Journal of Molecular Sciences* 2021, **22 (15)**: 7825; Licensed under Creative Commons Attribution [CC BY 4.0].

LIST OF ABBREVIATIONS

Abbreviations	Descriptions
aa	amino acid
AIDS	Acquired Immune Deficiency Syndrome
AP	Affinity Purification
APCs	Antigen-Presenting Cells
ApoE	Apolipoprotein E
ART	Antiretroviral Therapy
ASP	Antisense Protein
ATCC	American Type Culture Collection
BCA	Bicinchoninic Acid
BCR	B-cell Receptor
bFGF	Basic Fibroblast Growth Factor
BMs	Basement Membranes
bnAbs	Broadly neutralizing Antibodies
bp	base pair
BPE	Bovine Pituitary Extracts
BSA	Bovine Serum Albumin
BTLA	B- and T- lymphocyte Attenuator
C	Celsius
CA	Capsid
$CaCl_2$	Calcium chloride
cART	Combined Antiretroviral Therapy
CC	Cytosine-Cytosine
CCL	C-C motif Chemokine Ligand
CCR	C-C Chemokine Receptor
CD	Cluster of Differentiation
cDNA	Complementary DNA
CDS	Coding Sequence
CG	Cytosine-Guanine
CI	Confidence Interval
CIHR	Canadian Institutes of Health Research
CLPs	Common Lymphoid Progenitors
CLRs	C-type Lectin Receptors
CMV	Cytomegalovirus
CO_2	Carbon dioxide
CRFs	Circulating Recombinant Forms
CRM1	Chromosomal Region Maintenance 1 protein

CSF	Colony Stimulating Factor
CSPG	Chondroitin Sulfate Proteoglycan
CT	Cycle Threshold
CTL	Cytotoxic T-lymphocyte
CTLD	C-type Lectin domain
Ctrl	Control
CV	Coefficient of Variation
CVL	Cervicovaginal Lavage
CXCL	C-X-C motif Chemokine Ligand
CXCR	C-X-C Chemokine Receptor
DAMPs	Damage-associated Molecular Patterns
DAPI	4',6-diamidino-2-phenylindole
DCs	Dendritic cells
DC-SIGN	Dendritic cell-specific intercellular adhesion molecule-3-grabbing non-integrin
ddH_2O	Double distilled water
DIC	Differential Interference Contrast
DMEM	Dulbecco's modified eagle medium
DMP	Dimethyl Pimelimidate Dihydrochloride
DMSO	Dimethylsulfoxide
DNA	Deoxyribonucleic acid
dsDNA	Double-stranded DNA
DTT	Dithiothreitol
ECL	Enhanced Chemiluminescence
ECM	Extracellular Matrix
EDAC	1-ethyl-3-(3-dimethylaminopropyl) carbodiimide hydrochloride
EDTA	Ethylenediamine tetraacetic acid
EGF	Epidermal Growth Factor
eGFP	Enhanced Green Fluorescent Protein
EIA	Enzyme Immunoassay
env	Envelope
Fab	Fragment antigen-binding
FACS	Fluorescence-activated cell sorting
FBS	Fetal bovine serum
Fc	Fragment crystallizable
FCV	Final Confirmation and Validation
FGT	Female Genital Tract
FI	Fluorescent Intensity
FITC	Fluorescein isothiocyanate
FM	Follicular mature
FRAS1	Fraser syndrome 1

FREM1	Fras-related extracellular matrix 1
FSC-H	Forward scatter height
FSWs	Female Sex Workers
GAG	Glycosaminoglycan
gag	Group-specific antigen
GAPDH	Glyceraldehyde 3-phosphate dehydrogenase
GG	Guanine-guanine
GM-CSF	Granulocyte-macrophage colony-stimulating factor
gp	Glycoprotein
h	hour
HAART	Highly active antiretroviral therapy
HCl	Hydrochloride
HEK293	Human embryonic kidney 293
HeLa	Henrietta Lacks
HEPES	4-(2-hydroxyethyl)-1-piperazinethanesufonic acid
HESN	HIV-exposed seronegative
HIV	Human immunodeficiency virus
HIV-1	Human immunodeficiency virus type 1
HIV-2	Human immunodeficiency virus type 2
HMEC-1	Human microvascular endothelial cell-1
HPRT1	Hypoxanthine-guanine phosphoribosyltransferase 1
HRP	Horseradish peroxidase
HSX	Heterosexual
HVTN	HIV Vaccine Trials Network
IBM	International Business Machines
IFNg	Interferon-gamma
IFNs	Interferons
Ig	Immunoglobulin
IgG	Immunoglobulin G
IL	Interleukin
IL-1β	Interleukin-1beta
IL-1R1	Interleukin 1 receptor type 1
IL-1Ra	IL-1 receptor antagonist
IL-1RAcP	IL-1 receptor accessory protein
IL-6	Interleukin-6
IL-8	Interleukin-8
IN	Integrase
INIs	Integrase Inhibitors
IP-10	IFN-γ inducible protein-10
IQR	Interquartile range
IRAK4	IL-1R-associated kinase 4

kb	kilobyte
KCl	Potassium chloride
kDa	KiloDalton
KH_2PO_4	Potassium dihydrogen phosphate
KO	Knockout
LB	Luria-Bertani
LCs	Langerhan's cells
LDLR	Low-density lipoprotein receptor
LDS	Laemmli sample buffer
LecC	C-type lectin
LEDGF	Lens epithelium-derived growth factor
LLOQ	Lower limit of quantification
LPS	Lipopolysaccharides
LTR	Long terminal repeat
M	Molar
MA	Matrix
mAb	Monoclonal antibody
MERS-CoV	Middle East Respiratory Syndrome Coronavirus
MC	Multiple cloning
MCHT	Mother-child HIV transmission
MCP-1	Macrophage chemo-attractant protein
MCs	Mast cells
MDDCs	Monocyte-derived DCs
MES	2-(N-morpholino) ethanesulfonic acid
MFI	Mean fluorescence intensity
mg/ml	Milligrams per milliliter
MHC	Major histocompatibility complex
min	Minute
MIP-1α	Monocyte inflammatory protein-1alpha
MIP-1β	Monocyte inflammatory protein-1beta
ml	Milliliter
mM	Millimolar
MMID	Medical Microbiology and Infectious Diseases
mRNA	Messenger RNA
MSM	Men who have sex with men
MyD88	Myeloid differentiation primary response protein 88
MZ	Marginal zone
Na_2HPO_4	Disodium phosphate
NaCl	Sodium Chloride
NC	Nucleocapsid
ND	Not detected

nef	Negative regulatory factor
NEG	Negative
NF-κB	Nuclear factor kappa-light-chain-enhancer of activated B cells
ng/ml	Nanograms per milliliter
NG2	Neural/glial antigen 2
NHS	N-hydroxysulfosuccinimide
NIH	National Institute of Health
NK	Natural killer
NLRs	Nucleotide-binding oligomerization domains (NODs)-like receptors
nm	Nanometer
NML	National Microbiology Laboratory
NMWL	Nominal molecular weight limit
NNRTIs	Non-nucleoside reverse transcriptase inhibitors
NODs	Nucleotide-binding oligomerization domains
NRTIs	Nucleoside-analog reverse transcriptase inhibitors
N-terminus	NH2-terminus or amino-terminus
NVD	N-terminal variable region-containing domain
Ori	Origin of replication
PAMPs	Pathogen-associated molecular patterns
PBMCs	Peripheral blood mononuclear cells
PBS	Phosphate Buffered Saline
PBS-T	PBS-Triton X
PCP	Pneumocystic carinii pneumonia
PCR	Polymerase chain reaction
PCSs	Protease Cleavage Sites
PD-1	Programmed death-1
pDCs	Plasmacytoid Dendritic cells
PDGF	Platelet-derived growth factor
PDMS	Polydimethylsiloxane
PE	Phycoerythrin
pg/ml	Picograms per milliliter
pH	Potential hydrogen
PIC	Pre-integration complex
PIs	Protease inhibitors
PL	Parameter logistics
PLWH	People living with HIV
pol	Polymerase
PR	Protease
PRM	Percentage relative migration
PRR	Pattern recognition receptor
PSWC	Pumwani sex worker cohort

P-TEFb	Positive transcription elongation factor b
qPCR	Quantitative polymerase chain reaction
RANTES	Regulated on activation, normal T cell expressed and secreted
rev	Regulator of expression of virion proteins
rFREM1	Recombinant FREM1
RFU	Relative Fluorescence units
RGD	Arginine-glycine-aspartic acid
RIG-I	Retinoic acid-inducible gene-I
RIPA	Radioimmunoprecipitation assay
RLRs	Retinoic acid-inducible gene I (RIG-I)-like receptors
RM	Rhesus Monkey
RNA	Ribonucleic acid
RNA Pol II	RNA polymerase II
rpm	Revolutions per minute
RPMI	Roswell park memorial institute
rs	Reference SNP cluster ID
RT	Reverse transcriptase
RTC	Reverse transcription complex
RT-qPCR	Reverse transcription-quantitative PCR
SCON	Seroconverters
S	Standard
SARS-CoV-2	Severe Acute Respiratory Syndrome Coronavirus-2
SDF-1α	Stromal cell-derived factor-1alpha
SDS	Sodium dodecyl sulfate
SDS-PAGE	Sodium dodecyl sulfate-polyacrylamide gel electrophoresis
sec	Second
SEM	Standard error of the mean
SFM	Serum-free medium
SIV	Simian Immunodeficiency virus
SNP	Single-nucleotide polymorphism
spD	Specific domain
SPSS	Statistical Package for the Social Sciences
SSC-A	Side scatter area
ssRNA	Single-stranded RNA
sTILRR	Soluble TILRR
STIs	Sexually transmitted infections
SV40	Simian virus 40
T1 B	Transitional type 1 B cell
TAK1	Transforming growth factor β-activated kinase 1
tat	Transactivator of transcription
TCR	T-cell receptor

Th	T helper
TILRR	Toll-like interleukin 1 receptor regulator
TIR	Toll/interleukin-1 receptor
TLRs	Toll-like receptors
TNF-α	Tumor necrosis factor-alpha
TNFR	Tumor necrosis factor-α receptor
TRAF6	Tumor necrosis factor-α receptor-associated factor 6
TRIF	TIR domain-containing adaptor inducing IFN-β
Tris	Trisaminomethane
µg	Microgram
µg/ml	Micrograms per milliliter
µl	Microliter
µl/ml	microliters per milliliter
ULOQ	Upper limit of quantification
UV	Ultraviolet
Vec	Vector
vif	Viral infectivity factor
vpr	Viral protein R
vpu	Viral protein unique
WB	Western blot

1 CHAPTER 1: INTRODUCTION

1.1 HUMAN IMMUNODEFICIENCY VIRUS

1.1.1 History, global burden and strains classification

Human immunodeficiency virus (HIV) was first identified with an unusual clinical disease "*Pneumocystic carinii* pneumonia (PCP)" accompanying a rare form of malignancy called "Kaposi's sarcoma" in a group of young homosexual men (MSM, men who have sex with men) in 1981 [1-3]. The term "acquired immune deficiency syndrome (AIDS)" was later introduced to describe a new disease fatality primarily in infected MSM and a group of intravenous drug users in 1982 [4, 5]. Although the disease was reported between 1981 and 1982, the causative agent was first detected and reported in 1983 [6-9]. Since the beginning of the epidemic, an estimated 75.7 million people have been infected with HIV and 32.7 million people have died from AIDS-related illnesses [10]. Globally, an estimated 38.0 million people were living with HIV and 0.69 million people died due to AIDS-related illnesses in 2019 [10].

HIV is classified into two major types, HIV-1 and HIV-2 based on genetic characteristics and differences in the viral antigens [11]. HIV-1 is more common globally and more pathogenic than HIV-2 that is found mostly in West Africa [12]. The ancestor virus for HIV-1 was first appeared in approximately 1931 [13], and HIV-2 in around 1940 [14]. HIV-1 has been further classified into 4 major groups, namely M (major), O (outliers), N (non-M/non-O), and P [15, 16]. HIV-1 groups M and N originated following zoonotic transmission from Chimpanzees [17], whereas groups O and P arose from Gorillas [18, 19]. HIV-1 group M is widely distributed and mostly responsible for the worldwide pandemic, and groups O, N, and P are primarily confined to Central Africa, [19, 20]. Based on the diversity of viral genetics, HIV-1 group M is also classified into multiple subtypes/strains and recombinants, such as A, B, C, D, F, G, H, J, K, and

CRFs (circulating recombinant forms) [15]. HIV-1 subtype C is known to be primarily responsible for the majority of all HIV-1 infections in Africa and part of Asia, while subtype B mainly confined to Europe, Australia, and the Americas [20, 21]. HIV-2 is less pathogenic; however, multiple sub-groups A-I had also been proposed [22, 23]. *Because the aim of my thesis research is to investigate the role of a novel host factor (TILRR, toll-like interleukin-1 receptor regulator) in modulating inflammatory responses relevant to the HIV-1 acquisition, I will review the literature on HIV-1 only, and use the term HIV to denote HIV-1 hereafter unless otherwise stated. The overall literature review will focus on the topic of my thesis and include: basic knowledge of HIV, host immunology and HIV acquisition, and inflammatory immune responses relevant to HIV acquisition focusing on novel host factor TILRR.*

1.1.2 Viral structure and genome organization

HIV is a member of the genus *Lentivirus* under the family *Retroviridae* [24]. It is an envelope, spherical-shaped, positive sense, single-stranded RNA (ssRNA) virus with a diameter of 100-120 nm [25]. The mature virion consists of an outer lipid bilayer (called the envelope) derived from the host cell membrane that encloses the matrix protein (MA, P17) (lies immediately beneath the envelope) and a cone-shaped viral core. The envelope carries multiple outwards trimeric glycoprotein projections (spikes) comprising of a head (gp120), and a stalk (gp41) essential to bind with host cell receptors. The viral core contains a capsid (CA, p24), which encloses two 9.8 kb long linear ssRNA molecules, *gag* polyprotein, *env* protein, enzymes, such as integrase (IN), protease (PR), and reverse transcriptase (RT). Each ssRNA is tightly bound to nucleocapsid proteins (NC, p7) to stabilize genomic RNA dimers (**Figure 1.1**) [25, 26].

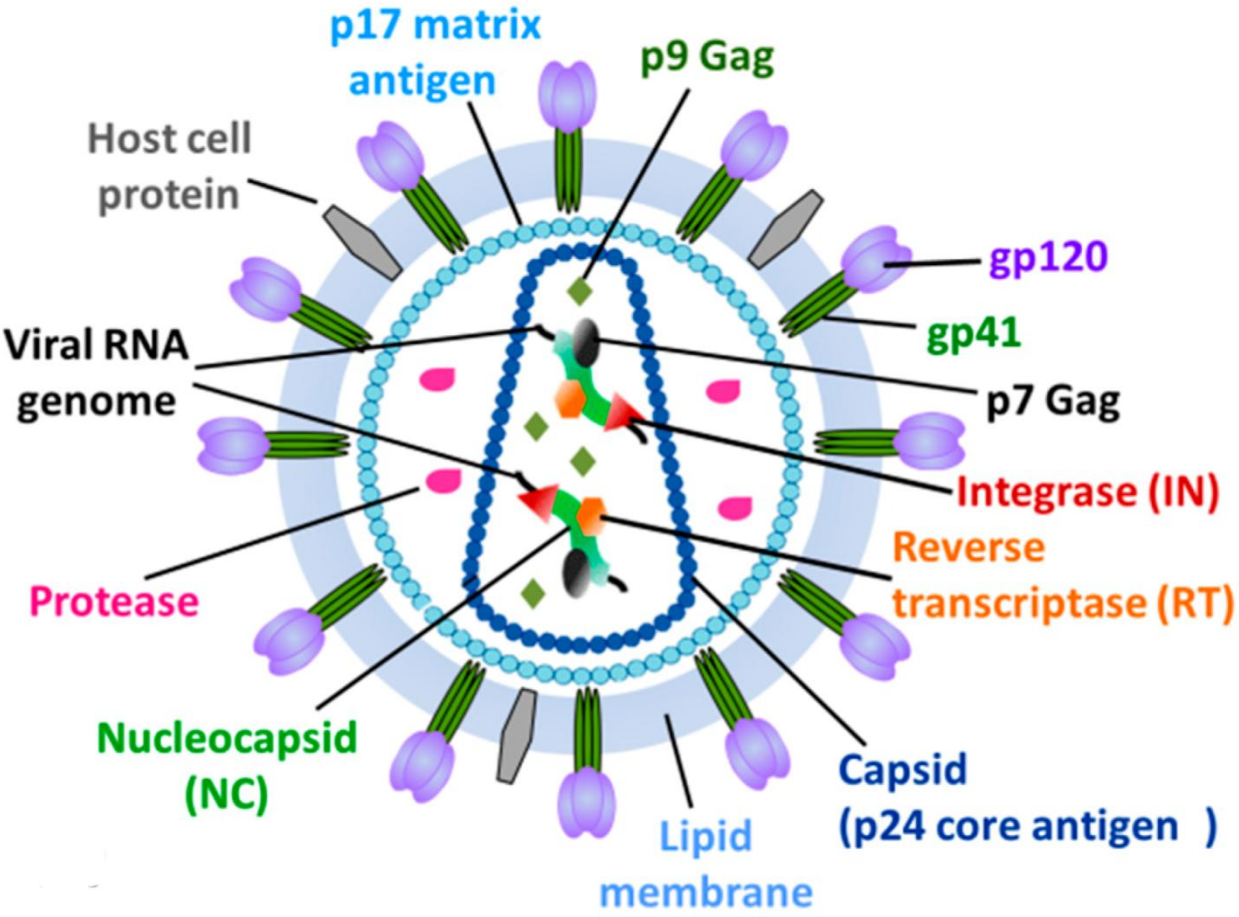

Figure 1.1: Diagram of mature HIV virion. The mature HIV virion contains a viral core, which is surrounded by the lipid bilayer bearing glycoprotein spikes. The viral core consists of capsid protein (CA, p24), nucleocapsid protein (NC, p7), RNAs, and enzymes including reverse transcriptase (RT) and Integrase. The inner wall of the membrane is lined by the matrix protein (MA, p17). This figure was reprinted with permission from Musumeci *et al.* [26] under the license of the Creative Commons Attribution (CC BY 4.0).

The genome of HIV contains several structural, regulatory, and accessory genes. In total, nine genes have been recognized in the HIV viral genome. These included three structural (*gag, pol,* and *env*), two regulatory (*tat* and *rev*), and four accessory (*vpr*, viral protein R; *vpu*, viral protein unique; *vif*, viral infectivity factor; and *nef*, negative regulatory factor) genes **(Figure 1.2**) [27, 28]. Structural genes *gag, pol,* and *env* encode core proteins, enzymes (RT, IN, and PR), and viral envelope protein (gp160, which cleaves into gp120 and gp41), respectively. The regulatory genes *tat* and *rev* function as RNA-binding. *Tat* protein also acts as a transactivator of transcription during proviral DNA transcription, and *rev* helps in shifting HIV gene expression as well as in exporting viral protein from the nucleus to cytoplasm. HIV accessory genes are involved in multiple functions, for instance, vpr functions as nucleocytoplasmic transport factor, vpu triggers the release of virions from the host cells, nef regulates T-cell activation accompanied by downregulation of MHC (major histocompatibility complex)-1 and CD4 marker on the surface of the immune cells, and vif enhances the viral replication in target cells [27, 29]. The HIV proviral DNA (provirus) genome is flanked by LTR (long terminal repeat) sequences at both ends **(Figure 1.2**). The 5' LTR region encodes the promoter for the transcription of the HIV genes [11].

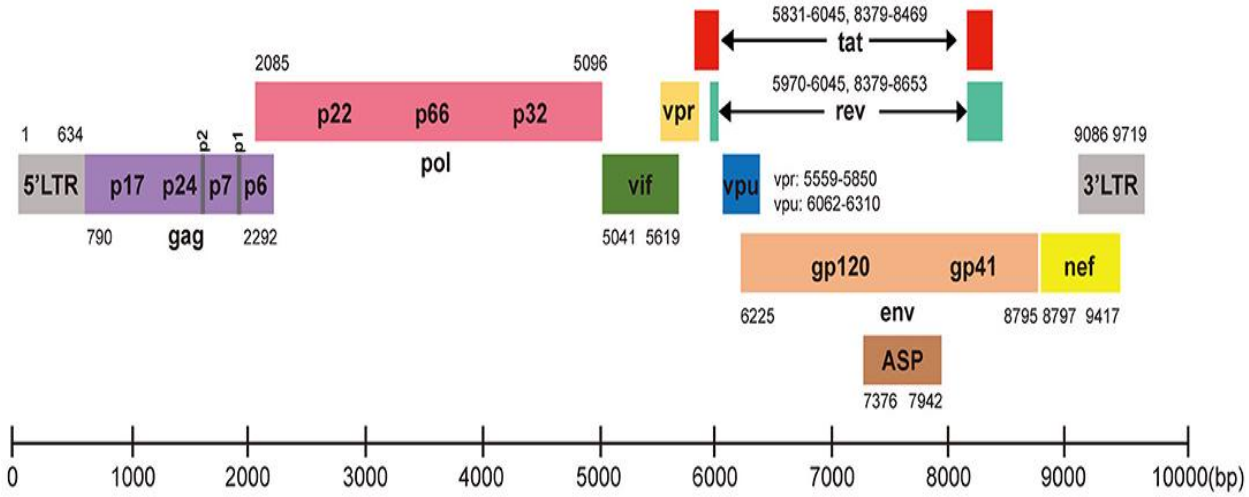

Figure 1.2: Organization of the HIV proviral genome. The genome is ~9.8 kb, which encodes several viral proteins with 5'- and 3'- LTRs. The location of each gene shows based on strain HXB2 (K03455). LTR, long terminal repeat; *vif*, viral infectivity factor; *vpr*, viral protein R; *vpu*, viral protein unique; and *nef*, negative regulatory factor; ASP, antisense protein; bp, base pair; p17: matrix protein; p24: capsid protein; p2: spacer peptide 2; p7: nucleocapsid protein; p1: spacer peptide 1; p22: protease; p66: reverse transcriptase; p32: integrase. This figure was adapted with permission from Xiao *et al.* [28] under the license of the Creative Commons Attribution (CC BY 4.0).

1.1.3 HIV transmission

Transmission of HIV occurs through direct contact of infected blood or mucosal secretions either by horizontal or vertical routes. Horizontal transmission can take place by either heterosexual (penile-vaginal/anal) or homosexual (penile-anal) intercourse between sexual partners [30], sharing needles among intravenous drug users [31], transfusion of infected blood [32, 33], and needle stick injury in the hospital setting [34]. On the other hand, vertical transmission occurs primarily from mother to child during perinatal (*in utero* or during birth) or postnatal periods, such as breastfeeding [35-37].

The majority of HIV infections (~80-90%) are acquired by sexual transmission [38-41], and the risk of HIV acquisition via heterosexual sex (male-to-female) observed 0.08% to 0.30% per sexual act in high- to low-income countries, respectively [42]. Following penile-vaginal intercourse, HIV entry to the target cells often involves a complex interaction with innate immune cells of the female genital tract (FGT). The virus can quickly enter the intraepithelial scavenging CD1a+ Langerhan's cells (LCs) by endocytosis or CD4+T cells via CD4 and CCR5/CXCR4 receptor-mediated direct fusion [43]. Once the virus enters into the CD4+T cell-rich sub-epithelial mucosa, it initiates systemic spread via the generation of local founder virus and establishes viral reservoirs/latency in secondary lymphoid organs [44, 45]. In addition, HIV can also directly penetrate the cervicovaginal epithelial cells through an alternative approach called transcytosis and get easy access to the target cell population in the sub-mucosal epithelia [46, 47] leading to the systemic spread and latency.

1.1.4 HIV life cycle

The HIV replication cycle is a complex event and involves multiple steps. These include i) attachment, ii) fusion, iii) uncoating, iv) reverse transcription, v) nuclear entry, vi) integration

with the host cell genome vii) transcription of proviral DNA, viii) nuclear export ix) translation, x) viral protein assembly xi) virion budding, xii) virion release, and xiii) virion maturation (**Figure 1.3**). The cycle starts with the interaction of viral envelope protein gp120 with host CD4-receptor expressed on target cells [48]. This binding initiates a conformational change in exposing the chemokine co-receptor binding domain of gp120, resulting in an interaction between the host cells CCR5 and/or CXCR4 and gp120-CD4 complex. The stable complex CCR5 and/or CXCR4-CD4-gp120 enables the N-terminal end of envelope gp41 to penetrate the plasma membrane and undergoes a second conformational change that brings both host cell membrane and viral envelope in close proximity leading to fusion [48].

Once the fusion occurred, the viral core delivers into the cytoplasm and release RNAs by uncoating the capsid proteins (p24) following cellular activation [49]. Viral RNAs are then converted into double-stranded DNAs (dsDNA) within a reverse transcription complex (RTC) by viral reverse transcriptase (RT) through a unique process termed reverse transcription [24]. The RTC then changes in a pre-integration complex (PIC) that helps to transport the proviral DNA to the nucleus where integration with the host cell genome occurs by the viral integrase (IN) and forms a functional provirus [48, 50]. The proviral form may either enter viral latency (transcriptionally silent) for a long period or undergo a transcriptionally active cycle [50, 51]. Activation of proviral DNA transcription in the nucleus is initiated by the combined effect of both *tat* and host transcription factors, including NF-κB, at the promoter site of the viral LTR [52]. Following the transcription, multiple HIV-specific mRNA transcripts are produced in the nucleus [48]. Among them, some are cotranscriptionally processed to generate multiply spliced mRNA transcripts, which are rapidly exported into the cytoplasm and translated to viral proteins. On the other hand, unspliced or singly spliced transcripts (called incompletely spliced

transcripts) retain in the nucleus and transport into the cytoplasm by the presence of viral protein rev [48, 53]. Viral Env glycoproteins are synthesized as gp160 (a polyprotein precursor), which is cleaved into gp120 (surface glycoprotein) and gp41 (transmembrane glycoprotein) by cellular proteases [54].

Afterward, viral assembly takes place at the inner surface of the cellular plasma membrane, which is facilitated by gag (and gag-pro-pol) polyprotein. The gag-pro-pol polyprotein is formed when translating ribosomes move to the 3' end of the gag ORF (open reading frame) and then translate the pol gene [55]. The immature virion is assembled with the incorporation of two copies of viral genomic RNAs (incompletely spliced transcripts), several viral proteins, and enzymes, and cellular tRNA molecules. The gp120/gp41 glycoprotein complex is integrated into the lipid bilayer of nascent virions as heterotrimeric spikes during virus assembly [54]. Budding of newly assembled immature virion takes place from the cell membrane, and the final maturation phase is accomplished by the protease (PR) cleavage of gag-pol polyprotein to generate fully processed structural proteins (capsid [CA], matrix [MA], nucleocapsid [NC], and p6), and the viral enzymes (integrase, protease, and reverse transcriptase) [55]. This mature virion is then fully functional to start another cycle by infecting the new host cells.

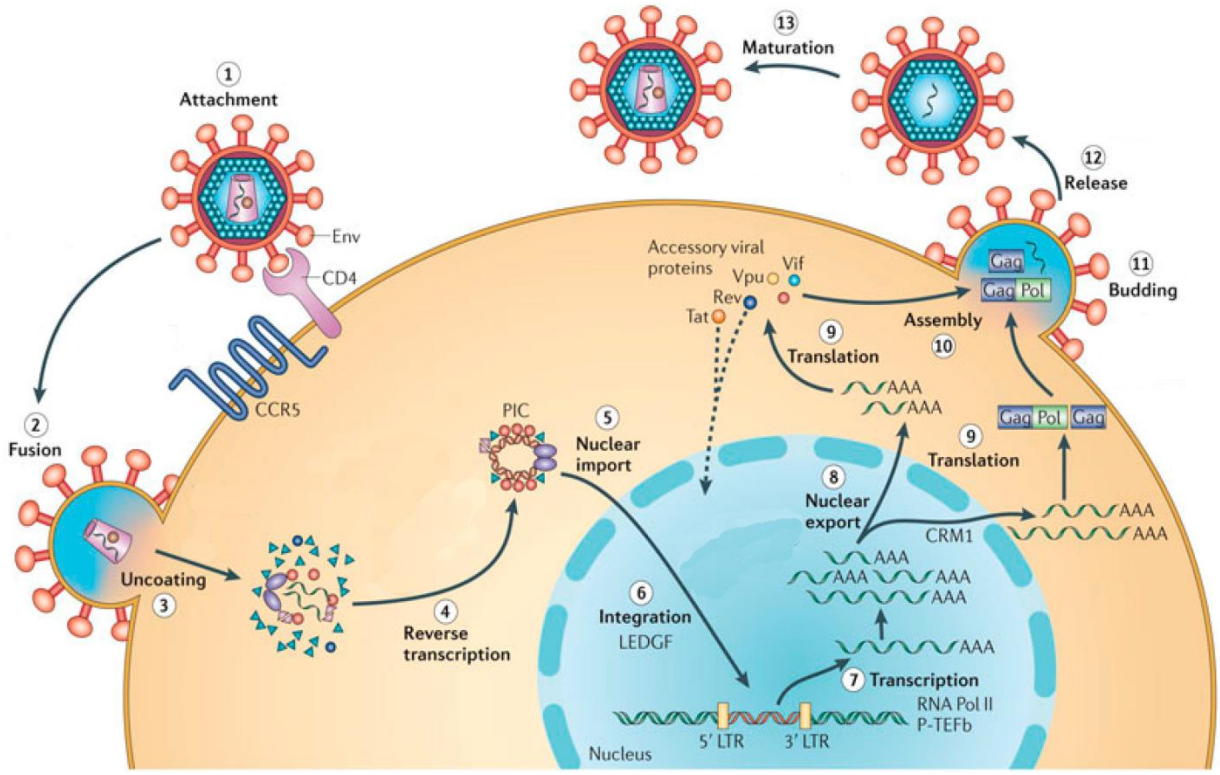

Figure 1.3: Replicative cycle of HIV. The cycle starts with the binding of HIV envelope proteins with host cell receptors CD4 and CCR5, resulting in fusion, and uncoating of viral nucleic acids in the cytoplasm. The release of nucleic acids facilitates reverse transcription and forms a pre-integration complex (PIC). With the help of PIC, dsDNAs transport into the nucleus and integrate with the host cell genome by the integrase (aided by host chromatin-binding protein lens epithelium-derived growth factor [LEDGF]). The proviral transcription is mediated by host positive transcription elongation factor b (P-TEFb) and RNA polymerase II (RNA Pol II), which produce viral mRNAs of different sizes. The mRNAs leave the nucleus (larger mRNAs require energy-dependent export through the host chromosomal region maintenance 1 protein [CRM1]) and serve as a template for protein translation. Afterward, viral assembly takes place in the host cell membrane followed by budding, release, and protease-mediated maturation to generate an infectious viral particle. This figure was adapted with permission from Musumeci *et al.* [26] under the license of the Creative Commons Attribution (CC BY 4.0).

1.1.5 HIV pathogenesis

HIV pathogenesis involves several critical phases: i) eclipse phase ii) acute phase, and iii) chronic asymptomatic or latency phase (occasionally death). Initiation of HIV pathogenesis begins with the entry of the virus through the mucosal epithelium, generation of founder virus in sub-epithelial mononuclear cells, and the transfer of the founder virus to the local draining lymph nodes to induce systemic immune activation and infection [56]. When the virus enters the CD4+T lymphocytes-rich submucosa, it productively infects activated and resting CD4+T cells and rapidly increases the local founder viral population [57, 58]. A short period between the initial entry to the cell and the production of new virions without detectable viremia (undetectable RNA in circulation) is called the "eclipse phase" which lasts for about 10 days. This narrow phase (also called 'window of opportunity') allows eliminating the infection before being disseminated systemically [59-61].

After the eclipse, the level of the virus is being increased exponentially to peak at ~3-4 weeks with characteristic acute retroviral symptoms [60, 62], and continues to persist at a high level for ~12 weeks. During this acute phase, the number of CD4+T cell count declined sharply with the high risk of viral transmission [63]. This massive depletion of CD4+T cells in infected individuals is a critical feature for the pathogenesis of HIV [64]. Immediately before the peak viremia, a systemic cytokine "storm" is induced [65], followed by the host HIV-specific immune responses, including cell-mediated, and humoral responses [66, 67]. Both HIV-specific cytotoxic T-lymphocyte (CTL) and humoral responses markedly control the viral replication, reducing the viremia to a "set point" level [66, 67], and undergo a chronic asymptomatic phase or viral latency. The chronic HIV latency can persist for decades with the gradual decay of the CD4+T cell count [68]. During the chronic phase, if the CD4+T cell count declined to <200 cells/cubic

mm of blood, the final phase (AIDS) is achieved. At this phase, the infected host becomes very susceptible to opportunistic pathogens, resulting in death due to AIDS-related complications [69, 70].

1.1.6 Treatment, control, and prevention

1.1.6.1 Antiretroviral therapy (ART)

Following the outbreak of HIV in 1981, the treatment regimen is improved because of the availability of antiretroviral (ARV) drugs, the discovery of several enzyme inhibitors targeting the HIV life cycle. Although monotherapy was introduced at the beginning of the treatment, a combination of at least 3 drugs called HAART (highly active antiretroviral therapy) has significantly changed the potential to decline HIV-related morbidity and mortality [71, 72]. The combination therapy partially improved the immune system by reducing viral load below the detection limit (<100 RNA copies/ml) and increased the CD4+T cell count [73, 74]. In 2010, the United States and European guidelines recommended using HAART once the level of CD4+T cells declined to 350/mm^3 of blood, at which phase the level of RNA copies reaches 10^4-10^5 copies/ml [72]. Despite the proper adherence to the treatment, the HAART cannot eradicate the HIV infection, which further reminds us to discover alternative approaches to manage HIV infection. Until recently, five different classes of antiretroviral agents are in use against HIV. These included: a) nucleoside-analog reverse transcriptase inhibitors (NRTIs), b) Non-NRTIs (NNRTIs), c) integrase inhibitors (INIs), d) protease inhibitors (PIs), and e) entry inhibitors (coreceptor antagonists and fusion inhibitors) [29].

1.1.6.2 Vaccine

Although HAART successfully improves the life span of HIV-infected patients, to end the HIV/AIDS pandemic requires a preventive vaccine. More than 250 clinical trials of HIV vaccine

candidates have been conducted since the first phase I human trial in 1987 [75], and most of them were stopped in phase I and II trials [76, 77]. Among them, HIV Vaccine Trials Network (HVTN) 502, also called the "STEP" trial was the most famous HIV vaccine candidate that mainly focused on T-cell immunity. The primary purpose of the STEP trial was to determine whether HIV-specific T-cell immunity generated by the vaccine prevents HIV infection or at least reduces plasma viral loads in infected patients [78]. A trivalent mixture of recombinant adenovirus type 5 (rAd5) vectors expressing gag, pol, and nef of HIV clade B, respectively, was utilized to formulate the candidate vaccine for the STEP trial. Although the vaccine was highly immunogenic in preclinical and phase I trial, the STEP trial was unexpectedly stopped in 2007 [79] because the vaccine neither prevented infection nor reduced plasma HIV viral loads in infected individuals [80]. Two years after the unsuccessful STEP trial, another vaccine trial called the "RV144 Thai trial" has shown modest protection for the first time with 31.2% efficacy against HIV infection [81]. In this trial, a "prime-boost" combination of AIDSVAX B/E gp120 subunit vaccine and vCP1521 (ALVAC-HIV) canarypox vectored vaccine was used. The correlates of protection analysis showed that antibodies to V1V2 may contribute to the protection against HIV infection. The data analysis failed to identify the neutralizing antibody as a potential correlate of protection, and the non-neutralizing antibodies involving antibody-dependent cell-mediated cytotoxicity (ADCC) were suggested to play a role in the protection [78]. This trial thus opened up the new door for more research in HIV vaccine development and clinical trials.

Following the RV144 Thai trial, a number of vaccine efficacy trials had been conducted including HVTN 702 clinical trial. In HVTN 702 trial, participants received an intramuscular (IM) injection of vCP2438 (ALVAC-HIV) at 0- and 1-month followed by a combination of vCP2438 (ALVAC-HIV) and bivalent subtype C gp120/MF59 at 3-, 6- and 12- months [82].

ALVAC-HIV vaccine contained gp120 of HIV clade C and the vaccine boost was co-formulated with ALVAC-HIV and MF59 adjuvant [83]. The usage of the MF59 adjuvant in the HVTN 702 trial was the primary difference from the RV144 Thai trial in addition to the incorporation of gp120 of HIV clade C instead of clade B/E. Unfortunately, after a decade of a glimmer of hope on the HVTN 702 clinical trial, the results have shown that the vaccine is ineffective in preventing transmission of HIV, and the trial was stopped in January 2020 [84, 85]. Currently, several major clinical trials are ongoing, including "HVTN 705/HPX2008 (Imbokodo trial)" and "HVTN 706/HPX3002 (Mosaico trial)" [84]. The regimen of the Imbokodo trial (HVTN 705/HPX2008) is composed of a tetravalent adenovirus vector vaccine (ad26.Mos4.HIV) and aluminum-phosphate adjuvanted clade C gp140 vaccine. The Imbokodo trial is to evaluate the efficacy, tolerability, and safety of a prime-boost vaccine regimen in healthy HIV-uninfected women [86]. Whereas, Mosaico trial (HVTN 706/HPX3002) is to assess the efficacy of a vaccine regimen utilizing Ad26.Mos4.HIV and aluminum phosphate-adjuvanted clade C gp140 and Mosaic gp140 in healthy MSM (men who have sex with men) and transgender people [87].

The study of our group has recently shown that a vaccine targeting protease cleavage sites (PCSs) offered 80% protection against repeated intravaginal SIVmac251 challenges in Mauritian cynomolgus macaques [88]. To generate a mature and infectious viral progeny, HIV protease needs to conduct 12 proteolytic reactions at 12 cleavage sites on the HIV polyproteins. A subtle disturbance during this process can interrupt the reactions and produce uninfectious viruses. Our group developed the PCS vaccine by targeting the highly conserved sequences surrounding the 12 PCSs. The PCS vaccine focuses immune responses on the sequences surrounding the twelve-viral PCSs. Twelve-peptide immunogens were administered as rVSVpcs (recombinant vesicular stomatitis virus pcs) and in nanoparticles (NANOpcs). The rVSVpcs and NANOpcs are

combinedly termed as PCS vaccine [89]. The vaccine regimen consists of a prime with rVSVpcs at week 0 followed by 4 boosts including rVSVpcs plus NANOpcs at weeks 6 and 51, NANOpcs alone at week 16, and rVSVpcs alone at week 72. The rVSVpcs and NANOpcs were given through intramuscular (IM) and intranasal routes, respectively [88]. Twenty-four weeks after the last boost, repeated low-dose intravaginal SIVmac251 challenges were carried out every two-week for 13-times. The study showed that the PCS-specific T-cell responses are significantly correlated with vaccine efficacy [88]. Thus, the PCS vaccine provides a novel approach for an effective HIV vaccine.

1.2 HOST IMMUNOLOGY AND HIV ACQUISITION

Immune responses directed against HIV are critical for viral acquisition and transmission. Since HIV mutates rapidly to escape the host immune system and targets CD4+ immune cells, including monocytes and T-lymphocytes, this section will therefore focus on the specific literature relevant to the basic host immunology and its functions in HIV acquisition and transmission. In general, the host immune system is classified into two major groups: innate and adaptive.

1.2.1 Innate immune responses

Innate immune machinery plays a central role in early detection and triggering pro-inflammatory responses to invading pathogens, and is therefore considered as the first line of defense against infection [90, 91]. It is principally composed of cellular (immune cells), physical (epidermis and mucosal surfaces), and chemical (pattern recognition molecules, cytokines/chemokines, complement fractions, and antimicrobial peptides) elements [92-94]. Innate recognition of pathogens mostly relies on germ line-encoded evolutionarily conserved pattern recognition receptors (PRRs) expressed on innate immune cells [91].

1.2.1.1 Innate immune cells

Innate immune cells include monocytes/macrophages, dendritic cells, natural killer (NK), granulocytes (including neutrophils, basophils, eosinophils, and mast cells [MCs]), and epithelial cells [93, 95, 96]. It also includes newly identified innate lymphoid cells [96]. The following few paragraphs will briefly describe the major innate immune cells, particularly involved in HIV acquisition and transmission.

1.2.1.1.1 Monocytes/Macrophages

Monocytes/macrophages are members of the mononuclear phagocyte system and are primarily involved in host innate immune responses. They play crucial roles in initiating inflammation via the production of inflammatory mediators and modulating adaptive immune responses [97, 98]. Monocytes are derived from common myeloid progenitor cells of bone marrow. Monocytes undergo spontaneous apoptosis during normal physiological conditions [98-100]; however, they can escape the apoptosis mechanism by differentiating to macrophages in the presence of appropriate stimulus [98, 100-103]. Differentiated macrophages function as professional antigen-presenting cells (APCs) and constitutively express high levels of MHC (major histocompatibility complex) class-II molecules, pattern recognition receptors (PRRs), and co-stimulatory molecules [95]. Activation of monocytes/macrophages is induced by recognizing specific stimuli with myriad surface and cytoplasmic receptors [101]. The activated macrophages present processed antigen/peptide to CD4+T-lymphocytes via MHC class-II molecules and induce the development of adaptive immune responses.

In HIV infection, monocytes/macrophages are the target cells [104] and potentially serve as a major contributor in initial infection, dissemination, person-to-person transmission, and long-term persistence [105, 106]. R5-tropic HIV preferentially infects monocytes/macrophages via

interaction between viral envelope protein gp120/gp41 and cellular dual surface markers, CD4 and CCR5 [107-109]. HIV envelope proteins gp120 and accessory protein Nef directly stimulate the activation of monocytes/macrophages, resulting in the production of pro-inflammatory cytokines/chemokines [110, 111]. Additionally, increased NF-κB transcription factor binding activity and HIV gene expression are observed during the maturation and differentiation of monocytes [112], supporting the critical roles of monocyte/macrophage in HIV infection.

1.2.1.1.2 Dendritic cells

Dendritic cells (DCs) derived from bone marrow precursors act as sentinels on the immune system [113]. They are considered the most efficient APCs because they uniquely initiate, coordinate, and modulate adaptive immune responses [95, 114]. DCs traffic from bone marrow to the body tissues where they reside as immature DCs and capture incoming antigens. Following antigen capture, the immature DCs migrate to the secondary draining lymphoid organs, transform to mature DCs, and promptly prime naive T-lymphocytes [113]. DCs present processed antigens (as a form of antigenic peptides) to naive CD4+ helper T and CD8+ cytotoxic T cells via MHC class-II and -I molecules, respectively [115]. Although HIV preferentially targets monocytes/macrophages as well as CD4+T cells, DCs serve as critical immune cells in mediating HIV transmission, target cell infection, antigen presentation, and shaping of adaptive immune responses [116]. During HIV infection, DCs (primarily skin DCs including epidermal Langerhan's cells) uptake the virus through a process, the so-called endocytosis, following the binding of Env gp120 to the C-type-lectin receptors (CLRs), DC-SIGN (Dendritic cell-specific intercellular adhesion molecule-3-grabbing non-integrin), and Langerin [117, 118]. Whereas, blood plasmacytoid DCs (pDCs) uptake the virus mostly via binding of Env gp120 to CD4-mediated endocytosis despite the expression of CLRs along with CD4 molecules [119].

Furthermore, effective HIV fusion with monocyte-derived DCs (MDDCs) is mainly dependent on the elevated level of surface-expressed CD4 molecules [120]. Thus, these data indicated the plasticity, preference, and importance of DCs in the event of HIV recognition and transmission.

1.2.1.2 Pattern Recognition Receptors (PRRs)

Innate immune cells naturally express multiple cell surface and cytoplasmic PRRs to recognize either PAMPs (pathogen-associated molecular patterns) or DAMPs (damage-associated molecular patterns), resulting in immediate immune activation and inflammatory responses [121]. PRRs include toll-like receptors (TLRs), nucleotide-binding oligomerization domains (NODs)-like receptors (NLRs), retinoic acid-inducible gene-I (RIG-I)-like receptors (RLRs), and C-type lectin receptors (CLRs) which recognize different viral RNA and proteins, bacterial lipopolysaccharides (LPS), lipoproteins and peptidoglycan [121, 122]. The binding of PAMPs with PRRs activates the downstream signaling events, resulting in the induction of interferons (IFNs) as well as pro-inflammatory mediators' production [123]. Among various PRRs, the TLR family members are the well-studied group. Until recently, ten and thirteen different TLRs have so far been discovered in humans (TLR1-10) and mice (TLR1-13), respectively [124, 125] where TLR10 is non-functional in mice [126]. TLRs 1, 2, 4, 5, 6, 10, 11, and 12 are exclusively expressed on the cell surface, whereas TLRs 3, 7, 8, 9, and 13 localized intracellularly in the cytosolic compartment inside the phagocytic vesicles [125, 127, 128]. In exception, TLR2 and TLR4 also express intracellularly in monocytes, DCs, epithelial as well as endothelial cells [129-131].

Using *in vitro* model, exposure of several TLR ligands showed that human TLR2-5 and TLR7-9 initiate memory and effector CD4+T and CD8+T lymphocyte activation [132]. In HIV-infected patients, TLR4 mediates the bacterial LPS (lipopolysaccharide)-induced cellular NF-κB

activation and HIV transcription via IL-1 signaling molecules, including MYD88 (Myeloid differentiation primary response 88), IRAK4 (IL-1R-associated kinase 4), TRAF6 (TNFR-associated factor-6), and NIK (NF-κB-inducing kinase). Activation of NF-κB then potently regulates HIV-LTR transactivation and replication [133]. The binding of LPS not only enhances HIV replication, but also directly modulates the secretion of cytokines/chemokines (IL-1β, IL-6, and TNFα) from peripheral infected macrophages and DCs [134], and induces aberrant systemic immune activation and inflammation [135-137]. Thus, these data demonstrated that PRRs of immune cells function as critical regulators in HIV acquisition.

1.2.2 Adaptive immune responses

The principal components of the adaptive immune system include T- and B- cells. The adaptive immune response is selective, proliferative, and generates memory responses [138].

1.2.2.1 CD4+ T cells

CD4+T (also known as helper T cells or Th) cells are the principal regulator of the adaptive arm of the immune system. The T-cell surface receptor (TCR) of CD4+T cells recognizes PAMPs presented by the MHC class-II molecule of APCs [139]. Following recognition of PAMPs, CD4+T cells become activated, undergo clonal expansion, and develop either memory or effector T-cell subsets depending on whether they are in draining lymph nodes or migrating towards other non-lymphoid organs, respectively [140]. Naive CD4+T cells proliferate and differentiate into Th (T helper) type 1 (Th1) and Th2 CD4+T cells in the presence of APCs-secreted IFNγ/IL-12 and IL-4/IL-2, respectively. Both Th1 and Th2 cells further contribute to T-cell proliferation and differentiation [141]. Activated CD4+T cells also provide essential signals for the survival and the generation of long-lived memory CD8+ cytotoxic T cells [142-144].

HIV preferentially infects CD4+T-lymphocytes [145]. The progressive loss of CD4+T-cells is considered a hallmark of HIV infection due to the imbalance in CD4+T-cell homeostasis, and gradual impairment of immunity [64]. Following successful entry, the single founder virus rapidly establishes an initial productive infection in CD4+T lymphocytes of regional lymph nodes, which serve as major viral reservoirs, from where HIV disseminates to the systemic circulation and other lymphoid tissue compartments, resulting in high levels of viremia [146, 147]. Over the course of infection, HIV infects a large proportion of CD4+ T-cells and the reduction of CD4+ T-cells leads to immunodeficiency and opportunistic infection [61].

1.2.2.2 CD8+ T cells

CD8+T (also known as cytotoxic T-lymphocytes or CTL) lymphocytes also require a signal for activation. The TCR of CD8+T cells binds to pathogenic peptides presented by MHC class I of APCs [139]. The binding of TCR with the MHC-peptide complex along with co-stimulation of neighboring CD4+T cells activates the CD8+T cells, which clonally differentiate into effector and memory CD8+T cells [144, 148]. Activation and early production of cytokines, such as IL-2, IL-12, type I IFNs, and IFNγ, instigate the proliferation, survival, effector differentiation, and abundance of CTLs during acute viral infection [149-152]. The CTLs kill the infected cells through the expression of granzymes and perforin.

In the case of acute HIV infection, the reduction of viral replication (viremia) is initially associated with the increased HIV-specific CD8+CTL responses resulted in slower disease progression [153-155]. Using a macaque model, the depletion of CD8+T cells has been shown to dramatically increase the plasma SIV viremia [156, 157]. Furthermore, activated mature CD8+T cells are susceptible to HIV infection due to the *de novo* expression of surface CD4 antigen [158]. Because the CD4 molecule functions as a binding receptor during HIV infection, its

expression on CD8+T cells thus increases HIV susceptibility. Thus, CD8+T cells can either control or augment HIV infection and disease progression.

1.2.2.3 B-cell and antibody responses

B-cells develop from bone marrow-derived common lymphoid progenitors (CLPs) in which sequential functional gene rearrangements occur in immunoglobulin (Ig) loci, resulting in the expression of identical surface Ig receptors recognizing specific antigenic epitopes [159]. After a series of initial development, immature B cells leave the bone marrow as short-lived, transitional type 1 B cell (T1 B) for peripheral development in the spleen where T1 B cells convert to transitional type 2 B (T2 B) cells followed by naive FM (follicular mature) and MZ (marginal zone) B cells. Once naive B cells encounter antigen with support signal from T cells, they further differentiate into long-lived plasma cells and memory B cells, which function to secrete antibodies and are responsible for recall responses, respectively [159, 160]. In HIV-infected individuals, several functional dysregulations have been documented in the B-cell population, including increased apoptosis and exhaustion, loss of morphologic integrity, and decreased quality of response to HIV [161]. Dysregulated B-lymphocytes in HIV-infected viremic subjects is evident by the disruption of peripheral B-cell subsets, which are accompanied by decreased BTLA (B- and T- lymphocyte attenuator), and an elevated level of PD-1 (programmed death-1) expression [162], and higher production of IgG or hypergammaglobulinemia [163].

During early HIV infection, the initial host antibody response is directed towards non-neutralizing epitopes on HIV envelope (Env), and the specific responses of broadly neutralizing activity to early infectious virus isolates are often delayed, and usually developed after several months (~6 months) or even years (2-4 years) after transmission event [164]. This initial antibody response against primary HIV viral isolates is inefficient to control viremia because the

selective pressure of the antibodies rapidly generates viral escape mutants [165, 166], and in some cases, the primary viral isolates are resistant to the antibody neutralization [167]. Furthermore, a very small proportion of HIV-infected individuals develop highly mutated, broadly neutralizing antibodies (bnAbs) capable to neutralize a broad range of HIV isolates [168-170]. Despite a wide range of broadly neutralizing activity of antibodies against HIV isolates, researchers are still struggling to develop an antibody-based vaccine in addition to the T cell-based vaccine strategies against HIV acquisition. Currently, two antibody-mediated prevention (AMP) vaccine trials are ongoing, such as HVTN703/HPTN081 and HVTN704/HPTN085 [171, 172]. Both HVTN703 and HVTN704 vaccine trials are assessing the safety, efficacy, and tolerability of VRC01 antibody (a potent bnAb, which designed against the CD4 binding site of HIV envelope glycoprotein) in heterosexual women [171], and men and transgender persons, who have sex with men (MSM) [172], respectively.

1.2.3 Genital mucosal immune cells and HIV acquisition

Multiple immune cells are responsible to generate antimicrobial immunity in the healthy female genital mucosa. These include mononuclear subsets, such as monocytes/macrophages, dendritic cells (DCs), Langerhan's cells, T-cells, and B- cells [173]. However, the proportions of these immune cells are variable in the female genital epithelium. T-lymphocytes are frequently found in the genital epithelium, where the levels of CD8+T lymphocytes are higher than CD4+T lymphocytes, and most of the T-lymphocytes (both CD4+ and CD8+T cells) are effector memory phenotype [174-178]. Flow cytometry analysis of normal genital tissues demonstrated that the upper genital tract (fallopian tubes, uterus, and endocervix) harbors higher levels of T-lymphocytes than the lower genital tract (ectocervix and vagina) [177]. A study also demonstrated that ectocervix contains elevated levels of T-lymphocytes (CD4+ and CD8+ T

cells) and B cells than endocervix [178]. Furthermore, ectocervix contains an increased number of CD14+ tissue hematopoietic cells, including macrophages (CD14+CD11c-) and dendritic cells (CD14+CD11c+), where macrophages are more frequent than dendritic cells [178].

During early vaginal HIV infection, the specific genital mucosal immune cells, such as macrophages, and dendritic cells, function as a vehicle carrying the virus to the CD4+T cell-rich sub-epithelial mucosa. Using genital mononuclear leukocytes, a study showed that vaginal and ectocervical DCs are the first to uptake HIV as early as 15 min followed by the macrophages and lymphocytes, suggesting that DCs primarily transfer HIV to the CD4+T target cells in sub-epithelial mucosa [179]. Therefore, the genital mucosal immune cells act as crucial modulators in vaginal HIV infection and transmission.

1.3 HOST INFLAMMATORY RESPONSES AND HIV ACQUISITION

Cellular immune responses following microbial insult or tissue injury induce the production of chemical mediators via intracellular signaling pathways, resulting in inflammation. Inflammation is a protective host physiological response characterized by vasodilatation and extravasation of immune cells and recruitment of plasma proteins to the site of tissue injury/infection. Inflammation is considered as a beneficial host response required to clear harmful pathogens and in promoting the healing process [180-182]. However, dysregulated inflammatory responses can cause aberrant tissue damage, which favors the pathogens, such as HIV, to access the target cells for productive infection. As the IL-1-NF-κB signal transduction pathway plays a critical role in host inflammatory responses, I will highlight the IL-1-NF-κB signaling pathways, and their downstream signaling effects on inflammatory mediators' production, including the effects of novel host factor(s) in augmenting inflammation, particularly relevant to HIV acquisition and transmission.

1.3.1 Inflammatory signaling pathways and HIV acquisition

The host immune system is equipped with various signaling networks to elicit host defense against microbial infection, including HIV. Interleukin (IL)-1 pathway is a master regulator of inflammatory cytokines/chemokines production through its downstream activation of NF-κB transcription factor. In the context of HIV, the IL-1 pathway functions as a driving force of inflammation-mediated HIV acquisition.

1.3.1.1 Interleukin-1 (IL-1) pathway

IL-1 family cytokines are widely known signaling molecules of host immune systems. It constitutes eleven members, including IL-1α, IL-1β, IL-1Ra (IL-1 receptor antagonist), IL-18, IL-33, and IL-1F5 to IL-1F10 encoded by 11 distinct human and mouse genes, which are central regulators of immunity and inflammation against a broad range of stimuli [183-186]. The prototypical, multifunctional agonists of IL-1 family members (IL-1α and IL-1β) typically bind with a cognate receptor called IL-1R1 (IL-1 receptor type I) and concurrently recruit a co-receptor IL-1RAcP (IL-1 receptor accessory protein, also known as IL-1R3) to form a heterotrimeric complex [187, 188]. Formation of extracellular ternary complex IL-1-IL-1R1-IL-1RAcP juxtaposes intracellular portions of cytoplasmic TIR (Toll/interleukin-1 receptor) domains connected to the cognate receptors and instigates downstream cytoplasmic signaling transduction [183, 186, 187]. These conformational changes allow the recruitment of adaptor molecules, most commonly MYD88, IRAK4, TRAF6, and other signaling intermediates. Following the assembly of all required molecules, subsequent biological reactions involve NF-κB (nuclear factor-κB) signaling pathway to induce inflammatory responses [189].

Studies showed that IL-1α and IL-1β induced HIV gene expression [190-193]. IL-1α and IL-1β induced the secretion of TNF-α [194], and IL-1β further promotes the TNF-α-induced HIV gene

expression [190]. The balance between the production of endogenous IL-1β (called viral inducers) and the inhibitor IL-1Ra modulates the HIV production and inflammatory process associated with HIV infection [195, 196]. For instance, an elevated level of IL-1α and IL-1β strongly induced the HIV gene expression in monocytes while IL-1Ra opposed the viral expression [190, 192]. Thus, the IL-1 signaling pathway plays an important role in generating inflammatory responses, and inflammation leading to HIV susceptibility, acquisition, and transmission.

1.3.1.2 NF-κB signaling pathway

NF-κB signaling orchestrates multiple aspects of innate and adaptive immunologic responses, including immune cell activation, survival, and differentiation together with the induction of inflammatory responses [181]. Activation of NF-κB signaling is mediated by two distinct pathways: canonical (also called classical) and non-canonical (alternative). The canonical pathway of NF-κB responds to multiple stimuli, including ligands of cytokine receptors (IL-1R1, and TNFR [tumor necrosis factor-α receptor] superfamily members), PRRs, TCR, and BCR (B-cell receptor) [181, 182]. This pathway of NF-κB activation is based on the inducible degradation of IκBα inhibitor with a multi-subunit IκB kinase (IKK) complex [197, 198]. The IKK complex comprises two catalytic subunits (IKKα and IKKβ) and a regulatory subunit (IKKγ; also called NF-κB essential modulator [NEMO]) [198] and activated by pro-inflammatory cytokines, microbial components, and growth factors [199]. Following activation, IKK complex phosphorylates IκBα inhibitor at two N-terminal serines, resulting in polyubiquitination and rapid degradation of IκBα in 26S proteasome [198]. Degradation of IκBα inhibitor triggers rapid and transient nuclear translocation of NF-κB family proteins, mostly p50/RelA and p50/c-Rel dimers, and bind to enhancers or promoters of target genes, leading to

NF-κB pathway activation. In this pathway, IKKβ but not IKKα is essential for inducible phosphorylation and degradation of IκBα inhibitor [181, 198].

The non-canonical NF-κB pathway, on the other hand, responds to a number of specific stimuli, such as ligands of TNFR superfamily member subsets, including BAFF (B-cell activating factor belonging to TNF family), and CD40L [200, 201]. The non-canonical pathway of NF-κB activation is strictly dependent on IKKα and independent of IKKβ and IKKγ (NEMO) [198]. This pathway is primarily involved in NF-κB2 precursor protein (p100) processing and does not involve degrading IκBα inhibitors [200]. The processing of NF-κB2 (p100) protein starts with its phosphorylation by IKKα together with the activation of NF-κB-inducing kinase (NIK), resulting in polyubiquitination and proteasomal degradation of inhibitory C-terminal IκB-like structure of NF-κB2 (p100). Degradation of inhibitory C-terminal region generates NF-κB2 p52 (mature form) and triggers nuclear translocation of NF-κB complex p52/RelB dimers, leading to activation of NF-κB signaling pathway [198].

Functionally, the canonical pathway of NF-κB activation associates with nearly all aspects of host immune responses while the non-canonical pathway acts as supplementary signaling axis, which cooperates with the canonical pathway in regulating specific functions of the adaptive immune system, including immune cell maturation and differentiation, and lymphoid organogenesis [181, 202]. In short, the binding of a ligand to a cognate receptor results in intracellular signaling cascades involving nuclear transportation of NF-κB molecules, and induction of innate inflammatory responses by producing inflammatory cytokines/chemokines, leading to inflammation [122, 182, 203]. NF-κB-induced dysregulated immune activation and inflammatory responses are the hallmarks of inflammation-mediated inflammatory disease pathogenesis [204, 205].

The replication and transmission of HIV can be augmented by activating host transcription factors including NF-κB. Because the HIV genome contains NF-κB binding sites in the 5'-untranslated leader region of HIV LTR, the binding of cellular NF-κB molecules can induce potent transcriptional activation of HIV gene expression [206, 207]. Indeed, activation or latency of HIV in infected cells is tightly controlled by HIV-LTR transcriptional activity regulated by host cellular NF-κB transcription molecules [208]. It is evident that the transmission of HIV can be promoted by IL-1-induced NF-κB activation, pro-inflammatory responses, and HIV target cell recruitment [209]. NF-κB activation in concert with the production of inflammatory mediators can directly enhance HIV replication, in addition to its effect on promoting target cell recruitment [209]. In fact, IL-1 itself or in combination with IL-6 and TNF-α induces HIV gene expression in latently infected monocytes and T-cells via activation of NF-κB singling pathway [190-192]. TNF-α also mediates HIV expression by elevating the level of free NF-κB which, in turn, binds to and transactivates HIV-LTR [191, 210]. In addition, the NF-κB transcription factor not only functions as a replication inducer of HIV gene expression but also acts as a regulator of HIV latency. The availability of activated NF-κB below a certain threshold can be the principal factor governing the establishment of HIV latency [211]. Thus, NF-κB functions as a double-edged sword in HIV acquisition, transmission, and latency establishment.

1.3.2 Inflammatory cytokines/chemokines and HIV acquisition

Inflammatory cytokines/chemokines (also called mediators) produced by the IL-1-NF-κB signaling transduction pathway function as critical regulators in inflammation-mediated HIV acquisition. Under physiological conditions, female genital cytokines/chemokines regulate mucosal integrity, chemotaxis of immune cells, and generate specific immune and inflammatory reactions to neutralize or kill pathogenic microbes [212]. Although the physiological level of

mucosal inflammatory mediators primarily controls the microbial transgression, an abnormally high level of mediators due to the microbial insult can directly compromise the tight junction permeability of epithelial and endothelial cells [213-216]. A persistently high level of female genital inflammatory cytokines/chemokines (MIP-1α/CCL3, MIP-β/CCL4, and IP-10/CXCL10) is associated with mucosal vulnerability to HIV infection, HIV seroconversion, and increased risk of HIV acquisition [217, 218]. The elevated level of these inflammatory mediators promotes HIV acquisition by recruiting and activating HIV target cells and distorting the mucosal epithelial barrier [217]. In HIV-uninfected Kenyan women, genital mucosal expression of GM-CSF, IL-1β, IL-8/CXCL8, IL-17, and MIP-3α (macrophage inflammatory protein-3α) has been shown to alter the expression of mucosal barrier proteins, proteases, and the recruitment of immune cells, which, in turn, become HIV target cells to establish productive infection [219]. Increased genital mucosal inflammatory mediators (IL-1α, IL-1β, IL-6, IL-8/CXCL8, IP-10/CXCL10, MCP-1/CCL2, MIP-1α/CCL3, and MIP-1β/CCL4) in cervicovaginal lavage (CVL) have been shown to cause an increased risk of HIV seroconversion and acquisition [218, 220, 221]. Studies also demonstrated that elevated level of genital mucosal RANTES/CCL5 in HIV-uninfected FSWs (female sex workers) is positively correlated with the level of cervical immune cells (CD4+T, CD8+T cells, and immature DCs), and pro-inflammatory mediators (IL-1, IL-6, IL-8/CXCL8, and TNF-α), suggesting the higher risk of HIV susceptibility [222, 223]. Furthermore, high levels of genital cytokines/chemokines and activated CD4+T cells are associated with an increased risk of HIV acquisition in adolescent girls and young women [224].

Besides, circulating inflammatory mediators also function as critical regulators of systemic immune activation, and inflammation in HIV acquisition and transmission. The elevated level of plasma cytokines/chemokines (IL-1β, IL-2, IL-6, IL-7, IL-12p70, IL-10, IP-10/CXCL10, and

TNF-α) have been shown to be strongly associated with increased HIV infection, seroconversion, and acquisition risk in women [221, 225, 226]. Taken together, these data underscore the importance of both female genital and circulatory inflammatory mediators in HIV susceptibility, acquisition, and transmission.

1.3.3 Inflammation and HIV infection

Cytokines/chemokines produced by activated immune cells cause aberrant inflammation, which is suggested to be a major driving force of HIV susceptibility, and acquisition. Indeed, the persistent inflammatory profile of genital mucosa contributes to the higher risk of vaginal HIV acquisition [217, 218, 227]. Genital inflammation accompanied by increased activated CD4+T-cells is shown to be associated with increased HIV acquisition risk in South African young women [224, 228]. It has also been shown that genital inflammation is a strong predictor of genital HIV RNA shedding, plasma viral load, and decreased systemic CD4+T-cell population [229, 230]. Thus, HIV acquisition is favored by inflammatory genital mucosa where inflammation fuels the recruitment and activation of HIV target cells [180].

Additionally, chronic systemic immune activation is considered as a driving force of sustained inflammation, CD4+T-cell depletion, and pathogenesis of AIDS. Although HIV replication is directly correlated with immune activation, accumulated evidence showed that high levels of HIV replication alone are neither enough nor necessary to initiate a pathological level of immune activation [231]. The abnormal systemic immune activation and inflammation are the major determinant of advanced HIV disease progression [232, 233].

HIV resistant women (HIV-exposed seronegative, HESN) demonstrated the immune quiescence phenotype in the genital mucosa [234], which is characterized by reduced expression of genes in

CD4+T cells, and reduced frequency of T cell subsets expressing CD69 activation marker together with limited production of soluble cytokines/chemokines [235-237]. HESN individuals have also shown low levels of CD4+T cell activation and reduced PBMC susceptibility to HIV infection [238]. Thus, these observations from HESN individuals indicated that the presence of both genital and systemic inflammation is a strong correlate of susceptibility to HIV infection.

1.3.4 Novel host factors in regulating inflammation and HIV acquisition

Because immune activation/inflammation during HIV infection is multifactorial, including biological, behavioral, and host genetics, in this section I will highlight the literature on two host factors, FREM1 (Fras-related extracellular matrix 1) and its splice variant, TILRR (Toll-like interleukin-1 receptor regulator- *the focus of this thesis*), in relevance to the inflammation and HIV acquisition.

1.3.4.1 FRAS-RELATED EXTRACELLULAR MATRIX 1 (FREM1)

FREM1 is an extracellular matrix protein that forms a ternary complex with other integral membrane proteins of epithelial cells, including FRAS1 (Fraser syndrome 1) and FREM2. It serves as an essential component during embryonic development, and a variant of FREM1, TILRR, functions as a mediator of innate immune responses and inflammation.

1.3.4.1.1 Molecular structure of FREM1 and its splice variants

Full-length human FREM1 contains multiple functional domains that interact with extracellular matrix molecules. It has an N-terminal signal sequence, positioned at 1-23 of its amino acid (aa) sequence, and an N-terminal variable region-containing (NV) domain (from aa 24-274) with an Arg-Gly-Asp (RGD) motif (from aa 199-201). Following the NV domain, there are 12 chondroitin sulfate proteoglycan (CSPG) tandem repeats. Each CSPG domain is approximately

120 aa long (from aa 275-1730) [239, 240]. At the C-terminal region, it contains a calcium-binding loop of approximately 89 aa long (Calx-β domain, from 1731-1820 aa), and an RGD motif sequence (from 1907-1909 aa). At the end of the C-terminus, it has a unique type C lectin-like (LecC) domain, which is ~131 aa long (from aa 2052-2179) [239]. Additionally, it bears two glycosaminoglycan (GAG) attachment sites located between CSPG10 and CSPG11 domains, and Calx-β and C-terminal RGD motif, which were shown to bind to the IL-1R1 receptor of IL-1-NF-κB signaling pathway (**Figure 1.4**) [241, 242].

The amino acid sequence of the N-terminal signal peptide is highly variable between human and mouse FREM1 protein and therefore termed as N-terminal variable region-containing domain (NVD) [239]. FREM1 RGD motif sequence is a well-studied cell-adhesive motif and functions as an integrin-binding region. It is recognized by a wide group of integrins, such as αv subunits (αvβ1 and αvβ3) and the β1 subunits (α5β1 and α8β1), which transduce signals to the cells [239]. Twelve CSPG repeats, also known as cadherin repeat-like repetitive elements [240, 243] initially identified in NG2 (neural/glial antigen 2) core protein [244], are the hallmark of Fras/FREM family proteins because they are common to all members of the family [243]. Studies have demonstrated that NG2 core protein (CSPG motifs) frequently interact with an array of extracellular matrix (ECM) proteins, including collagen type II, V, and VI [245-247], platelet-derived growth factor (PDGF-AA, a longer isoform of PDGF) [248], and basic fibroblast growth factor (bFGF2) [248]. Thus, it is suggested that FREM1 binds with ECM proteins of basement membranes (BMs) through its repetitive CSPG domains [249] to conduct its biological functions, including cell adhesion, cell proliferation, and migration. The Calx-β domain of FREM1 is a calcium-binding loop of Na^{+}-Ca^{+} exchange β. The Calx-β domain is characterized by a cytoplasm-localized, calcium chelating, and calcium-binding region of transmembrane proteins,

such as integrin β4 [250]. Additionally, the unique feature of FREM1 protein is having a C-terminal LecC domain (CTLD) which is associated with carbohydrate residues of ECM. The other members of Fras/FREM family proteins do not have CTLD [251].

According to AceView [252, 253], FREM1 has approximately 15 splice variants. Of them, a full-length isoform 1 encoding the 2179 amino acids long full FREM1 protein (NM_144966.5/NP_659403.4), and a shorter isoform 2 encoding a 715 aa protein (NM_001177704.1/NP_001171175.1) were described [249]. The FREM1 isoform 2 (TILRR) has a structurally different N-terminal region and only has 3 CSPG domains with a Calx-β domain and a C- terminal LecC domain [241, 254]. Similar to isoform 1, it contains an RGD motif and two GAG attachment sites that are associated with cell adhesion and IL-1β signal transduction, respectively (**Figure 1.4**).

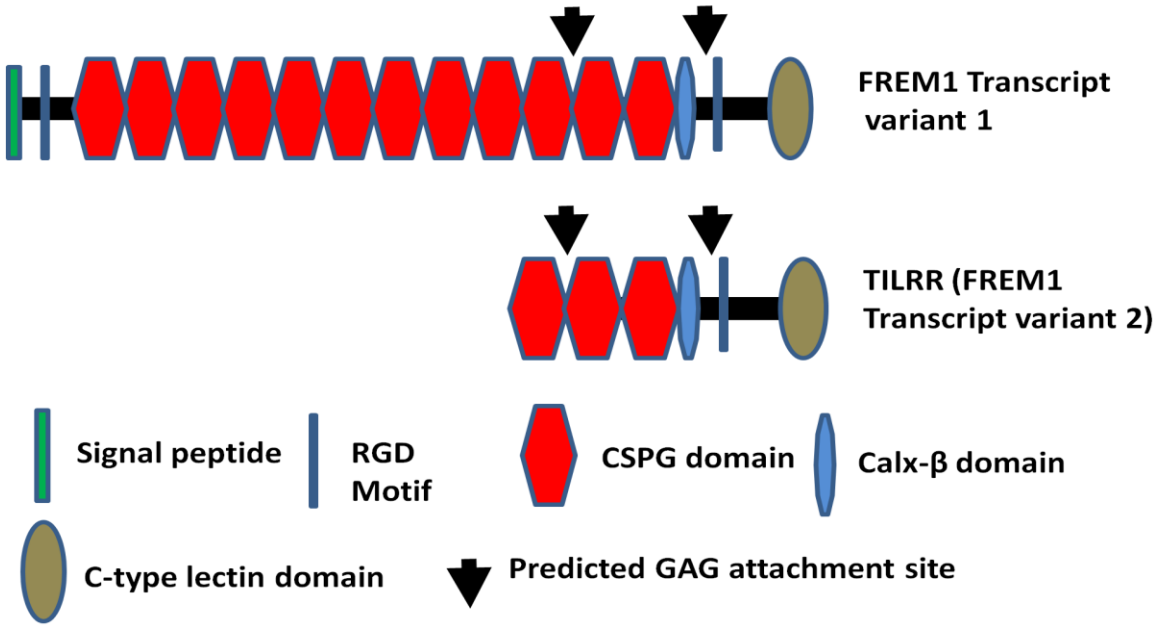

Figure 1.4: Diagram of FREM1 and its splice variant. Full-length FREM1 transcript variant 1 (top) and FREM1 truncated variant 2 (also called TILRR) (bottom); CSPG, chondroitin sulfate proteoglycan; RGD, arginine-glycine-aspartic acid; GAG, glycosaminoglycan. This figure was reprinted with permission from Kashem et al. [254] under the license of Creative Commons Attribution (CC BY).

1.3.4.1.2 FREM1 expression, localization, and interactions

FREM1 protein is expressed in a wide variety of human and animal cells and tissues. It functions as an important extracellular molecule either in developing embryos or in the pathogenesis of multiple abnormalities. FREM1 is primarily secreted by the mesenchymal cells underlying the basement membrane of visceral pleura and in epithelial and mesothelial cells [255, 256]. The protein is localized in the dermal layer where it forms a stable complex with other Fras/FREM-related proteins called ternary complex [257]. Although both dermal and epidermal cells express FREM1 [251, 256], its expression is most prominent in dermal cells of the eyelids, head, and limbs of mice [243]. It is also expressed in the diaphragm [255], intestine, lung, kidney, and skin [256], craniofacial structures, such as ears, forehead, midface, nose, teeth, and hair follicles in mice [243, 258, 259].

A previous study from our group showed that mRNA of FREM1 is expressed in various human tissues, including cervix, colon, esophagus, heart, kidney, lung, ovary, placenta, prostate, skeletal, small intestine, testes, thymus, thyroid, and trachea [260]. The expression of FREM1 was observed at a high level in cervical tissues, the small intestine, and kidneys. Immuno-histochemistry staining of human ectocervical biopsy specimens from two different groups of women (HIV-negative new enrollees and HIV resistant) of the Pumwani sex worker cohort (PSWC) demonstrated that FREM1 protein is expressed in the epithelial and sub-mucosal layer underneath the basement membrane (BM), particularly the upper lamina propria [260].

Recently, we also found that FREM1 is expressed in the stratified epithelium of human ectocervix, sub-epithelial tissues, and columnar epithelium of endocervix (Omange et al. Submitted). FREM1 is also identified in the ectocervix of Rhesus monkeys (RM). Surprisingly, FREM1 was not only expressed in the epithelial tissues, but also in PBMCs, including

monocytes, B-, NK-, and T- cells of humans, and RM. The frequency of FREM1 expression was highest in monocytes followed by B-, NK- and T-cells. Classical monocytes ($CD14^{+}CD16^{-}$) showed a relatively higher frequency of FREM1 expression compared to non-classical monocytes ($CD14^{dim/-}CD16^{+}$) in humans. The pattern of FREM1 expression frequency in PBMCs of RM was also shown to be similar to that in humans (Omange et al. Submitted). Thus, FREM1 is expressed in a variety of immune cells, which may have particular importance in the pathogenesis of HIV/SIV infection.

1.3.4.1.3 FREM1 and immune cell infiltration

Extracellular matrix (ECM) proteins function as mediators of inflammation and infiltration of immune cells [261-264]. Because FREM1 is an extracellular matrix protein and is widely expressed in the regions of epithelial-mesenchymal interaction [243], its expression in epithelial tissues may promote immune cell infiltration. Using immunohistochemistry (IHC) and immunofluorescence (IF) assays, a study demonstrated that elevated expression of FREM1 in normal breast/mammary epithelial tissues is positively correlated with the infiltration of several immune cells, such as CD4+, and CD8+T -cells, and M1 (inflammatory) macrophages [265]. In addition, analysis of breast cancer (BC) epithelial tissues showed that high FREM1-expressed BC tissues harbor abundant CD4+T memory cells (resting and activated), CD8+T-cells, M1 macrophages, resting dendritic cells, gamma-delta T cells (γδT), B-cells (naive and memory), plasma cells, and resting mast cells. Whereas, low FREM1-expressed BC tissues were trended to have a higher proportion of M2 (anti-inflammatory) macrophages, neutrophils, and resting NK (natural killer) cells [265]. It has also been shown that the RGD motif of ECM binds with integrins and promotes migration of effector T cells into the interstitial inflamed tissues [266]. Thus, the binding of FREM1 with integrins may function as a critical regulator in infiltrating

immune cells, especially in cervicovaginal tissues. Although the direct role of FREM1 in infiltrating immune cells in cervical tissues is yet to be examined, the expression of FREM1 in the cervix of humans [260], and RM (Omange et al. manuscript submitted) supports the notion that FREM1 may functions as an inducer of immune cell infiltration, including HIV target cells, facilitating vaginal HIV infection.

1.3.4.1.4 FREM1 in innate signaling and vaginal HIV/SIV infection

Because toll-like receptor (TLR) and IL-1 signaling pathways shared many components [189], and TLRs, including TLR4, play a key role in producing pro-inflammatory cytokines/chemokines and HIV pathogenesis [267], we have recently examined the interactions between FREM1 and TLR4 in monocytes and CD4+T cells. Our study showed that stimulation with LPS (lipopolysaccharide), a TLR4 agonist, altered FREM1 expression in monocytes and CD4+ T-cells of human PBMCs. TLR4 agonist stimulation increased the frequency of FREM1+TLR4+ monocytes whereas reduced that of FREM1+TLR4- monocytes (Omange et al. manuscript submitted). We further observed that blocking FREM1 with anti-FREM1 monoclonal antibodies (mAbs) reduced the frequency of FREM1+TLR4+ monocytes in human PBMCs. Thus, FREM1 potentially functions as a TLR4 signaling co-receptor capable of modulating pro-inflammatory and co-stimulatory functions in monocytes in response to LPS. Using the macaque model, our study further showed that FREM1 and TLR4 colocalize in the stratified layer of cervicovaginal epithelial cells, and the expression of both FREM1 and TLR4 was increased in the cervicovaginal sub-mucosa of RM following intravaginal SIVmac239 infection (Omange et al. manuscript submitted). Taken together, these results suggested that the association of FREM1 and TLR4-induced inflammatory responses may influence vaginal HIV/SIV infection and transmission.

1.3.4.1.5 FREM1 polymorphism and HIV resistance

In 1985, an observational cohort study was established in the heart of Pumwani slum, Nairobi, Kenya called the Pumwani sex worker cohort (PSWC). It is an open prospective cohort study of the immunobiology and epidemiology of sexually transmitted infections (STIs), and the patients enrolled in the cohort have been followed biannually since the cohort establishment [268-271]. This cohort is not only involved in the research, but also provides services related to STI and HIV prevention and care, such as consultation, provision of free condoms, and treatment of other infections. Between 1985 and 2008, more than 3000 sex workers have been enrolled in the cohort. A sub-group of women in PSWC remained HIV uninfected despite the frequent exposure to high-risk HIV-infected sexual partners [271]. These women demonstrated a significantly high-level expression of various potentially HIV inhibitory molecules, including RANTES [272], serpins, elafin, and many other factors [272-274] at their genital mucosa. Multiple immunological [275-278], genetic [279-283], and proteomics [273, 274] factors are associated with this phenotype.

Our group has conducted a genome-wide analysis of SNP (single nucleotide polymorphism) among women of PSWC to identify the genetic polymorphism associated with the HIV-resistant phenotype [260]. The study showed that the minor allele of SNP rs1552896 of FREM1 is enriched in HIV-resistant women. The rs1552896 was located at the intron 11 (57 bp) close to the 3' end of the exon 11 of the FREM1 gene. Besides, the frequency of the minor allele of rs1552896 was also found higher in HIV-uninfected women in comparison to HIV-infected individuals in a mother-child HIV transmission (MCHT) cohort. Thus, the minor allele of FREM1 SNP rs1552896 is associated with the HIV-resistant phenotype.

Since the minor allele "G" (GG/GC genotype, protective) of the FREM1 SNP rs1552896 is associated with the HIV-resistant women and the major allele "C" (CC genotype, wild-type) of the SNP rs1552896 is associated with HIV susceptible women [260], we recently studied FREM1 expression in relation to the activation status of immune cells collected from individuals with different FREM1 SNP genotypes. We found that the activation status of FREM1-expressed T cells was lower in individuals with protective genotype (GG/GC) of FREM1 SNP rs1552896 compared to the wild-type genotype (CC) individuals (Omange et al. Submitted). However, we know very little about the specific roles of FREM1 in HIV resistance/susceptibility and how this intronic FREM1 SNP influences the function of FREM1.

1.3.4.1.6 Current advances in studying FREM1 and its splice variant TILRR

Antibodies are important tools to study the function of proteins and have been used as therapeutics for many diseases [284]. To study the function of FREM1 and its role in HIV infection, our group developed anti-FREM1 antibodies [241]. To develop anti-FREM1 monoclonal antibodies, we expressed two recombinant proteins of FREM1, rspD (376 amino acids, 56.8 kDa), and rspF (255 amino acids, 29.5 kDa). The two recombinant proteins overlap the C-terminal region of full-length FREM1 isoform 1 and the majority portion of FREM1 isoform 2 (TILRR). Structurally, rspD protein contains a small portion of the CSPG9 domain as well as the CSPG10, CSPG11, CSPG12, and Calx-β domains of FREM1, whereas rspF only contains C-type Lectin domain (CTLD) (**Figure 1.5)**. Our group developed 17 anti-FREM1 mouse monoclonal antibodies (mAbs) and mapped their epitopes [241]. These anti-FREM1 mAbs target different major and minor epitopes of multiple domains of FREM1 and its splice variants. These in-house developed anti-FREM1 mAbs and recombinant FREM1 proteins are used as tools to study the role of FREM1 and its variants in inflammation responses and vaginal

HIV/SIV acquisition. Using these anti-FREM1 mAbs, we have recently demonstrated that FREM1 modulates pro-inflammatory responses (Omange et al. Submitted).

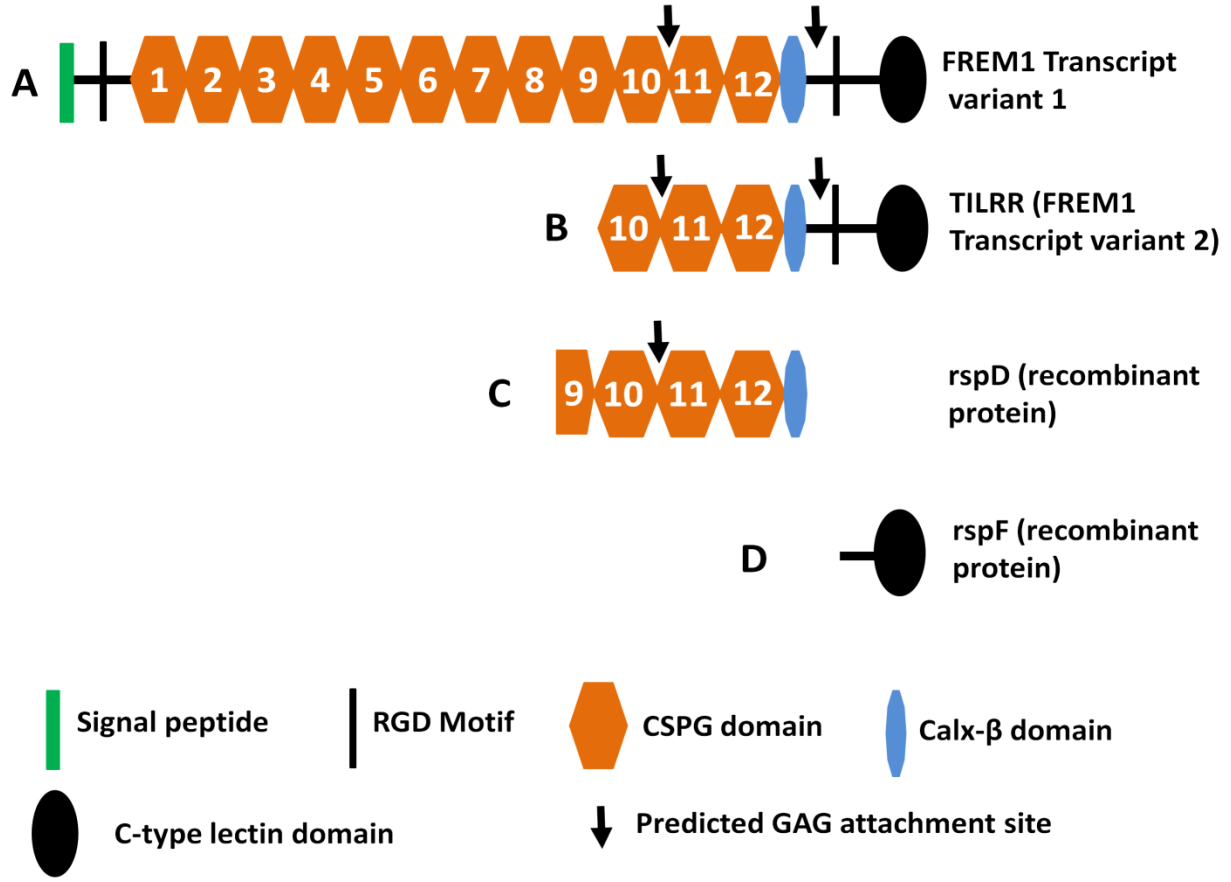

Figure 1.5: Diagram of FREM1 variants and recombinant proteins. A) Full-length FREM1 transcript variant 1; **B)** TILRR; **C)** rFREM1 spD protein; and **D)** rFREM1 spF protein. RGD, arginine-glycine-aspartic acid; CSPG, chondroitin sulfate proteoglycan; and GAG, glycosaminoglycan. This figure was adapted from Yuan et al. [241] with permission.

1.3.4.2 TOLL-LIKE INTERLEUKIN-1 RECEPTOR REGULATOR (TILRR)

TILRR, a FREM1 variant, is an IL-1R1 co-receptor and has been identified as a unique and highly conserved membrane-bound glycosylated protein [285].

1.3.4.2.1 Characteristics of TILRR

TILRR is a shorter FREM1 transcript consisting of 715 aa residues [285, 286]. It associates with IL-1/IL-1R1 signaling receptor, binds with the host cell membrane by its structural C-terminal LecC domain, and increases the cell surface receptors expression and ligand binding activities [285]. As a truncated variant of FREM1, its transcriptional start site is located within an intronic segment between exons 24 to 25 of the FREM1 gene called 5' TILRR coding sequence (CDS) [287]. The 5' TILRR CDS was found in human and mouse FREM1 and therefore used to identify ortholog of TILRR in other organisms for its evolutionary history and development. Analysis of 5' CDS in tetrapods (amphibians), teleosts (fish), and invertebrates (*Drosophila melanogaster*, *Caenorhabditis elegans,* and *Ciona intestinalis*) showed that only tetrapod organisms possess 5' TILRR CDS within the FREM1 ortholog. Although teleost organisms possess at least one FREM1 ortholog, no 5' TILRR CDS was recognized in these organisms [287].

In invertebrates, in contrast, neither FREM1 ortholog nor 5' TILRR CDS were found. Thus, FREM1 appeared following the evolution of vertebrates; however, TILRR was only identifiable after the divergence of teleosts. These suggest that FREM1/TILRR may evolve from the common ancestor of tetrapod and teleost organisms and subsequently extinct in FREM1 paralogs prior to the modern teleosts evolution [287]. In addition, FREM1/TILRR may emerge due to the divergence of a common ancestor in the tetrapod lineage [287].

1.3.4.2.2 TILRR expression

TILRR is expressed in a wide variety of human and animal cells. The mRNA expression analysis of PBMCs, and several epithelial, endothelial, and other immune cell lines demonstrated that TILRR mRNA was expressed in all cells, but the level of expression is variable [285]. In humans, TILRR mRNA is relatively highly expressed in several cell lines, including microvascular endothelial cell (HMEC-1), human embryonic kidney cells (HEK293), leukemic cells (K562, ML-1, HL-60, and MOLT-4), and macrophage cell line (U937); however, lower expression of TILRR mRNA was reported in cervical epithelial cell (HeLa), monocytes (THP-1) and PBMCs. In animals, on the other hand, high levels of TILRR mRNA were observed in murine mammary epithelial cells (C127), fibroblast (3T3), and monocyte/macrophage cells (J774.2), and relatively low expression was reported in a murine macrophage cell line (RAW 264.7). Zhang *et al*. [285] further demonstrated that TILRR is a 70 kDa protein and its protein expression level is consistent with the level of mRNA expression.

Smith *et al.* [288] showed that TILRR mRNA is expressed in murine monocyte-derived macrophages (RAW 264.7). A high level of TILRR mRNA expression was also found in PBMCs of myocardial infarction-diagnosed patients [288]. Additionally, immunohistochemistry staining of the carotid artery revealed a significantly elevated level of TILRR expression in the atherosclerotic plaque [288]. A recent study further demonstrated that TILRR mRNA is highly expressed in normal human breast/mammary epithelial cells [286]. Taken together, TILRR mRNA is expressed in multiple immune and epithelial cells in humans and animals, and its expression implicates the importance of TILRR in innate immune responses and inflammatory diseases.

1.3.4.2.3 TILRR in innate signal transduction and inflammation

Toll-like/IL-1 receptors regulate the innate immune and inflammatory responses through association with the IL-1R1 receptor complex followed by engagement of MYD88 adaptor protein to the cytoplasmic TIR (toll/IL-1 receptor) domain, and transcriptional modification of NF-κB transcription factor [289-291]. As a co-receptor of IL-1R1, TILRR interacts with the IL-1R1-TIR complex and augments the signal transduction by enhancing ligand-binding activities and the expression of IL-1R1 receptor [285, 292]. The association of TILRR with IL-1R1 not only potentiates the receptor expression, but also enhances the recruitment of cytoplasmic MYD88 adapter on the TIR domain resulting in the expression of pro-inflammatory genes after NF-κB signaling pathway activation (**Figure 1.6**) [285, 293]. TILRR mediates the activation of inflammatory genes in a wide variety of cells including macrophages, epithelial cells, and fibroblasts via TIR regulatory components [285].

Smith *et al*. [288] demonstrated that inflammatory conditions, such as lung fibrosis, and myocardial infarction, trigger an elevated TILRR expression in blood monocytes/macrophages. It has been also shown that blocking with an anti-TILRR antibody or genetic deletion of TILRR has significantly reduced the monocyte/macrophage population in the inflamed areas [288]. Microarray analysis of blood samples revealed that knockout of the TILRR gene greatly reduced inflammatory gene expression [288]. Gabhann [294] elucidated that the binding of IL-1 with its cognate receptor IL-1R1 forms the IL-1-IL-1R1 complex, which initiates a medium level of NF-κB activation. Whereas the association of co-receptor TILRR with IL-1-IL-1R1 complex, like IL-1-IL-1R1-TILRR, instigates a higher level of NF-κB activation, resulting in increased pro-inflammatory responses during pathological conditions **(Figure 1.7)**. Thus, TILRR mediates inflammation. Targeting TILRR to reduce its function may significantly reduce inflammatory

responses, immune cell migration, and infections or diseases associated with inflammation. The reduced TILRR expression may reduce HIV acquisition.

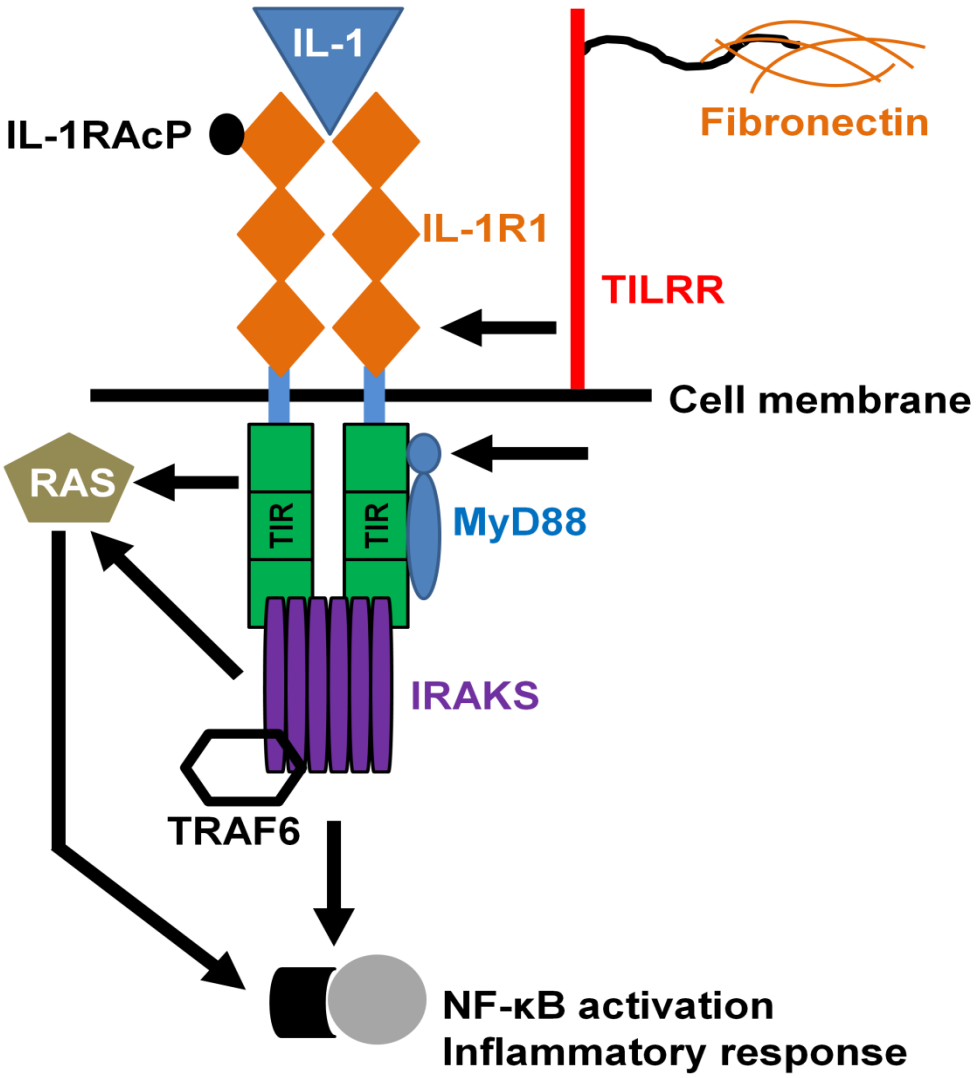

Figure 1.6: TILRR potentiates MYD88 recruitment to IL-1RI to induce NF-κB signaling and inflammatory responses. TILRR binds with IL-1R1 as a co-receptor and potentiates the recruitment of MYD88 adapter to the cytoplasmic TIR domain. The association of an adapter molecule with the TIR domain induces the signal amplification and directs the Ras GTPase-controlled enhancement of NF-κB induction and inflammatory genes. This figure was adapted with permission from Zhang *et al*. [285] under a Creative Commons Attribution Non-Commercial License (CC-BY-NC 3.0).

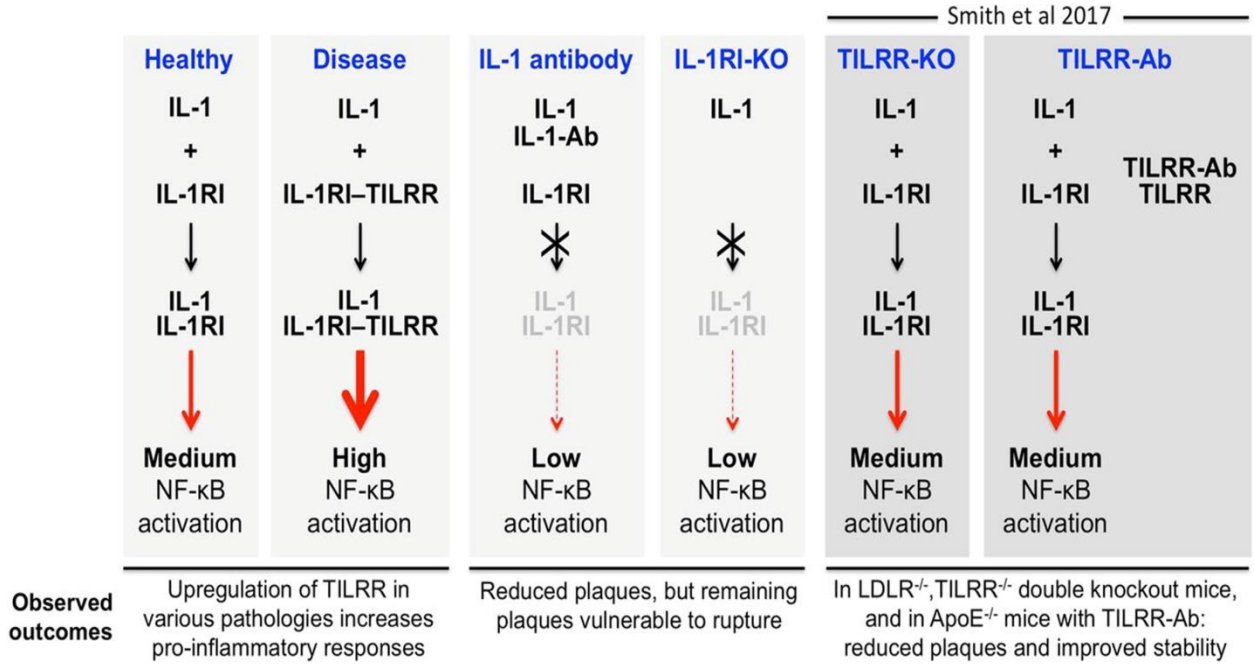

Figure 1.7: Three levels of IL-1R1 signaling. Activation of NF-κB in healthy (medium level), disease (high level) conditions, and in overly aggressive therapy targeting co-receptor TILRR (low level) as demonstrated by Smith et al. [288]. **Darker gray areas** demonstrated the work contributed by Smith et al. [288]. Ab, antibody; ApoE, apolipoprotein E; IL, interleukin; IL-1RI, interleukin 1 receptor type I; KO, knockout; LDLR, low-density lipoprotein receptor; NF, nuclear factor; TILRR, toll-like interleukin-1 receptor regulator. This figure was reprinted with permission from Gabhann [294] under a Creative Commons Attribution-NonCommercial-NoDerivatives 4.0 International License (CC BY-NC-ND 4.0).

1.3.4.2.4 TILRR and production of inflammatory mediators

Because TILRR is involved in IL-1-IL-1R1 signal transduction events [285], it may potentiate the production of soluble pro-inflammatory cytokines/chemokines through modulation of mRNA expression of genes associated with the NF-κB signaling pathway. Studies have shown that activation of cytoplasmic sequestered NF-κB transcription factor together with nuclear translocation of NF-κB is the key step to initiate mRNA and protein expression of genes involved in inflammatory responses [181, 295]. Rhodes *et al.* [292] demonstrated that binding of TILRR with IL-1R1 potentiates the release of NF-κB from its cytoplasmic inhibitory molecules, resulting in NF-κB nuclear translocation, activation, and inflammatory cascade reactions. Using TILRR knockout mice, Smith *et al*. [288] demonstrated that mRNA expression of inflammatory genes encoding MCP-1/CCL2, IL-6 and TNFα was significantly reduced in bone marrow-derived macrophages and splenic samples compared to that of wild type control. A recent study also showed that overexpression of TILRR in BT474, a human breast tumor cell line, significantly potentiates the expression of immune and inflammation-associated genes, including IL-6, IL-8/CXCL8, IP-10/CXCL10, MCP-1/CCL2, and RANTES/CCL5 [286]. Using human breast tumor tissues, Xu et al. [286] further demonstrated that elevated expression of TILRR is positively correlated with mRNA expression of IP-10/CXCL10. However, these studies did not measure the protein level expression of these genes.

Although we know little about the effect of TILRR on the pro-inflammatory cytokines/chemokines production, the existing data suggested that TILRR may play a crucial role in the production of soluble mediators from genital epithelial cells, and may be a risk factor for vaginal HIV acquisition due to its role in enhancing inflammation. This can be investigated

by using an appropriate *in vitro* model to mimic the vaginal microenvironment and HIV acquisition.

1.3.4.2.5 TILRR and migration of immune cells

Activation of IL-1-IL-1R1-TILRR-NF-κB signaling complex potentiates mRNA expression of inflammatory genes in epithelial cells [285, 288]. Production of cytokines/chemokines by epithelial cells initiates the cognate receptor-mediated signal that attracts immune cells into the tissues. Monocyte chemotactic protein (MCP)-1 or CCL2 produced from epithelial cells promotes infiltration of various immune cells (monocytes/macrophages, T-lymphocytes, and NK-cells) through the CCR2 receptor expression on target cells [296]. Thus, it is possible that the TILRR-induced production of inflammatory mediators by genital epithelial cells would promote the migration of immune cells. Although currently there is no report on the role of TILRR in promoting immune cell migration in cervicovaginal tissues, a recent study showed that TILRR influenced the infiltration of monocytes under pathological conditions [288]. Recently, a study showed that higher expression of TILRR in breast/mammary epithelial tissues is significantly positively correlated with immune cell infiltration, mostly CD4+ and CD8+ T cells, and to a lesser extent of B cells, macrophages, dendritic cells, and neutrophils [286]. Because TILRR augments the NF-κB signaling pathway via the IL-1-IL-1R1 receptor complex [285, 293], TILRR may well play an important role in the migration of immune cells that is relevant to vaginal HIV acquisition through attracting immune cells to the site of inflammation.

1.4 GAPS IN KNOWLEDGE AND STUDY RATIONALE

Among thousands of components of the host immune system, the NF-κB transcription factor has been identified as one of the central regulators of innate and adaptive immune responses and involved in regulating the expression of many pro-inflammatory genes [181, 297]. NF-κB coordinates the production of pro-inflammatory cytokines/chemokines and the rapid influx of immune cells into the injured tissues, resulting in profound inflammatory responses and inflammation [295, 298]. Activation of NF-κB is critical for viral infection [299]. It has been shown that the IL-1-NF-κB signaling pathway functions as an enhancer of HIV acquisition/susceptibility via recruitment and/or activation of HIV target cells [209]. Because NF-κB activation is potentiated by the association of TILRR with IL-1R1 [285, 294] and TILRR-mediated NF-κB activation instigates the inflammatory responses [285, 292, 294], it is important to know the effects of TILRR in modulating inflammatory reactions during microbial infection, including vaginal HIV acquisition. To date, very little is known whether TILRR interacts with or regulates other genes in the NF-κB inflammatory signaling pathway, and influences the production of soluble inflammatory mediators by genital epithelial cells, and migration of immune cells, including HIV target cells, into cervicovaginal tissues.

Since cervicovaginal epithelial cells express TILRR, the presence of TILRR in female genital epithelial cells may augment the inflammatory responses via NF-κB activation and the production of inflammatory mediators. It is also important to know whether TILRR circulates in human blood plasma and involves in regulating plasma cytokines/chemokines and systemic inflammatory responses, and plays a role in increasing susceptibility to HIV infection. Our group has previously shown that the minor allele of FREM1 SNP rs1552896 is associated with HIV resistant phenotype [260], and TILRR mRNA is less likely detected in the women with the minor

allele of rs1552896. Thus, understanding the role of TILRR in mucosal and systemic immune activation and inflammation is important. These motivate me to investigate the role of TILRR in inflammation-mediated vaginal HIV acquisition. As immune activation fuels inflammation and pro-inflammatory mediators promote infiltration of immune cells, identifying the root cause may help to control vaginal HIV infection in the future.

1.5 GLOBAL HYPOTHESIS

I hypothesized that **FREM1 transcript variant 2, TILRR, regulates genes involved in immune activation, inflammatory responses, and target cell recruitment, and plays a role in the susceptibility of vaginal HIV acquisition.**

1.6 SUB-HYPOTHESES

I further divided the global hypothesis into four sub-hypotheses that will be tested with relevant specific objectives.

- **A.** TILRR increases mRNA expression of genes in the NF-κB signal transduction pathway and inflammatory responses.
- **B.** TILRR induces the production of pro-inflammatory cytokines/chemokines in cervicovaginal epithelial cell lines.
- **C.** TILRR promotes the migration of immune cells through the modulation of soluble cytokines/chemokines production from epithelial cells.
- **D.** TILRR protein circulates in the blood and its level is associated with susceptibility to HIV acquisition.

1.7 OVERALL AND SPECIFIC OBJECTIVES

A. Determination of the effect of overexpression of TILRR on the expression of genes involved in inflammatory responses and inflammation.

Specific objectives

a. To overexpress TILRR in human cervical epithelial (HeLa) and vaginal mucosal epithelial (VK2/E6E7) cell lines.

b. To determine the effect of TILRR overexpression on mRNA expression of genes in the NF-κB signal transduction and inflammatory response pathways.

B. Evaluation of the effect of TILRR on the production of pro-inflammatory cytokines/chemokines in cervicovaginal epithelial cells.

Specific objectives

Quantification of pro-inflammatory cytokines/chemokines in supernatants of HeLa and VK2/E6E7 cells.

C. Assessment of the effect of TILRR on the migration of immune cells (HIV target cells).

Specific objectives

a. To test the effect of TILRR on immune cell migration using the Transwell approach.

b. To assess the TILRR effect on immune cell migration using microfluidic real-time migration assay.

D. Determination of the level of TILRR in archived plasma samples of women enrolled in the Pumwani sex worker cohort (PSWC) and its association with susceptibility to HIV acquisition.

Specific objectives

a. To develop a multiplex quantification method using anti-FREM1 monoclonal antibodies and a multiplex bead array system for measuring soluble TILRR in human plasma samples.

b. To confirm the presence of plasma TILRR by affinity purification and Western blot analysis.

c. To validate the in-house developed methods utilized to measure plasma TILRR.

d. To analyze the association of plasma TILRR level with the FREM1 SNP rs1552896 genotypes.

e. To determine the relationship between the plasma TILRR level with the levels of plasma inflammatory cytokines/chemokines, and its association with HIV susceptibility in the Pumwani cohort.

The following review article has been published from the introduction of this thesis:

The potential role of FREM1 and its isoform TILRR in HIV-1 acquisition through mediating inflammation. International Journal of Molecular Sciences, 2021. 22(15): p.7825.

Mohammad Abul Kashem[1,2], Hongzhao Li[1,3], Lewis Ruxi Liu[1,2], Binhua Liang[2,3,4], Robert Were Omange[5], Francis A. Plummer[1††], Ma Luo[1,2,3*]

Authors' affiliation(s):
[1]Department of Medical Microbiology and Infectious Diseases, University of Manitoba, Winnipeg, MB, Canada.
[2]JC Wilt Infectious Diseases Research Centre, Winnipeg, MB, Canada.
[3]National Microbiology Laboratory, Public Health Agency of Canada, Winnipeg, MB, Canada.
[4]Department of Biochemistry & Medical Genetics, University of Manitoba, Winnipeg, MB, Canada.
[5]Vaccine and Gene Therapy Institute, Oregon Health and Science University, Portland, Oregon, United States.

AUTHORS' CONTRIBUTIONS
MAK and ML conceived and designed the review; **MAK** performed the literature search and wrote the manuscript; HL, LL, BL, RWO, and ML reviewed the manuscript; **MAK** revised, formatted, and submitted to the journal. All authors have approved this article.

FUNDING
The study was funded by an operating grant from the Canadian Institutes of Health Research (CIHR), operating grant- PA: CHVI Vaccine Discovery and Social Research (http://www.cihr-irsc.gc.ca/e/193.html).

2 CHAPTER 2: MATERIALS AND METHODS

A complete list of general materials/reagents used in this thesis research is mentioned in chapter 7 (**Appendix A).**

2.1 METHODS SPECIFIC TO RESULTS SECTION 3.1

2.1.1 Study outline

The studies were conducted using two human epithelial cell lines, HeLa and VK2/E6E7. TILRR-plasmid DNA was used to transfect cells using a lipid-based transfection reagent. Transfected cells were selected by puromycin dihydrochloride, and incubated with serum-free medium with or without IL-1β for different time points. TILRR overexpression was confirmed by confocal microscopy, flow cytometry, Western blotting, and real-time RT-qPCR analyses. RNA was harvested and purified. RNA quality and quantity were measured by Agilent BioAnalyzer and NanoDrop 1000 spectrophotometer, respectively. Complementary DNA (cDNA) synthesized from purified RNA was utilized to analyze the mRNA expression of 84 genes using NF-κB signaling pathway PCR array and RT-qPCR primer assay. The overall workflow undertaken in this section of the study is presented in **Figure 2.1**.

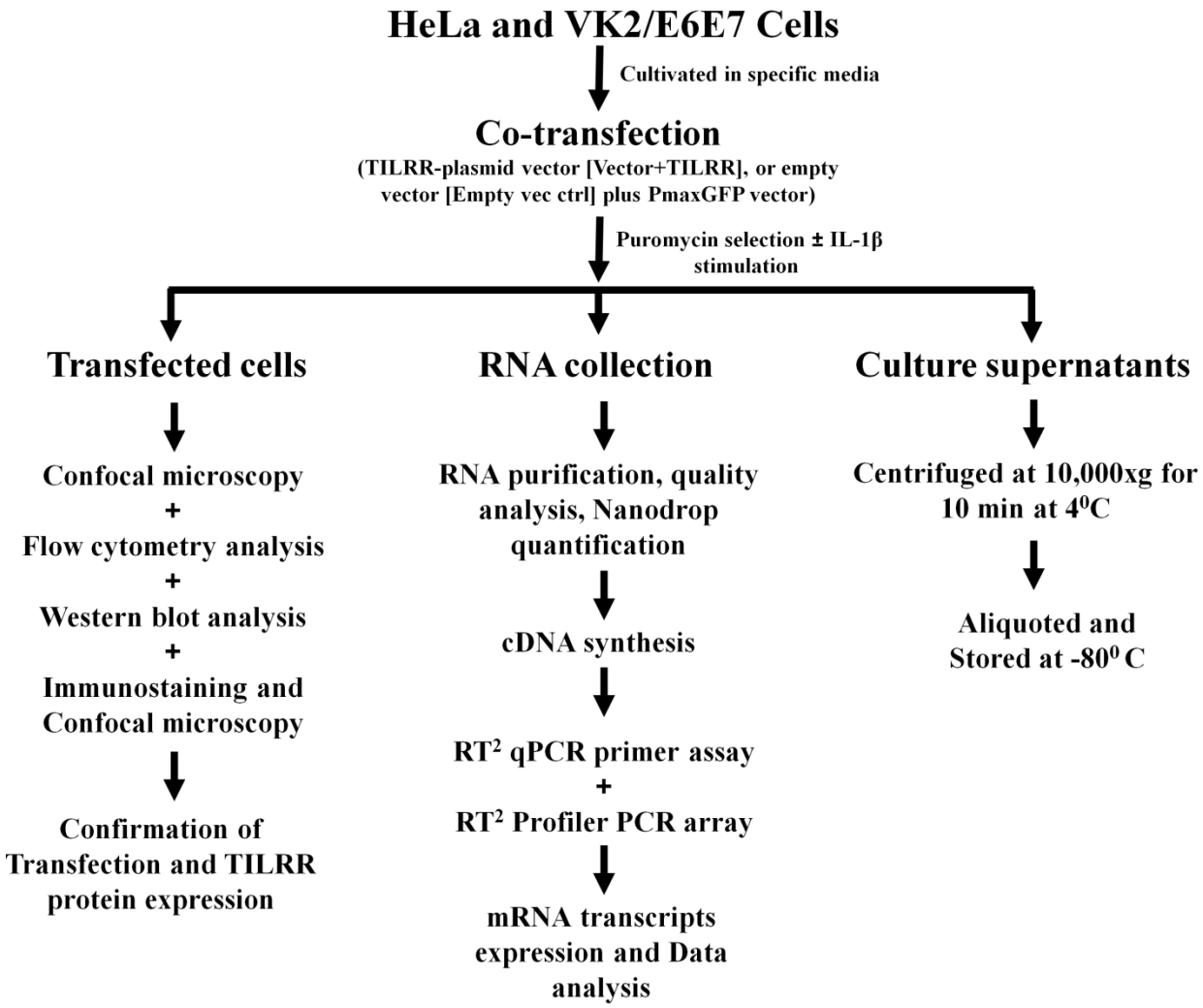

Figure 2.1: Schematic diagram of the overall workflow conducted for testing sub-hypothesis I.

2.1.2 Cell lines and culture condition

Our group previously showed that FREM1 mRNA is highly expressed in human cervical cells [260]. To study the effect of FREM1 variant TILRR expression on cervical cells, I used two model cervical epithelium cell lines, HeLa and VK2/E6E7. RNA-seq analysis and RT-qPCR analysis showed that these two cell lines do not express TILRR mRNA under the cell culture conditions I used in the study. Thus, I can use them to overexpress TILRR to study the effect on other inflammatory response-related genes.

HeLa cells were maintained in Dulbecco's Modified Eagle's Medium (DMEM) supplemented with 10% FBS (fetal bovine serum) and 1% Antibiotic-Antimycotic. VK2/E6E7 cells were maintained in Keratinocyte-SFM (1X) growth medium, supplemented with human recombinant EGF (Epidermal Growth factor, 0.1 ng/ml), and BPE (Bovine Pituitary Extracts, 50 µg/ml), 0.4 mM $CaCl_2$ and 1% Penicillin-Streptomycin solution. Adherent cells in culture were detached from the T175 flask with 0.25% Trypsin-EDTA, and the enzyme was deactivated with sufficient volume of complete DMEM growth medium for HeLa, and DMEM Nutrient mixture F-12 Ham supplemented with 10% FBS plus 1% Penicillin-Streptomycin solution for VK2/E6E7 based on the recommended protocols (ATCC). All the cells were then incubated at 37^0 C with 5% CO_2 for 2-3 days until 90-100% confluent.

2.1.3 Plasmid constructs

Both TILRR-plasmid (GeneCopoeia, Catalog# EX-I2135-68) and Empty vector-plasmid control (GeneCopoeia, Catalog# EX-NEG-68) containing a CMV promoter, an ampicillin marker, and a puromycin marker, were used for transfecting cells **(Figure 2.2).** PmaxGFP (Lonza, Walkersville, MD, USA) was used as a standard enhanced GFP (Green fluorescence protein)

control vector to monitor the transfection efficiency by Flow Cytometry and Confocal Microscopy.

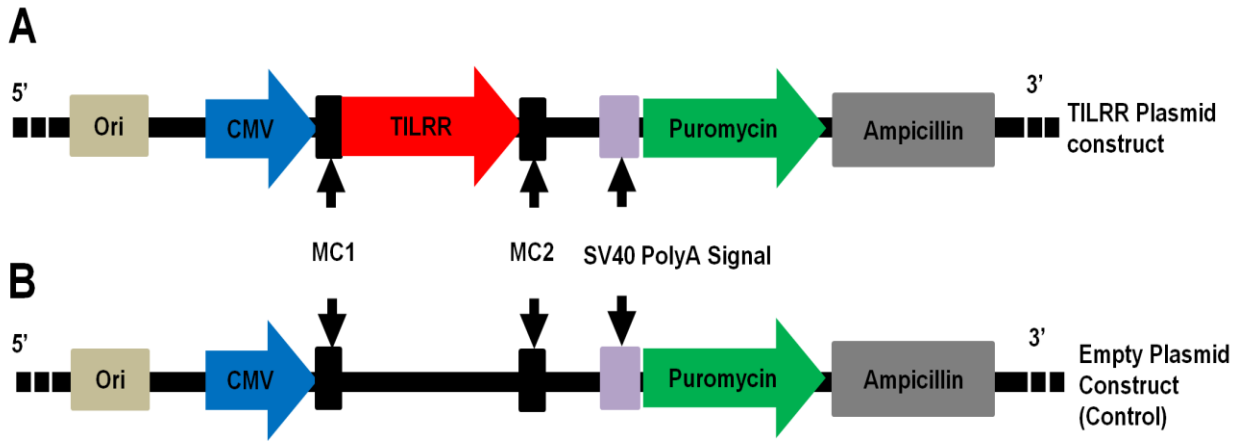

Figure 2.2: Diagram of plasmid constructs. A) TILRR (2148bp) inserted pEZ-M68 vector containing Ori, CMV promoter, puromycin selection marker (mammalian selection), and ampicillin selection marker (bacterial selection) (top); **B)** Empty control pEZ-M68 vector containing Ori, CMV promoter, puromycin marker, and ampicillin marker (bottom). The arrowhead of the TILRR insert and puromycin-resistant marker denotes the direction of gene transcription (5' to 3'). Puromycin marker was used to select plasmid-transfected HeLa and VK2/E6E7 cells following 24h transfection with EndofectinMax transfection reagent. Ampicillin marker was used to select plasmid-transformed *Escherichia coli* bacteria on selective Luria-Bertani (LB) agar plate and LB broth containing ampicillin during the production and purification of plasmids. Ori, origin of replication; CMV, Cytomegalovirus; MC, multiple cloning; and SV40, simian virus 40. This figure was adapted from GeneCopoeia, Inc., Rockville, MD (https://www.genecopoeia.com/wp-content/uploads/oldpdfs/tech/omicslink/pReceiver-M68.pdf).

2.1.4 Plasmid DNA purification

TILRR-plasmid DNA or empty-vector plasmid DNA was purified using an Endofree plasmid Maxi kit according to the supplier's instructions. Briefly, the bacterial stock was plated on the selective Luria-Bertani (LB) agar plate containing ampicillin and then inoculated into LB broth. The bacteria were harvested by spinning at 6000xg for 15 min at 4^0C. The pellet was resuspended in 10 ml Buffer P1 containing RNase A and then mixed with 10 ml Buffer P2 followed by incubation at Room temperature (RT) for 5 min. Ten milliliters of Buffer P3 was added to the lysate and mixed immediately. The lysate was poured into the QIAfilter Cartridge, incubated at RT for 10 min, and filtered into a 50 ml BD Falcon tube. Buffer ER (2.5 ml) was added to the lysate and incubated on ice for 30 min. The lysate was then poured into the QIAGEN-tip, washed 2X with 30 ml Buffer QC, and the plasmid DNA was eluted with 15 ml Buffer QN. Eluted DNA was precipitated by adding 10.5 ml RT 100% isopropanol, and centrifuged immediately at ≥15000x g for 30 min at 4^0C. The pellet was washed with endotoxin-free RT 70% ethanol and centrifuged immediately at ≥15000 x g for 10 min at 4^0C. Finally, the pellet (plasmid DNA) was air-dried for 5-10 min and redissolved into 1 ml endotoxin-free Buffer TE. The purified DNA was quantified by NanoDrop 1000, aliquotted into the Eppendorf tube, and immediately stored at -80^0C for downstream transfection of cells.

2.1.5 Transfection of cells

Approximately $2.5x10^5$ cells per ml were plated into each well of a 12-well culture plate in complete DMEM growth medium (HeLa) or complete Keratinocyte-SFM (1X) (VK2/E6E7) a day before transfection and incubated at 37^0 C with 5% CO_2 for 24 h. Once the cells reached 80-90% confluency, the media was replaced with antibiotic-free fresh growth media. Co-transfection was performed using different concentration of either TILRR-plasmid

(vector+TILRR) (0.25 µg, 0.5 µg, 1.0 µg, and 2.0 µg per well) or empty vector-plasmid (empty vector control) (0.25 µg, 0.5 µg, 1.0 µg, and 2.0 µg per well) in combination with PmaxGFP-plasmid DNA (0.05 µg, 0.1 µg, 0.2 µg or 0.4 µg per well respectively; 1:5 ratio) with 2 µl of EndofectinMax transfection reagent following to the protocol recommended by the manufacturer. After incubation at 37^0 C with 5% CO_2 for 24h, the effect of TILRR overexpression on the mRNA expression of 4 genes was analyzed. The optimized concentration of TILRR-plasmid (1.0 µg/well) or empty vector (1.0 µg/well) in combination with PmaxGFP vector (0.2 µg/well; 1:5 ratio) was used to transfect HeLa and VK2/E6E7 cells with 2 µl of EndofectinMax transfection reagent to analyze the effect of overexpression of TILRR on mRNA expression of NF-κB signal transduction pathway-related genes and pro-inflammatory cytokines/chemokines.

2.1.6 RNA extraction, purification, and quantification

RNA was extracted from cells under different experimental conditions using RLT buffer from RNeasy Mini Kit. Extracted and purified RNA from $5x10^5$ cells/experimental condition using RNAeasy Mini Kit according to the manufacturer's instructions. The purified RNA was quantified using a NanoDrop 1000 Spectrophotometer (Thermofisher Scientific, USA), and the *A260:A230* ratio of the isolated RNA was >1.7 and their *A260:A280 ratio* was between 1.8 and 2.0.

2.1.7 RNA quality analysis

RNA quality was also assessed with 2100 Agilent$^{(R)}$ Bio-analyzer (Agilent Technologies, USA) using an RNA 6000 Nano LabChip$^{(R)}$ kit, and verified the quality with sharp bands/peaks for both the 18S and 28S ribosomal RNAs. The RIN was maintained at ≥7.0 for each sample.

2.1.8 RNA Clean up

When the *A260:A230* ratio of the purified RNA was <1.7 and the *A260:A280* ratio was <1.8 in NanoDrop 1000 Spectrophotometer analysis, the RNA samples were further cleaned to achieve standard ratio (*A260:A230* ratio >1.7 and *A260:A280* ratio between 1.8 and 2.0). RNeasy MinElute cleanup kit was used according to the manufacturer's recommended protocol. In brief, the RNA was adjusted to 100 µl volume with RNase-free water, and 350 µl buffer RLT was added. Next, 250 µl of 96-100% ethanol was added and mixed well. The diluted sample was transferred to an RNeasy MinElute Spin column and centrifuged at 8000xg for 15sec. The column was transferred to a new 2 ml collection tube, added 500 µl Buffer RPE, and centrifuged at 8000xg for 15sec. Following buffer RPE wash, 500 µl of 80% ethanol was added and centrifuged at 8000xg for 2 min. The column was again placed in a new 2 ml collection tube and centrifuged at 14000xg for 5 min with an open lid. Next, the column was placed in a new 1.5 ml collection tube, and 14 µl of RNase-free water was directly added to the center of the column membrane and centrifuged at 14000xg for 1 min. The eluted RNA was quantified by NanoDrop 1000 Spectrophotometer. All steps of the RNA cleaning process were performed at 15-25^0 C.

2.1.9 cDNA synthesis

The cDNA was synthesized using an RT^2 first strand kit with 500 ng purified RNA per reaction as recommended by the manufacturer's protocol.

2.1.10 RT^2 qPCR Primer Assay

Real-time quantification of TILRR overexpression was done using a commercial RT^2 qPCR primer assay and RT^2 SYBR$^{(R)}$ Green ROX qPCR Mastermix. RT^2 qPCR primer assay was also performed for some selective immune responsive genes, CCL5, CXCL8, IL-6, and TNFα to

measure the mRNA transcript expression with similar Mastermix as mentioned above. All primers were purchased from Qiagen.

2.1.11 RT^2 Profiler PCR array

NF-κB signaling pathway expression was quantified using RT^2 profiler qPCR array (Qiagen, Catalog# PAHS-025Z) and similar Mastermix as mentioned above. The list of genes included in the NF-κB signaling pathway PCR array is shown in **Appendix Table C7.1.**

2.1.12 Amplification conditions for RT-qPCR

One microliter of cDNA was used in a 25µl reaction volume. Amplification of cDNA was performed in 40 cycles, consisting of an initial 1 cycle at 95^0 C for 10 min followed by 40 cycles, each cycle run at 95^0 C for 15 sec followed by 60^0 C for 1 min. After 40 cycles, a dissociation cycle was also performed for all 84 genes and the threshold was manually corrected at 0.4. Data were exported and finally organized in Microsoft Office Excel sheet and analyzed by GeneGlobe Data Analysis Centre (Qiagen). Applied BioSystem 7900 HT Fast Real-time PCR 96-well standard block (ThemoFisher Scientific, USA) was used for all RT-qPCR analysis.

2.1.13 Confocal microscopy

Transfected cells expressing eGFP and TILRR protein were visualized using a confocal microscopy imaging system (Zeiss LSM 700, Laser Scanning Microscope). For visualization of overexpressed TILRR protein in transfected cells, the TILRR-plasmid (vector+TILRR) transfected cells (after puromycin selection) and parental control (non-transfected) cells were plated in Glass bottom 6-well plate (MatTek Corporation, Cat# P06G-1.5-20-F) for 24h. The cells were washed once with 1X PBS, then fixed with 4% paraformaldehyde (pH 7.4) for 10 min at 37^o C. The fixed cells were washed 3 times with 1X PBS and permeabilized with 0.1%

TritonX-100 for 10 min at room temperature (RT). After further washes (3 times with 1X PBS), the cells were blocked with 3% BSA containing 0.1% TritonX-100 in 1X PBS at RT for 1h. Following blocking, the cells were incubated at RT for 3h with a mixture of two in-house developed mouse monoclonal antibodies (mAbs) targeting epitopes of TILRR (F218G1 and F218G5) (2µg/ml, diluted in 1X PBS containing 0.1% BSA and 0.1% TritonX-100) [241]. An isotype control experiment with a mAb (2µg/ml) (F400G3S) specific for a *Chlamydia trachomatis* antigen was conducted in parallel. After washing (three times with PBS-T blocking buffer containing 0.05% TritonX-100+1.5% BSA), the cells were stained with Alexa Fluor 647-labeled goat anti-mouse IgG secondary antibody (Invitrogen, Catalog# A-21235) (2µg/ml, diluted in 1X PBS containing 0.1% BSA and 0.1% TritonX-100) for 45 min at room temperature. As a negative control, cells were also incubated with only Alexa Fluor 647-labeled goat anti-mouse IgG secondary antibody (2µg/ml) without primary mAbs cocktail. Following washes (3 times with PBS-T), the cells were incubated for 5 min with counterstain for nucleus, DAPI (300nM) (Invitrogen, Catalog# D1306). After staining, the cells were kept in 1 ml of 1X PBS and sealed with Parafilm M (Sigma Aldrich, Catalog# P7793-1EA) and examined with a Confocal microscopy imaging system using three color channels for DAPI, FITC, and Alexa Fluor 647.

2.1.14 Flow Cytometry

The overexpression of TILRR protein in transfected HeLa and parental cells was also quantified by FACS analysis (BD Accuri C6, BD Biosciences). The cells were stained according to the BD Biosciences (California, USA) protocol. Briefly, $5x10^5$ HeLa cells from each of the experimental conditions were prepared and washed with 1X PBS containing 2% FBS (fetal bovine serum), then incubated with 50 µl Alexa Fluor 647 labeled in-house developed mAbs (F218G1 and

F218G5) (2µg/ml, diluted in 1X PBS containing 3% BSA) for 30 min at 4^{o} C in dark (APEX Antibody Labeling kit, Invitrogen, Catalog# A10475). After washing (PBS containing 2% FBS), 100 µl BD permeabilizing solution (BD Biosciences, Catalog# 554714) was added. After 10 minutes of permeabilization, the cells were washed twice with 1X Perm/Wash buffer, and then 50 µl of Alexa Fluor 647 labeled mAbs cocktail (F218G1 and F218G5) (2µg/ml, diluted in 1X Perm/Wash buffer) was further added and incubated for 30 min at 4^{o} C in dark. Finally, the cells were resuspended in PBS containing 2% FBS after two times washes with 1X Perm/Wash buffer and analyzed with BD Accuri C6 after. In parallel, the cells were also stained with isotype control mAb (F400G3S) (2µg/ml) labeled with Alexa Fluor 647. FlowJo software (Treestar, USA) was used for analysis. Cell viability by FACS was measured using Live/Dead Fixable Red Dead Cell Stain (Life Technologies, Catalog# L34971) following the company's recommended protocol.

2.1.15 Western blot analysis

2.1.15.1 Gel preparation

NuPAGE Bis-Tris 4-12% 1.0 mm x 10 well gel cassette was taken from the pouch and rinsed with deionized water. Gently peeled off the tape from the bottom of the cassette and pulled the comb with one smooth motion. The sample wells were rinsed with 1X NuPAGE MES Running buffer, inverted to remove, and repeated the rinsing steps twice. The cassette was then placed in the Mini-Cell gel tank with cassette face inwards toward the Buffer Core and securely locked with Gel Tension Wedge. Next, the upper/inner buffer chamber was filled with a small volume of 1X MES Running buffer containing antioxidants to check the tightness of the seal and gradually filled up with the rest of the volume up to the maximum level. An appropriate volume

of samples and protein molecular weight marker was loaded into the wells and the lower/outer buffer chamber was filled with 600 ml 1X MES Running buffer.

2.1.15.2 Western blot Protocol

A previously published method was used with slight modifications [300]. Briefly, SDS-PAGE was conducted using NuPAGE Bis-Tris mini gel electrophoresis. Approximately 1×10^6 cells were lysed with 50 µl RIPA lysis and extraction buffer, then passed through a QIAshredder column (Qiagen, Catalog# 79654) by centrifugation at 15,000 g for 2 min. The lysate was then prepared and loaded into a NuPAGE 4-12% Bis-Tris 1.0 mm×10well gel (Thermo Fisher Scientific). Several monoclonal antibodies were used to detect the TILRR protein including F218, F208, F217, F244, F220, and F237 previously developed in our lab [241]. The monoclonal antibodies were diluted in antibody buffer (wash buffer containing 0.5% skimmed milk) to give a concentration of 1 µg/ml for each antibody and then incubated overnight with membranes at 4°C with shaking. Then, the secondary antibody, goat anti-mouse IgG-HRP (Santa Cruz Biotechnology, Catalog# sc-2005) was diluted at 1:5,000 in antibody buffer and incubated with the membrane for 1 h at RT with shaking. Chemiluminescent detection was performed on a ChemiDoc XRS instrument using Quantity One 4.6.9 software (Bio-Rad). The level of TILRR protein expression was defined as the ratio of the band intensity of TILRR to that of GAPDH and finally normalized to parental cells.

2.1.16 Venn diagram and Heat Map generation

Venn diagram was made by using pyvenn (https://github.com/tctianchi/pyvenn). Heat Map was created using RStudio (https://www.rstudio.com/).

2.2 METHODS SPECIFIC TO RESULTS SECTION 3.2

2.2.1 Study outline

This section of the study was to evaluate cytokines/chemokines in culture supernatants from TILRR-overexpressed cervicovaginal epithelial cells (HeLa and VK2/E6E7). An in-house developed 13-plex Bio-Plex assay method was used for the cytokines/chemokines analysis. An overview of the workflow is shown in **Figure 2.3.**

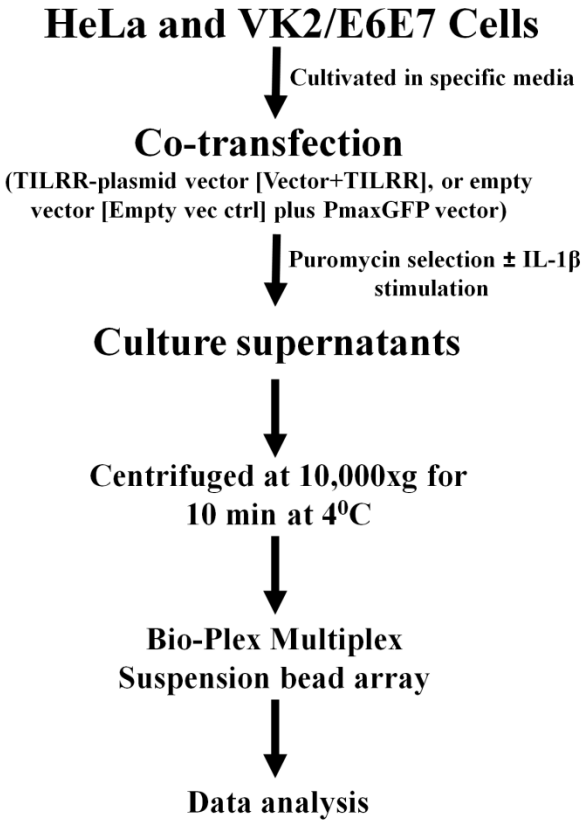

Figure 2.3: Schematic diagram of the workflow for cytokines/chemokines analysis relating to sub-hypothesis II.

2.2.2 Panel of Analytes

A panel of 13 cytokines/chemokines was selected based on their importance and functional involvement in innate immune responses, inflammation, and inflammatory disease progression, especially HIV infection and transmission. These include granulocyte-macrophage colony-stimulating factor (GM-CSF), interferon-gamma (IFNγ), interleukin (IL)-1β, IL-6, IL-8 (CXCL8), IL-10, IL-17A, IFN-γ inducible protein (IP)-10, macrophage chemoattractant protein (MCP)-1, monocyte inflammatory protein (MIP)-1α, MIP-1β, regulated on activation, normal T cell expressed and secreted (RANTES), and tumor necrosis factor (TNF)-α. All uncoupled primary antibodies and biotinylated secondary antibodies were purchased from different suppliers as listed in **Table 2.1.**

Table 2.1: List of primary and secondary antibodies used in Bioplex Multiplex cytokines/chemokines bead assay

Primary antibody			
SL	**Name**	**Catalog#**	**Vendor**
1	Human CXCL8/IL-8 MAb	M801	ThermoFisher Scientific
2	Human CCL5/RANTES PAb	P230E	ThermoFisher Scientific
3	Rat Anti-Human GM-CSF-UNLB	10111-01	SouthernBiotech
4	Human IFNγ MAb	M700A	ThermoFisher Scientific
5	Human IL-1beta/ IL-1F2 Antibody	MAB601-500	R&D System
6	Human IL-6 MAb	M620	ThermoFisher Scientific
7	Rat Anti-Human IL-10-UNLB	10100-01	SouthernBiotech
8	Human/Primate IL-17/IL-17A Antibody	MAB317-500	R&D System
9	Human IP-10/ CXCL10/CRG-2 Antibody	MAB266-500	R&D System
10	Human MCP-1/CCL2/JE Antibody	MAB679-500	R&D System
11	Human MIP-1α/CCL3Antibody	AF-270-NA	R&D System
12	Human MIP-1β/CCL4 Antibody	MAB271-100	R&D System
13	Human TNFα MAb	M303	ThermoFisher Scientific
Secondary antibody (Biotinylated)			
SL	**Name**	**Catalog#**	**Vendor**
1	Human CXCL8/IL-8 MAb, Biotin-labeled	M802B	ThermoFisher Scientific
2	Human CCL5/RANTES MAb, Biotin-labeled	M230B	ThermoFisher Scientific
3	Rat Anti-Human GM-CSF-BIOT	10112-08	SouthernBiotech
4	Human IFNγ MAb, Biotin-labeled	M701B	ThermoFisher Scientific
5	Human IL-1beta/IL-1F2 Biotinylated Antibody	BAF201	R&D System
6	Human IL-6 MAb, Biotin-labeled	M621B	ThermoFisher Scientific
7	Rat Anti-Human IL-10-BIOT	10110-08	SouthernBiotech
8	Human/Primate IL-17/IL-17A Biotinylated Antibody	BAF317	R&D System
9	Human IP-10/CXCL10/CRG-2 Biotinylated Antibody	BAF266	R&D System
10	Human MCP-1/CCL2/JE Biotinylated Antibody	BAF279	R&D System
11	Human MIP-1α/CCL3 Biotinylated Antibody	BAF270	R&D System
12	Human MIP-1β/CCL4 Biotinylated Antibody	BAF271	R&D System
13	Human TNFα MAb, Biotin-labeled	M302B	ThermoFisher Scientific

2.2.3 Coupling of primary antibodies to magnetic beads

The primary antibodies to different cytokines/chemokines were coupled to the selected beads using an amine coupling kit according to the manufacturer's instructions. Magnetic COOH beads with different fluorescent spectrum (26, 28, 29, 34, 37, 43, 46, 52, 53, 55, 62, 64, 65) were used to couple TNFα, IL-6, IL-10, IL-8, MIP-1β, MIP-1α, RANTES, IL-1β, IP-10, IFNγ, GM-CSF, IL-17A and MCP-1 antibodies, respectively. Briefly, 100 µl of $1.25x10^6$ monodisperse COOH beads with a unique region was coupled to the primary antibody in a single coupling reaction. Four separate coupling reactions were performed for each antibody. Stock beads were vortexed for 30 sec, and 100 µl of bead was transferred to a coupling reaction tube (supplied). After 1X wash with washing buffer, beads were resuspended in 80 µl of bead activation buffer and vortexed for 30 sec. Ten microliters of 50 mg/ml Sulfo-NHS and 10 µl of 50 mg/ml EDAC were added to the beads containing activation buffer and incubated for 20 min at RT on a rotor. The beads were washed 1X with PBS pH 7.4 and added to each diluted antibody (20µg). Beads-antibody mixture was incubated for 2 h at RT on a rotor. After incubation, non-specific binding sites were blocked by using 250 µl blocking buffer for 30 min at RT on a rotor. Using a magnetic separator, supernatants were discarded, and then 500 µl of storage buffer was added and vortexed for 20 sec. Storage buffer was carefully removed, and 150 µl of fresh storage buffer was again added as a final bead volume. All four separate reactions of each antibody were combined in a single tube and the concentration of coupled beads was estimated using a hemocytometer as previously described [301, 302]. Coupled beads were stored at 4^0 C for downstream application. The principle of the coupling reaction is schematically presented in **Figure 2.4.**

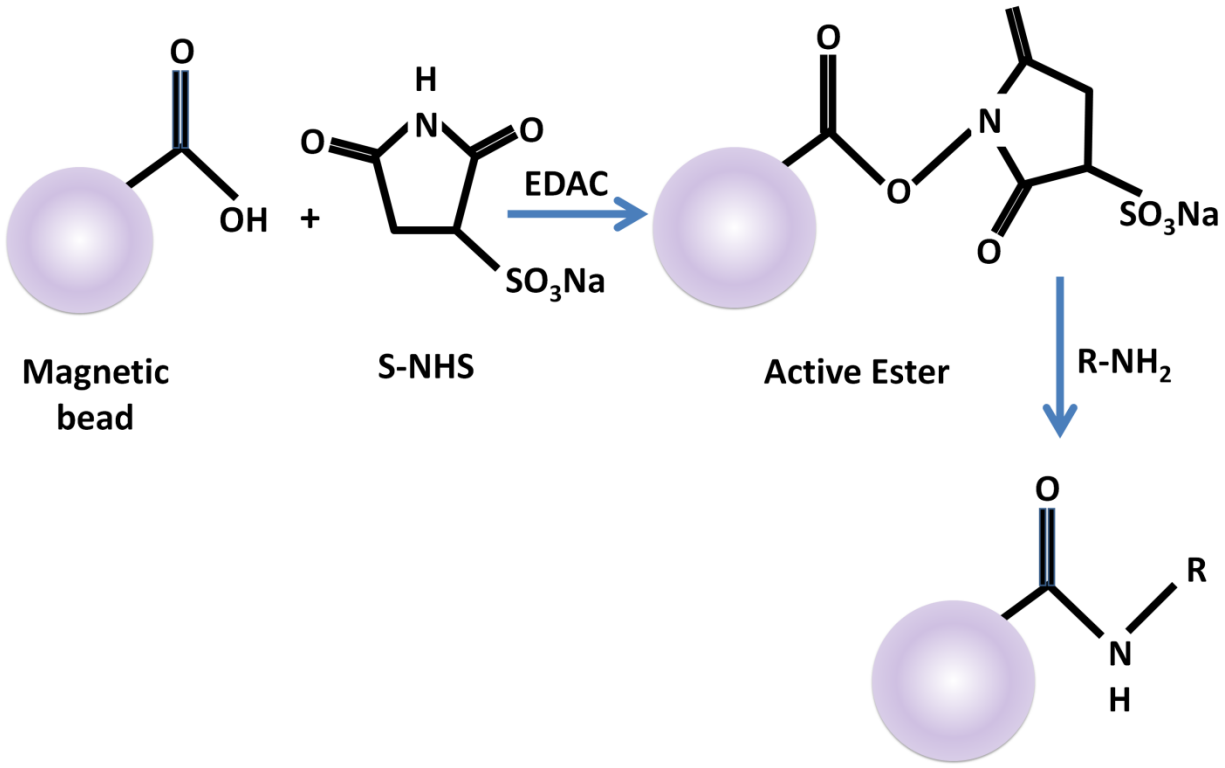

Figure 2.4: Principle of the magnetic bead coupling reaction. The coupling of antibodies to the beads was achieved by two different steps of Carbodiimide reactions. The reaction occurred between carboxyl functional groups on the bead surface and the primary amine groups on the protein. Following activation of beads with EDAC (1-ethyl-3-[3-dimethylaminopropyl] carbodiimide hydrochloride) and S-NHS (N-hydroxysulfosuccinimide), an active O-acylisourea ester was formed which then covalently bind with amines of proteins/antibody (This figure was adapted from Bio-Rad).

2.2.4 Optimization of coupled beads

The 13-plex cytokines/chemokines panel was optimized to ensure the optimal measurement of proteins from culture supernatants. Each antibody coupled bead stock (~$5x10^6$/ml) was diluted into multiple working concentrations, such as 1:100, 1:200, 1:400, 1:800, 1:1000, 1:2000, 1:4000 and 1:10000 dilutions with assay buffer (Bio-Plex Pro^{TM} reagent kit, BioRad). Bio-Plex Pro Human Cytokine Standards Group I 27-plex (BioRad, Catalog# 171D50001) was used to optimize the beads. The assay was conducted according to the Bio-Rad recommended protocol. Results of the assay were checked for parameters required to maintain the optimal assay condition, including the number of bead count (≥50 for each bead region), %CV (coefficient of variation) (≤15%), and bead recovery range (70-130%). The optimized bead concentration was used to measure cytokines/chemokines from cell culture supernatants.

2.2.5 Collection of conditioned media for cytokines/chemokines assay

The HeLa and VK2/E6E7 cells were transfected with TILRR-plasmid or empty vector-plasmid control as described in **section 2.1.5.** Twenty-four hours after transfection, the cells were treated with puromycin dihydrochloride (Gibco, Catalog# A11138-03) for 24 hours to remove non-transfected cells. The cells were then incubated in serum-free DMEM (HeLa) or Keratinocyte SFM (1X) (VK2/E6E7). In parallel experiments, the cells were incubated with human interleukin-1β (IL-1β; 1nM) (Sigma-Aldrich, Catalog# I9401) in serum-free HeLa and VK2/E6E7 cells medium. The cell culture medium was collected at 1, 3, 6, 15, and 24 hours for cytokine/chemokine(s) analysis. All culture supernatants were supplemented with 0.5% BSA, mixed gently, and centrifuged at 10,000xg for 10 min at 4^0C. The sample was aliquotted into a protein low binding tube and stored at -80^0C until further analysis.

2.2.6 Culture supernatants preparation for the assay

Cell culture supernatants from the -80^0 C freezer were thawed on ice. All samples were kept on ice until the assay plate was ready to use. The samples were vortexed for 15 sec before being added to the plate. One freeze-thaw cycle was allowed for all culture supernatants to minimize sample degradation.

2.2.7 Bioplex Cytokine/chemokine(s) Multiplexed bead assay

An in-house developed 13-plex cytokine/chemokine assay was used for the analysis of the cell culture supernatants according to the previously described methods with slight modification [300]. Briefly, the antibody-coupled beads were vortexed and combined at 1:600 dilutions in assay buffer (Bio-Plex Pro^{TM} reagent kit, BioRad, Catalog# 171-304070M). 50 µl of combined beads from all the 13 individual cytokine/chemokine was added to the Bio-Plex Pro^{TM} Flat bottom plate (BioRad, Catalog# 171025001) and washed twice with 100 µl Bio-Plex wash buffer (BioRad, Catalog# 171-304070M) at RT. 50 µl of culture supernatants was added to the plate and shaken for 30 sec at 1000 rpm and then incubated for 30 min on a plate shaker (850±50 rpm) at RT. The plate was washed twice and 25 µl of the combined detection antibody (1 µg/ml) was added per well, incubated again for 30 min on a plate shaker. 50 µl streptavidin-PE conjugate (1X) (BioRad, Catalog# 171304501) was added per well after three washes and incubated for 10 min at RT. Finally, the plate was washed three times, added 150 µl of assay buffer into each well, shaken for 10 sec, and then run by Bio-Plex^{TM} 200 System (Luminex xMAP technology) (Bio-Rad, Canada). Complete growth media (HeLa and VK2/E6E7 cell-specific) were used as diluents for Bio-Plex Pro Human Cytokine Standards Group I 27-plex (BioRad, Catalog# 171D50001) and as a background (blank) control. To generate the standard curve, 50 µl of 4-fold standard dilutions was added in 6-wells in duplicates and the correlation coefficient (R^2) was

being calculated in each experiment to see the linearity of the standard curve. Data were generated by Bio-Plex Manager 6.1 software. The principle of the Bio-plex magnetic suspension array system is depicted in **Figure 2.5.**

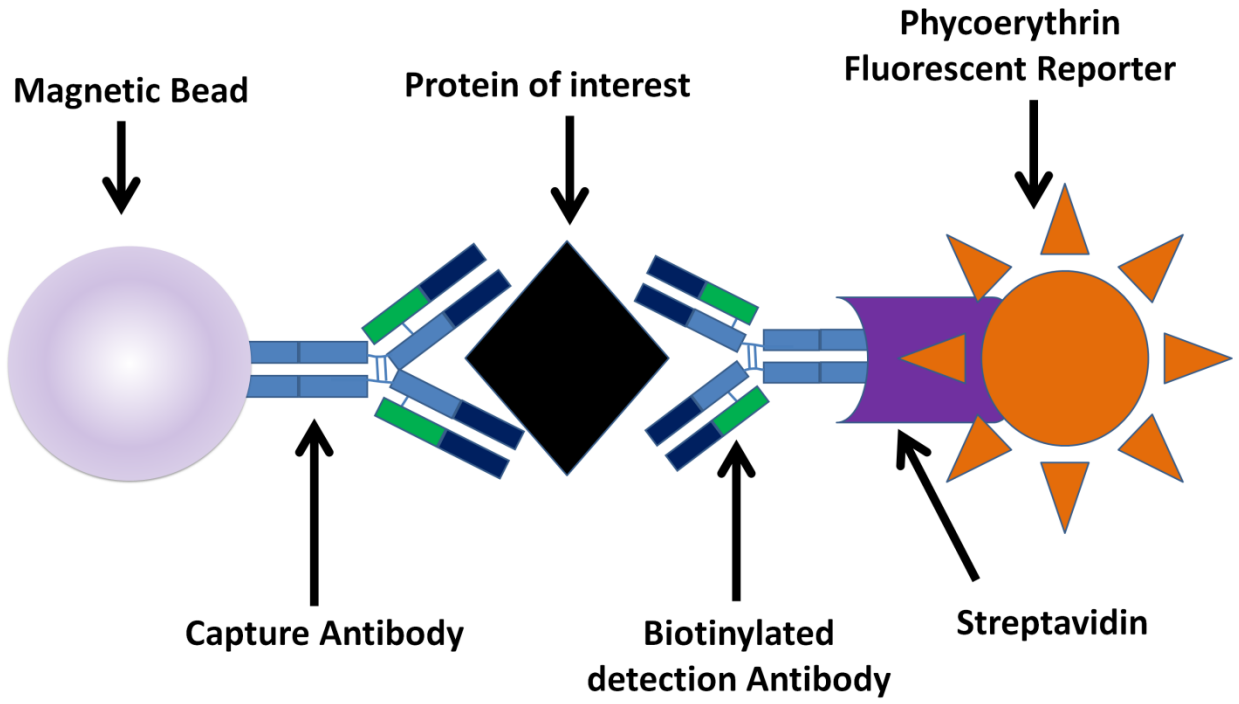

Figure 2.5: Bio-plex multiplex suspension magnetic bead array method. The primary antibody coupled with magnetic bead binds to the cognate epitopes on target protein through "Fab" arms. The secondary biotinylated antibody then binds to the free epitopes of the same protein via "Fab" arms to form a sandwich complex. Streptavidin-PE conjugates bind to the "Fc" arm of the secondary antibody. This complex is then detected by a Bio-Plex detection system with two specific lasers (This figure was adapted from Bio-Rad).

2.3 METHODS SPECIFIC TO RESULTS SECTION 3.3

2.3.1 Study outline

The study was conducted to evaluate the effect of TILRR on the migration of immune cells. Culture supernatants were harvested from TILRR-transfected HeLa cells. The effect of the culture supernatants on the migration of THP-1 and MOLT-4 cells was evaluated using Transwell assay and microfluidic device assay. In the Transwell assay, cells and chemo-attractants were placed in the upper chamber (insert) and bottom chamber, respectively, whereas in the microfluidic device, the cells were allowed to migrate towards the gradient of chemo-attractants. A brief study outline is shown in **Figure 2.6.**

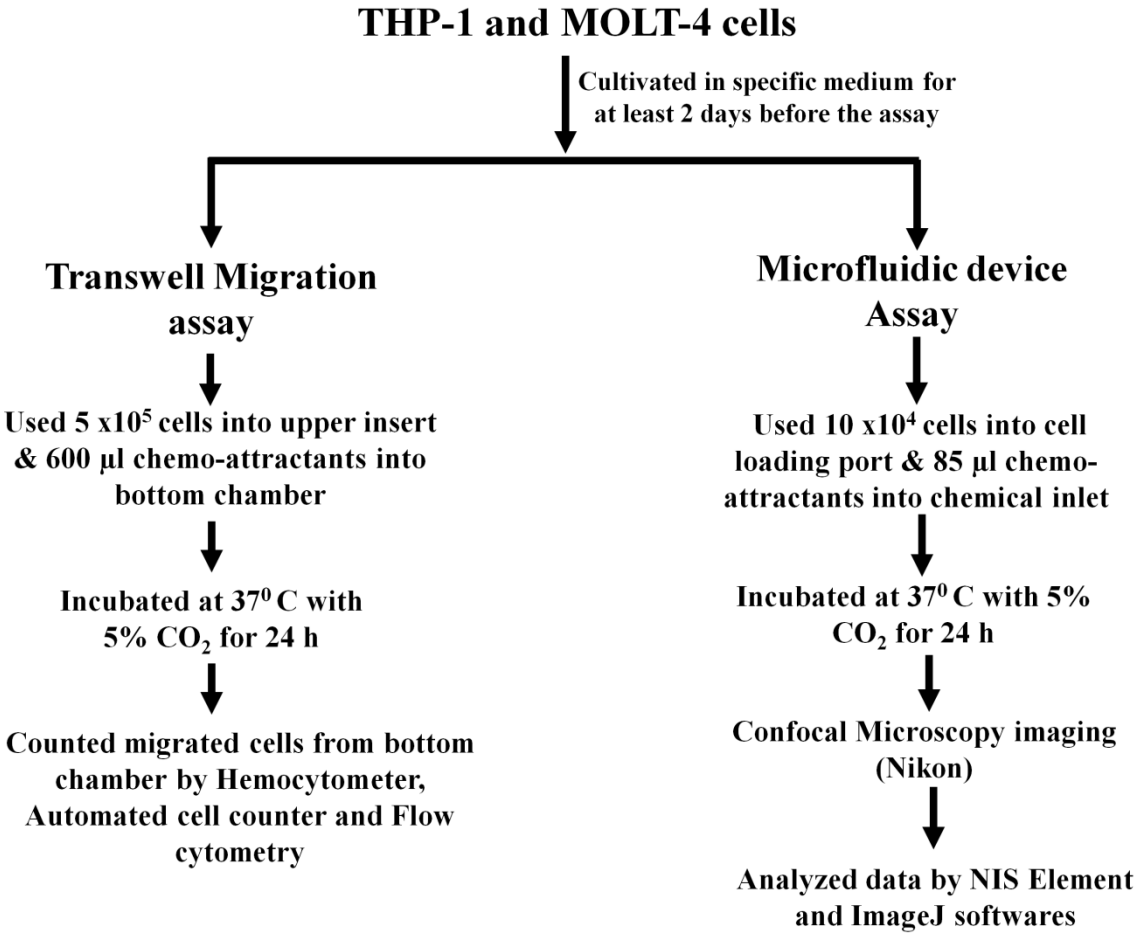

Figure 2.6: Diagram of workflow conducted for testing sub-hypothesis III.

2.3.2 Cell lines and culture conditions

THP-1 (ATCC) (NIH, Catalog# 9942), a human monocytic cell line, and MOLT-4 (NIH, Catalog# 175), a human T lymphoblastic cell line, were used for *in vitro* migration assay. MOLT-4 cells were maintained in complete RPMI 1640 growth medium (Sigma-Aldrich, Catalog# R0883) supplemented with 10% fetal bovine serum (FBS) (Giboco, Catalog# 12483), 2 mM GlutaMax-I (Gibco, Catalog# 35050-061), 10 mM HEPES (Gibco, Catalog# 15630-080), 1 mM sodium pyruvate (Gibco, Catalog# 11360070), and 1% Pen-Strep (Gibco, Catalog# 15140-122). THP-1 cells were also maintained in a complete RPMI 1640 growth medium similar to the MOLT-4 cells with an additional supplement of 0.05 mM 2-Mercaptoethanol (Sigma-Aldrich, Catalog# M3148). The medium was replaced every 2-3 days. HeLa cells (NIH, Catalog# 153) were maintained as described in **section 2.1.2**. Because THP-1 (monocytes) and MOLT-4 (lymphocytes) cells express HIV-1 receptor/co-receptors CD4, CCR5, and CXCR4 essential for R5- and X4- tropic HIV-1 strains to infect the host [303-306], and these cells are widely used as *in vitro* model for HIV-1 infection [303, 304, 307-311], I, therefore, utilized these cell lines as a model for *in vitro* cell migration assay.

2.3.3 Collection of cervical epithelial cell culture supernatants

Secretion of inflammatory mediators from female genital epithelial cells demonstrated a critical role in the rapid influx of immune cells at mucosal epithelia, resulting in heightened inflammation and vaginal microbial infection including HIV-1 [180, 209, 222, 312, 313]. Thus, to mimic the physiological conditions of the cervical epithelial microenvironment, TILRR-transfected HeLa cell culture supernatant was used as chemo-attractants in this study to investigating the effect on the migration of THP-1 monocytes and MOLT-4 lymphocytes. Culture supernatants from HeLa cells were produced as described in **section 2.2.5**. Briefly, HeLa

cells were co-transfected with TILRR- or empty vector- plasmid and selected with puromycin treatment after 24 h of transfection. Cells were then incubated with FBS- and antibiotic-antimycotic free DMEM medium (Sigma Aldrich, Catalog# D5796) for another 24h, and the supernatants were collected in sterile centrifuge tubes. The culture supernatants were centrifuged at 10,000xg for 10 min at 4^0 C, aliquoted in protein low binding tubes (Thermofisher Scientific, Catalog# 90410), and stored at -80^0C for downstream experiments.

2.3.4 Bio-Plex analysis of culture supernatants

I analyzed the cytokines/chemokines in HeLa cell culture supernatants using a custom 13-plex panel as described in **section 2.2.7**. These cytokines/chemokines include granulocyte-macrophage colony-stimulating factor (GM-CSF), interferon-gamma (IFNγ), interleukin (IL)-1β, IL-6, IL-8/CXCL8, IL-10, IL-17A, IFN-γ inducible protein (IP)-10/CXCL10, macrophage chemoattractant protein (MCP)-1/CCL-2, monocyte inflammatory protein (MIP)-1α, MIP-1β, regulated upon activation, normal T cell expressed and secreted (RANTES)/CCL5, and tumor necrosis factor-alpha (TNF-α).

2.3.5 Preparation of THP-1, and MOLT-4 -cells for the cell migration assays

The cell lines, following revival from the liquid nitrogen tank, were cultured for at least one passage before being used for the migration experiment. I used cells that were passaged for <10 times for this study. On the day of the migration experiment, the cells were mixed gently and transferred to a 50 ml BD Falcon tube, centrifuged for 10 min at 130xg, and the supernatants were discarded. Ten milliliters of RPMI 1640 complete medium without FBS and Pen-Strep was added to the pelleted cells, mixed gently, and the cell numbers were counted. For the Transwell-based cell migration assay, a total of $5x10^5$cells/100µl/assay was used, whereas $1x10^4$cells/10µl/unit was used for microfluidic-based cell migration assay.

2.3.6 Preparation of positive control chemo-attractants

Since HeLa cells were incubated with DMEM medium during the production of culture supernatants, DMEM medium was used as a medium control and diluent in this study. MCP-1/CCL2 (Sigma-Aldrich, Catalog# SRP3109-20UG) and stromal cell-derived factor (SDF)-1α/CXCL12 (Sigma-Aldrich, Catalog# SRP3276-10UG) were used as positive chemo-attractant controls for the migration assays. Positive chemo-attractant controls were diluted to concentrations (5 ng/ml, 10 ng/ml, 50 ng/ml, 100 ng/ml and 200 ng/ml) with DMEM medium (Sigma-Aldrich, Catalog# D5796) without FBS and antibiotic-antimycotic for the optimization assay.

2.3.7 Cell migration experiments in Transwell

Migration of cells was performed using a 24-well polycarbonated membrane insert with 5 µm pore size (Corning, Catalog# CLS3421) (**Figure 2.7**). In the bottom chamber of the Transwell plate, 600 µl of each chemo-attractant (DMEM control, diluted positive controls, culture supernatants of TILRR overexpressed HeLa cells, culture supernatants of empty plasmid-transfected HeLa cells, or culture supernatants of non-transfected HeLa cells) was added. One hundred microliters of cells ($5x10^5$ cells) in RPMI 1640 migration media were added to the upper chamber (Transwell insert) and incubated for 24 h at 37^0 C with 5% CO_2. The number of input cells was calculated using three different counting methods, such as hemocytometer, automated cell counter (Invitrogen, Catalog# C10227), and flow cytometry (BD accuri C6, BD Biosciences, California, USA). After 24 h of migration, Transwell insert was carefully removed from the well, and the medium containing the migrated cells in the bottom chamber was gently mixed and transferred to the 1.5 ml Eppendorf tube and migrated cells in the 50 µl medium were counted using a hemocytometer and automated cell counter as described previously [301, 302,

314]. For flow cytometry counting, the remaining ~550 µl volume of the medium containing the migrated cells was gently vortexed and analyzed with BD accuri C6 (BD Biosciences, California, USA). The data obtained from flow cytometry were analyzed with FlowJo software (Treestar, USA). The data obtained from each counting method were separately presented as percentage relative migration (PRM).

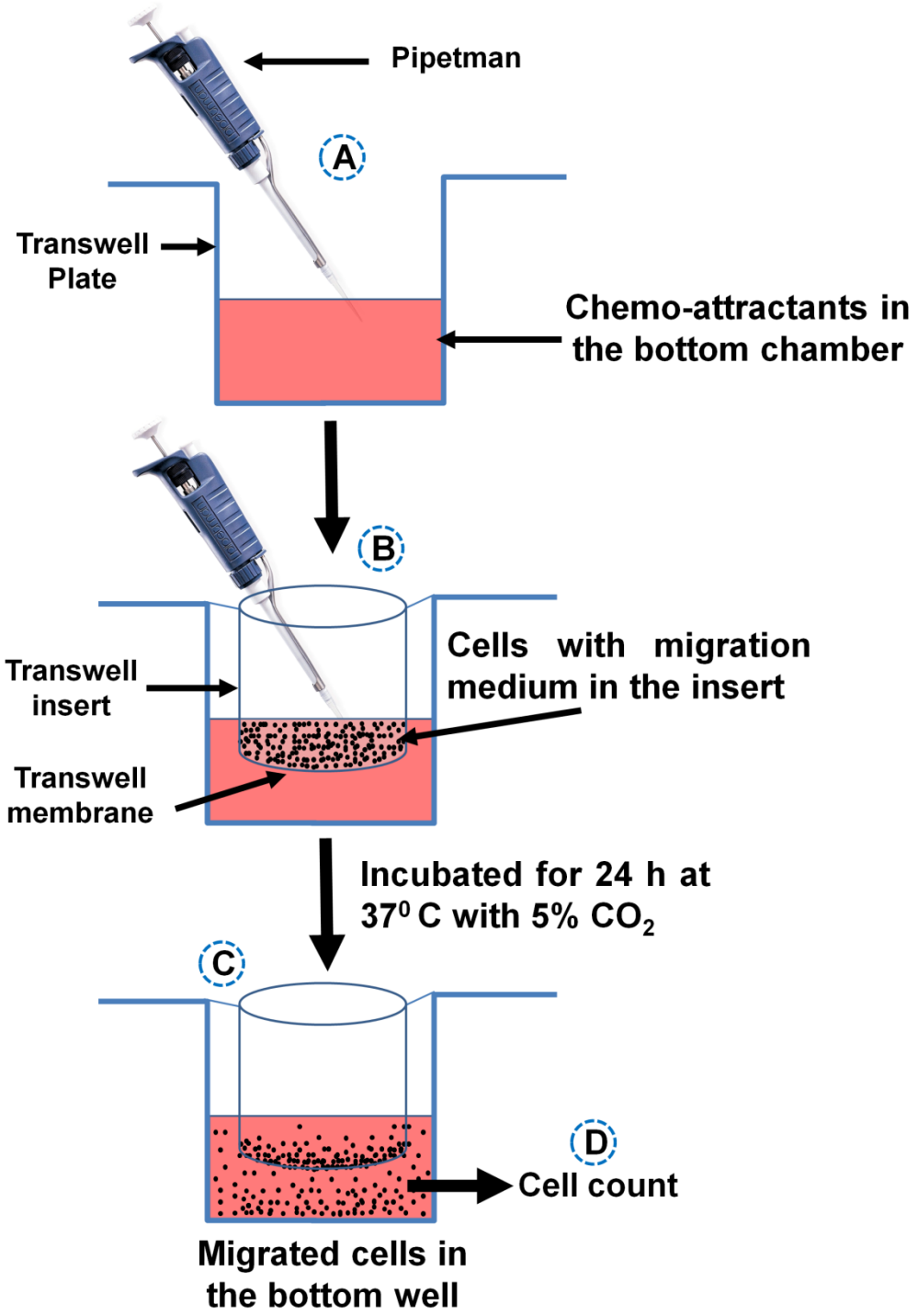

Figure 2.7: Illustration of the Transwell migration assay. **(A)** TILRR-overexpressed HeLa cell culture supernatants (light red color) were added to the bottom chamber of the Tranwell plate. **(B)** Immune cells ($5x10^5$/insert) (THP-1 or MOLT-4) containing migration media dispensed in Transwell insert. **(C)** Following 24h of incubation at 37^0 C, the migrated cells in the bottom chamber were examined under a microscope. **(D)** Media containing migrated cells were collected from the bottom chamber and estimated for cell numbers using a hemocytometer, automated cell counter, and flow cytometry analysis.

2.3.8 Preparation of the microfluidic device

A previously in-house built radial microfluidic device was used in this study **(Figure 2.8**) [315]. The device consisted of two layers with different thicknesses, the first layer (~7 μm high) forms the cell docking structure to trap cells inside the cell loading channels; while the second layer (~ 40 μm high) includes the cell loading ports and channels, and the gradient channels with chemical inlets and waste outlets. This device contains 8 independent units, each one has its own two chemical inlets, one waste inlet, and one cell loading port, which allows 8 independent experiments performed simultaneously. The device was fabricated by using previously described standard photolithography and soft lithography procedures [315-317]. Briefly, the device pattern was designed by AUTOCAD and printed onto a transparent film at 24,000 resolution (Fineline Imaging) served as the photomask for later photolithography. The pattern was then replicated by selected exposure of UV light through the photomask on top of a 3-inch silicon wafer (Silicon, Inc., ID) with a pre-coat of SU-8 negative photoresist (MicroChem). The wafer with patterns was used as the mold to reproduce polydimethylsiloxane (PDMS) (Sylgard 184, Dow Corning, Manufacturer SKU# 2065622) replicas, and then the replicas were cut off from the mold after 2h of baking at 80°C. The chemical inlets (6 mm diameter), waste outlets (4 mm diameter), and cell loading ports (2 mm diameter) were punched out of the PDMS replica, and the replica was bonded onto a glass slide after air plasma treatment. The design of micropillar supports below the docking barrier increased the structural stability during the bonding process. The device channels were coated with rat-tail collagen type I (20 μg/mL; Corning, Catalog# 354236) for 1h, and then incubated with DMEM medium for another 30 min inside the incubator before the cell migration experiments.

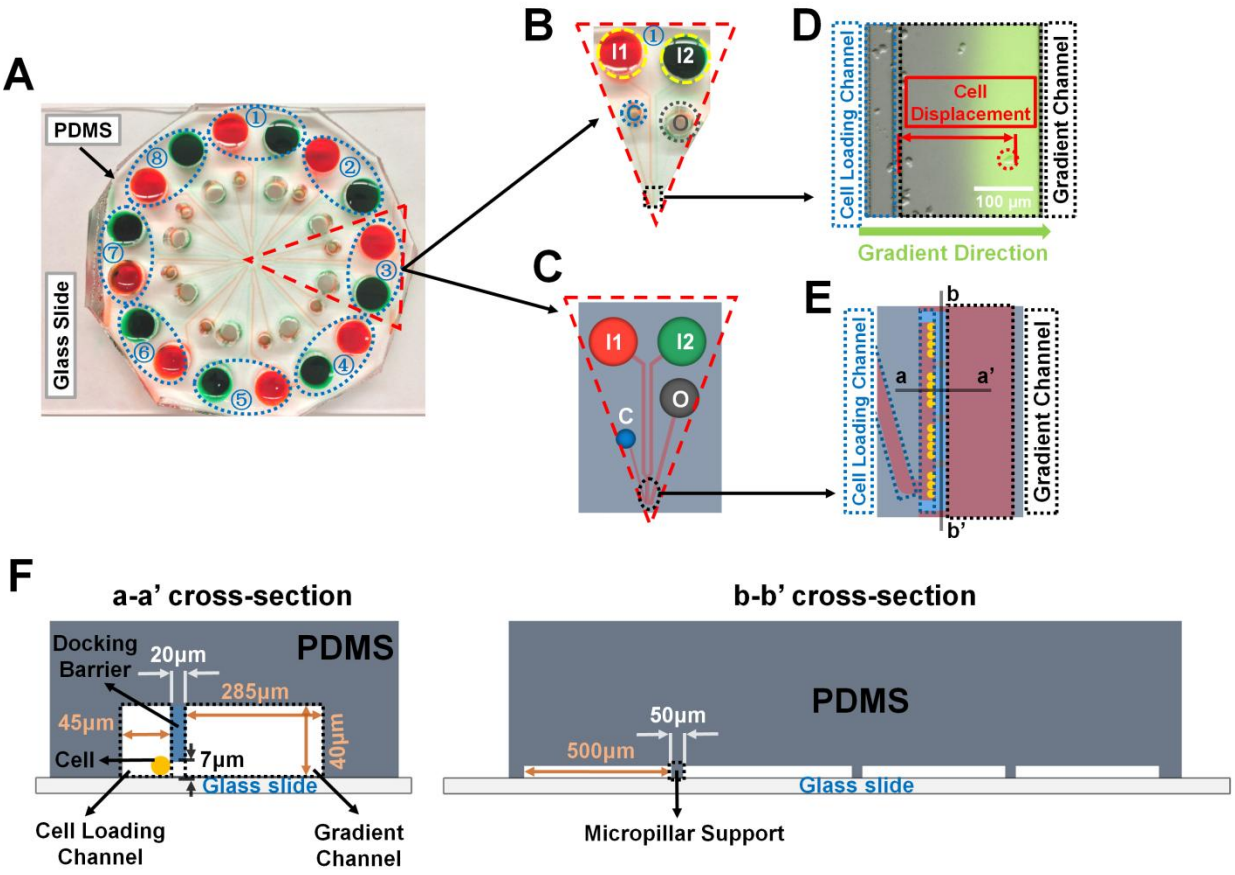

Figure 2.8: Illustration of the radial microfluidic device and cell migration analysis. A) A representative image of the real radial microfluidic device with colored dyes to show the major networks in each unit. The upper transparent part is a PDMS replica, which is bonded onto the bottom part of the glass slide; the blue elliptical-dashed box and the number (1-8) show the chemical inlets of each independent unit. **(B-C)** Magnified view of the selected unit 3 of figure A in a real device (B) and the schematic diagram (C). I1 and I2: chemical inlets; C: cell loading port; O: waste outlet. **(D)** A representative experimental image to illustrate the data analysis of cell migration displacement in the magnified view of the selected black-dashed box in figure B. **(E)** Magnified view of the black elliptical-dashed box of schematic figure C. In figures D and E, the blue- and black-dashed boxes represent the cell loading and gradient channels, respectively; the green arrow indicates the gradient direction; the red arrow shows the displacement of an individual migrated cell. **(F)** Cross-sectional views to illustrate the detailed designs of the device as indicated in figure E.

2.3.9 Cell migration experiments with the microfluidic device

Cells and chemo-attractants were prepared as described above. Cells were loaded into the cell loading ports. Fluorescein isothiocyanate (FITC)-dextran (10 kDa, Sigma-Aldrich, Catalog# FD10S) was added into the chemo-attractant solutions to indicate the gradient profile. DMEM medium and chemo-attractants were injected into the chemical inlet 1 and 2, respectively, to generate the gradient (**Figure 2.8B-C**). In addition, the two chemical inlets of each unit were covered by silicone oil (Alfa Aesar, Tewksbury, USA, Catalog# A12728-22) to balance the pressure difference for a better gradient generation as previously described [315]. The device was then placed under an inverted fluorescence microscope (Nikon Ti-U) inside an environmental controlled chamber (InVivo Scientific) at 37° C. Differential interference contrast (DIC) images of cell migration were taken for all the units at 0h and 24h, respectively. The microfluidic device was incubated inside the incubator when not taking images. The DIC images of cell migration were obtained using NIS Element Viewer (Nikon) and ImageJ software (NIH). Specifically, cells that migrated away from the docking boundary to the gradient direction inside the gradient channel within the microscope field were recorded, and the displacement of each targeted cell was measured in each group at the end of the experiment using ImageJ (**Figure 2.8D-F**).

2.4 METHODS SPECIFIC TO RESULTS SECTION 3.4

2.4.1 Study outline

TILRR epitope-specific mouse monoclonal antibodies were utilized to develop an in-house Bio-Plex (multiplex suspension array) method. Recombinant FREM1 spD (rFREM1 spD) protein containing TILRR-specific domains was used as a standard. The TILRR protein measured by the in-house developed Bio-Plex method was confirmed by in-house developed affinity purification

and Western blot analysis. A quick schematic workflow of TILRR protein measurement is shown in **Figure 2.9**. The established method was used to measure soluble TILRR (sTILRR) protein in plasma samples from women of the Pumwani sex worker cohort (PSWC) between 1985 and 2008, and the FREM1 SNP rs1552896 genotype and HIV status at the time of blood collection were included in analysis.

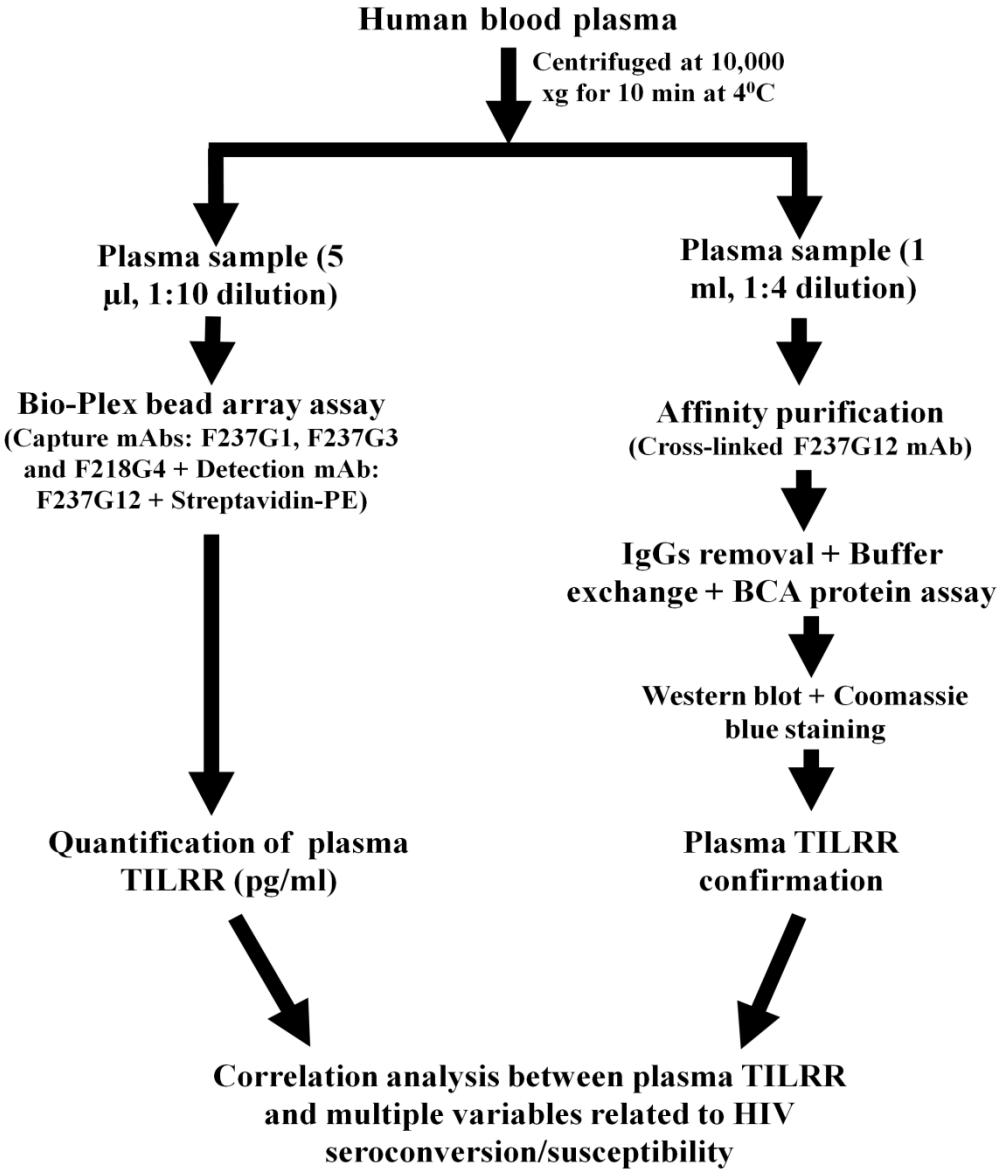

Figure 2.9: Schematic representation of plasma TILRR quantification and confirmation and downstream analysis to correlate with HIV seroconversion/susceptibility. mAb, monoclonal antibody; pg/ml, picograms per milliliter; BCA, Bicinchoninic Acid.

2.4.2 Ethics statement

This study was guided by the Helsinki Declaration on ethical principles for medical research involving human subjects. Ethics approval to conduct this study using human plasma samples was obtained from the University of Manitoba and the University of Nairobi/Kenyatta National Hospital Ethics Committee. All enrolled subjects gave written informed consent to participate in the study.

2.4.3 Study participants

Women of the Pumwani sex worker cohort (PSWC), Nairobi, Kenya enrolled between 1985 and 2008 were the participants of this study. The design, methods, and follow-up of this cohort have been described earlier [271]. In brief, all enrolled women were screened for anti-HIV p24 using enzyme immunoassays (EIA). Women who identified HIV negative for antibodies on EIA were further confirmed by immunoblot testing. All participants were routinely screened for HIV infection by PCR (polymerase chain reaction) assay. In this cohort, a group of women was categorized as HIV resistant or HESN (HIV-exposed seronegative) who were continually engaged in active sex work and remained HIV seronegative and PCR negative for at least three years post-enrolment. The average follow-up time of HESN women was 9.6±4.3 years. Additionally, a group of women was identified as HIV seroconverters [HIV SCON] who were HIV negative at the time of enrolment but later identified as positive by EIA, immunoblot testing, and PCR assay. I examined 640 plasma samples from 316 participants with different HIV status to quantify TILRR protein in this study. The overall demographic information of study subjects is shown in **Appendix Table C7.2.**

2.4.4 Multiplex bead array method for quantification of soluble TILRR in blood plasma

2.4.4.1 Method design

The full-length FREM1 (2179 amino acid) contains multiple functional domains: a putative N-terminal signal sequence, 12 chondroitin sulfate proteoglycan (CSPG) tandem repeats, a Calx-β domain, and a unique type C lectin-like (LecC) domain towards the C-terminal region [239]. It has two Arg-Gly-Asp (RGD) motifs and two glycosaminoglycan (GAG) attachment sites. FREM1 splice variant, TILRR, is a shortened FREM1 (715 amino acid) and contains protein sequence from CSPG domains 10 to the LecC domain (**Figure 2.10**) [241, 254]. With 699 out of 715 amino acid sequences of TILRR are identical to FREM1 except for the 16 amino acids at its N-terminal, it is very difficult to differentiate TILRR from FREM1 except that TILRR is a smaller protein.

Our lab previously developed a panel of mouse monoclonal antibodies (mAbs) to FREM1 [241]. Of them, some are specific to major epitopes located on CSPG-9, CSPG-10, CSPG-11/12, and Calx-β domains (**Table 2.2**). Since TILRR does not have CSPG9, I can use a combination of these monoclonal antibodies to differentiate TILRR from FREM1 with a multiplex bead array method. I can use mAbs specific to CSPG-9, CSPG-11/12, and Calx-β domains to capture FREM1 and TILRR and use the mAb to CSPG-10 to detect the captured protein. With a combination of different fluorescent beads conjugated with these mAbs, I should be able to differentiate the detected protein as FREM1 or TILRR. Three mAbs (F237G1, F237G3, and F218G4) recognizing different FREM1 domains were used as capture antibodies (**Table 2.2**). The mAb, F237G1 targeting epitopes on CSPG9 of FREM1, was used to capture full-length FREM1 protein. The F237G1 mAb was used to differentiate full-length FREM1 from TILRR

protein. F237G12 was used as a detection antibody. The TILRR protein detection methods using four anti-FREM1 mAbs in a multiplex suspension array system are shown in **Figure 2.10**.

Table 2.2: List of mouse anti-FREM1 mAbs selected for TILRR and full-length FREM1 isoform measurement in human plasma samples.

Anti-FREM1 mAbs	Target epitope sequence	Domain	Class	Type	Reference
F237G1	HTGAMDSQNQDSFTF	CSPG9	IgG1/κ	Major	[241]
F237G3	LSPDLLQLTDPDTPA	CSPG11 and CSPG12	IgG1/κ	Major	[241]
F237G12	KPEELLYVITSPPRY	CSPG10	IgG1/κ	Major	[241]
F218G4	YEVCENVGLLPLEII	Calx-β	IgG1/λ	Major	[241]

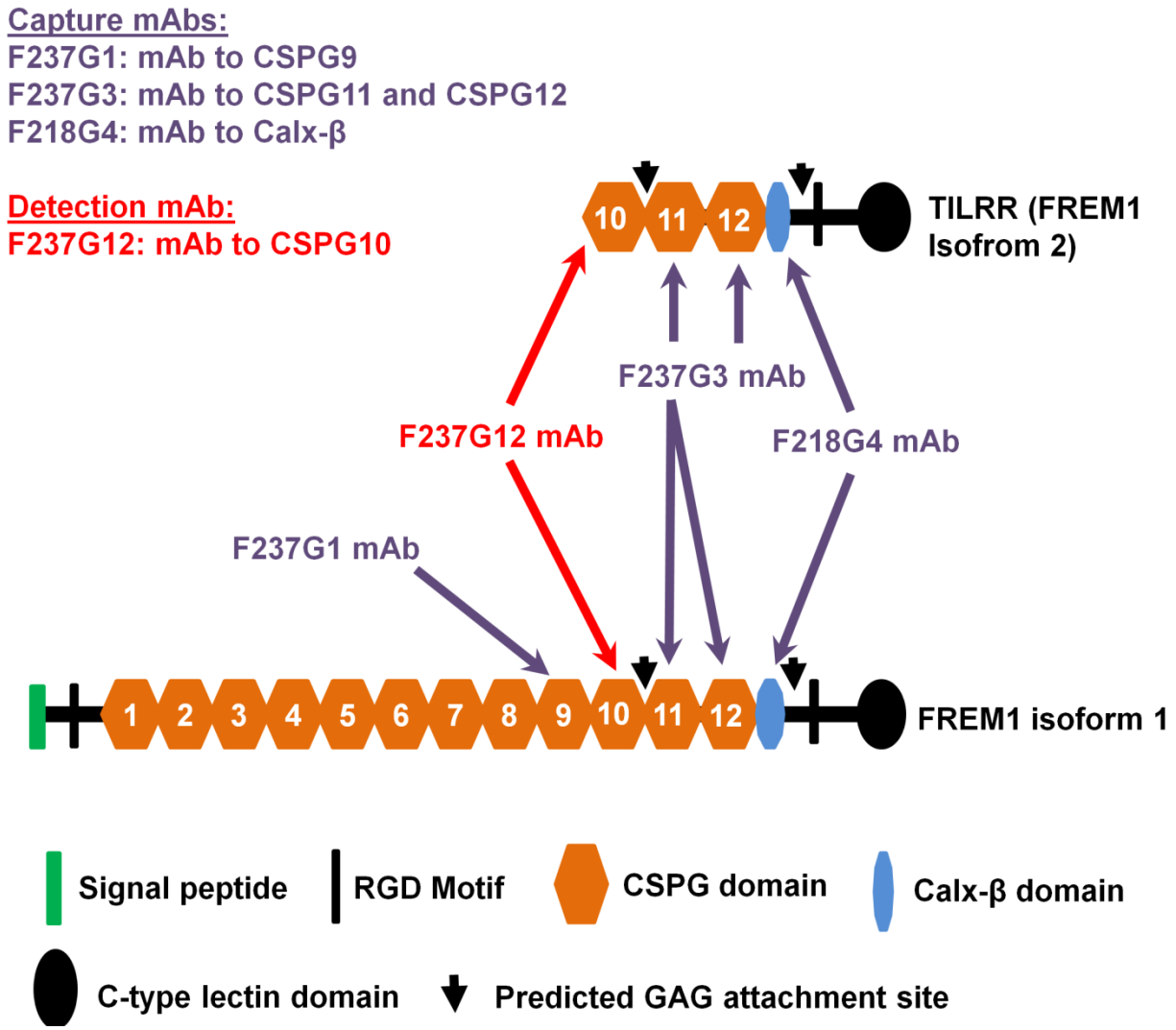

Figure 2.10: Soluble TILRR detection methods from human plasma samples using four mouse anti-FREM1 monoclonal antibodies with the Bio-Plex suspension array system. F237G3, F218G4, and F237G1 mAbs were used as capture antibodies, and F237G12 mAb was used as a detection antibody. Legends of the figure are mentioned in the bottom and upper left side. mAb, monoclonal antibody; RGD, arginine-glycine-aspartic acid; CSPG, chondroitin sulfate proteoglycan; and GAG, glycosaminoglycan. This figure was adapted from Kashem et al.[254].

2.4.4.2 Coupling of anti-FREM1 mAbs to magnetic beads

In-house developed mouse monoclonal anti-FREM1 IgG antibodies F237G1, F237G3, and F218G4 were coupled to magnetic beads using an amine coupling kit (Bio-Rad, Catalog# 171406001) according to the manufacturer's instructions [318] and as described in **section 2.2.3**. Briefly, 100 µl of 1.25 x 10^6 monodisperse COOH beads with different fluorescent spectrum (34, 36, and 64) were used to couple F218G4, F237G3, and F237G1 mAbs targeting major epitopes on Calx-β, CSPG11-12, and CSPG9 domains in a single coupling reaction, respectively. Four separate coupling reactions were performed for each antibody with each concentration (20 µg, 40 µg, or 60 µg). All four separate reactions were combined in a single tube and the concentration of coupled beads was estimated using a hemocytometer as previously described [301, 302]. Coupled beads were stored at 4^0 C for downstream application.

2.4.4.3 Detection antibody labeling

Anti-FREM1 IgG F237G12 mAb targeting major epitopes on the CSPG10 domain of TILRR was used as a detection antibody. This antibody was biotinylated by using an apex antibody labeling kit (Invitrogen, Catalog# A10495) according to the manufacturer's instructions [319]. Briefly, the resin inside the labeling tip was settled down at the bottom and hydrated with 100 µl wash buffer using a gel-loading tip. Wash buffer was gently pushed through the tip into a microcentrifuge tube with a syringe (supplied). After washing, 10 µl of diluted F237G12 mAb (20 µg maximum) was slowly pushed through the resin and then added 10 µl Biotin-XX reactive dye mixed with dimethyl sulfoxide (DMSO) and labeling buffer. The reaction mixture was incubated overnight at 4^0C. The resin bed was carefully washed 2X with 50 µl wash buffer. Next, 10 µl of neutralization buffer was taken in a clean microcentrifuge tube, and 40 µl of elution buffer was slowly pushed through the resin into the collection tube containing

neutralization buffer. The eluted antibody (~50 µl) was mixed gently and stored at 4^0 C for a maximum of 2 weeks. For longer storage, the buffer in the labeled antibody was exchanged with exchange buffer (PBS pH 7.2 containing 1 mM EDTA and 154 mM NaCl) using Amicon$^{(R)}$ Ultra-2 Centrifugal filter with 10K NMWL.

2.4.4.4 Optimization of coupled beads, detection antibody, and recombinant FREM1 spD protein

I optimized the assay condition for the required amount of coupled anti-FREM1 mAb beads using in-house developed recombinant FREM1 spD (rFREM1 spD) protein (**Figure 1.5)**. Anti-FREM1 mAbs coupled bead stock (~$5x10^6$ beads/ml) were diluted together (3-plex; equal concentration) with custom assay buffer (PBS pH 7.2 containing 2 mM EDTA, 150 mM NaCl, and 1% IGEPAL CA-630) into multiple working concentrations, 1:100, 1:200, 1:400, 1:800, 1:1000, 1:2000, 1:4000 and 1:10000 dilutions. The rFREM1 spD protein in duplicates was used as a sample for bead optimization assay. The assay was conducted according to the Bio-Rad recommended protocol. Data were checked for some cut-off parameters required to maintain the optimal assay condition, including the number of bead count (≥100 for each bead region), % CV (coefficient of variation) (≤15%), and bead recovery range (70-130%). The results showed that 1:100 bead dilutions (20 µg concentration) were satisfied with the cut-off parameters. Next, detection antibody concentration (1-2 µg/ml) was optimized using an optimal bead dilution of 1:100. The detection antibody concentration of 1 µg/ml was satisfied with the cut-off parameters.

Additionally, rFREM1 spD protein was optimized using an optimal concentration of captured and detection antibodies. I generated a standard curve by using rFREM1 spD protein for each captured antibody (**Appendix Figure B7.1**). A 5-fold dilution of rFREM1 spD protein (lab ID# F5) was prepared ranges from standard 1 (S1; conc. 10000ng/ml) to S7 (conc. 0.64 ng/ml). Each

point of diluted rFREM1 spD protein in duplicates was added to the assay plate containing capture beads followed by the addition of detection antibody and streptavidin-PE. The optimal dilution of rFREM1 spD protein (based on the upper limit of quantification [ULOQ] and lower limit of quantification [LLOQ]) was utilized for all downstream assays to measure TILRR protein from human plasma samples.

2.4.4.5 Preparation of plasma samples for the assay

Archived human plasma samples collected from HIV seroconverters, and HESN women of Pumwani Sex Worker Cohort, Kenya, between 1985 and 2008 were used to measure the TILRR protein. Samples were pulled from the -80^0 C freezer and kept on ice to thaw. The thawed plasma was centrifuged at 10,000xg for 10 min at 4^0 C to pellet the leftover blood cells along with other solid particles. Supernatants were collected and diluted with custom plasma diluents (PBS pH 7.2 containing 2 mM EDTA, 150 mM NaCl, and 1% IGEPAL CA-630) in a ratio of 1:10. A total of 120 µl samples (12 µl of plasma + 108 µl of plasma diluents) were prepared to use in duplicates from each individual. Diluted samples were kept on ice and vortexed for 15 sec before being added to the assay plate.

2.4.4.6 Measurement of TILRR protein from human plasma samples

A modified in-house developed cytokine/chemokine measurement protocol was used to measure TILRR in plasma samples as described in **section 2.2.7**. The assay was conducted using an in-house developed custom 3-plex anti-FREM1 mAbs panel. Briefly, anti-FREM1 mAbs coupled magnetic beads (50 µl) were diluted in custom assay buffer (PBS pH 7.2 containing 2 mM EDTA, 150 mM NaCl, and 1% IGEPAL CA-630) at 1:100 dilutions and added to the 96-well assay plate. Following 2X washes, 50 µl of diluted plasma (1:10) was added to the wells in duplicates and incubated for 2h at RT on a plate shaker (850±50 rpm). After 3X washes, a 30 µl

custom biotinylated secondary detection antibody (1 µg/ml) was added and incubated again for 30 min at RT on a plate shaker. Fifty microliters of streptavidin-PE conjugate (1X) were added following 3X washes, and further incubated for 10 min at RT on a shaker. Finally, 125 µl PBS (pH 7.2) was dispensed into each well, and run the plate in Bio-Plex^{TM} 200 System (Luminex xMAP technology) (Bio-Rad, Canada). For the standard curve, rFREM1 spD protein was diluted into 5-fold dilution (S1 to S7), and 50 µl of each dilution was added in duplicates. For blank (background control), 50 µl of dilution buffer (PBS pH 7.2 containing 2 mM EDTA, 150 mM NaCl, and 1% IGEPAL CA-630) was added in duplicates. Bio-Plex software version 6.1 was used to acquire data, which were optimized to calculate the ULOQ (pg/ml) and LLOQ (pg/ml) using logistic-5PL regression analysis with fitness probability ≥ 0.95.

2.4.4.7 Measurement of plasma inflammatory cytokines/chemokines

A panel of cytokines/chemokines in plasma samples was also analyzed by the in-house developed Bio-Plex method as described in **section 2.2.7** [254]. The cytokines/chemokines include granulocyte-macrophage colony-stimulating factor (GM-CSF), interferon-gamma (IFNγ), interleukin (IL)-1α, IL-1β, IL-6, IL-8/CXCL8, IL-10, IL-17A, IFN-γ inducible protein (IP)-10/CXCL10, macrophage chemoattractant protein (MCP)-1/CCL-2, monocyte inflammatory protein (MIP)-1α, MIP-1β, regulated upon activation, normal T cell expressed and secreted (RANTES)/CCL5, and tumor necrosis factor-alpha (TNF-α).

2.4.5 Affinity purification and Western blot analysis methods for the validation of plasma TILRR

2.4.5.1 Cross-linking of anti-FREM1 IgG mAb with Protein G agarose beads

The cross-linking procedure was performed with modified protocol as described by New England BioLabs Inc. After uniform mixing of protein G agarose beads (by inverting the vial

several times), 500 µl was taken into a clean 5 ml affinity purification column (ThermoFisher Scientific, Catalog# 29922). The buffers were removed from the beads by gravitational force (end volume obtained 50% bead slurry) and washed twice with 5 ml of 0.1 M sodium phosphate buffer (binding buffer, pH 8.0). Beads were resuspended in 400 µl of binding buffer, and 150 µl of diluted anti-FREM1 F237G12 IgG mAb (100 µg concentrations in binding buffer) was added, mixed gently, and incubated for 30 min at 4^0 C on a rotor. Following incubation, the buffers were removed and washed 3X with 5 ml of binding buffer. Then, 5 ml of 0.2 M triethanolamine (cross-linking buffer, pH 8.2) was added to the column containing protein G immobilized anti-FREM1 IgG mAb and allowed to drain through the membrane. Washing of protein G immobilized mAb column was repeated for one more time with cross-linking buffer and added 5 ml of 25 mM DMP cross-linking reagent (6.5 mg/ml in cross-linking buffer, prepared immediately prior to use). The reaction was mixed gently and incubated at RT for 45 min on the rotor. After incubation, excess buffers were removed, and the beads were washed 1X with 5 ml of 0.1 M ethanolamine (blocking buffer, pH 8.2). The beads were again resuspended in a 5 ml blocking buffer and incubated for 1 h at RT on the rotor. Following a 2X wash with 5 ml PBS pH 7.2, 5 ml elution buffer (0.1 M glycine-HCl, pH 2.5) was added to elute the unlinked anti-FREM1 F237G12 IgG mAbs. Finally, 1 ml of PBS pH 7.2 containing 0.1% Tween 20 and 0.02% sodium azide was added to the cross-linked IgG mAb, and stored at 4^0 C. Cross-linked anti-FREM1 IgG mAb was used for affinity purification of TILRR protein from plasma samples. The cross-linking procedures of anti-FREM1 F237G12 IgG mAb with protein G agarose beads are shown in **Figure 2.11**.

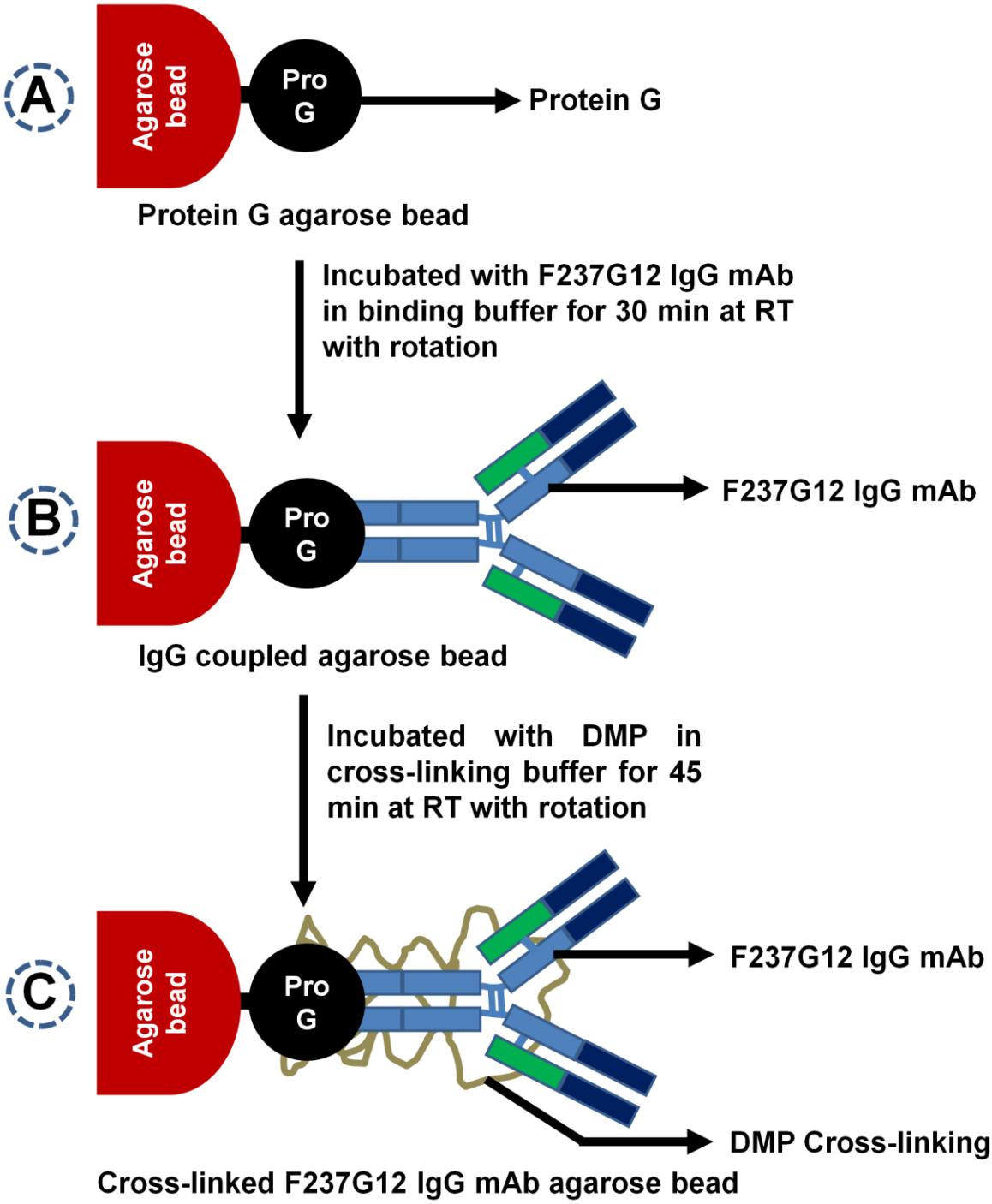

Figure 2.11: Graphical representation of anti-FREM1 F237G12 IgG mAb cross-linking procedure with Protein G agarose beads. A) Protein G coupled agarose bead, **B)** Protein G bound with Fc region of anti-FREM1 F237G12 mAb, **C)** Anti-FREM1 F237G12 mAb cross-linked with protein G agarose bead by DMP. mAb, monoclonal antibody; IgG, immunoglobulin G; DMP, Dimethyl pimelimidate dihydrochloride; and RT, room temperature.

2.4.5.2 Verification of anti-FREM1 IgG mAb cross-linking efficiency

Cross-linking efficiency of anti-FREM1 F237G12 IgG mAb with protein G agarose beads was examined by Pierce BCA Protein Assay (ThermoFisher Scientific, Catalog# 23227) using filter through (collected from each step of cross-linking procedure) according to the manufacturer's instructions. Briefly, a set of diluted albumin (bovine serum albumin, BSA) standards was prepared ranges from 25 to 2000 µg/ml concentrations (S1 to S8). The working reagent of BCA was prepared by adding 50 parts of reagent A with 1 part of reagent B (50:1). Each point of diluted standard and unknown filter through samples (10 µl) in duplicates was dispensed into 96-well flat-bottom microtitre plate (ThermoFisher Scientific, Catalog# 269620**)**. Two hundred microliter of BCA working reagent was added, and the plate was covered with plate seal (Bio-Rad, Catalog# MSF1001). The plate was gently mixed for 30 sec at RT on a plate shaker (850±50 rpm) and incubated for 30 min at 37^0 C. Following incubation, the plate was cooled down at RT, and the absorbance was measured at or near 562 nm on SpectraMax M2e plate reader (Molecular Devices, USA) using SoftMax version 6.2.2 software. The protein concentration in unknown samples (µg/ml) was automatically calculated based on the standard curve generated by software, where R^2 value and coefficient of variation (CV) were maintained at ≥ 95.0 and <15, respectively.

2.4.5.3 Affinity purification of TILRR protein from human plasma samples

Storage buffer from cross-linked anti-FREM1 F237G12 IgG mAb protein G agarose beads in the column was drained and washed with 5 ml of PBS pH 7.2, and further with 5 ml of 0.1 M sodium phosphate buffer pH 8.0. Four milliliters of 1:4 dilution plasma samples were added to approximately 250 µl bead slurry, mixed gently, and incubated overnight at 4^0 C on the rotor. Following incubation, the beads were washed five times with 1 ml washing buffer to remove

unbound non-specific proteins. After 5X washes, TILRR protein was eluted from the bead slurry with 250 µl elution buffer (0.2 M glycine-HCl pH 2.5) into a tube containing 250 µl neutralization buffer (1.0 M Tris-HCl, pH 8.0). Elution with 0.2 M glycine-HCl was performed two more times, and all elutes were combined in a single tube. After elution, the bead slurry was neutralized twice with 900 µl bead neutralization buffer. The regenerated IgG cross-linked bead column was stored with 2 ml of PBS pH 7.2 containing 0.02% sodium azide at 4^0 C. The procedure of affinity purification of TILRR protein is presented in **Figure 2.12**.

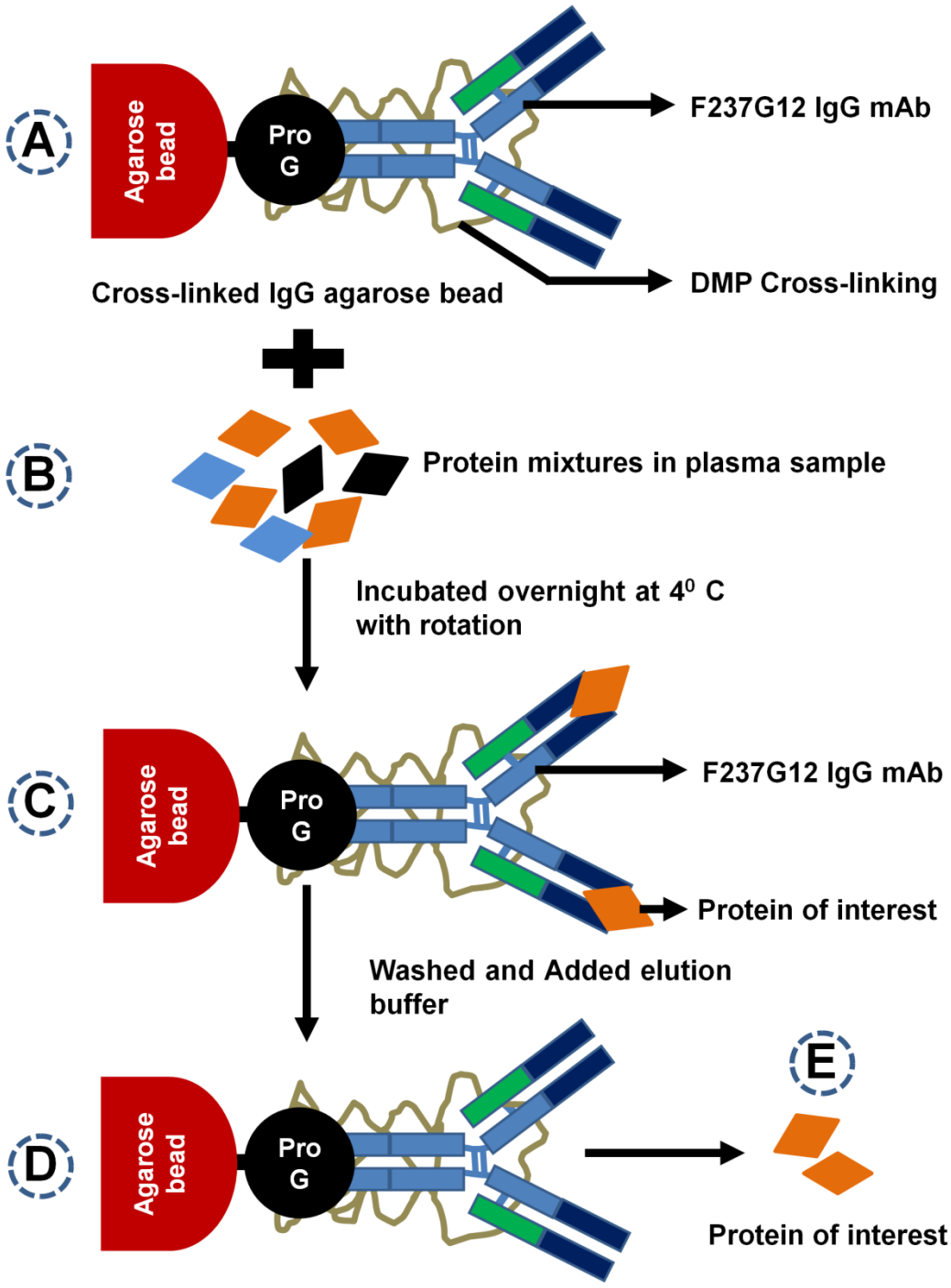

Figure 2.12: Affinity purification procedure of TILRR protein. A) Anti-FREM1 F237G12 mAb cross-linked protein G agarose bead, **B)** Mixture of proteins in plasma samples, **C)** Protein of interest (TILRR) bound with Fab region of anti-FREM1 mAb, **D)** Neutralized cross-linked anti-FREM1 mAb following affinity purification of target protein, **E)** Target proteins (TILRR). mAb, monoclonal antibody; IgG, immunoglobulin G; and DMP, Dimethyl pimelimidate dihydrochloride.

2.4.5.4 Removing plasma immunoglobulin G (IgG) from eluted protein

Because IgG in plasma can bind to the protein G agarose beads that might not be fully cross-linked to the mouse mAb, the plasma IgGs were co-eluted with the affinity-purified TILRR. The plasma IgGs need to be removed from the eluted TILRR proteins. Thus, following affinity purification, human plasma IgG was removed from eluted protein using Protein G agarose beads that were not cross-linked to the mouse antibodies as follows: the eluted protein was diluted with 6 ml of PBS pH 7.2 containing 1 mM EDTA, 154 mM NaCl, and protease inhibitor (10 µl per ml), and went through a human IgG cleaning process. Briefly, 3 ml protein G agarose bead resin was pipetted into a clean 5 ml column, and allowed to drain off buffers by gravitational force. Bead slurry (~50% of the initial volume) was washed twice with 5 ml of sodium phosphate buffer (0.1 M, pH 8.0), and then the diluted protein was slowly added to the column. The protein passed through the agarose beads was collected in a new collection tube and should contain protein with reduced plasma IgG. This process was repeated once more to obtain purified protein without plasma IgG. The final purified protein was concentrated by a 10K Amicon Ultra-2 centrifugal filter for downstream analysis. The plasma IgG bound to the Protein G agarose beads was eluted with 5 ml of glycine-HCl (0.1 M, pH 2.5) and neutralized with 0.5 ml of Tris HCl (1 M, pH 8.0).

2.4.5.5 Protein concentration and buffer exchange

Affinity purified protein was concentrated using a 10k Amicon Ultra- 2 centrifugal filter unit (Ultracel- 10K) (Millipore, Catalog# UFC201024) according to the manufacturer's recommended protocol. Briefly, a maximum of 2 ml purified protein was loaded into the centrifugal filter at a time and spun at 4000xg for 30 min at 6^0 C. The buffer in concentrated protein was exchanged twice with 1 ml of 1X PBS pH 7.2 containing 1 mM EDTA, 154 mM NaCl, and protease

inhibitor (10 µl in 1 ml buffer). After centrifugation, the filter was inversed into a collection tube and spun at 1000xg for 2 min. The final volume of concentrated protein was adjusted to 300 µl, and Pierce BCA protein assay was used to measure protein concentration. Affinity purified protein was analyzed by Western blot with anti-FREM1 IgG mAbs.

2.4.5.6 Western blot analysis

Western blot analysis of affinity-purified proteins was conducted using a slightly modified method as described in **section 2.1.15**. Briefly, Odyssey$^{(R)}$ One-color protein molecular weight marker (LI-COR, P/N: 928-40000) was used as a protein marker (2 µl/lane). Each protein sample was run separately in a precast NuPAGE 4-12% Bis-Tris 1.0 mm x 15 well gel (Thermo Fisher Scientific, Catalog# NP0323BOX) for 45 min with 200 V, and then transferred to a nitrocellulose membrane by iBlot transfer (cycle p3 for 7 min). After 1X wash with 5 ml double distilled water (ddH_2O) and further with 5 ml of PBS-T for 5 min on a shaker at 60 rpm, the membrane was dried at 37^0 C for 30 min. The dried membrane was blocked with 5% skim milk (Difco, BD Biosciences, Catalog# 232100; diluted in PBS-T) for 1 h at RT on a shaker. After the removal of the blocking buffer, the membrane was incubated separately with 20 µg/ml (diluted in PBS-T containing 0.25% bovine serum albumin, BSA) of anti-FREM1 primary mAb (F237G3, F218G4, and F237G1) overnight at 4^0 C on a shaker (60 rpm). Anti-FREM1 F237G3 and F218G4 mAbs were used to identify TILRR, whereas anti-FREM1 F237G1 mAb was used for full-length FREM1 isoform. After 3X washes with PBS-T, the membrane was probed with IRDye$^{(R)}$ 800CW goat anti-mouse IgG secondary antibody (LI-COR, P/N: 926-32210) (at 1:2000 dilution in PBS-T) for 1h at RT on a shaker (60 rpm). The gel was kept covered with aluminum foil to prevent light exposure from the secondary antibody incubation step and onwards. Following 3X washes with PBS-T and a final 1X wash with PBS pH 7.2, the membrane was

carefully laid on the clean scanning surface of the Odyssey CLx imager (LI-COR, USA). Before placing the membrane, the glass scanning surface was carefully cleaned with 100% methylene chloride (Fisher Scientific, Catalog# D151-1) followed by double distilled water and 50% isopropanol (Fisher Scientific, Catalog# A464-4), and dried with lint-free wipes. Image Studio software version 5.0 (Image Acquisition Odyssey CLx) was utilized to obtain the images with the following settings: auto intensity (both 700 and 800 channels), 42µm scan size with high scan quality, and 0 (zero) mm focal offset. Post-acquisition image analysis for TILRR protein signal intensity was conducted using Image Studio Lite version 5.2. The intensity of both 700 and 800 channels was further manually adjusted to minimize the background effect.

2.4.5.7 Coomassie blue gel staining

To perform quick visualization of the expected ~70 kDa band of affinity-purified TILRR protein in transferred gels, Coomassie gel staining was conducted in parallel using BioSafe^{TM} Coomassie stain (Bio-Rad, Catalog# 1610786) according to the company's recommended protocol [320]. In brief, after iBlot transfer onto nitrocellulose membrane using iBlot gel transfer device (Invitrogen, Catalog# IB1001), the gel was placed in a staining container bearing 200 ml ddH_2O and washed 3X with ddH_2O for 5 min. Twenty milliliters of BioSafe^{TM} Coomassie stain was added to the staining container following complete removal of ddH_2O and incubated for 1 h at RT on a plate shaker with 60 rpm. After 1 h incubation, the Coomassie stain was removed and further rinsed into 200 ml ddH_2O for 30 min at RT. The gel was then scanned with the Odyssey CLx imaging system (LI-COR, USA) using the auto intensity of 700 channel, 42µm scan size, high scan quality, and 0.5 mm focal offset. Additionally, the gel was kept in fresh 200 ml ddH_2O until to conduct gel drying.

2.4.5.8 Gel drying

To preserve data for an indefinite period, BioSafe^{TM} Coomassie-stained gel was dried using DryEase$^{(R)}$ Mini-Gel Drying System (Invitrogen, Catalog# NI2387) according to manufacturer's instructions [321, 322]. Double distilled water was completely removed from the gel tray and equilibrated in 35 ml of fresh Gel-Dry^{TM} Drying solution for 20 min at RT on a shaker. During the incubation, DryEase$^{(R)}$ gel drying base was set up by placing a drying frame with the corner pin facing up. Two pieces of cellophane were used for each gel and immersed into a drying solution one after another for a maximum of 2 min. A sheet of completely soaked cellophane was placed on the center of the drying base and laid the stained gel on the center making sure not to trap any bubbles between the gel and the cellophane. Gel images were taken with a digital camera while lying down horizontally on the drying base and then covered with a second sheet of entirely soaked cellophane. Another drying frame was aligned with holes in the bottom frame and left standing for 24 h. Once the gel was fully dried, the excess cellophane was trimmed off and the gel was placed between the pages of the notebook under light pressure for 2 days to keep flat of the gel for future use.

2.5 DATA ANALYSIS

RT^2 Primer qPCR assay and RT^2 profiler PCR array data were analyzed using the GeneGlobe Data Analysis Centre (Qiagen) (https://www.qiagen.com/us/shop/genes-and-pathways/data-analysis-center-overview-page/). The mRNA transcript fold changes in the threshold cycle (CT) were calculated relative to the CT level of empty vector control. Fold change 1.0 was assigned as a baseline control and threshold cycle (CT) assays were performed in three independent experimental replicates. All mRNA transcript data were normalized against the HPRT1 housekeeping gene. The cytokine/chemokine(s) data were analyzed by GraphPad Prism version

8.3.0 (GraphPad Software, Inc. USA) and presented as relative to the concentration of empty vector control, and show mean±SEM of three independent experiments. The data obtained with the transwell assay was also analyzed by GraphPad Prism software. The cell migration data obtained with the microfluidic device was processed by the OriginPro software (OriginLab Corporation, USA) and ImageJ (NIH, USA). Western blot and Coomassie blue staining data were analyzed by Image Studio Lite software version 5.2 (https://www.licor.com/bio/image-studio-lite/) (LI-COR, USA). Western blot analysis for TILRR overexpression was also performed by Quantity One (Bio-Rad). The final statistical comparisons conducted using student t-test with 95% CI, all $p<0.05$ were reported and indicated using asterisks' *p<0.05, **p<0.01, ***p<0.001, and ****p<0.0001.

3 CHAPTER 3: RESULTS

3.1 TILRR REGULATES MRNA EXPRESSION OF GENES ASSOCIATED WITH THE NF-KB SIGNALING PATHWAY AND INFLAMMATION

The results of this section are based on the following article:

Toll-like Interleukin 1 Receptor Regulator Is an Important Modulator of Inflammation Responsive Genes. Frontiers in Immunology, 2019. **10**(272): p. 1-16.

Mohammad Abul Kashem[1,3], Hongzhao Li[1,3], Nikki Pauline Toledo[1,3], Robert Were Omange[1,3], Binhua Liang[2,3], Lewis Ruxi Liu[1,3], Lin Li[1,3], Xuefen Yang[3], Xin-Yong Yuan[4], Jason Kindrachuk[1], Francis A Plummer[1], Ma Luo[1,3,4]

[1]Department of Medical Microbiology and Infectious Diseases, University of Manitoba, Winnipeg, MB, Canada
[2]Department of Biochemistry & Medical Genetics, University of Manitoba, Winnipeg, MB, Canada
[3]JC Wilt Infectious Diseases Research Centre, National Microbiology Laboratory, Winnipeg, MB, Canada
[4]National Microbiology Laboratory, Public Health Agency of Canada, Winnipeg, MB, Canada.

Authors' Contributions

MK, FP, and ML conceived and designed research; **MK** performed all research, analyzed the data, generated figures/tables, organized the writing materials, and wrote the paper; HL helped in Western blot study; NT helped in Bio-Plex assay, LL and XY helped in Confocal microscopy study; FP and ML acquired funding; XYY supported reagents; BL, FP, and ML supervised research; and ML, HL, RO, LRL, BL, and JK edited the paper. **MK** revised, formatted, submitted, and responded to the reviewers' comments.

Funding

The study was funded by an operating grant from the Canadian Institutes of Health Research (CIHR), Operating grant- PA: CHVI Vaccine Discovery and Social Research. URL: http://www.cihr-irsc.gc.ca/e/193.html.

3.1.1 TILRR overexpression in transfected cells

To assess the effect of TILRR overexpression on genes in the NF-κB inflammatory pathway, I overexpressed TILRR in HeLa (a cervical epithelial cell-line) **(Figure 3.1A and B**) and VK2/E6E7 (a normal human vaginal mucosal epithelial cell-line) cells (**Figure 3.1E and F**). Confocal microscopy image analysis showed that cells containing plasmids with either TILRR plus puromycin selection marker (vector+TILRR) or only puromycin marker (empty vector control) were alive after 24h puromycin dihydrochloride selection as shown by the cells attached to the culture plate with active pseudopods and intact morphology **(Figure 3.1A and B; Figure 3.1E and F**). Whereas, within the same period of time under puromycin selection the non-transfected cells or the cells that only contain PmaxGFP vector were died, showing complete loss of pseudopodia and detachment from the culture plate with distracted morphology (**Figure 3.1C and D; Figure 3.1G and H**). Flow cytometry quantification of GFP expressing cells showed that the transfection efficiency was between 87.0% and 90.9% of empty vector control- and TILRR (vector+TILRR)-transfected HeLa cells, respectively (**Figure 3.1I and J**).

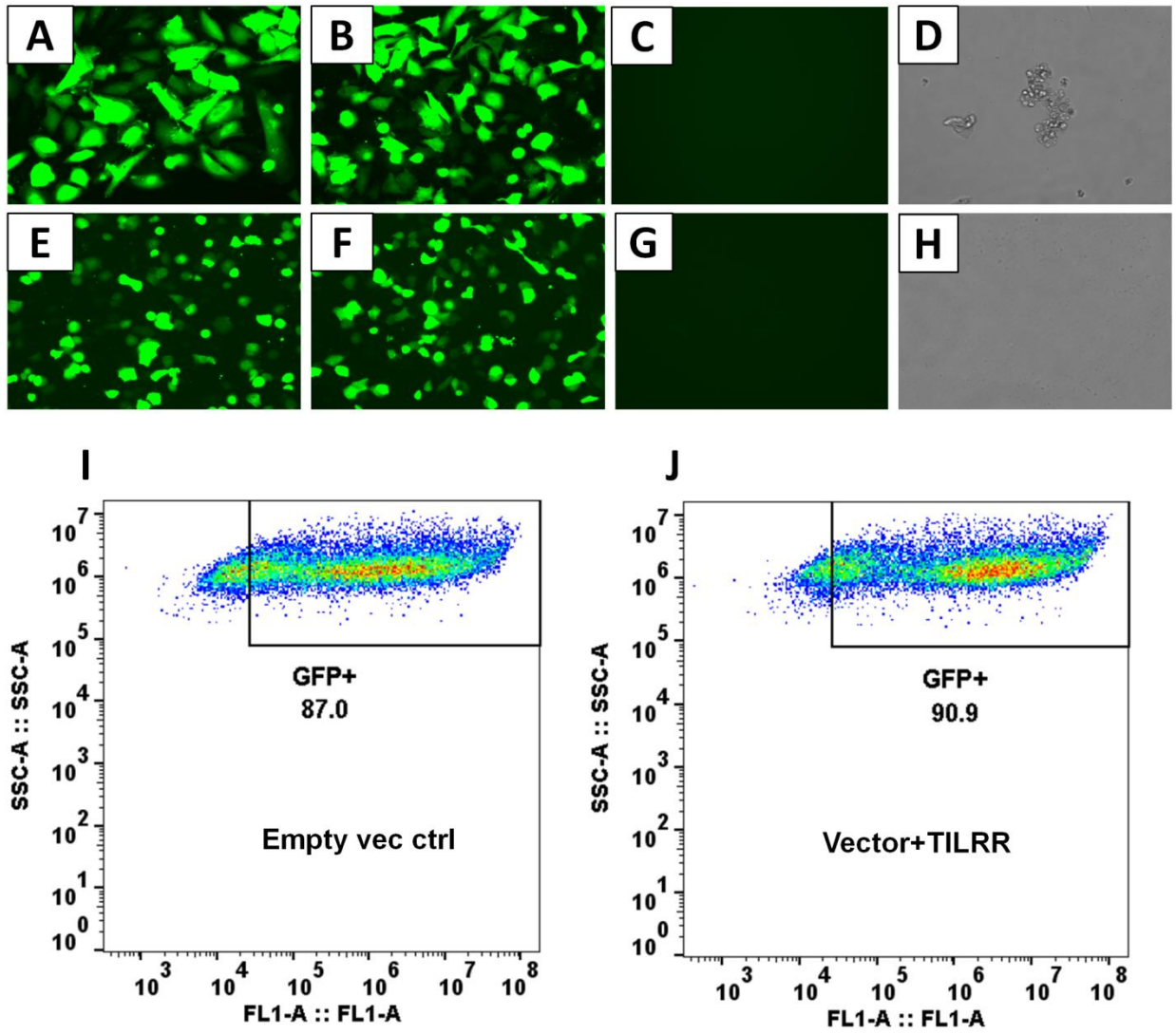

Figure 3.1: Expression of TILRR in transfected cell lines. Confocal microscopy imaging of transfected HeLa (**A to D**) and VK2/E6E7 (**E to H**) cells showing eGFP expression following co-transfection with pEZ-TILRR-M68 (vector+TILRR) (1.0µg/5x10^5 cells) (**A and E**) or pEZ-NEG-M68 (empty vector control) (1.0µg/5x10^5 cells) (**B and F**) along with PmaxGFP (0.2 µg/5x10^5 cells) and non-transfected control (C to D and G to H). **(I-J)** Flow cytometry quantitation of transfected HeLa cells (I, empty vector control–transfected cells; J, TILRR-overexpressed cells).

Western blot analysis of transfected cells showed that cells transfected with TILRR expressed a significantly higher amount of TILRR protein compared to parental-HeLa cells and cells transfected with empty vector ($p<0.05$) (**Figure 3.2A**; full-length original blots presented in **Appendix Figure B7.2**). RT^2 qPCR Primer analysis showed that cells transfected with TILRR containing plasmid significantly overexpressed the TILRR mRNA compared to non-transfected parental control and empty vector ($p<0.0001$) (**Figure 3.2B**). Confocal microscopy imaging analysis further confirmed the overexpressed TILRR protein in HeLa cells (**Figure 3.3A-D**) compared to the respective controls (**Figure 3.3E and F; Appendix Figure B7.3E-H and I-L**). I also confirmed the TILRR protein expression in transfected HeLa cells by flow cytometry analysis using Alexa Fluor 647 labeled monoclonal antibodies (F218G1 and F218G5) recognizing epitopes in TILRR. The mean fluorescence intensity (MFI) of TILRR transfected cells showed significantly higher expression of TILRR compared to the parental control, isotype control, and empty vector-transfected control (**Figure 3.4A-C)**. These data indicated that TILRR transfected HeLa and VK2/E6E7 cells overexpressed TILRR.

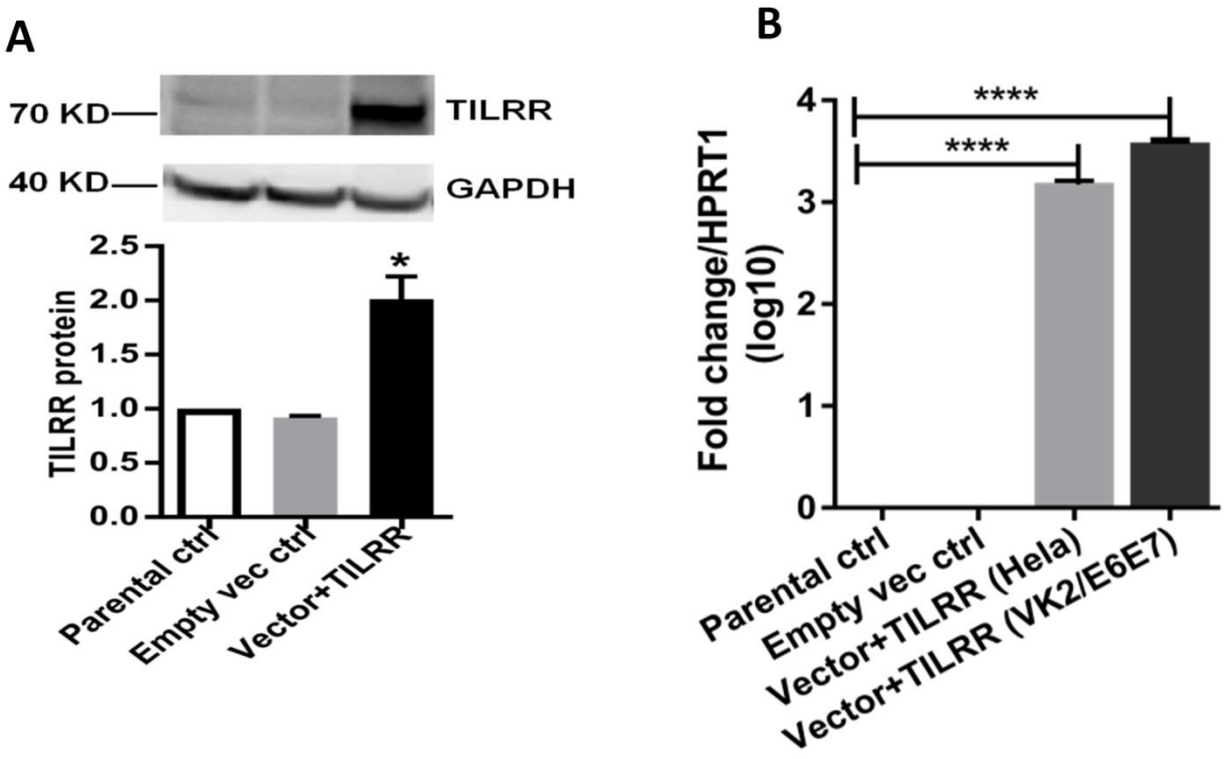

Figure 3.2: Expression of TILRR in transfected cell lines. A) Western blot of TILRR proteins following 24h post-transfection, as compared to GAPDH control (full-length original blots presented in **Appendix Figure B7.2**), **(B)** Confirmation of the TILRR mRNA transcripts overexpression in both cells using RT^2 qRT-PCR primer assay and data presented as log10 fold change, which was normalized against HPRT1 housekeeping gene. Student t-test with 95% CI performed for the statistical analysis using GraphPad Prism version 7.03, all $p<0.05$ were reported and indicated using asterisks' *p<0.05, and ****p<0.0001.

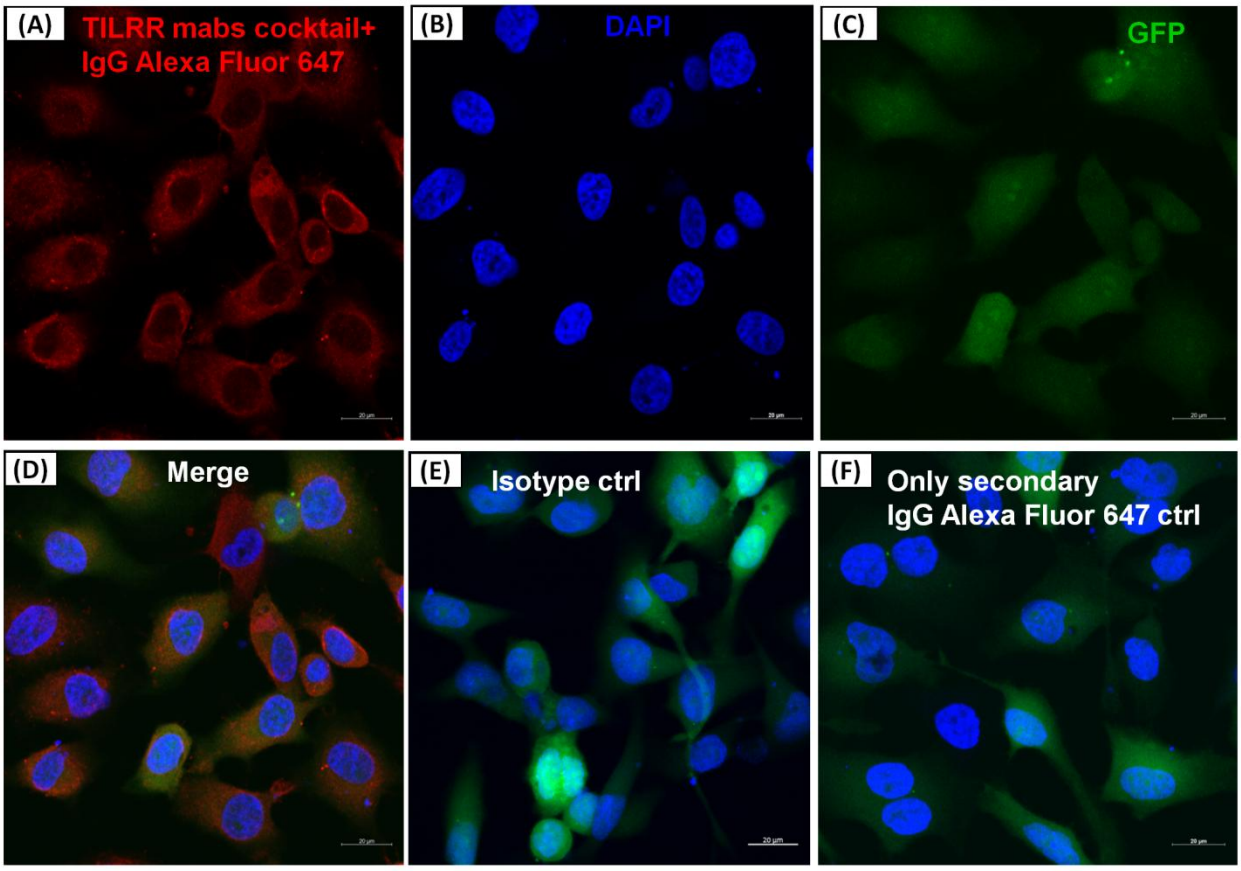

Figure 3.3: Confocal microscopy analysis of TILRR protein overexpression in transfected cells. (**A)** TILRR protein expression in HeLa cells transfected with TILRR plasmid DNA, (**B)** DAPI staining shown cell nuclei, **(C)** Transfected cells showing eGFP, **(D)** Merged expression of TILRR protein, eGFP, and nucleus, **(E)** Isotype control monoclonal antibody (F400G3S) staining, and **(F)** Alexa Fluor 647 labeled goat anti-mouse IgG secondary antibody only control. Color code: red, TILRR protein (Alexa Fluor 647 channel); blue, nuclear DNA (DAPI channel); and green, eGFP (FITC channel). Image captured using 20x objectives with a 20µm scale.

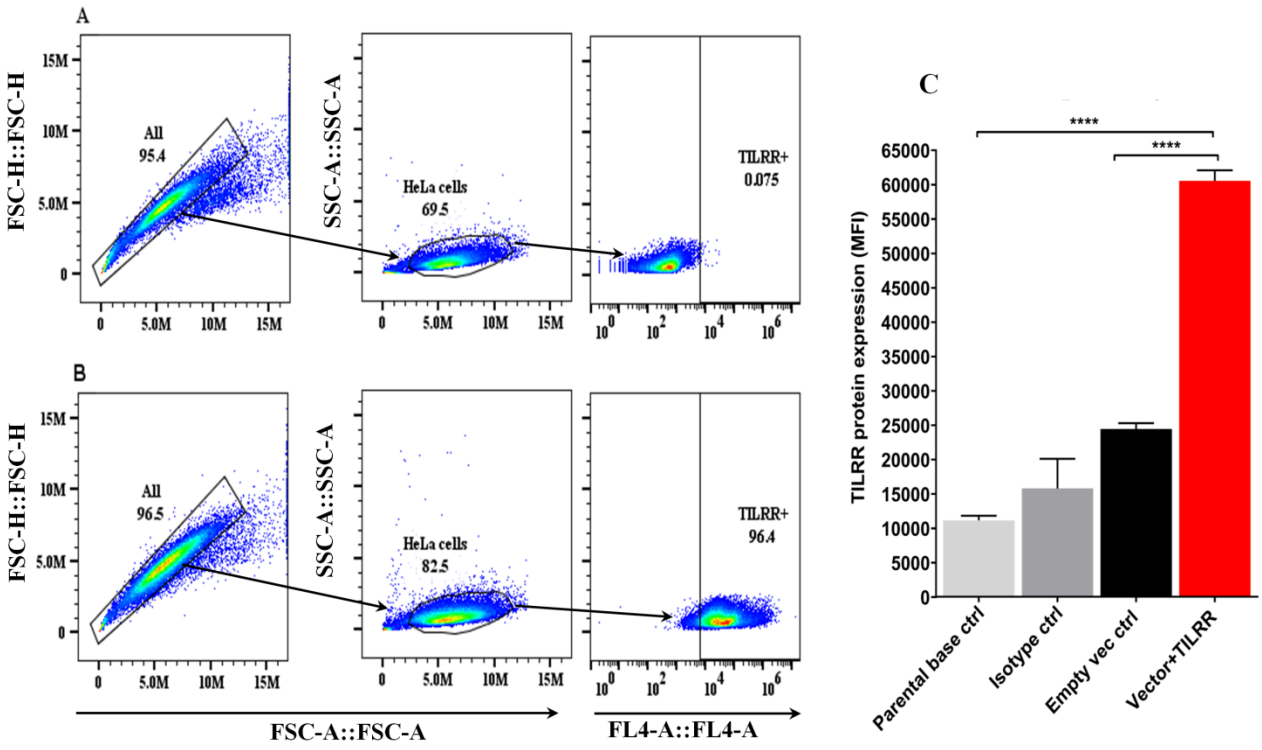

Figure 3.4: Flow cytometry analysis of TILRR protein overexpression in transfected cells. Flow cytometry confirmation of overexpressed TILRR protein in transfected HeLa cells. Cells were prepared by the recommended protocol as illustrated in the materials and methods chapter (**section 2.1.14**). (**A-B)** Gating strategy for TILRR protein expressed cells, A) Parental control cells, and B) TILRR overexpressed cells, (**C)** The overexpressed TILRR protein confirmed by analyzing the mean fluorescence intensity (MFI) in TILRR-transfected cells compared to the parental base, isotype, and empty vector-transfected control cells. Student t-test with 95% CI performed for the statistical analysis using GraphPad Prism version 7.03, all $p<0.05$ were reported and indicated using an asterisks' ****p<0.0001.

3.1.2 TILRR overexpression regulates the mRNA transcript expression of inflammation responsive genes in a dose-dependent manner

To examine the effect of different amounts of TILRR on immune and inflammation responsive genes, I co-transfected both HeLa and VK2/E6E7 cells with different concentrations of TILRR (vector+TILRR) (0.25-2.0 µg/well) or empty vector control (0.25-2.0 µg/well) plasmid DNA in combination with PmaxGFP plasmid DNA (0.05- 0.4 µg/well) and incubated at 37^{o} C for 24h as described in materials and methods chapter. Four genes (CCL5/RANTES, CXCL8/IL-8, IL-6, and TNFα) that play important role in immune activation and inflammatory response were selected to evaluate the effect of different amounts of TILRR on their mRNA expression. Different amounts of TILRR-plasmid DNA transfection did result in a dose-dependent increase in mRNA expression in HeLa cells **(Figure 3.5A and Appendix Table C7.3)** and VK2/E6E7 cells **(Figure 3.5B and Appendix Table C7.4).** HeLa cells transfected with 0.25-2.0 µg/well of TILRR-plasmid DNA significantly increased mRNA of all 4 genes in a dose-dependent manner except TNFα, which was only significantly increased with the dose of 0.5 µg/well or above (**Figure 3.5A**). In the case of VK2/E6E7 cells, the effect of different amounts of TILRR-plasmid DNA transfection was only observed for the mRNA of CXCL8 and IL-6 (**Figure 3.5B**). The data showed that one microgram of plasmid DNA per well worked best in upregulating the selected inflammation responsive genes (GeneCopoeia recommended protocol). Thus, 1.0 µg of plasmid DNA per well was used for all subsequent experiments in this study.

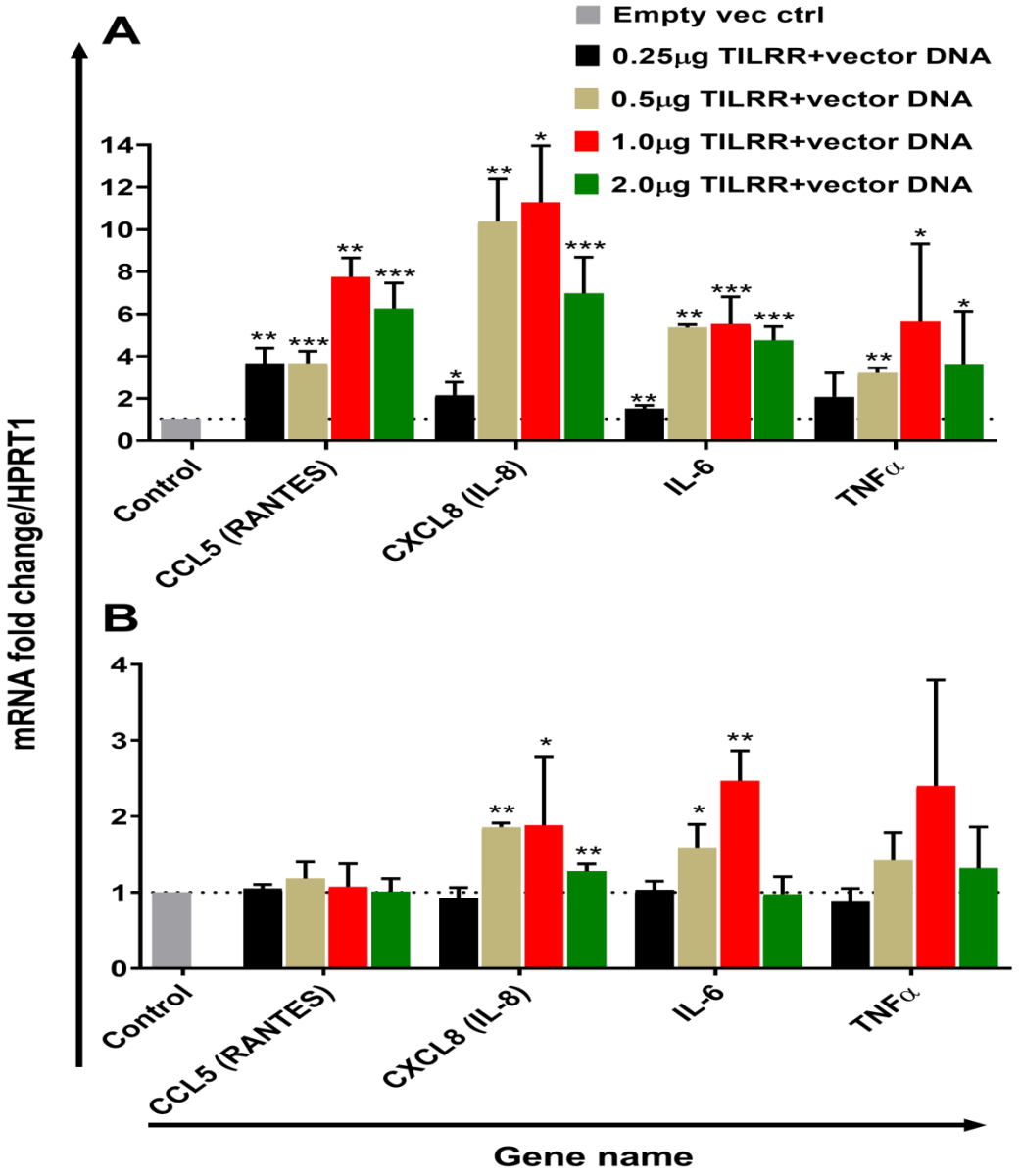

Figure 3.5: Dose-response effect of TILRR overexpression on the regulation of inflammation responsive genes. RT^2 qPCR Primer assay for mRNA transcripts of the 4 immune and inflammation responsive genes in HeLa **(A)** and VK2/E6E7 **(B)** cells. Data were analyzed using the GeneGlobe Data Analysis Centre (Qiagen) for RT^2 qPCR Primer assay. Fold induction for the individual gene in each concentration of TILRR-plasmid DNA transfected cells expressed as relative to levels of the respected concentration of empty vector-transfected control and show mean±SEM of three independent experiments. All data were normalized against the HPRT1 housekeeping gene. The statistical comparisons conducted using student t-test, all $p<0.05$ were reported and indicated using asterisks' *p<0.05, **p<0.01, and ***p<0.001. Legends on the upper right corner represent the experimental conditions with plasmid DNA concentrations.

3.1.3 Overexpression of TILRR significantly influenced the mRNA level of genes in the NF-κB signal transduction pathway

Next, I investigated the effect of TILRR overexpression on the 84 genes in the NF-κB signal transduction pathway. I hypothesized that upon interaction with the IL-1R1 receptor, TILRR would influence the downstream signaling events by regulating the mRNA transcript of genes in the NF-κB signal transduction pathway. To test this, I investigated the effect of overexpression of TILRR on a panel of 84-genes (grouped in several categories in **Table 3.1)** that are directly related to the NF-κB signaling pathway, immune activation, and inflammatory responses using the Human NF-κB pathway RT^2 profiler PCR array.

Table 3.1: Categories of NF-κB signaling pathway-related genes. (PAHS-025Z, Qiagen)

Category	Gene
NFκB Signaling Ligands	CXCL8(IL-8), IL-1A, IL-1B, IL-10, TNF
NFκB Signaling receptors	CD27 (TNFRSF7), CD40 (TNFRSF5), EGFR (ERBB1), F2R (PAR1), FASLG (TNFSF6), IL-1R1, LTBR, NOD1 (CARD4), TLR1, TLR2, TLR3, TLR4, TLR6, TLR9, TNFRSF1A (TNFR1), TNFRSF10A (TRAIL-R), TNFRSF10B (DR5), TNFSF10 (TRAIL), TNFSF14
NFκB Transcription Factors	ATF1, EGR1, ELK1, FOS, JUN, STAT1, NFKB1 (p105/p50), NFKB2 (p100/p52), REL (p65), RELA, RELB
Signaling Downstream of NFκB	BIRC2 (cIAP1), FADD, IRAK1, IRAK2, IRF1, MYD88, RIPK1, TBK1, TICAM1 (TRIF), TICAM2 (TRAM), TNFAIP3, TRADD, TRAF2, TRAF3, TRAF6
Immune Responsive genes	CCL2 (MCP-1), CCL5 (RANTES), CSF1 (M-CSF), CSF2 (GM-CSF), CSF3 (G-CSF), CXCL8 (IL-8), ICAM1, IFNA1, IFNG, LTA (TNFB), TNF
Cytoplasmic Sequestering / Releasing of NFκB	BCL3, CHUK (IKKα), IKBKB (IKKβ), IKBKE (IKKε), IKBKG, NFKBIA (IκBα), NFKBIB (IκBβ), NFKBIE
Apoptosis	AGT, BCL2A1 (BFL1), BCL2L1 (BCLXL), BIRC3 (c-IAP2)
Other NFκB Signaling	AKT1, MAP3K1 (MEKK1), RAF1, BCL10, CARD11, CASP1 (ICE), CASP8 (FLICE), CFLAR (Casper), HMOX1, MALT1, PSIP1, RHOA, TIMP1

I first assessed the mRNA transcript fold change of NF-κB signal transduction-related genes in transfected HeLa cells after 3 hours of incubation with serum-free DMEM. The result showed fold increase (FI) in mRNA expression of a few genes were significantly upregulated (CCL5, FI: 3.08±0.78, p=0.0026; CXCL8, FI: 1.48±0.26, p=0.0181; IRAK2, FI: 1.30±0.13, p=0.0256; IRAF1, FI: 1.26±0.18, p=0.0316; RIPK1, FI: 1.08±0.03, p=0.0417, TICAM1, FI: 1.13±0.08, p=0.0273; TLR4, FI: 1.14±0.07, p=0.0113) by TILRR overexpression at the 3 hour time point (**Figure 3.6A-F**).

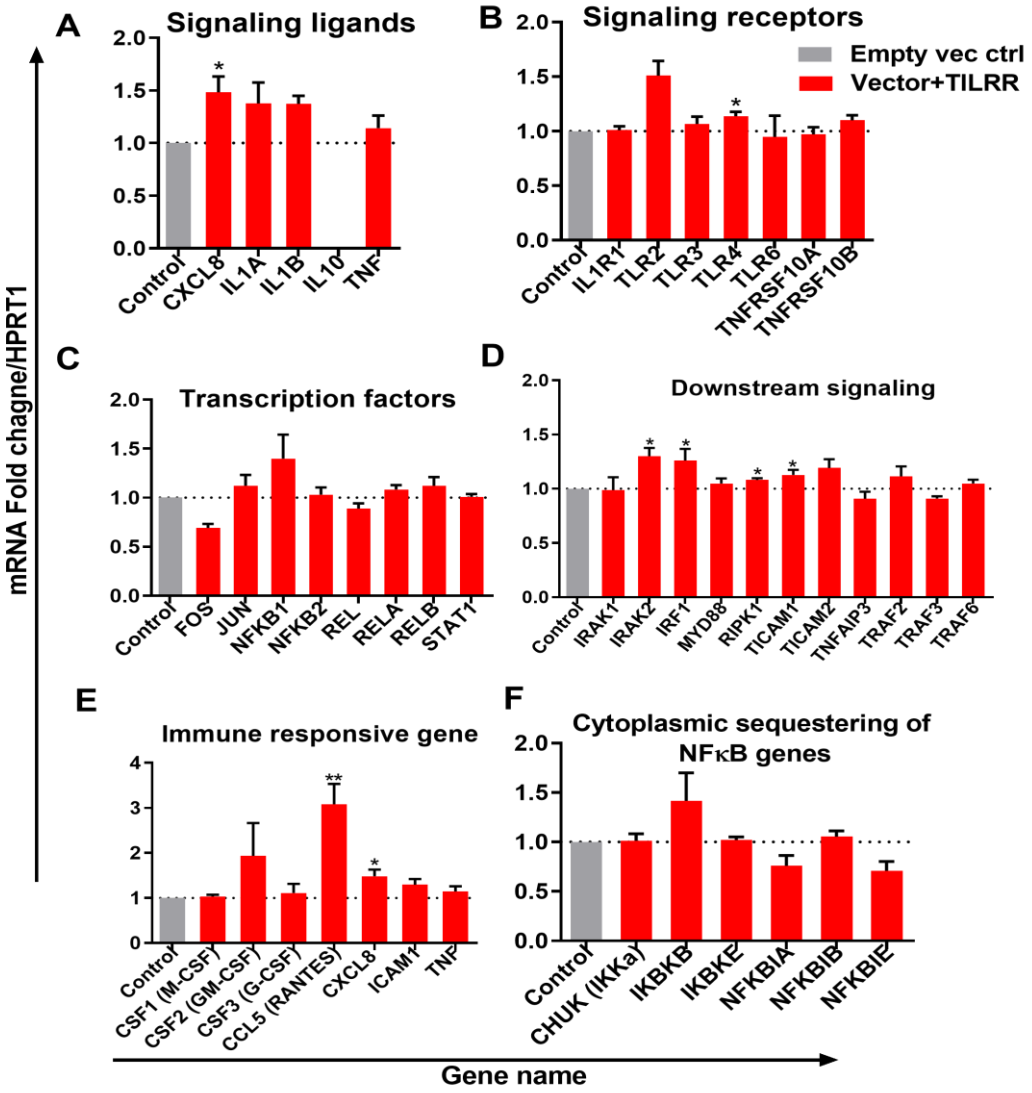

Figure 3.6: The mRNA transcripts fold change of NF-κB signal transduction pathway after three hours incubation following transfection. HeLa cells were transiently co-transfected with either pEZ-TILRR-M68 (Vector+TILRR) (1.0µg/5x10^5 cells) or pEZ-NEG-M68 (empty vector control) (1.0µg/5x10^5 cells) along with PmaxGFP (0.2µg/5x10^5 cells) in parallel experiments for 24h at 37^0C with 5% CO_2 as described in the materials and methods chapter. The cells were incubated in serum-free DMEM for 3h. Harvested RNAs from both cells used for the synthesis of cDNAs that finally run with RT^2 profiler qPCR array targeting NF-κB signaling components such as signaling ligands **(A),** signaling receptors **(B)**, transcription factors **(C),** downstream signaling genes **(D)**, immune responsive genes **(E)**, and cytoplasmic sequestering of NF-κB genes **(F).** Data were analyzed using the GeneGlobe Data Analysis Centre (Qiagen) for the RT^2 profiler PCR array. Fold induction for the individual gene in TILRR transfected cells expressed as relative to levels of empty vector-transfected control and show mean±SEM of three independent experiments. All data were normalized against the HPRT1 housekeeping gene. The statistical comparisons conducted using student t-test, all $p<0.05$ were reported and indicated using asterisks' *p<0.05, and **p<0.01. Legends on the upper right corner represent the experimental conditions.

The mRNA expressions of more genes were significantly influenced by the overexpression of TILRR in both cell lines at 24 hours as presented in the heat map (**Figure 3.7**).

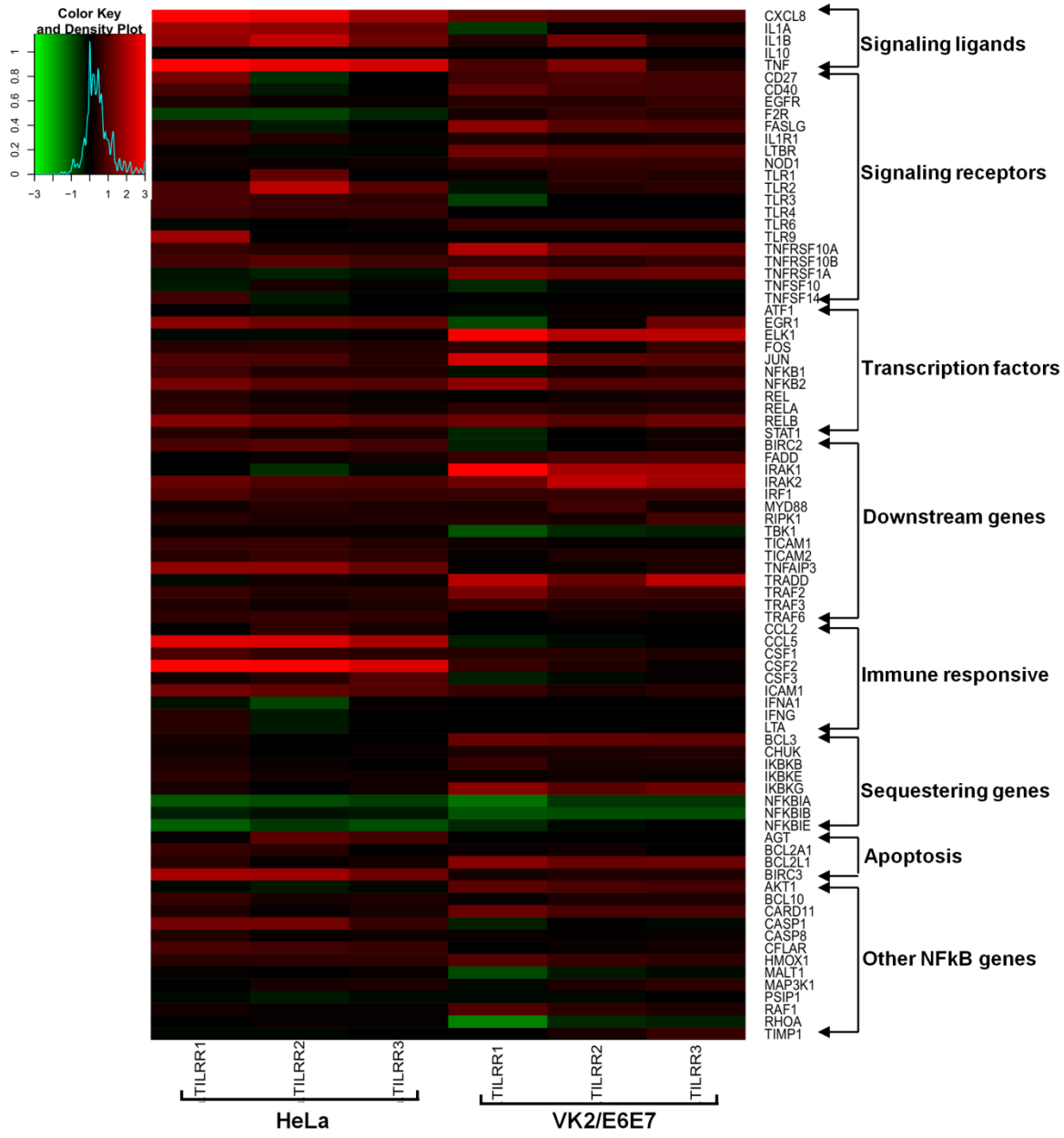

Figure 3.7: Heat map presentation of up- and down-regulated genes in the NF-κB pathway for the presence of TILRR. Log2 fold changes of gene expression in HeLa and VK2/E6E7 cells generated by RStudio (https://www.rstudio.com). Gradient red color indicates the up-regulated genes; gradient green represents the down-regulated genes. Solid black means baseline, which represents the fold change 1 or log2= 0 (control). The X-axis showing the triplicate biological samples for each cell line, the Y-axis (right side) represents the 84 tested genes categorized into different groups. Legend on the upper left side shows the scale of log2 fold change.

Of the 84 genes, 49- and 41-genes were significantly up-regulated in HeLa and VK2/E6E7 cells, respectively (**Figure 3.8A**). Seven genes were significantly down-regulated in HeLa (AKT1, FI: 0.87±0.09, p=0.0277; F2R, FI: 0.64±0.20, p=0.0046; NFKBIA, FI: 0.54±0.06, p=0.0011; NFKBIB, FI: 0.80±0.04, p=0.0020; NFKBIE, FI: 0.54±0.09, p=0.0015; PSIP1, FI: 0.87±0.08, p=0.0098; TNFRSF1A, FI: 0.81±0.06, p=0.0055); 3 genes were down-regulated in VK2/E6E7 cells (NFKBIB, FI: 0.53±0.01, p=0.0057; STAT1, FI: 0.55±0.16, p=0.0442; and TBK1, FI: 0.67±0.14, p=0.0309) (**Figure 3.8B).** No significant fold change observed for 28 and 40 genes in HeLa and VK2/E6E7 cells, respectively (**Figure 3.8C**).

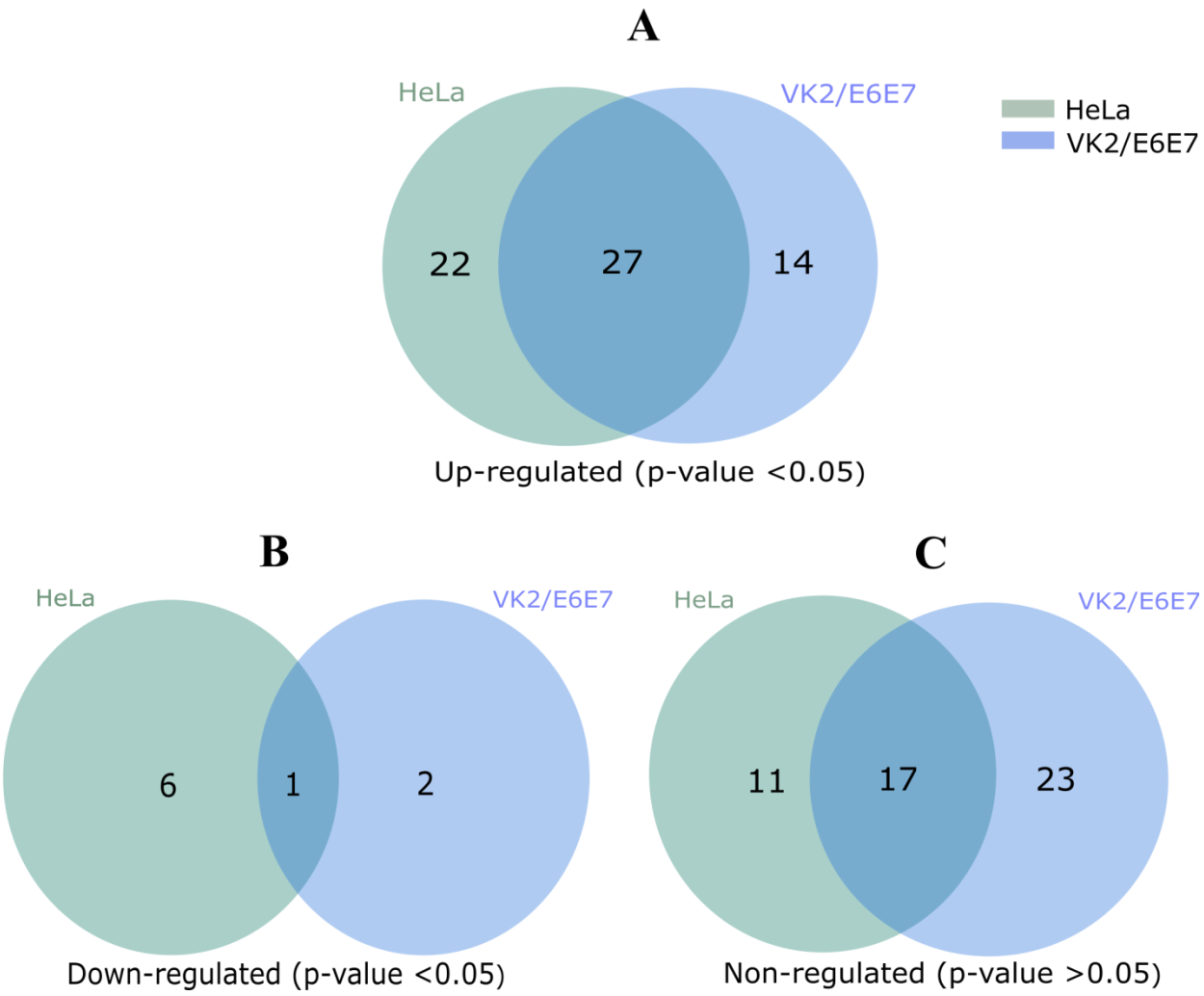

Figure 3.8: Venn diagram presentation of total regulated genes in the NF-κB signal transduction pathway. A) The significantly up-regulated genes in HeLa and VK2/E6E7 cells (p<0.05), **B)** The significantly down-regulated genes in both cell lines (p<0.05), and **C)** Non-influenced genes in both HeLa and VK2/E6E87 for the presence of TILRR (p>0.05). Legends on the upper right corner represent the cell lines. The right circle represents the HeLa cells, the left circle for VK2/E6E7 cells, and the center overlapping circle represents the combined regulated genes in both cell lines. Venn diagrams were made using pyvenn (https://github.com/tctianchi/pyvenn).

The expression of NF-κB signaling ligands, such as CXCL8 (IL-8) and IL-1β was significantly up-regulated in HeLa cells (CXCL8, FI: 6.33±2.48, p=0.0154; and IL-1β, FI: 3.44±1.15, p=0.0084) and in VK2/E6E7 cells (CXCL8, FI: 2.55±0.92, p=0.0252; IL-1β, FI: 2.23±0.64, p=0.0379). The magnitude of increase of these signaling ligands is higher in HeLa cells. Significant increases in IL-1α (FI: 3.05±0.70, p=0.0126) and TNFα (FI: 5.63±3.69, p=0.0100) expression were only observed in HeLa cells. Overexpression of TILRR appears to have no effect on mRNA of IL-10 detection in these two cell lines **(Figure 3.9A**).

Overexpressing TILRR in HeLa cells significantly increased the expression of 6 out of 7-signaling receptors including IL-1R1 (FI: 1.36±0.24, p=0.0263), TLR2 (FI: 2.82±1.52, p=0.0278), TLR3 (FI: 1.58±0.17, p=0.0004), TLR4 (FI: 1.57±0.10, p=0.0055), TNFRSF10A (FI: 1.42±0.08, p=0.0003) and TNFRSF10B (FI: 1.80±0.21, p=0.0012) (**Figure 3.9B**). In particular, IL-1R1 and TNFRSF10B receptor expression were significantly up-regulated in both HeLa (IL-1R1, FI: 1.36±0.24, p=0.0263 and TNFRSF10B, FI: 1.80±0.21, p=0.0012) and VK2/E6E7 (IL-1R1, FI: 1.23±0.03, p=0.0238 and TNFRSF10B, FI: 1.49±0.06, p=0.0032) cells, respectively. However, TLR6 (FI: 1.57±0.03, p=0.0007) expression was only significantly increased in VK2/E6E7 cells, and TLR6 mRNA was unaltered in TILRR transfected HeLa cells. Further, there was no significant effect on TLR4 mRNA detection in VK2/E6E7 cells.

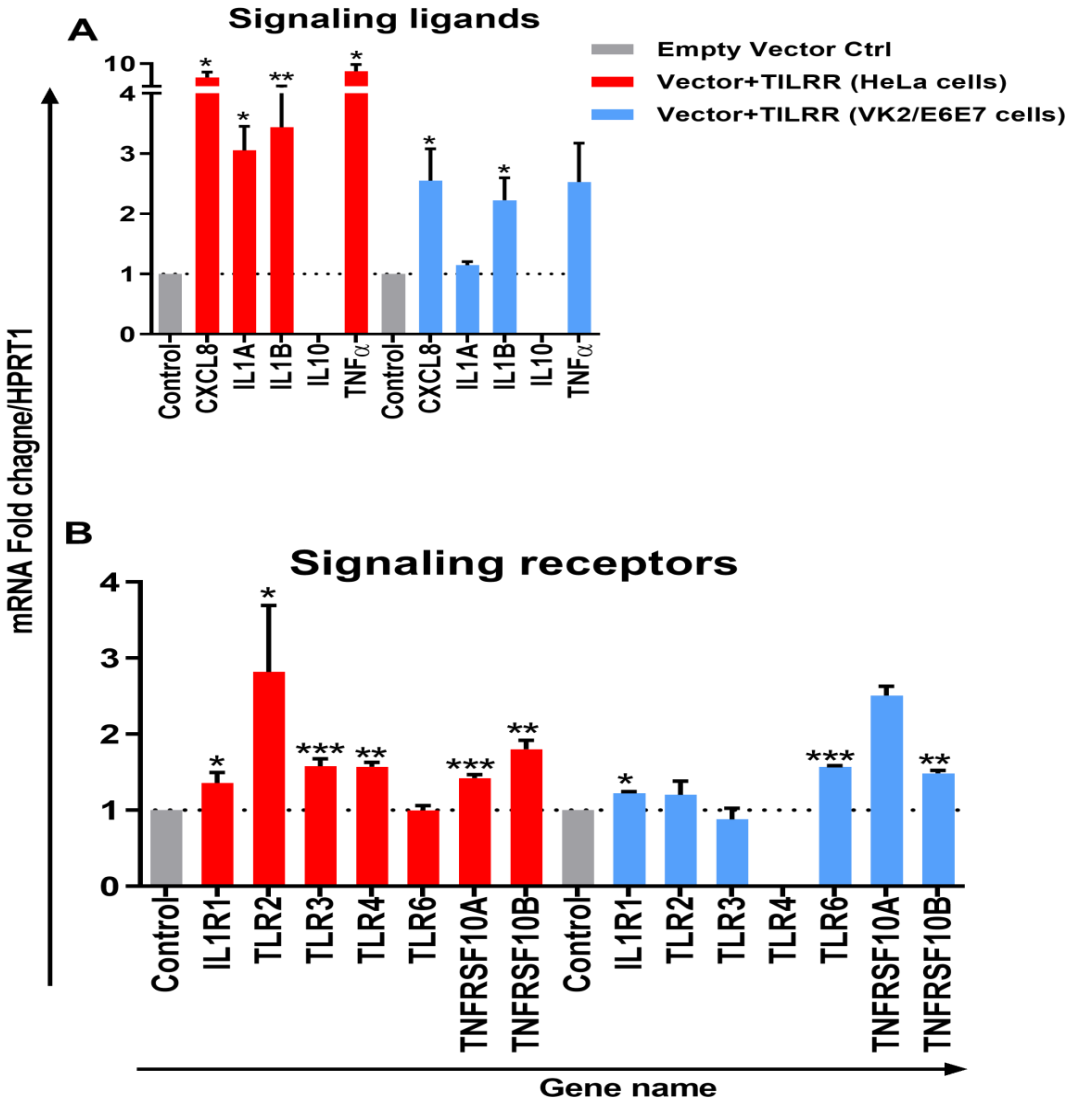

Figure 3.9: TILRR induces expression of signaling ligands and singling receptor genes in the NF-κB signal transduction pathway. HeLa and VK2/E6E7 cells were transiently co-transfected with either pEZ-TILRR-M68 (vector+TILRR) (1.0µg/5x10^5 cells) or pEZ-NEG-M68 (empty vector control) (1.0µg/5x10^5 cells) along with PmaxGFP (0.2µg/5x10^5 cells) in parallel experiments for 24h at 37^0C with 5% CO_2 as described in the material and methods chapter. Harvested RNAs from both cells were used for the synthesis of cDNAs that finally run with RT^2 profiler qPCR array targeting NF-κB signaling components, such as signaling ligands **(A),** signaling receptors **(B).** Data were analyzed using the GeneGlobe Data Analysis Centre (Qiagen) for the RT^2 profiler PCR array. Fold induction for the individual gene in TILRR transfected cells expressed as relative to levels of empty vector-transfected control and show mean±SEM of three independent experiments. All data were normalized against the HPRT1 housekeeping gene. The statistical comparisons conducted using student t-test, all $p<0.05$ were reported and indicated using asterisks' *p<0.05, **p<0.01, and ***p<0.001. Legends on the upper right corner represent the cells with experimental conditions.

TILRR overexpression enhanced the expression of 8 NF-κB transcription factors (**Figure 3.10A**) in HeLa cells. Of which, the expression of FOS (FI: 1.41±0.07, *p*=0.0124), JUN (FI: 1.68±0.25, *p*=0.0266), NFκB1 (p105/p50) (FI: 1.44±0.16, *p*=0.0036), NFκB2 (p100/p52) (FI: 2.16±0.27, *p*=0.0004), REL (p65) (FI: 1.25±0.14, *p*=0.0182), RELA (FI: 1.31±0.15, *p*=0.0091), RELB (FI: 2.40±0.48, *p*=0.0066), and STAT1 (FI: 1.27±0.12, *p*=0.0046) was significantly increased. However, only the expression of four NF-κB transcription factors significantly increased in VK2/E6E7 cells, including JUN (FI: 2.28±0.92, *p*= 0.0499), NFκB1 (p105/p50) (FI: 1.41±0.24, *p*=0.0421), NFκB2 (p100/p52) (FI: 1.82±1.09, *p*=0.0494) and RELB (FI: 2.32±0.21, *p*= 0.0173).

The expression of mRNA of genes directly connected to the downstream NF-κB signaling was significantly increased following TILRR overexpression in both cell lines (**Figure 3.10B**). These included IRAK2 (FI: 2.01±0.27, *p*=0.0024 and FI: 2.08±0.48, *p*=0.0182), IRF1 (FI: 1.64±0.18, *p*=0.0043 and FI: 1.32±0.24, *p*=0.0002), RIPK1 (FI: 1.34±0.04, *p*=0.0002, and FI: 1.45±0.27, *p*=0.0361), and TICAM1 (FI: 1.51±0.15, *p*=0.0030, and FI: 1.19±0.06, *p*=0.0247) in HeLa and VK2/E6E7 cells, respectively. Furthermore, TICAM2 (FI: 1.45±0.05, *p*=0.0093, and FI: 1.21±0.11, *p*=0.0093), TRAF2 (FI: 1.43±0.11, *p*=0.0023, and FI: 1.96±0.59, *p*=0.0319), TRAF3 (FI: 1.27±0.09, *p*=0.0080, and FI: 1.39±0.09, *p*=0.0061) and TRAF6 (FI: 1.47±0.03, *p*=0.0004, and FI: 1.12±0.06, *p*=0.0247) were also increased in HeLa and VK2/E6E7 cells, respectively. In addition, MYD88 (FI: 1.30±0.12, *p*=0.0425) and TNFAIP3 (FI: 2.81±0.48, *p*=0.0049) were enhanced in HeLa cells whereas IRAK1 (FI: 2.86±1.67, *p*=0.0013) in VK2/E6E7 cells only.

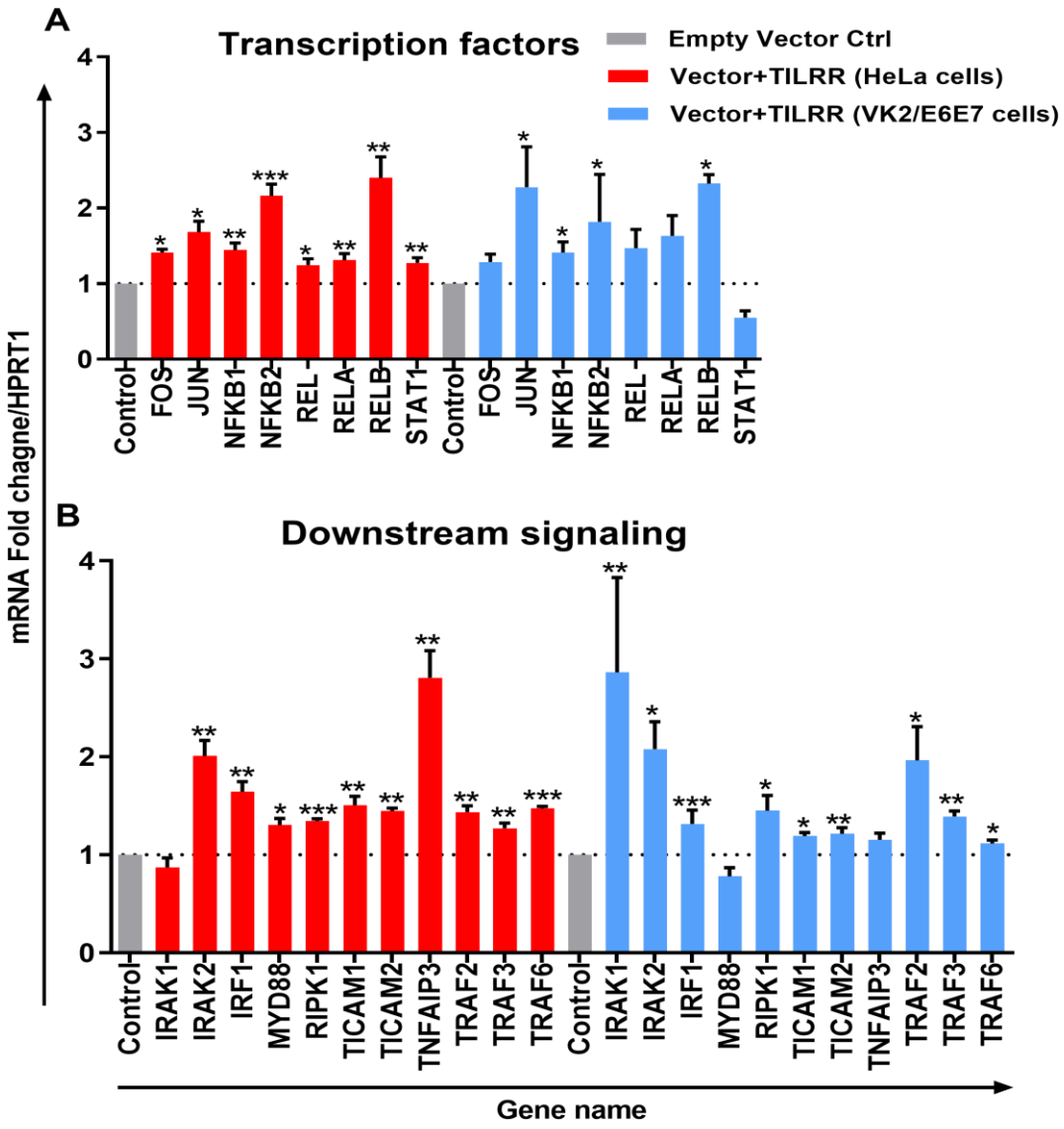

Figure 3.10: TILRR induces expression of transcription factors and downstream signaling genes in the NF-κB signal transduction pathway. HeLa and VK2/E6E7 cells were transiently co-transfected with either pEZ-TILRR-M68 (vector+TILRR) (1.0µg/5x10^5 cells) or pEZ-NEG-M68 (empty vector control) (1.0µg/5x10^5 cells) along with PmaxGFP (0.2µg/5x10^5 cells) in parallel experiments for 24h at 37^{0}C with 5% CO_2 as described in the material and methods chapter. Harvested RNAs from both cells were used for the synthesis of cDNAs that finally run with RT^2 profiler qPCR array targeting NF-κB signaling components such as transcription factors **(A),** downstream signaling genes **(B).** Data were analyzed using the GeneGlobe Data Analysis Centre (Qiagen) for the RT^2 profiler PCR array. Fold induction for the individual gene in TILRR transfected cells expressed as relative to levels of empty vector-transfected control and show mean±SEM of three independent experiments. All data were normalized against the HPRT1 housekeeping gene. The statistical comparisons conducted using student t-test, all p<0.05 were reported and indicated using asterisks' *p<0.05, **p<0.01, and ***p<0.001. Legends on the upper right corner represent the cells with experimental conditions.

The expression of immune responsive genes directly associated with the NF-κB signaling pathway was also examined. I observed significant induction of mRNA transcripts for 7 immuno-regulatory genes when TILRR was overexpressed **(Figure 3.11A)**. The expression of CSF1 (M-CSF) (FI: 1.56±0.20, p=0.0065 and FI: 1.35±0.08, p=0.0031), CSF2 (GM-CSF) (FI: 8.46±2.93, p=0.0261 and FI: 1.34±0.23, p=0.0249), CXCL8 (IL-8) (FI: 6.33±2.48, p=0.0154, and FI: 2.55±0.92, p=0.0252), and ICAM1 (FI: 2.22±0.33, p=0.0011 and FI: 1.42±0.14, p=0.0155) was enhanced in TILRR transfected HeLa and VK2/E6E7 cells, respectively. CSF3 (G-CSF) and CCL5 (RANTES) were only significantly regulated in HeLa cells.

Finally, I examined the effect of TILRR on the expression of genes that are involved in cytoplasmic sequestration or release of NF-κB complex proteins (**Figure 3.11B**). The expression of three out of six genes evaluated was significantly up-regulated in the HeLa cell line, including CHUK (IKKa), IKBKB (IKKβ), and IKBKE (IKKε). Only the expression of CHUK was up-regulated in VK2/E6E7 cells. Thus, TILRR has a direct influence on genes involved in the formation of transcription factors NFκB1 (p50) and NFκB2 (p52) that subsequently translocate to the nucleus and potentiate signal transduction.

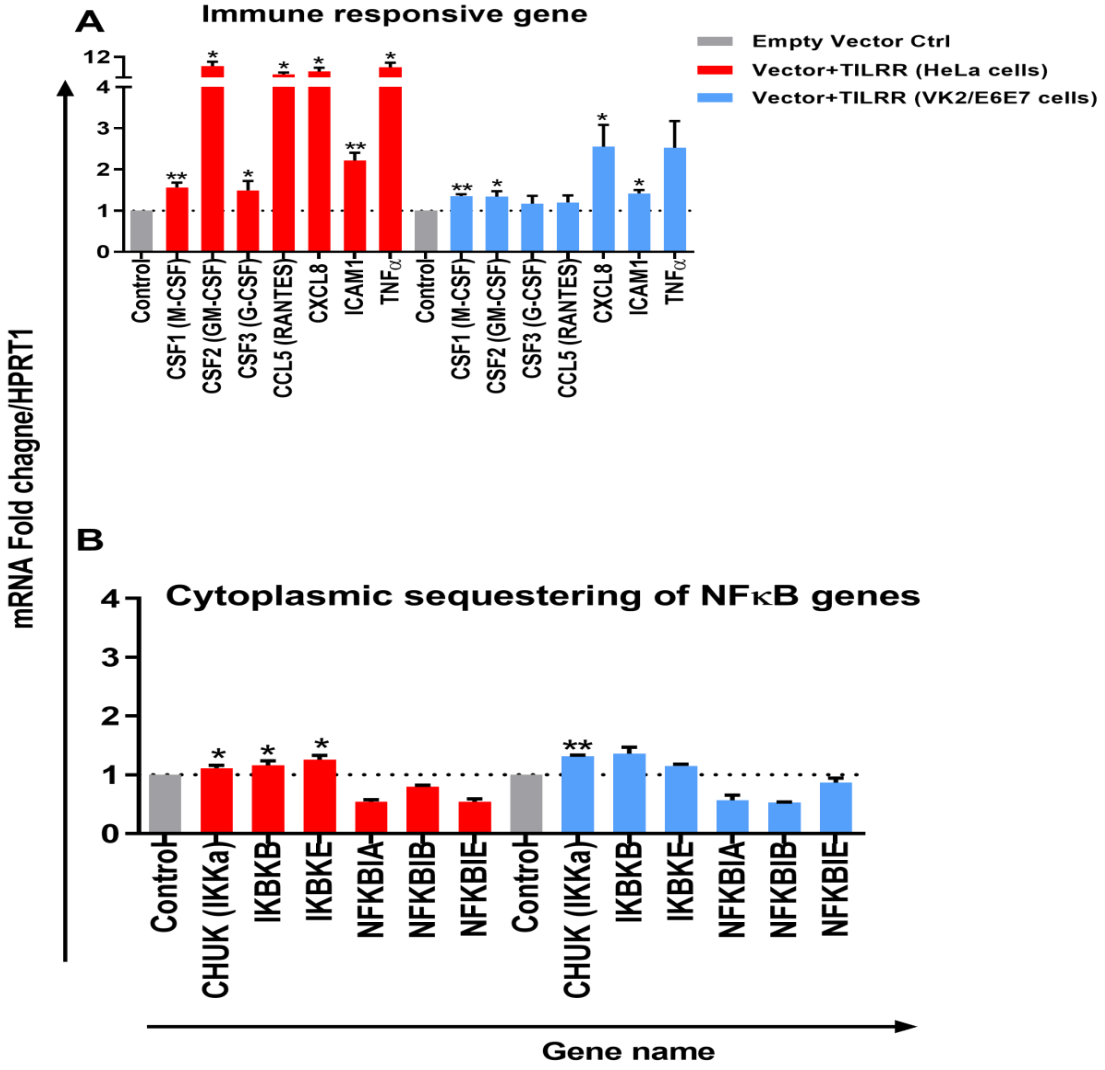

Figure 3.11: TILRR induces expression of immune responsive and cytoplasmic sequestering genes in the NF-κB signal transduction pathway. HeLa and VK2/E6E7 cells were transiently co-transfected with either pEZ-TILRR-M68 (vector+TILRR) (1.0µg/5x10^5 cells) or pEZ-NEG-M68 (empty vector control) (1.0µg/5x10^5 cells) along with PmaxGFP (0.2µg/5x10^5 cells) in parallel experiments for 24h at 37^0C with 5% CO_2 as described in the material and methods chapter. Harvested RNAs from both cells were used for the synthesis of cDNAs that finally run with RT^2 profiler qPCR array targeting NF-κB signaling components such as immune responsive genes **(A)**, and cytoplasmic sequestering of NF-κB genes **(B).** Data were analyzed using the GeneGlobe Data Analysis Centre (Qiagen) for the RT^2 profiler PCR array. Fold induction for the individual gene in TILRR transfected cells expressed as relative to levels of empty vector-transfected control and show mean±SEM of three independent experiments. All data were normalized against the HPRT1 housekeeping gene. The statistical comparisons conducted using student t-test, all $p<0.05$ were reported and indicated using asterisks' *p<0.05, **p<0.01, and ***p<0.001. Legends on the upper right corner represent the cells with experimental conditions.

3.1.4 TILRR along with IL-1β increases the mRNA transcript expression of various inflammatory cytokines/chemokines related genes

I further tested the effect of TILRR overexpression in the presence of IL-1β on selected genes directly involved in immune activation and inflammatory response in HeLa and VK2/E6E7 cells. TILRR transfected HeLa and VK2/E6E7 cells were incubated with or without IL-1β in parallel experiments and the expression of mRNA transcript was quantified using RT^2 qPCR Primer assay. The results showed that TILRR overexpression, in the presence or absence of added IL-1β, significantly increased the expression of 4 immune and inflammation responsive genes in HeLa and VK2/E6E7 cells (**Figure 3.12)**. In the absence of added IL-1β, TILRR overexpression significantly increased mRNA transcript fold change of CXCL8 (IL-8) (FI: 6.33±2.48, p=0.0154), IL-6 (FI: 5.52±1.30, p=0.005), and TNFα (FI: 5.63±3.69, p=0.0100) in HeLa cells; and CXCL8 (IL-8) (FI: 2.55±0.92, p=0.0252) and IL-6 (FI: 2.47±0.40, p=0.0031) in VK2/E6E7 cells compared to empty vector control. CCL5 (RANTES) (FI: 5.24±1.23, p=0.0116) was an exception, which was only significantly enhanced in HeLa cells for the TILRR overexpression.

In the presence of added IL-1β, TILRR overexpression also significantly increased mRNA transcripts of these immune and inflammation responsive genes in comparison to the empty control vector. These include CCL5 (RANTES) (FI: 27.48±3.25, p=0.0006), CXCL8 (IL-8) (FI: 63.58±5.94, p<0.0001), IL-6 (FI: 28.03±11.08, p=0.0057) and TNFα (FI: 8.67±1.53, p=0.0005) in HeLa cells; and CCL5 (RANTES) (FI: 3.66±0.54, p=0.0016), CXCL8 (IL-8) (FI: 3.72±1.23, p=0.0183), IL-6 (2.98±0.40, p=0.0010) and TNFα (FI: 2.73±0.54, p=0.0051) in VK2/E6E7 cells. These results support that TILRR acts as a co-receptor of IL-1R1, which enhances the activation of NFκB signaling genes in the inflammatory response during microbial infection.

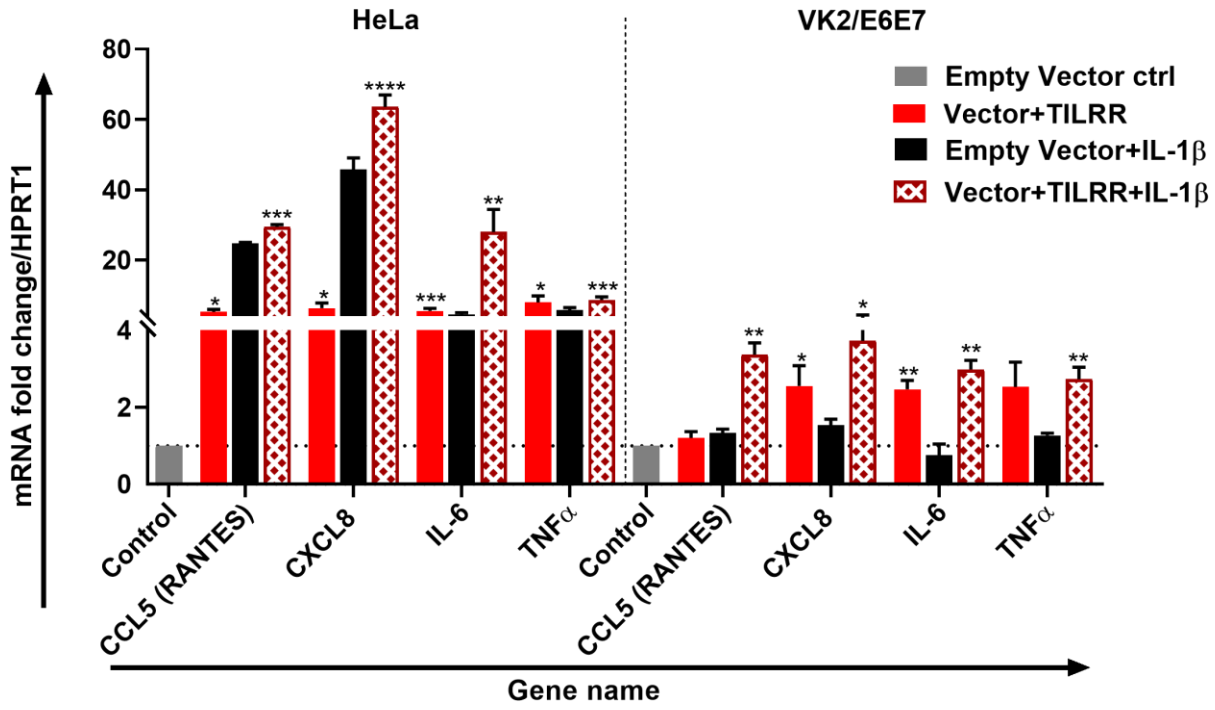

Figure 3.12: TILRR enhances the expression of immune-responsive genes in the presence or absence of added IL-1β. HeLa ($5x10^5$/well) and VK2/E6E7 ($5x10^5$/well) cells were transiently co-transfected with either pEZ-TILRR-M68 (vector+TILRR) (1.0µg/well) or pEZ-NEG-M68 (empty vector control) (1.0µg/well) along with PmaxGFP (0.2µg/well) in parallel experiments as described in materials and methods. In parallel experiments, the cells were incubated with the addition of IL-1β (1nM) in serum-free DMEM (HeLa) or Keratinocyte SFM (1X) (VK2/E6E7) media for 24 hours at 37^o C. Data were analyzed using GeneGlobe Data Analysis Centre (Qiagen) for RT^2 qPCR Primer assay. Fold increase for individual gene in TILRR transfected (vector+TILRR) cells, in the presence or absence of IL-1β, expressed as relative to levels of empty vector-transfected control and show mean±SEM of three independent experiments. All data were normalized against the HPRT1 housekeeping gene. The statistical comparisons conducted using student t-test, all $p<0.05$ were reported and indicated using asterisks' *p<0.05, **p<0.01, ***p<0.001, and ****p<0.0001. Legends on the upper right corner represent the cells with experimental conditions.

3.1.5 SUMMARY

This study examined whether the overexpression of TILRR could lead to the increase of mRNA expression of genes associated with the IL-1-NF-κB inflammatory signaling pathway using *in vitro* model systems (HeLa and VK2/E6E7 cell lines). I overexpressed TILRR in HeLa and VK2/E6E7 epithelial cell lines and analyzed the mRNA expression of 84 genes in the NF-κB signaling pathway using a PCR array system. The results showed that TILRR was successfully overexpressed in transfected HeLa and VK2/E6E7 cells and overexpression of TILRR significantly increased the mRNA expression of inflammation responsive genes in a dose-dependent manner. Overexpressed-TILRR significantly influenced the mRNA level expression of many genes in the NF-κB signaling pathway, including signaling ligands, signaling receptors, transcription factors, immune responsive genes, and downstream signaling molecules. Additionally, TILRR alone or in combination with IL-1β increased the mRNA transcript expression of many inflammatory cytokines/chemokines-related genes. Thus, TILRR overexpression significantly increased the mRNA transcript expression of immune and inflammation responsive genes in cervicovaginal epithelial cell lines.

Since TILRR increased the expression of many downstream signaling genes in the NF-κB pathway, its overexpression in cervicovaginal epithelial cells may promote the production of soluble pro-inflammatory cytokines/chemokines in transfected cell culture supernatants. Thus, I examined the culture supernatants of TILRR-overexpressed HeLa and VK2/E6E7 cells using an in-house developed multiplexed bead array method to quantify soluble pro-inflammatory mediators. The results of the analysis of pro-inflammatory mediators are described in the next section.

3.2 EFFECT OF TILRR ON THE PRODUCTION OF SOLUBLE CYTOKINES/CHEMOKINES IN CERVICOVAGINAL EPITHELIAL CELLS

The results of this section are based on the following article:

Toll-like Interleukin 1 Receptor Regulator Is an Important Modulator of Inflammation Responsive Genes. Frontiers in Immunology, 2019. **10**(272): p. 1-16.

Mohammad Abul Kashem[1,3], Hongzhao Li[1,3], Nikki Pauline Toledo[1,3], Robert Were Omange[1,3], Binhua Liang[2,3], Lewis Ruxi Liu[1,3], Lin Li[1,3], Xuefen Yang[3], Xin-Yong Yuan[4], Jason Kindrachuk[1], Francis A Plummer[1], Ma Luo[1,3,4]

[1]Department of Medical Microbiology and Infectious Diseases, University of Manitoba, Winnipeg, MB, Canada
[2]Department of Biochemistry & Medical Genetics, University of Manitoba, Winnipeg, MB, Canada
[3]JC Wilt Infectious Diseases Research Centre, National Microbiology Laboratory, Winnipeg, MB, Canada
[4]National Microbiology Laboratory, Public Health Agency of Canada, Winnipeg, MB, Canada.

Authors' Contributions

MK, FP, and ML conceived and designed research; **MK** performed all research, analyzed the data, generated figures/tables, organized the writing materials, and wrote the paper; HL helped in Western blot study; NT helped in cytokines/chemokines study, LL and XY helped in Confocal microscopy study; FP and ML acquired funding; XYY supported reagents; BL, FP, and ML supervised research; and ML, HL, RO, LRL, BL, and JK edited the paper. **MK** revised, formatted, submitted, and responded to the reviewers' comments.

Funding

The study was funded by an operating grant from the Canadian Institutes of Health Research (CIHR), Operating grant- PA: CHVI Vaccine Discovery and Social Research. URL: http://www.cihr-irsc.gc.ca/e/193.html.

3.2.1 TILRR overexpression significantly increased the production of pro-inflammatory cytokine/chemokine proteins in HeLa cell culture supernatants

To examine whether the production of specific cytokine/chemokine was also influenced by the overexpression of TILRR, I quantified the production of 13 cytokines/chemokines in TILRR transfected HeLa and VK2/E6E7 cell culture supernatants using an in-house developed 13-plex bead array assay. The 13-plex bead array assay was designed to measure most of the important cytokines/chemokines that are associated with the induction of innate immune responses, inflammation, and inflammatory diseases, and enhanced HIV acquisition. This 13-plex bead array assay was developed to quantify inflammatory mediators in several other projects in our lab. It performed well and was cost-effective.

The results showed that TILRR overexpression, in the absence of added IL-1β, significantly increased the production of several pro-inflammatory cytokines/chemokines in HeLa cells compared to the empty vector control during the observed time points from 1 to 24 h **(Figure 3.13** and **Appendix Table C7.5**; fold change [mean±SEM] for cytokines/chemokines is shown in **Appendix Table C7.5)**. After 1h incubation with serum free media, IL-6 (p= 0.0014), IL-8 (CXCL8) (p< 0.0001), IP-10 (p<0.0001), and MCP-1 (p= 0.0064) were significantly increased in culture supernatants. After 3-, 6- and 15-h incubation, I observed significantly higher production of IL-6 (p= 0.0004, <0.0001, and 0.0011), IL-8 (CXCL8) (p= 0.0004, 0.0005, and <0.0001), IP-10 (p= 0.0012, <0.0001, and <0.0001), and MCP-1 (p= 0.0035, 0.0013, and 0.0001) in HeLa cell culture supernatants, except RANTES (CCL5) (p= 0.0024), which was only increased after 15h incubation. The level of IL-6 (p< 0.0001), IL-8 (CXCL8) (p= 0.0002), IP-10 (p< 0.0001), RANTES (CCL5) (p= 0.0001), and MCP-1 (p< 0.0001) in the cell culture supernatant of TILRR-transfected HeLa cells remained high at 24 h. The data showed the consistency between mRNA

and protein level expression of IL-8 (CXCL8) and RANTES (CCL5). However, CSF2 (GM-CSF), IFNγ, IL-10, IL17A, MIP-1α, and TNFα were not detected in the HeLa cell culture supernatant (data not shown). Thus, overexpression of TILRR enhanced the production of many pro-inflammatory cytokine/chemokine(s) in HeLa cell culture supernatants.

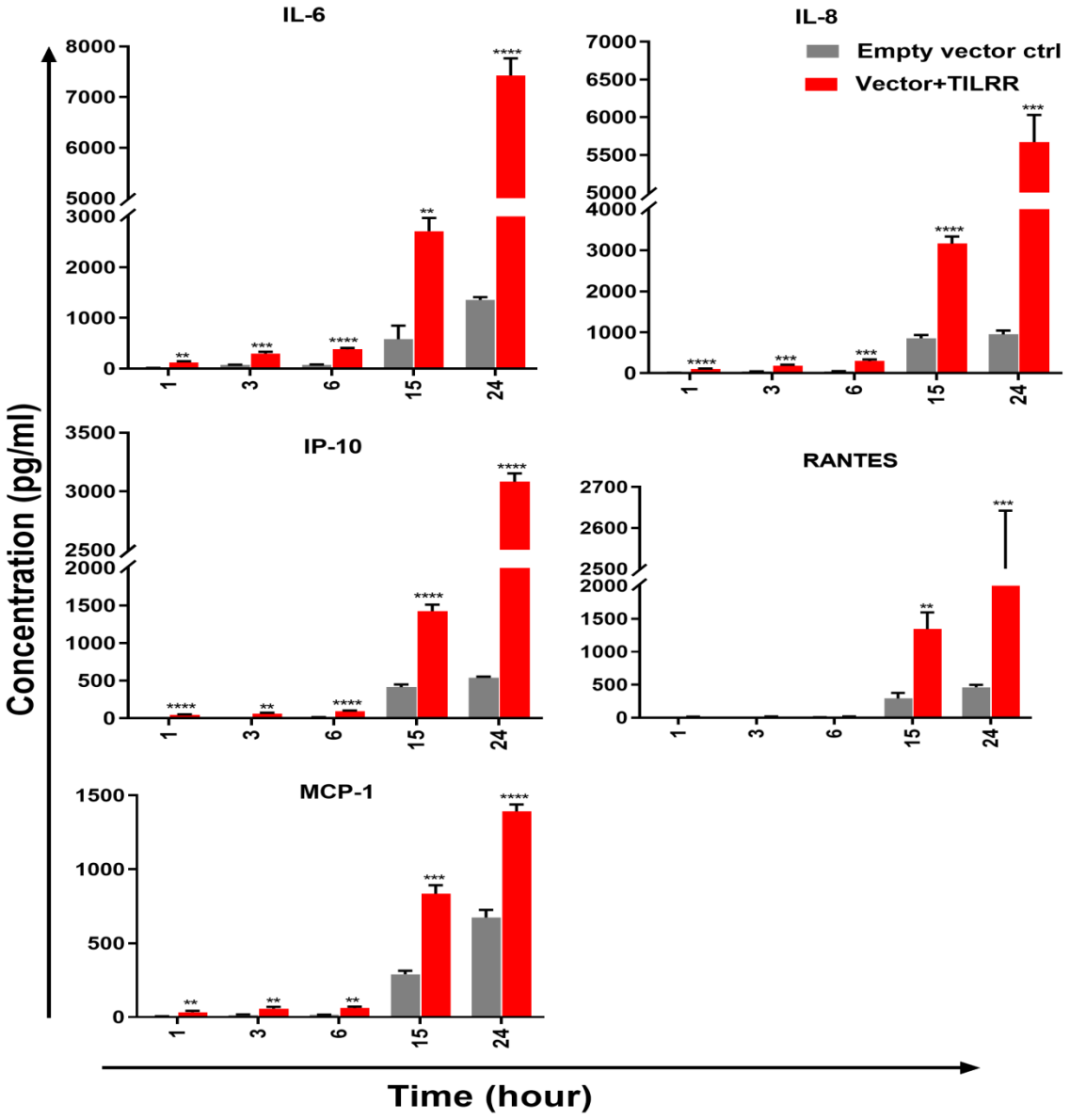

Figure 3.13: TILRR overexpression in HeLa cells increased the production of pro-inflammatory cytokines/chemokines. HeLa ($5x10^5$cells/well) cells were co-transfected with either pEZ-TILRR-M68 (1.0µg/$5x10^5$ cells) or pEZ-NEG-M68 (1.0µg/$5x10^5$ cells) with PmaxGFP (0.2µg/$5x10^5$ cells) vector as explained in the materials and methods chapter. Cells were incubated with serum-free DMEM medium for different time points and supernatants were collected. Thirteen different inflammatory cytokines were measured using an in-house developed multiplex cytokines/chemokines bead assay with Bio-Plex 200 (Bio-Rad). The data represent the relative level of vector+TILRR compared to the empty vector control. The sample measurements below the detection limit were assigned as zero. The data represent the mean of three independent experiments (mean±SEM). Statistical comparisons conducted using student t-test with 95% CI, all $p<0.05$ were reported and indicated using an asterisks' *$p<0.05$, **$p<0.01$, ***$p<0.001$, and ****$p<0.0001$.

3.2.2 TILRR overexpression significantly increased the production of pro-inflammatory cytokine/chemokine proteins in normal vaginal mucosal (VK2/E6E7) cell culture supernatants

I next examined the level of cytokines/chemokines production in culture supernatants of TILRR-overexpressed VK2/E6E7 cells. Similar to the HeLa cells, in the absence of IL-1β, there was a gradual increase of cytokine/chemokine(s) production in VK2/E6E7 cell culture supernatants at different time points compared to the empty vector-transfected cells **(Figure 3.14** and **Appendix Table C7.6**; fold change is shown in **Appendix Table C7.6).** Unlike the HeLa cells, I observed that after 1h incubation with serum-free media, only IP-10 (p= 0.0109) was significantly increased in TILRR overexpressed VK2/E6E7 cell supernatants. However, after longer incubations time (3-, 6-, 15-, and 24-h incubation), the levels of IL-6 (p= 0.0061, 0.0013, 0.0077, and 0.0084), IL-8 (CXCL8) (p= 0.0007, 0.0243, 0.0050, and 0.0319), IP-10 (p= 0.0061, 0.0109, <0.0001, and 0.0301), and RANTES (CCL5) (p= 0.0283, 0.0435, 0.0016, and 0.0007) were all significantly increased. Whereas, the level of MIP-1β (p= 0.0025, and 0.0007) was only significantly increased after 15h and 24h incubation. CSF2 (GM-CSF), IFNγ, IL-10, IL17A, MCP-1, MIP-1α, and TNFα were not detected in the VK2/E6E7 cell culture supernatant after these incubation times (data not shown). Thus, overexpression of TILRR enhanced the production of many pro-inflammatory cytokine/chemokine(s) in VK2/E6E7 cell culture supernatants.

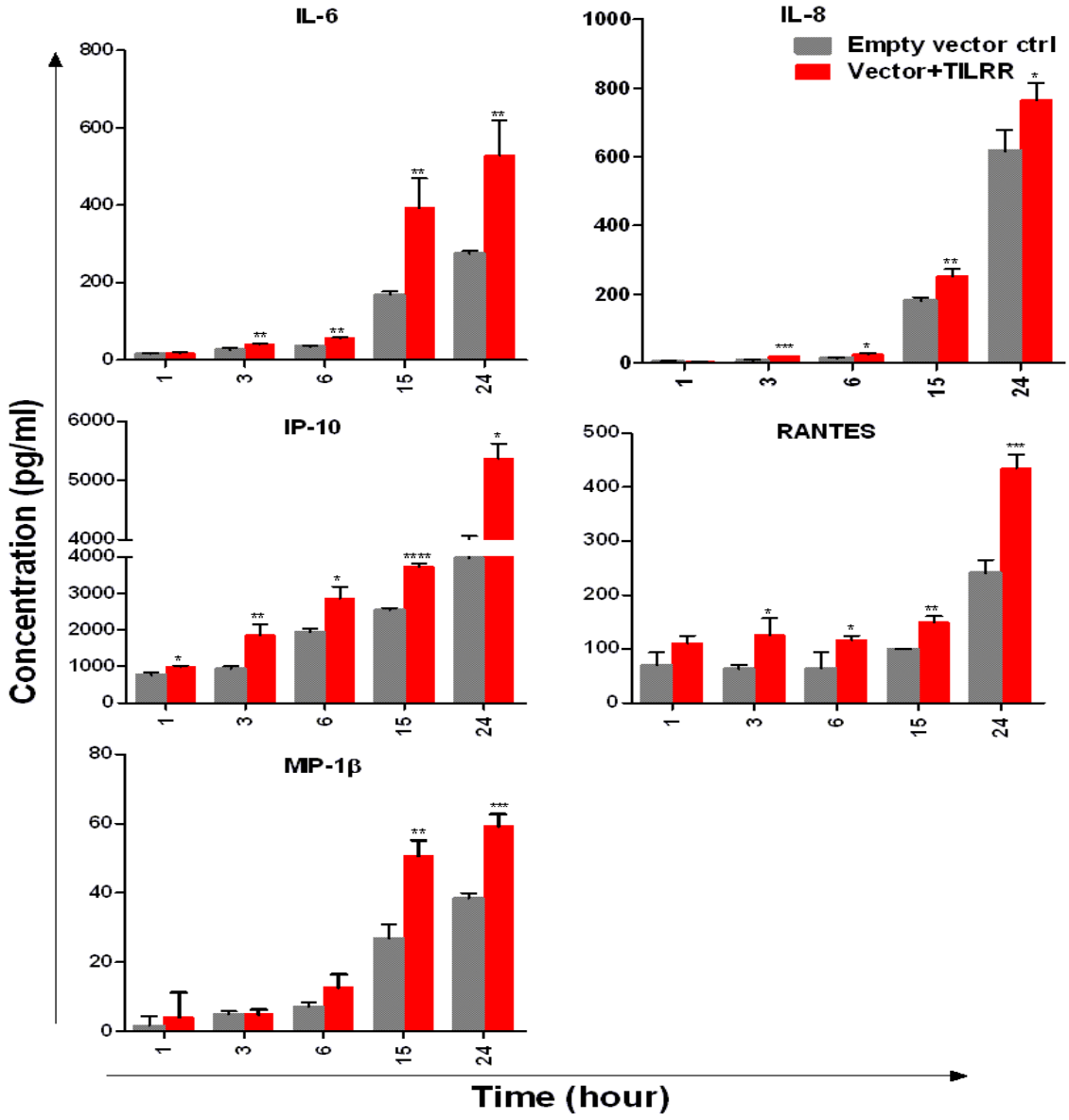

Figure 3.14: TILRR overexpression in VK2/E6E7 cells increased the production of pro-inflammatory cytokines/chemokines. VK2/E6E7 ($5x10^5$cells/well) cells were co-transfected with either pEZ-TILRR-M68 (1.0µg/$5x10^5$ cells) or pEZ-NEG-M68 (1.0µg/$5x10^5$ cells) with PmaxGFP (0.2µg/$5x10^5$ cells) vector as explained in the materials and methods chapter. Cells were incubated with serum-free Keratinocyte SFM (1X) medium for different time points and supernatants were collected. Thirteen different inflammatory cytokines were measured using an in-house developed multiplex cytokines/chemokines bead assay with Bio-Plex 200 (Bio-Rad). The data represent the relative level of vector+TILRR compared to the empty vector control. The sample measurements below the detection limit were assigned as zero. The data represent the mean of three independent experiments (mean±SEM). Statistical comparisons conducted using student t-test with 95% CI, all $p<0.05$ were reported and indicated using asterisks' *$p<0.05$, **$p<0.01$, ***$p<0.001$, and ****$p<0.0001$.

3.2.3 TILRR along with IL-1β stimulation significantly induced the production of cytokine/chemokine proteins in HeLa cell culture supernatants

To determine whether TILRR overexpression augments the production of pro-inflammatory cytokines/chemokines in the presence of IL-1β, I analyzed the effect of TILRR in the presence of IL-1β in cell culture supernatants of HeLa and VK2/E6E7 cells. The analysis showed that in HeLa cells the level of these cytokines/chemokines increased in a time-dependent manner with the presence of TILRR and added IL-1β in comparison to the empty vector-transfected control **(Figure 3.15** and **Appendix Table C7.7**; fold change is shown in **Appendix Table C7.7).** After 1h incubation in serum-free media, the level of IL-6 (p= 0.0002), IL-8 (CXCL8) (p= 0.0001), IP-10 (p= 0.0002), and MCP-1 (p= 0.0368) was significantly increased in HeLa cells. After longer incubation times (3-, 6-, 15-, 24-h incubation), the level of IL-6 (p= 0.0005, 0.0029, 0.0002, and <0.0001), IL-8 (CXCL8) (p< 0.0001, =0.0042, <0.0001, and =0.0008), IP-10 (p< 0.0001, =0.0014, <0.0001, and 0.0001), and MCP-1 (p= 0.0001, 0.0088, <0.0001, and <0.0001) was significantly increased due to the combined effect of TILRR and IL-1β. The chemokine RANTES (CCL5) was only significantly increased at 15h (p= 0.0002) and 24h (p< 0.0001) after incubation with IL-1β in serum-free media. CSF2 (GM-CSF), IFNγ, IL-10, IL17A, MIP-1α, MIP-1β, and TNFα were not detected in the HeLa cell culture supernatant with TILRR overexpression and added IL-1β (data not shown). Thus, these data demonstrated that TILRR overexpression in the presence of added IL-1β enhanced the production of specific cytokines/chemokines in HeLa cell culture media.

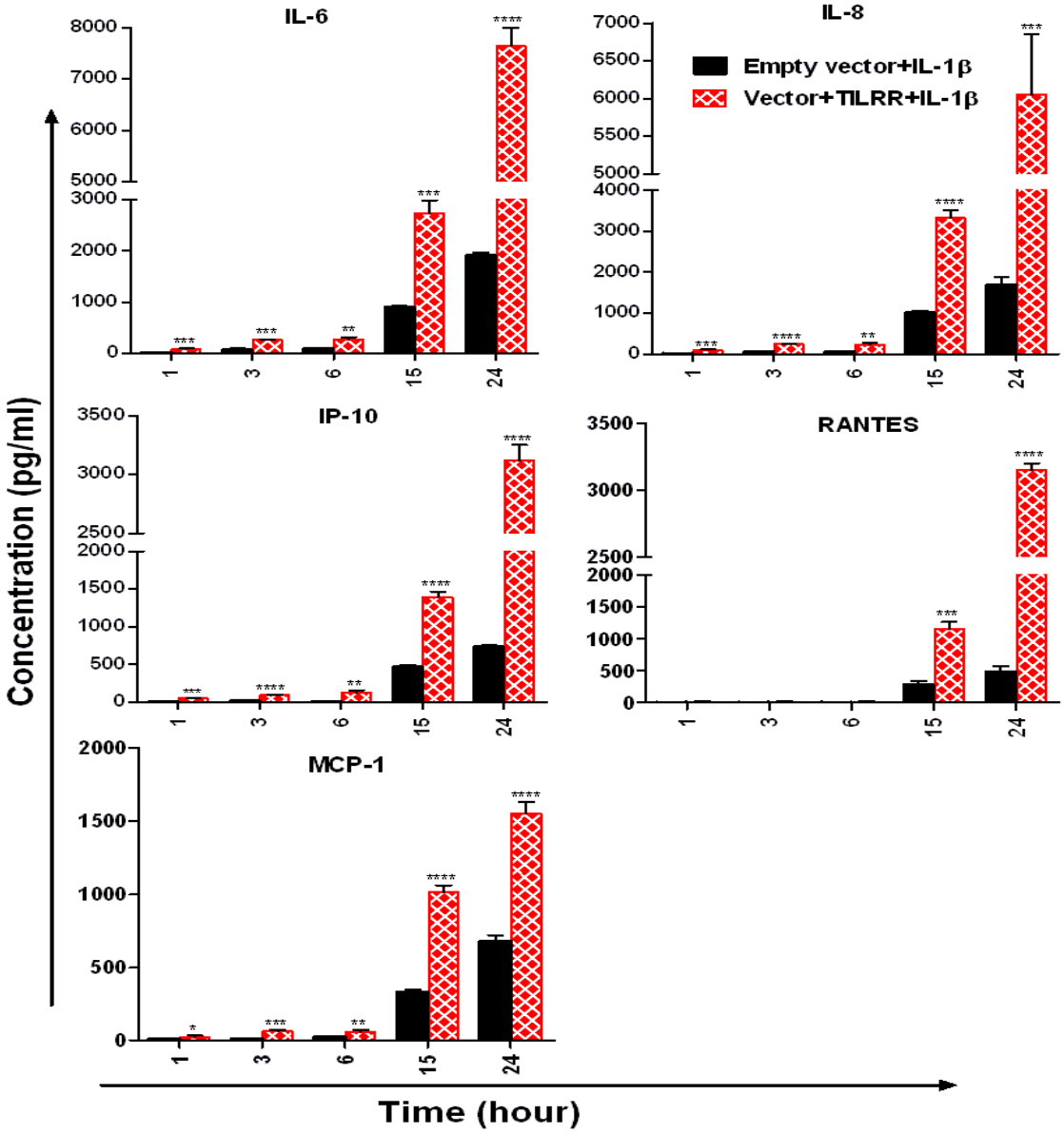

Figure 3.15: TILRR overexpression in HeLa cells increased the production of pro-inflammatory cytokines/chemokines in the presence of added IL-1β. HeLa cells ($5x10^5$cells/well) were co-transfected with either pEZ-TILRR-M68 (1.0µg/$5x10^5$ cells) or pEZ-NEG-M68 (1.0µg/$5x10^5$ cells) with PmaxGFP (0.2µg/$5x10^5$ cells) vector as explained in the materials and methods chapter. Cells were incubated with the addition of IL-1β (1nM) in serum-free DMEM medium for different time points and then the cultured media were collected. Thirteen different inflammatory cytokines were measured. The data represent the relative level of vector+TILRR, in the presence of IL-1β, compared to the empty vector control. The sample measurements below the detection limit were assigned as zero. The data represent the mean of three independent experiments (mean±SEM). Statistical comparisons conducted using student t-test with 95% CI, all $p<0.05$ were reported and indicated using asterisks' *$p<0.05$, **$p<0.01$, ***$p<0.001$, and ****$p<0.0001$.

3.2.4 TILRR along with IL-1β stimulation significantly induced the production of cytokine/chemokine proteins in VK2/E6E7 cell culture supernatants

Next, I examined the effect of TILRR overexpression in the presence of added IL-1β on the production of cytokines/chemokines in VK2/E6E7 cells. I observed a trend of increase of pro-inflammatory cytokines/chemokines production in the presence of TILRR and IL-1β compared to the empty vector control in serum-free media **(Figure 3.16** and **Appendix Table C7.8**; fold change is shown in **Appendix Table C7.8).** Unlike the HeLa cells, only IP-10 (p= 0.0004) was significantly higher with the TILRR overexpression and added IL-1β in VK2/E6E7 cell supernatants after 1h incubation. Similar to the HeLa cells, after longer incubation time (3- and 24-h incubation) the levels of IL-6 (p= 0.0058, and 0.0439), IL-8 (CXCL8) (p= 0.0011, and 0.0045), IP-10 (p= 0.0362, and 0.0004) and RANTES (p= 0.0281, and 0.0329) were significantly increased in VK2/E6E7 cell culture supernatants. The significant increase of IL-8 (CXCL8) (p= 0.0049), IP-10 (p= 0.0384) and RANTES (p= 0.0021) was also observed after 6h incubation and the higher level of IL-6 (p= 0.0022), IP-10 (p= 0.0004), RANTES (CCL5) (p= 0.0012) and MIP-1β (p= 0.0332) was also observed after 15h incubation. However, the production of CSF2 (GM-CSF), IFNγ, IL-10, IL17A, MCP-1, MIP-1α, and TNFα was not detected following the addition of IL-1β in the VK2/E6E7 cell culture supernatant (data not shown). In summary, these data showed that TILRR, in the presence of added IL-1β, can promote the production of pro-inflammatory cytokine/chemokines by VK2/E6E7 cells.

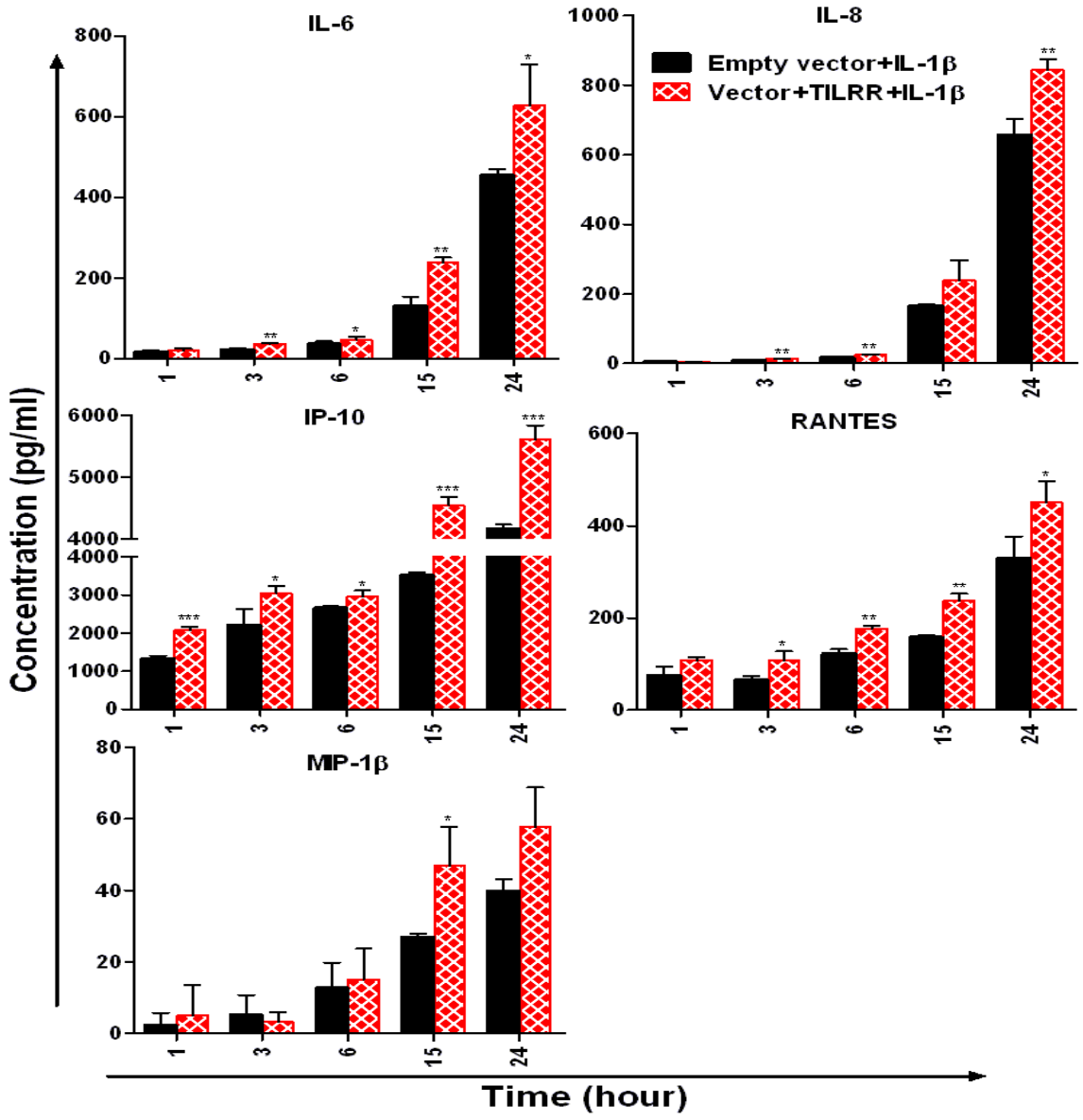

Figure 3.16: TILRR overexpression in VK2/E6E7 cells increased the production of pro-inflammatory cytokines/chemokines in the presence of added IL-1β. VK2/E6E7 ($5x10^5$cells/well) cells were co-transfected with either pEZ-TILRR-M68 (1.0µg/$5x10^5$ cells) or pEZ-NEG-M68 (1.0µg/$5x10^5$ cells) with PmaxGFP (0.2µg/$5x10^5$ cells) vector as explained in the materials and methods chapter. Cells were incubated with the addition of IL-1β (1nM) in a serum-free Keratinocyte SFM (1X) medium for different time points and then the cultured media were collected. Thirteen different inflammatory cytokines were measured. The data represent the relative level of vector+TILRR, in the presence of IL-1β, compared to the empty vector control. The sample measurements below the detection limit were assigned as zero. The data represent the mean of three independent experiments (mean±SEM). Statistical comparisons conducted using student t-test with 95% CI, all $p<0.05$ were reported and indicated using asterisks' *$p<0.05$, **$p<0.01$, ***$p<0.001$, and ****$p<0.0001$.

3.2.5 SUMMARY

The results of this section demonstrated that overexpression of TILRR in cervicovaginal epithelial cells significantly increased the production of multiple pro-inflammatory cytokines/chemokines in the culture supernatants of the transfected cells in a time-dependent manner. Specifically, an elevated level of IL-6, IL-8/CXCL8, IP-10/CXCL10, and RANTES/CCL5 was observed in TILRR-overexpressed HeLa and VK2/E6E7 cell culture supernatants compared to that of empty vector-transfected controls. The chemokines MCP-1/CCL2 and MIP-1β/CCL4 were only significantly increased in HeLa and VK2/E6E7 cell culture supernatants, respectively. In addition, the levels of IL-6, IL-8/CXCL8, IP-10/CXCL10, and RANTES/CCL5 were also increased in the culture supernatants in the presence of added IL-1β. Collectively, these data showed that TILRR overexpression significantly induced the production of soluble pro-inflammatory cytokines/chemokines in cervicovaginal epithelial cells.

Inflammatory mediators in the female genital tract induce the rapid infiltration of immune cells, and these infiltrated immune cells secrete inflammatory mediators upon activation resulting in the cycles of inflammation, which increase the risk of HIV acquisition. Because the overexpression of TILRR increased the level of pro-inflammatory mediators in culture supernatants, it is possible that TILRR-modulated production of inflammatory mediators by cervical epithelial cells promotes the migration of immune cells, including HIV target cells. To test this, I examined the migration behavior of HIV target cells under the influence of the TILRR-overexpressed HeLa cell culture supernatants using Transwell assay and microfluidic device assay. The results of the analysis of migration behavior of immune cells are described in the next section of this thesis.

3.3 EFFECT OF TILRR ON THE MIGRATION OF IMMUNE CELLS THROUGH THE MODULATION OF SOLUBLE CYTOKINES/CHEMOKINES PRODUCTION FROM EPITHELIAL CELLS

The results of this section are based on the following article:

TILRR promotes migration of immune cells through induction of soluble inflammatory mediators. Frontiers in Cell and Development Biology, 2020. 8(563): p. 1-13.

Mohammad Abul Kashem[1,2,3,4], Xiaoou Ren[5,6], Hongzhao Li[4], Binhua Liang[2,4,7], Lin Li[2,4], Francis Lin[5,6,8], Francis A. Plummer[1], Ma Luo[1,2,4]

[1]Department of Medical Microbiology and Infectious Diseases, University of Manitoba, Winnipeg, MB, Canada.
[2]JC Wilt Infectious Diseases Research Centre, Winnipeg, MB, Canada.
[3]Department of Microbiology and Veterinary Public Health, Chittagong Veterinary and Animal Sciences University, Chittagong, Bangladesh.
[4]National Microbiology Laboratory, Public Health Agency of Canada, Winnipeg, MB, Canada.
[5]Department of Biosystems Engineering, University of Manitoba, Winnipeg, MB, Canada.
[6]Department of Physics and Astronomy, University of Manitoba, Winnipeg, MB, Canada.
[7]Department of Biochemistry & Medical Genetics, University of Manitoba, Winnipeg, MB, Canada
[8]Department of Immunology, University of Manitoba, Winnipeg, MB, Canada.

Authors' contributions

FAP and ML acquired funding; **MK**, ML, and FL conceived and designed the research; **MK** performed all research, analyzed the data, generated figures/tables, organized the writing materials, and wrote the full paper; XR participated in microfluidic device migration assay study and drew the microfluidic device cartoon; ML and FL supervised the research; ML, FL, HL, BL, and LL edited the manuscript; **MK** revised, formatted and submitted to the journal. All authors have approved this article.

Funding

The study was funded by an operating grant from the Canadian Institutes of Health Research (CIHR), operating grant- PA: CHVI Vaccine Discovery and Social Research (http://www.cihr-irsc.gc.ca/e/193.html) and by a discovery grant from the Natural Sciences and Engineering Research Council of Canada (NSERC) (RGPIN-2014-04789).

3.3.1 Optimization of Transwell cell migration assay

To determine the optimal concentration of positive control chemo-attractants for inducing chemotaxis of the monocytes and lymphocytes in Transwell assay, a series of dilution experiments were conducted using MCP-1/CCL2 and SDF-1α/ CXCL12. One hundred microliters of $5x10^5$ cells diluted in RPMI 1640 medium were seeded into the apical chamber (insert) of the Transwell plate and allowed for migration at 37^0 C for 24 h. The results showed that THP-1 monocyte migration was gradually increased with increasing MCP-1/CCL2 concentration, and migration efficiency was gradually decreased to close to the baseline level after 50 ng/ml MCP-1/CCL2 **(Figure 3.17A).** The highest percentage of THP-1 cell migration was observed at 50 ng/ml chemokine concentration, and the lowest percentage was with 5 ng/ml of MCP-1/CCL2 using three different cell counting methods. More specifically, the percentage of relative migration (PRM) was observed at 10 ng/ml (PRM: 51.53±5.05%, p= 0.0077), 50 ng/ml (PRM: 78.57±1.44%, p= 0.0007), 100 ng/ml (PRM: 70.41±18.76%, p= 0.0424), and 200 ng/ml (PRM: 37.76±1.45%, p= 0.0037) compared to the DMEM only control (PRM: 7.65±2.16) by counting with hemocytometer. Similar migration behavior was also observed with automated cell counter, and flow cytometry analysis [10 ng/ml (PRM: 52.94±4.16%, p= 0.0111; and PRM: 56.22±6.18%, p= 0.0110), 50 ng/ml (PRM: 80.89±18.72%, p= 0.0476; and PRM: 82.01±9.92%, p= 0.0106), and 200 ng/ml (PRM: 33.82±2.08%, p= 0.0299; and PRM: 43.02±4.96%, p= 0.0153) of MCP-1/CCL2, respectively]. The highest PRM at 50 ng/ml of MCP-1/CCL2 was consistently determined with all three methods. MCP-1/CCL2 concentration higher than the 50 ng/ml diminished the effect of attracting THP-1 cells, and at 200 ng/ml the PRM was close to the baseline. Thus, 50 ng/ml of MCP-1/CCL2 is the best concentration to induce the maximum percentage of THP-1 cell migration in a conventional Transwell migration assay.

Similarly, the optimal concentration of SDF-1α/CXCL12 for MOLT-4 T-lymphocyte migration in Transwell assay was also determined **(Figure 3.17B)**. The PRM of MOLT-4 T-lymphocyte significantly increased at 100 ng/ml (PRM: 49.64±9.89%, p= 0.0184), and 200 ng/ml (PRM: 53.90±9.19%, p= 0.0098) of SDF-1α/CXCL12 compared to that of DMEM control by counting with a hemocytometer. MOLT-4 T-cell was also significantly migrated at 100 ng/ml (PRM: 46.92±7.98%, p= 0.0359) and 200 ng/ml (PRM: 81.41±14.70%, p= 0.0169) with automated cell counter and flow cytometry analysis, respectively. However, the PRM of MOLT-4 was reduced at 200 ng/ml of SDF-1α/CXCL12 by counting with an automated cell counter. Because MOLT-4 T-cell significantly migrated at 100 ng/ml of SDF-1α/CXCL12, and the rate of migration was declined at 200 ng/ml by automated cell counter, I selected 100 ng/ml as the optimal concentration to induce maximum percentage of MOLT-4 cell migration in Transwell migration assay. This concentration was also found to be the best in inducing T-lymphocyte migration in earlier studies [323, 324]. Taken together, the optimal concentrations of both MCP-1/CCL2 and SDF-1α/CXCL12 were used as positive controls in Transwell and microfluidic real-time migration assays.

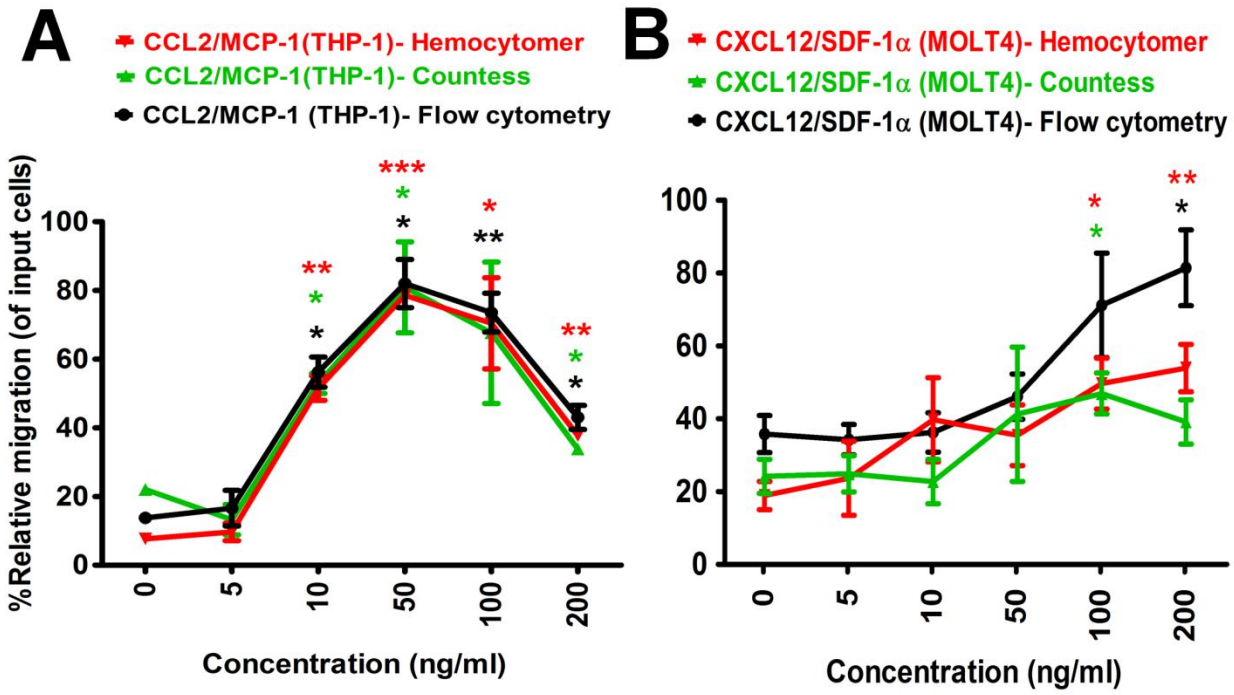

Figure 3.17: Optimization of positive control chemo-attractants for monocytes and lymphocytes migration using Transwell assay. A) THP-1 monocytes, and **B)** MOLT-4 T-lymphocytes migration was optimized using known chemo-attractants of MCP-1/CCL2 and SDF-1α/CXCL12, respectively. Chemo-attractants were diluted in DMEM without FBS and antibiotic-antimycotic. Approximately $5.0x10^5$ cells were used as input cells on the upper chamber (insert) of Corning 24-well plate with a 5.0 µm pore size polycarbonated membrane and incubated for 24h. The line graph represents three independent experiments (mean±SEM) compared to the DMEM base control (0 ng/ml chemo-attractants). Color-coded lines show different counting methods. A red line with red asterisks represents hemocytometer count, a green line with green asterisks for the automated countess, and a black line with black asterisks indicates flow cytometry count. Statistical comparisons were conducted using student t-test with 95% CI, all $p<0.05$ were reported and indicated using asterisks' *$p<0.05$, **$p<0.01$, and ***$p<0.001$. Legend on the top of the figures represents the chemoattractants, type of cell used, and counting method. The X-axis shows the different concentrations of MCP-1/CCL2 and SDF-1α/CXCL12.

3.3.2 The culture supernatant of TILRR-transfected HeLa cells significantly induced migration of THP-1 cells in Transwell assay

To examine if the presence of TILRR-modulated soluble cytokines/chemokines influences the migration of monocytes, a Transwell migration assay was conducted using THP-1 monocytes and HeLa cell culture supernatants. The results demonstrated that the TILRR-transfected HeLa cell culture supernatant attracted a significantly higher amount of THP-1 cells (11-40%) than the controls **(Figure 3.18A-D).** Data analysis showed that approximately 16-46% higher amount of THP-1 cells were migrated towards the culture supernatants of TILRR overexpressed HeLa cells compared to the supernatant of empty vector-transfected (PRM: 52.26±6.88% vs 37.04±3.09%, p= 0.0250), non-transfected (PRM: 52.26±6.88% vs 31.69±9.35%, p=0.0373) HeLa cell supernatants, or DMEM controls (PRM: 52.26±6.88% vs 6.58±2.49%, p=0.0004) (hemocytometer counts) **(Figure 3.18B)**. Similarly, it was observed that significantly higher amount of THP-1 cells (12-39%) migrated towards TILRR-transfected culture medium than the empty vector-transfected (PRM: 49.39±3.90% vs 38.04±4.22%, p= 0.0267), non-transfected (49.39±3.90% vs 36.32±5.90%, p= 0.0328) HeLa cell supernatants, or DMEM controls (49.39±3.90% vs 10.96±8.39%, p= 0.0020) (automated cell counter) **(Figure 3.18C)**. Flow cytometry analysis also showed that the higher numbers of THP-1 cells migrated towards the TILRR-transfected culture medium (11-35%) than the controls **(Figure 3.18D)**. As expected, THP-1 cells were also significantly migrated towards the positive control chemo-attractant MCP-1/CCL2 compared to that of DMEM controls as determined by all three counting methods **(Figure 3.18B-D).** Thus, the supernatant of TILRR-overexpressed HeLa cells attracted the THP-1 monocytes, suggesting that cervical tissue TILRR may attract immune cells to the cervical tissues by promoting the secretion of inflammatory cytokines.

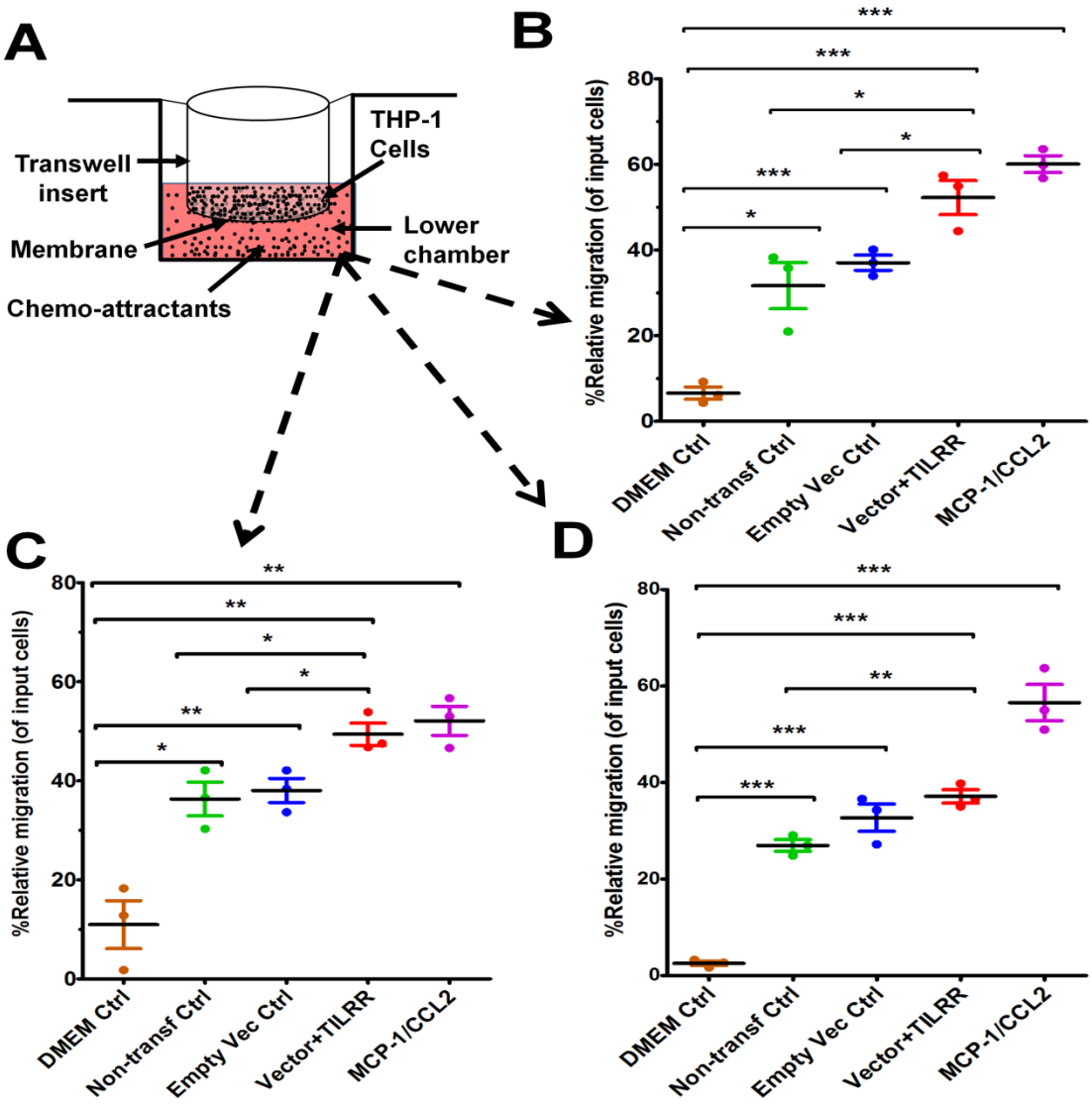

Figure 3.18: THP-1 monocytes migration towards TILRR-modulated cervical cell culture supernatants in Transwell assay. A) A representative image of polycarbonated membrane Transwell unit. Approximately $5.0x10^5$ THP-1 cells were used as input cells on the upper chamber, and 600 µl of each chemo-attractant (either HeLa cell culture supernatants or MCP-1/CCL2) was dispensed in the bottom chamber of the Transwell plate as described in the materials and methods chapter. MCP-1/CCL2 (50 ng/ml diluted in DMEM) was used as a positive control chemo-attractant. Corning 24-well plate with 5.0 µm pore membrane used to conduct migration assay for 24 h. The migrated cells were counted with three independent counting methods, **B)** hemocytometer, **C)** automated countess, and **D)** flow cytometry. Scatter dot plots represent the percent relative migration of cells in the presence of TILRR-transfected HeLa cell culture supernatants compared to the empty vector- and non-transfected control supernatants, and DMEM control. The data represent the mean±SEM of three independent experiments. Statistical comparisons were conducted using student t-test with 95% CI, all $p<0.05$ were reported and indicated using asterisks' *$p<0.05$, **$p<0.01$, and ***$p<0.001$. The X-axis indicates the condition of chemo-attractants.

3.3.3 The culture supernatant of TILRR-transfected HeLa cells significantly induced migration of MOLT-4 T-lymphocytes in Transwell assay

To assess whether the supernatant of TILRR-overexpressed HeLa cells attracts T-lymphocytes, MOLT-4 cell migration was conducted using a similar approach. MOLT-4 cells were also showed higher PRM (14-17%) towards TILRR-modulated HeLa cell culture supernatants compared to that of controls **(Figure 3.19A-D**). Approximately 16-19% higher amount of MOLT-4 cells were significantly attracted to TILRR overexpressed HeLa cell supernatants than the supernatants of empty vector-transfected (PRM: 27.63±3.57% vs 11.67±1.17%, p= 0.0018), non-transfected (PRM: 27.63±3.57% vs 8.95±2.94%, p= 0.0022) cells, or DMEM control (PRM: 27.63±3.57% vs 8.95±1.78%, p= 0.0013) (hemocytometer counting method) **(Figure 3.19B)**. A similar trend of MOLT-4 cell migration was observed by automated cell counter and flow cytometry analysis where the PRM was observed approximately 14-18% and 12-14% higher in TILRR-overexpressed HeLa cell culture supernatants than that of controls, respectively **(Figure 3.19C-D)**. Similar to the THP-1 cells, MOLT-4 cells were also significantly migrated to the positive control chemo-attractant SDF-1α/CXCL12 compared to the DMEM controls (**Figure 3.19B-D)**. Collectively, these data showed that the supernatant of TILRR-overexpressed HeLa cells also attracts T-lymphocytes.

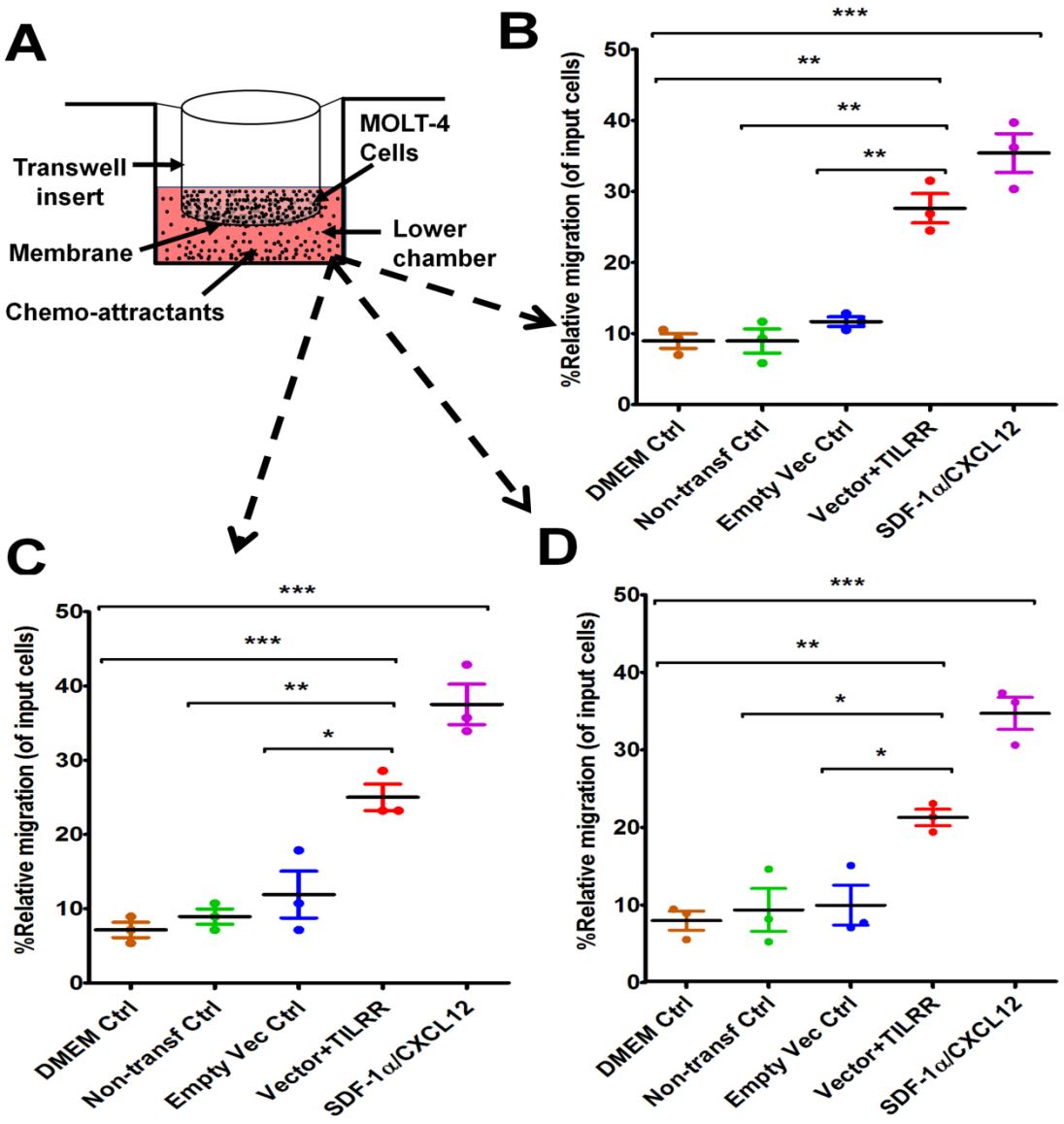

Figure 3.19: MOLT-4 T lymphocytes migration towards TILRR-modulated cell culture supernatants in Transwell assay. A) A representative image of polycarbonated membrane Transwell unit. Approximately 5.0x10^5 MOLT-4 lymphocytes cells were used, and 600 µl of HeLa culture media or positive control chemoattractant slowly dispensed into the Transwell plate (bottom chamber) as described in the materials and methods chapter. SDF-1α/CXCL12 (100 ng/ml diluted in DMEM) was used as a positive control. A similar Transwell plate (as THP-1) was used to conduct the migration of MOLT-4 cells for 24 h. The migrated cells were counted with three independent counting methods such as **B)** hemocytometer, **C)** automated countess, and **D)** flow cytometry. Scatter dot plots represent the percent relative migration of cells in the presence of TILRR-transfected HeLa cell culture supernatants compared to the empty vector- and non-transfected control supernatants, and DMEM control. The data represent the mean±SEM of three independent experiments. Statistical comparisons were conducted using student t-test with 95% CI, all $p<0.05$ were reported and indicated using asterisks' *$p<0.05$, **$p<0.01$, and ***$p<0.001$. The X-axis indicates the condition of chemo-attractants.

3.3.4 The culture supernatant of TILRR-transfected HeLa cells significantly induced migration of THP-1 monocytes by the microfluidic device analysis

Because Transwell assay does not provide the data on how far (directional displacement) a cell can migrate towards the HeLa cell culture supernatants, I next sought to examine the displacement of THP-1 monocytes from their original location towards the gradient of culture supernatants by a novel microfluidic device. The microfluidic device offers a better-controlled chemical gradient with single-cell analysis, which enables the data analysis of the displacement and distribution of individual migrated cells during the experiment. The results showed that TILRR-overexpressed HeLa cell culture supernatants attracted more THP-1 cells with significantly higher average cell displacement compared to the controls (**Figure 3.20A-E**). Furthermore, my study data showed that THP-1 cells migrated further to the supernatant of TILRR overexpressed HeLa cells in comparison to the supernatant of the empty vector-transfected HeLa cells (52.00±52.00 vs 34.00±48.00 µm, p= 0.0180), non-transfected HeLa cells (52.00±52.00 vs 28.00±29.00 µm, p< 0.0001), or DMEM control (52.00±52.00 vs 19.00±23.00 µm, p< 0.0001) (**Figure 3.20E**). Thus, the TILRR-transfected HeLa cell supernatants promoted the migration of THP-1 monocytes in microfluidic device assay.

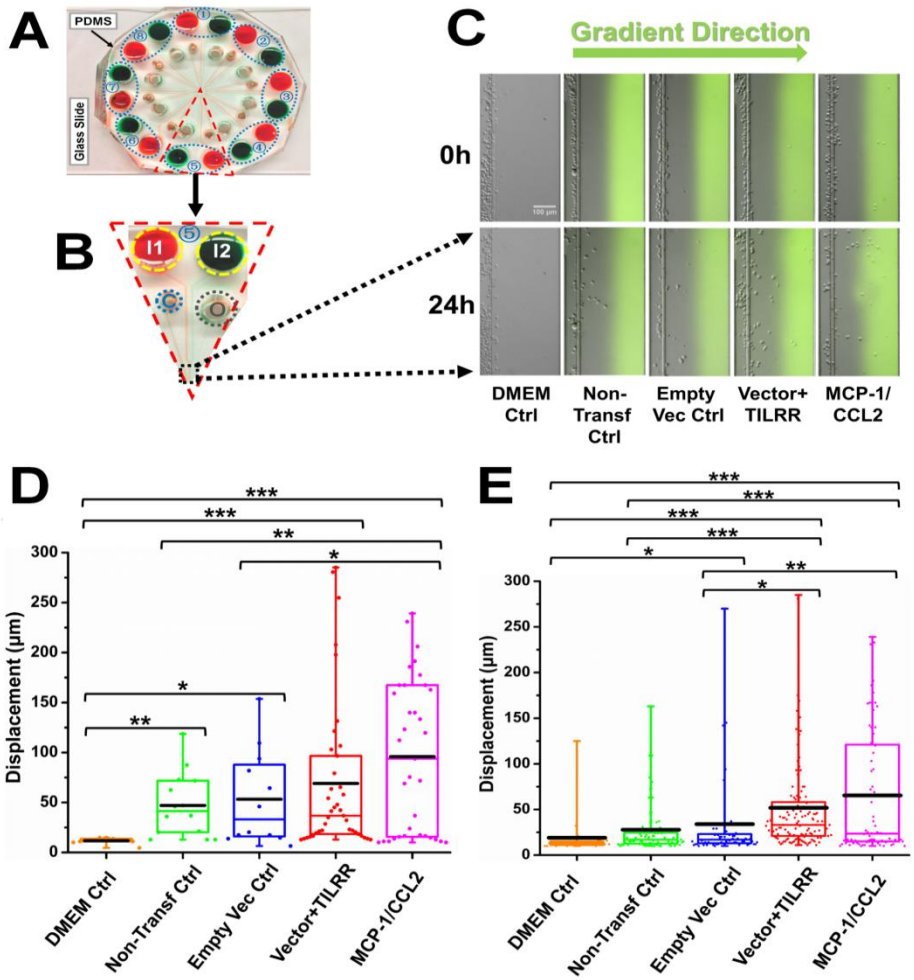

Figure 3.20: THP-1 monocytes migration towards TILRR-modulated cell culture supernatants in the microfluidic device. A) A representative image of the real radial microfluidic device with colored dyes to show the major networks in each unit. The upper transparent part is a PDMS replica, which is bonded onto the bottom part of the glass slide; the blue elliptical-dashed box and the number (1-8) show the chemical inlets of each independent unit. **(B)** One magnified triangular unit (randomly selected) from figure A showing the black-dashed square area from where migrated cells were analyzed. I1 and I2: chemical inlets; C: cell loading port; O: waste outlet. **(C)** Representative images of the migration of THP-1 cells in different conditions at 0h and 24h analyzed from figure B. Green color in the image of all experimental conditions except DMEM control indicates the profile and most concentrated area of a chemical gradient. **(D)** The colored box plots show the total displacement of each cell in the corresponding experimental groups in figure C (from a single experiment). **(E)** The colored box plots show the total displacement of each cell in three independent experiments. MCP-1/CCL2 (50 ng/ml diluted in DMEM) was used as a positive control chemo-attractant. The top and bottom of the whisker show the maximum and minimum values; the box shows the migrated cells within the range from 25% - 75% of total cells based on the ranked displacement value; the black bold line indicates the mean displacement. The data in different groups were compared using the Student t-test with 95% CI, all $p<0.05$ were reported and indicated using asterisks' *$p<0.05$, **$p<0.01$, and ***$p<0.001$.

3.3.5 The culture supernatant of TILRR-transfected HeLa cells significantly induced migration of MOLT-4 T-lymphocytes by the microfluidic device analysis

I also evaluated the effect of the culture supernatant of TILRR-transfected HeLa cells on the migration of MOLT-4 T-lymphocytes with the microfluidic device. The results showed that TILRR-overexpressed culture supernatants also attracted more MOLT-4 cells with significantly higher average cell displacement (**Figure 3.21A-E**). Similar to the THP-1 cells, MOLT-4 T-lymphocytes migrated further towards the supernatant of TILRR overexpressed HeLa cells compared to the supernatant of empty vector-transfected HeLa cells (25.00±10.00 vs 19.00±8.00 µm, $p<0.0001$), non-transfected (25.00±10.00 vs 20.00±13.00 µm, $p= 0.0025$) HeLa cells, or DMEM control (25.00±10.00 vs 14.00±3.00 µm, $p<0.0001$) (**Figure 3.21E**). Thus, TILRR-transfected HeLa cell supernatants also promoted MOLT-4 T-lymphocytes migration with microfluidic device assay.

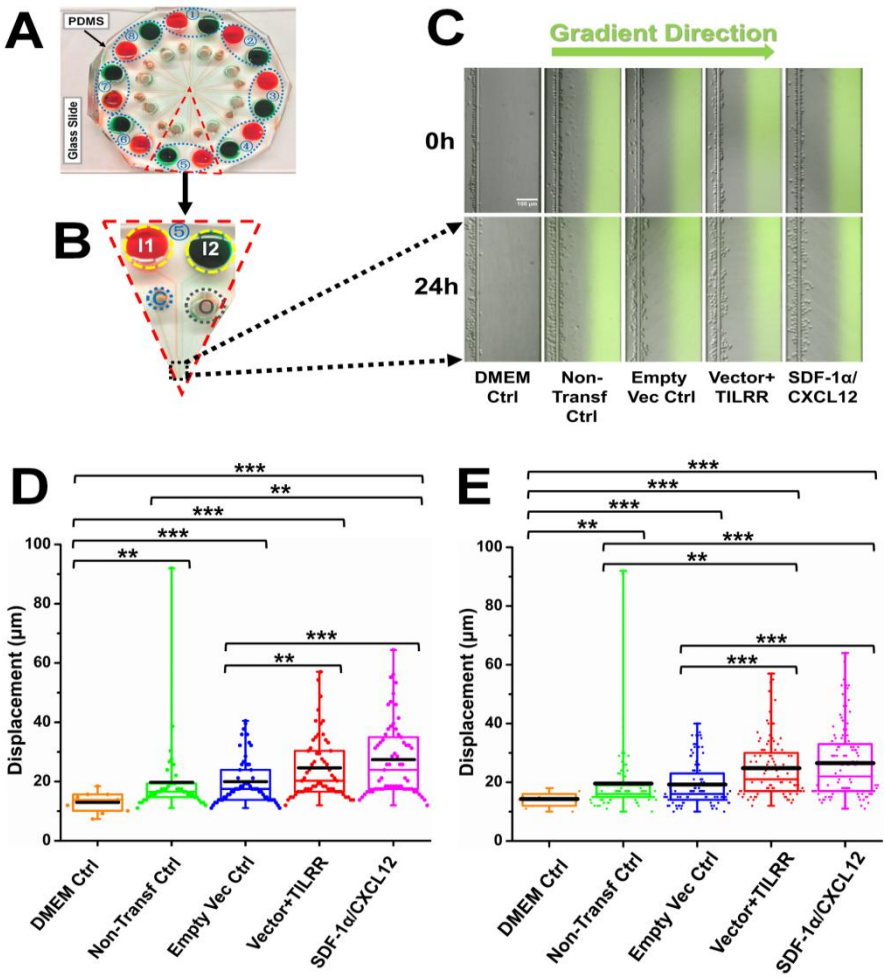

Figure 3.21: MOLT-4 T cells migration towards TILRR-modulated cell culture supernatants in the microfluidic device. A) A representative image of the real radial microfluidic device with colored dyes to show the major networks in each unit. The upper transparent part is a PDMS replica, which is bonded onto the bottom part of the glass slide; the blue elliptical-dashed box and the number (1-8) show the chemical inlets of each independent unit. **(B)** One magnified triangular unit (randomly selected) from figure A showing the black-dashed square area from where migrated cells were analyzed. I1 and I2: chemical inlets; C: cell loading port; O: waste outlet. **(C)** Representative images of the migration of THP-1 cells in different groups at 0h and 24h analyzed from figure B. Green color image of all experimental conditions except DMEM control indicates the profile and most concentrated area of a chemical gradient. **(D)** The colored box plots show the total displacement of each cell in the corresponding experiment conditions in figure C (from a single experiment). **(E)** The colored box plots show the total displacement of each cell in three independent experiments. SDF-1α/CXCL12 (100 ng/ml diluted in DMEM) was used as a positive control. The top and bottom of the whisker show the maximum and minimum values; the box shows the migrated cells within the range from 25% - 75% of total cells based on the ranked displacement value; the black bold line indicates the mean displacement. The data in different groups were compared using the Student t-test with 95% CI, all $p<0.05$ were reported and indicated using asterisks' *$p<0.05$, **$p<0.01$, and ***$p<0.001$.

3.3.6 SUMMARY

This study investigated whether TILRR-modulated production of cytokines/chemokines in cervical epithelial cells promotes the migration of immune cells, such as monocytes and T-lymphocytes, the HIV target cells. Using Transwell assay, I demonstrated that the culture supernatants of TILRR-transfected HeLa cells significantly promoted the migration of THP-1 (monocytes) and MOLT-4 (T-lymphocytes) cells compared to that of empty vector-transfected and non-transfected HeLa cell culture supernatants. The data from the microfluidic device assay also showed that TILRR-transfected HeLa cell culture supernatants induced the longer migration distance of THP-1 and MOLT-4 cells. Altogether, these results support the hypothesis that TILRR-mediated induction of soluble pro-inflammatory mediators by cervical epithelial cells promotes the migration of immune cells, the HIV target cells.

The results described in the above three sections of this thesis research demonstrated that TILRR is an important modulator of the NF-κB signaling pathway, production of chemotactic mediators, and migration of HIV target cells. These studies provided further understandings of the role of TILRR in inflammatory responses in addition to the published studies [285, 288]. However, all earlier studies measured the mRNA expression of TILRR and downstream NF-κB signaling molecules. In these studies, TILRR was associated with cells and tissue, and there is no report on the existence of TILRR in human blood. It is possible that TILRR also exists as a soluble protein in human blood. If this is the case, it may modulate systemic inflammation. I hypothesized that TILRR may circulate as a soluble protein in human blood, and its level in blood is associated with differential susceptibility to HIV acquisition. I examined the human plasma TILRR using an in-house developed multiplex bead array method and Western blot analysis and presented the data in the next section of this thesis.

3.4 TILRR CIRCULATES IN THE BLOOD AND THE LEVEL OF PLASMA TILRR IS ASSOCIATED WITH SUSCEPTIBILITY TO HIV INFECTION

The results (first part) of this section are based on the following article:

TILRR (Toll-like interleukin-1 receptor regulator), an important modulator of inflammatory responsive genes, is circulating in the blood. Journal of Inflammation Research (in revision)

Mohammad Abul Kashem[1,2,3,4], Xin-Yong Yuan[4], Lin Li[2], Joshua Kimani[5], Francis A Plummer[1††], Ma Luo[1,2,4*]

Authors' affiliation(s):
[1]Department of Medical Microbiology and Infectious Diseases, University of Manitoba, Winnipeg, MB, Canada.
[2]JC Wilt Infectious Diseases Research Centre, Winnipeg, MB, Canada.
[3]Department of Microbiology and Veterinary Public Health, Chittagong Veterinary and Animal Sciences University, Chittagong, Bangladesh.
[4]National Microbiology Laboratory, Public Health Agency of Canada, Winnipeg, MB, Canada.
[5]Institute for Tropical and Infectious Diseases, University of Nairobi, Nairobi, Kenya.
[††] In memoriam (passed away on February 4, 2020)

Authors' contributions
FAP and ML acquired funding; **MAK** and ML conceived and designed the research; **MAK** performed all research, analyzed the data, generated figures/tables, organized the writing materials, and wrote the paper; LL helped in Western blot study; JK coordinated the plasma sample collection and shipment; ML supervised the research; X-YY provided reagents; LL and ML edited the manuscript; **MAK** revised, formatted and submitted to the journal. All authors have approved this article.

Funding
The study was funded by an operating grant from the Canadian Institutes of Health Research (CIHR), operating grant- PA: CHVI Vaccine Discovery and Social Research (http://www.cihr-irsc.gc.ca/e/193.html).

3.4.1 Identification of soluble TILRR protein in human plasma

3.4.1.1 TILRR protein is detected in human plasma samples

To test whether TILRR exists as a soluble protein in human plasma, I examined plasma samples collected from women of PSWC between 1985 and 2008 (n=640). I quantified plasma TILRR protein using an in-house developed multiplex bead array method (Bio-Plex). TILRR was detected by two anti-FREM1 mAbs (F237G3 and F218G4, targeting epitopes on CSPG11+12 and Calx-β domain, respectively) and full-length FREM1 by anti-FREM1 F237G1 mAb (targeting epitopes on CSPG9). Because the CSPG9 domain does not exist in TILRR, the use of F237G1 mAb can differentiate TILRR from full-length FREM1 (the detailed method is described in section **2.4.4.1**). The results of my study showed that the in-house developed method successfully detected TILRR protein in plasma, and the quantity of plasma TILRR protein is variable among different individuals. Furthermore, the quantity of TILRR protein estimated by the two anti-FREM1 mAbs, F237G3 (CSPG 11 and 12) and F218G4 (Calx-β) is different. ***Based on the detection value of these two mAbs, I classified the examined plasma samples into 4 different patients' groups as shown in Table 3.2*** (*these patients' groups will be referred back for the data analysis in this section of my thesis*). Of 640 samples, the plasma TILRR protein was detected by both F237G3 and F218G4 mAbs in 186 samples with concentration ranges from 0.57 ng/ml to 1449.62 ng/ml. Since the intact TILRR protein should have both CSPG 11/12 and Calx-β domains, I thought that the lower value detected by the two mAbs should be the quantity of the TILRR protein (**Table 3.2, patient group 1**). In addition, 303 (**patient group 2**) and 19 (**patient group 3**) plasma samples only have detectable value using F237G3 mAb (ranges from 2.38 ng/ml to 5196.79 ng/ml) or F218G4 mAb (ranges from 15.81 ng/ml to 201.08 ng/ml), respectively **(Table 3.2).** TILRR was not detected in 132 plasma

samples using either F237G3 or F218G4 mAbs (**Table 3.2, patient group 4**). Full-length FREM1 protein was barely detected in patients' plasma using F237G1 mAb (data not shown). Thus, these data showed that TILRR protein is indeed present in human plasma and their amount is variable among the patients.

Table 3.2: Blood plasma TILRR protein detection and quantification by Bio-Plex assay (as an example).

Patient groups classified based on TILRR value using Bio-Plex method	F237G3 mAb (CSPG 11 and 12) (ng/ml)	F218G4 mAb (Calx-β) (ng/ml)	F237G1 mAb (CSPG9) (ng/ml)	TILRR	TILRR level (ng/ml)
Group 1	104.22	156.36	Not detected	Yes	104.22
Group 2	29.64	Not detected	Not detected	Not sure	?
Group 3	Not detected	201.08	Not detected	Not sure	?
Group 4	Not detected	Not detected	Not detected	Not sure	0

3.4.1.2 Confirmation of TILRR protein in human plasma samples

To confirm the detected TILRR protein in human plasma using the in-house developed multiplex bead array system (Bio-Plex), I selected 3 patient plasma samples from each of the 4 classified patient groups (**Table 3.2**) based on the detection values with different mAbs. The TILRR protein was affinity-purified from the selected samples and analyzed by Western blot. The TILRR was probed using anti-FREM1 F237G3 and F218G4 mAbs, and Full-length FREM1 was probed using anti-FREM1 F237G1 mAb. Because F237G3 and F218G4 mAbs can detect both TILRR and FREM1, I can only differentiate TILRR from FREM1 by their protein size with protein molecular weight (MW) marker. TILRR is a ~70 kDa protein, whereas full-length FREM1 is a ~235 kDa protein. The Western blot analysis showed that TILRR protein (a 70 kDa protein) can be detected from all groups of patient plasma samples with variable signal intensity **(Figure 3.22A-D; Appendix Figure B7.4**). Even the plasma samples with no signal using the Bio-Plex method have a 70 kDa band with Western Blot analysis **(Figure 3.22D, Group 4**) except that the TILRR protein intensity varies. The TILRR protein intensity was consistent with the TILRR quantity measured with Bio-Plex assay among different patients' groups (**Figure 3.22A-D;** and tables on the top of **Figure 3.22A-D).** Coomassie blue staining showed that the affinity-purified proteins were not completely transferred (especially for group 1) from the gel to the nitrocellulose membrane **(Figure 3.22A-D; Appendix Figure B7.5**)**.** The protein intensity (mostly 70 kDa) in group 1 following Coomassie blue staining showed significantly higher than the other groups (**Figure 3.22A).** Thus, although Western blot validated the presence of TILRR in the blood plasma, it cannot provide accurate quantification of the protein since a portion of proteins were not transferred to the nitrocellulose membrane. F237G1 mAb (binds with epitopes on CSPG9 of FREM1) was used to detect the full-length FREM1 by Western blot; no band of

~235 kDa (the expected size of full FREM1 protein) was detected (**Appendix Figure B7.6A-B**). Thus, only TILRR protein (70 kDa) and other FREM1 variants (either <70 kDa or >70 kDa) are present in the human plasma samples. Other variants of FREM1 have not been consistently detected in all plasma samples examined. The role of these FREM1 protein variants in host inflammatory response could be interesting studies in the future.

mAbs	Group 1			Group 2		
	ML2492 (ng/ml)	ML2802 (ng/ml)	ML2442 (ng/ml)	ML326 (ng/ml)	ML2170 (ng/ml)	ML2443 (ng/ml)
F237G3	104.22	198.60	414.81	29.64	83.50	34.32
F218G4	156.36	156.36	458.27	ND	ND	ND

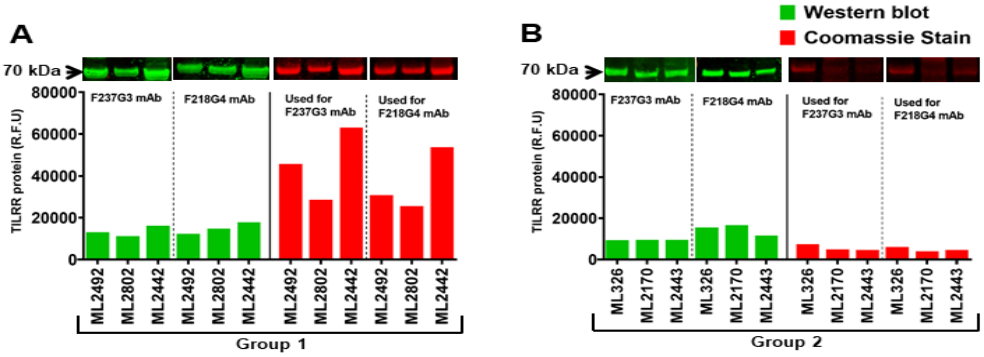

mAbs	Group 3			Group 4		
	ML2292 (ng/ml)	ML2772 (ng/ml)	ML109 (ng/ml)	ML887 (ng/ml)	ML893 (ng/ml)	ML1070 (ng/ml)
F237G3	ND	ND	ND	ND	ND	ND
F218G4	55.18	91.17	201.08	ND	ND	ND

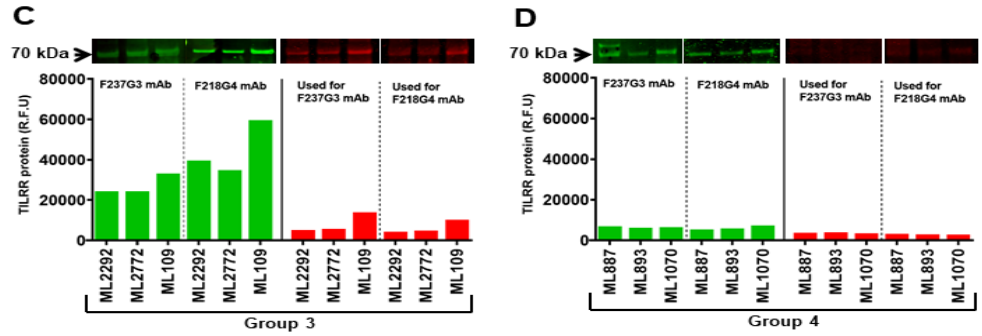

Figure 3.22: Western blot and Coomassie blue staining confirmation of purified TILRR from plasma after affinity purification for classified TILRR groups 1 to 4. The tables on the top of the figures show the amount of plasma TILRR protein quantified by Bio-Plex using plasma from patients' groups 1-4 (**Table 3.2). A-D**) Affinity purified plasma TILRR was analyzed by Western blot (left, green color) and Coomassie blue staining of NuPAGE gel after iBlot transfer, showing the untransferred protein (right, red color) in Group 1 **(A)**, Group 2 **(B),** Group 3 **(C)**, and Group 4 **(D)**. Each group shows data from 3 patients. Top panels (left) of figures A-D show the Western blot bands (green color) for TILRR protein (cropped) detected by two different anti-FREM1 IgG mAbs (F237G3 and F218G4) (full-length un-cropped blot images are shown in **Appendix Figure B7.4**). Top panels (right) of figures A-D show the protein bands in the gel after Coomassie blue staining (red color) (cropped); Full-length un-cropped gels are shown in **Appendix Figure B7.5**. The corresponding TILRR protein (R.F.U) for each patient is shown in the bar graph beneath the cropped blots and gels. Western blot and Coomassie blue staining images were acquired by Odyssey CLx imaging system (LI-COR, USA) with auto channels (both 700 and 800), 42 µm resolution, high image quality, and 0mm focal offset for blots and 0.5mm focal offset for gels. The X-axis of all figures indicates the patients' identification number. ND, Not detected; kDa, kiloDalton; RFU, relative fluorescence units. Legends on the top right corner of figure B show the assay techniques.

Based on the data from Bio-Plex (multiplex bead array) and Western blot analysis, I conclude that TILRR exists in the plasma of all patients' groups **(Table 3.3)**. Based on the Western blot results, I revised my assessment on the TILRR plasma level **(Table 3.4).** My conclusion is that TILRR presents in the blood plasma of all patients and its level varies greatly among the patients, ranges from 2.38 ng/ml to 5196.79 ng/ml. The highest level of plasma TILRR was observed in patient group 1 (median [IQR]: 143.74 [76.69-247.73] ng/ml). In this group, TILRR can be detected by both F237G3 and F218G4 mAbs with the highest detection value between these two mAbs as the level of plasma TILRR. The plasma TILRR level of group 3 is determined with F218G4 mAb (median [IQR]: 97.14 [55.18-134.63] ng/ml, second-highest level), and the one for group 2 is determined with F237G3 mAb (median [IQR]: 50.36 [35.44-74.08] ng/ml, lowest level) (**Figure 3.23A**).

Next, I analyzed the detection frequency of plasma TILRR protein among 640 samples to determine whether the detection frequency is correlated to the level of plasma TILRR protein in different patient groups (**Figure 3.23B**). Since patient group 4 did not show TILRR detection (below the limit of detection), I calculated the frequency (%) for groups 1-3 by subtracting the numbers of samples of group 4. Based on the defined groups in **Table 3.2,** group 2 is the highest with a detection frequency of 59.65% (303/508), followed by group 1 (36.61%, 186/508), and group 3 (3.74%, 19/508). Thus, the level of plasma TILRR protein is not correlated with the detection frequency in patients' groups 1-3. Although patient group 4 showed no TILRR detection by Bio-Plex, Western blot analysis confirmed that this group of patients also carries TILRR in their blood plasma. Therefore, I considered patient group 4 as the lowest plasma TILRR group in this study.

Table 3.3: Blood plasma TILRR protein detection and confirmation by Bio-Plex assay and Western blot analysis.

The plasma of Patient groups (n=640)	Bio-Plex detection				Western Blot Confirmation (70 kDa band)				FCV
	F237G3 mAb	F218G4 mAb	F237G1 mAb	TILRR	F237G3 mAb	F218G4 mAb	F237G1 mAb	TILRR	TILRR
Group 1 (n=186)	D	D	ND	Yes	C	C	ND	Yes	Yes
Group 2 (n=303)	D	ND	ND	Not sure	C	C	ND	Yes	Yes
Group 3 (n=19)	ND	D	ND	Not sure	C	C	ND	Yes	Yes
Group 4 (n=132)	ND	ND	ND	Not sure	C	C	ND	Yes	Yes
D, detected; ND, not detected; C, confirmed; FCV, final confirmation and validation; kDa, kiloDalton									

Table 3.4: Blood plasma TILRR protein detection and quantification by Bio-Plex assay (after Western Blot analysis).

Patient groups	F237G3 mAb (CSPG 11 and 12) (ng/ml)	F218G4 mAb (Calx-β) (ng/ml)	F237G1 (CSPG9) (ng/ml)	TILRR	TILRR level (ng/ml)
Group 1	104.22	156.36	Not detected	Yes	156.36
Group 2	29.64	Not detected	Not detected	Yes	29.64
Group 3	Not detected	201.08	Not detected	Yes	201.08
Group 4	Not detected	Not detected	Not detected	Yes	Below detection

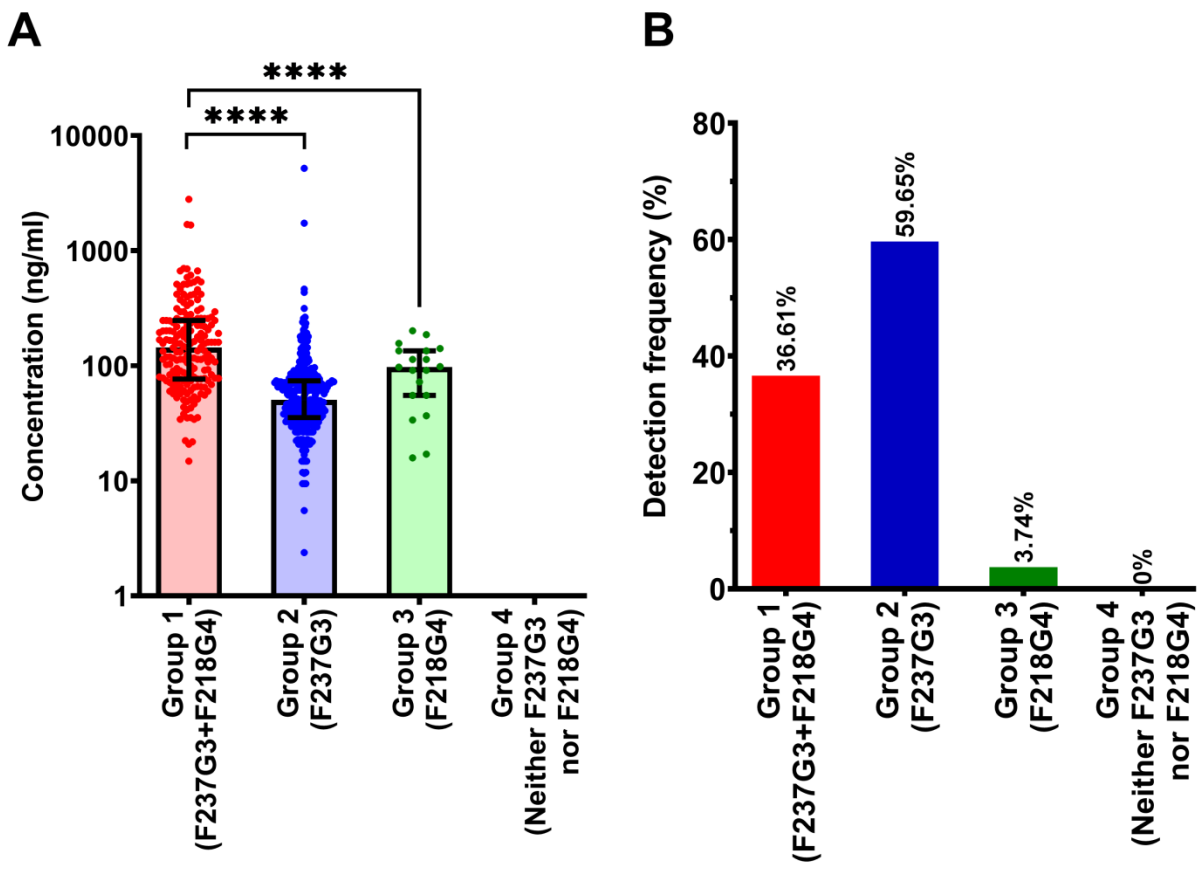

Figure 3.23: Variable quantity and the detection frequency of TILRR protein in human plasma samples. A) The level of plasma TILRR detected by anti-FREM1 mAbs (F237G3 and F218G4) among patients' groups 1-4 (n=640) (as classified in **Table 3.2)** is shown (median with interquartile range [IQR]). In the case of group 1, both anti-FREM1 mAbs (F237G3 and F218G4) detected the plasma TILRR, thus the higher detection value between these two mAbs was plotted (patient group 1). In the case of patient groups 2 and 3, TILRR was only detected by F237G3 mAb (group 2) and F218G4 mab (group 3), respectively. TILRR was detected neither by F237G3 mAb nor by F218G4 mAb in patient group 4 (below the detection limit). Thus, the data for group 4 was plotted as 0 (zero). F237G3 mAb targets epitopes on CSPG11 and 12 domains of FREM1/TILRR protein. F218G4 mAb binds epitopes on the Calx-β domain of FREM1/TILRR protein. **B)** The detection frequency of plasma TILRR protein among patients' groups 1-4 (n=640). As plasma from patient group 4 did not show TILRR detection by Bio-Plex, the detection frequency for group 4 showed 0 (zero) %. For groups 1-3, the detection frequency was calculated based on the total detected samples (n=508). Statistical comparisons were conducted using student t-test with 95% CI, all $p<0.05$ were reported and indicated using asterisks' ****$p<0.0001$.

3.4.1.3 Validation of in-house developed multiplex bead array method for plasma TILRR quantification

3.4.1.3.1 In-house developed Multiplex bead array method detected and quantified added recombinant FREM1 spD proteins

To investigate whether the in-house developed Bio-Plex method accurately quantified TILRR in plasma samples, the plasma samples from different patients' groups (as classified in **Table 3.2**) were spiked with rFREM1 spD protein. Quantification of the rFREM1 spD protein in these plasma samples will validate the in-house developed method. The data demonstrated that the multiplex bead array method successfully detected and quantified the spiked rFREM1 spD in these plasma samples (**Figure 3.24A, Table 3.5**). Thus, the in-house developed multiplex bead array method can successfully measure TILRR proteins in most patient samples as indicated in **Table 3.2**.

Next, I examined whether the Bio-Plex system can effectively measure the purified plasma TILRR protein from different patients' groups as categorized in **Table 3.2**. I used Bio-Plex assay to quantify the affinity-purified protein (the volume of affinity-purified protein was adjusted based on the input volume of plasma samples used in Bio-Plex assay). The results demonstrated that TILRR was detected in the affinity-purified protein of all patients' groups including group 4, which was undetectable by Bio-Plex assay before conducting affinity purification (**Figure 3.24B).** The reason for plasma TILRR detection by Bio-Plex assay in patient group 4 after affinity purification could be due to that the mAb-specific epitopes of TILRR are accessible to the mAbs in the purified TILRR solution, while in plasma samples the antibody specific epitopes might be blocked by other proteins. Taken together, these data suggested that the low limit of

TILRR detection using the in-house developed multiplex bead array method (Bio-Plex) was at the level of ≥2.38 ng/ml in human plasma samples.

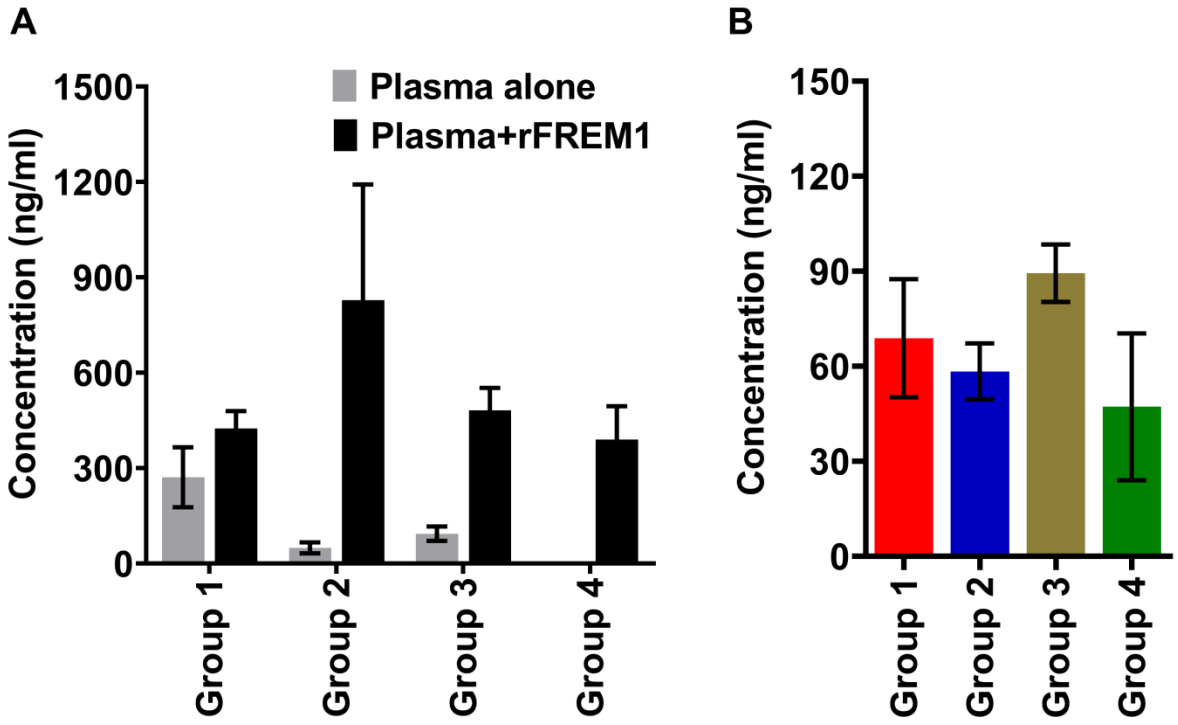

Figure 3.24: TILRR protein quantified by multiplexed bead array method in plasma samples of patients with different patients' groups before and after spiked with rFREM1 spD protein and following affinity purification. A) TILRR of plasma samples (n=3 from each of patient groups 1-4 in **Table 3.2**) spiked with rFREM1 spD protein (conc. 106.58 ng/ml). **B)** Quantification of affinity-purified TILRR protein (after removal of plasma IgG) obtained from plasma samples of different groups of patients (groups 1-4 in **Table 3.2**) (n=3 for each group). The input volume of affinity-purified protein was adjusted based on the amount of plasma samples used for the Bio-Plex assay. The data presented as mean±SEM of three independent samples. Legends on the top of Figure A represent the experimental conditions. The X-axis of both Figure A and B indicated the patients' groups.

Table 3.5: Validation of the detection efficiency of the in-house developed multiplex bead array assay

Patient group (as mentioned in Table 3.2)	Patient ID#	TILRR detection (Bio-Plex)	TILRR confirmation (WB, 70 kDa)	Amount of rFREM1 spD protein spiked to the plasma (ng/ml)	Bio-Plex detection after spiked with rFREM1 spD
Group 1	ML002492	Yes	Yes	106.58	Yes
	ML002802				
	ML002442				
Group 2	ML000326	Yes	Yes	106.58	Yes
	ML002170				
	ML002443				
Group 3	ML002292	Yes	Yes	106.58	Yes
	ML002772				
	ML000109				
Group 4	ML000887	Below detection	Yes	106.58	Yes
	ML000893				
	ML001070				

kDa, kiloDalton; WB, Western blot

3.4.1.3.2 TILRR protein purified by affinity purification with anti-FREM1 F237G12 IgG mAb

To verify whether the agarose beads cross-linked with anti-FREM1 F237G12 IgG mAb captured FREM1 variants including TILRR in human plasma, I spiked patient plasma samples with rFREM1 spD protein. After affinity purification, Western blot analysis was conducted. The results showed that only a ~57 kDa band was observed in rFREM1spD protein alone, whereas both 70 kDa and ~57 kDa sized protein were found in patients' plasma samples spiked with rFREM1 spD protein (**Figure 3.25A** and **Appendix Figure B7.7A)**. Intriguingly, the plasma sample itself without the added rFREM1 spD protein had also a ~57 kDa-sized protein in addition to the 70 kDa TILRR protein (**Figure 3.25A** and **Appendix Figure B7.7A**). Additionally, Coomassie blue staining showed that the remaining proteins in the gel had also strong signal intensity for both ~57 kDa and 70 kDa proteins in all conditions (**Figure 3.25B** and **Appendix Figure B7.7B).** Overall, the plasma samples with spiked rFREM1 spD protein demonstrated higher signal intensity for ~57 kDa protein compared to the rFREM1 spD alone and plasma itself (**Figure 3.25C-D)**. Thus, this study confirmed that agarose beads cross-linked with anti-FREM1 F237G12 IgG mAb can efficiently capture TILRR protein or other minor variants of FREM1 from patients' plasma.

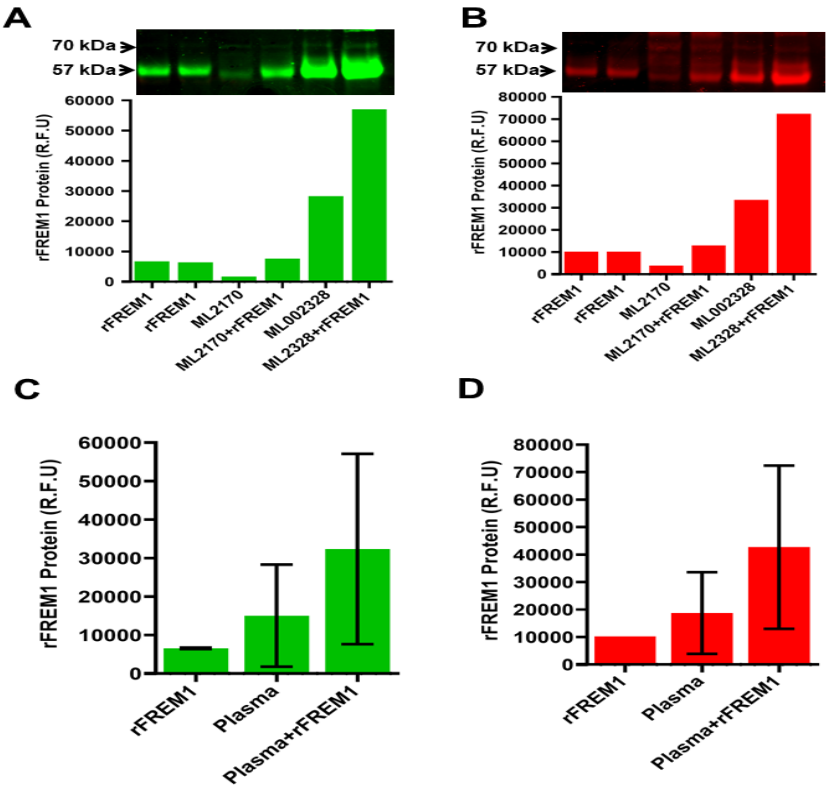

Figure 3.25: Western blot and Coomassie blue staining confirmation of plasma TILRR protein before and after spiked with rFREM1 spD and affinity purification. The plasma sample (1ml) was spiked with rFREM1 spD (106.58 ng/ml) in a single tube. In parallel, the plasma sample alone, and rFREM1 spD alone were separately taken into the tubes. The final volume of all samples was adjusted to 4 ml (1:4 dilution), and the concentration of spiked rFREM1 spD protein was adjusted similar to the concentration of TILRR protein (median) in the patient's plasma observed by Bio-Plex. Affinity purification (AP) was conducted by cross-linked anti-FREM1 F237G12 IgG mAb. **A)** Western blot confirmation of ~57kDa rFREM1 spD protein (cropped; Full-length un-cropped bot is shown in **Appendix Figure B7.7A**). The bar graph underneath the cropped blot shows the corresponding protein intensity (R.F.U) for only ~57kDa protein. **B)** Coomassie blue staining of ~57kDa rFREM1 spD protein (cropped; the full-length un-cropped gel is shown in **Appendix Figure B7.7B)**. The bar graph underneath the gel shows the corresponding rFREM1protein intensity (R.F.U) for ~57kDa protein. TILRR protein intensity (R.F.U) with bar graph for 70 kDa protein is not shown. **C-D)** Plasma samples with spiked rFREM1 spD protein (R.F.U) compared to the rFREM1 spD alone and plasma alone following Western blot analysis (C) and Coomassie blue staining (D). Western blot and Coomassie blue staining images were acquired by Odyssey CLx imaging system (LI-COR, USA) with auto channels (both 700 and 800), 42 µm resolution, high image quality, and 0mm focal offset for blots and 0.5mm focal offset for gels. kDa, kiloDalton; RFU, relative fluorescence units.

3.4.2 Association of plasma TILRR with HIV seroconversion

3.4.2.1 Detection frequency of TILRR protein in archived plasma samples

To assess whether archived human plasma samples (n= 640) are suitable to further analysis of TILRR protein, I first estimated the overall detection frequency of TILRR protein in plasma samples collected between 1985 and 2008 following Bio-Plex quantification. Data analysis showed that overall detection frequency was higher in plasma samples collected between 2001 and 2008 (**Figure 3.26A,** detailed breakdown is presented in **Appendix Figure B7.8 and Appendix Figure B7.9).** More specifically, the highest detection frequency was recorded as 93.08% (121/130) between 2001 and 2005, and the least frequency was 64.25% (124/193) from 1991 to 1995. The frequency of 80.77% (84/104), 79.28% (88/111), and 89.22% (91/102) was also observed during 1985-1990, 1996-2000, and 2006-2008, respectively. These data suggest that the overall detection frequency of TILRR protein in archived plasma samples is suitable to use for further analysis.

Next, I analyzed whether the level of plasma TILRR protein was correlated with the frequency of detection in archived plasma samples. The analysis demonstrated that the highest level of TILRR protein was observed in samples collected between 1985 and 1990 (median [IQR]: 134.63 [41.43-257.37] ng/ml) whereas the lowest level of plasma TILRR was observed in samples collected during 2001-2005 (median [IQR]: 42.31 [23.39-65.03] ng/ml) (**Figure 3.26B**). Thus, the levels of TILRR protein in the archived plasma samples are not correlated with the frequencies of plasma TILRR protein detection and the plasma samples collected between 1985 and 2008 are suitable for further analysis with other factors, such as plasma inflammatory cytokines, FREM1 SNP rs1552896 genotype, and HIV acquisition.

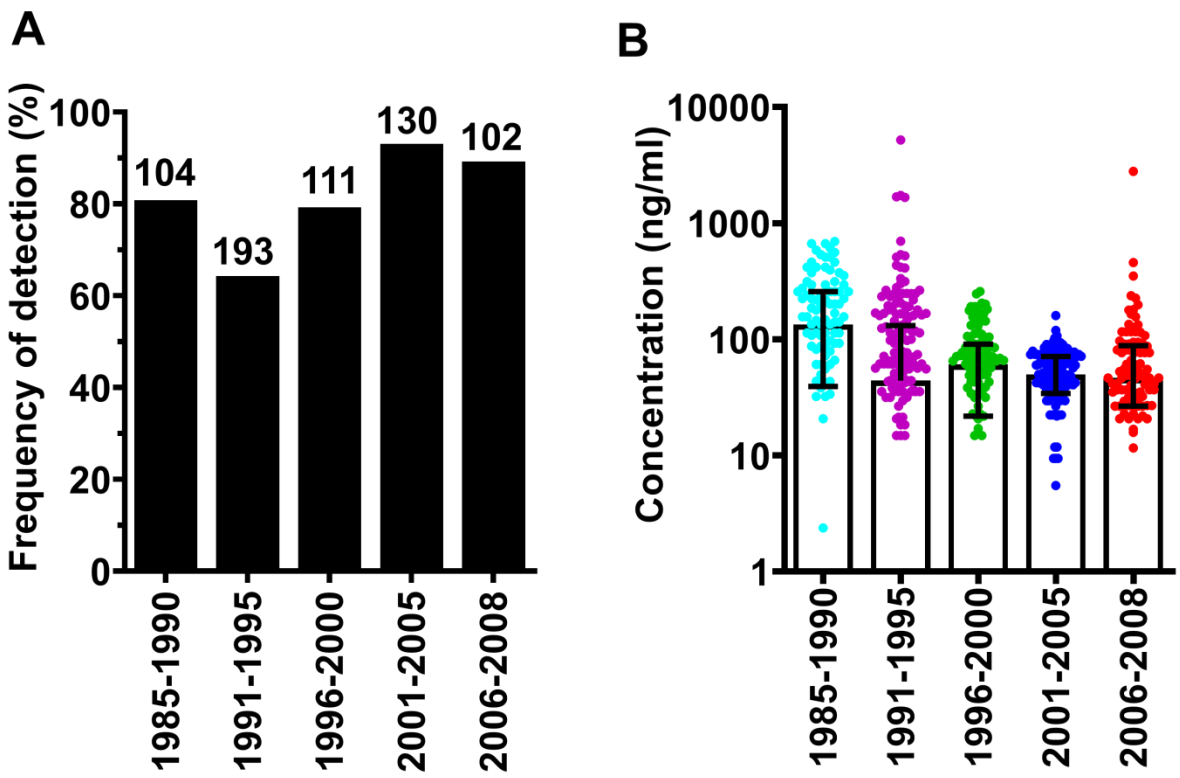

Figure 3.26: Overall detection frequency and the level of plasma TILRR in archived samples of all patients (groups 1-4) collected from women of PSWC. A) Frequency of blood plasma TILRR detection among different groups of patients (as mentioned in **Table 3.2**) collected between 1985 and 2008 (n=640); **B)** The level of TILRR protein (median with IQR) in plasma samples collected between 1985 and 2008 (n=640). The number above and within each bar of Figure **A** represents the total samples (n) tested and the TILRR protein detection frequency (%), respectively.

3.4.2.2 Higher frequency of high plasma TILRR protein was observed in patients with FREM1 SNP rs1552896 CC genotype (major allele) in the Pumwani sex worker cohort

An earlier study from our group showed that the minor allele "G" (GG/GC genotype) of FREM1 SNP rs155896 is correlated with HIV resistant individuals and the major allele "C" (CC genotype) of FREM1 SNP is associated with HIV susceptible individuals [260]. To examine whether women with CC genotype of FREM1 SNP rs1552896 are more likely to have a high level of TILRR in their blood than women with GG/GC genotype of the FREM1 SNP, I analyzed the frequency and the level of plasma TILRR protein expression between CC and GG/GC genotypes of women of PSWC. Of 640 samples (316 subjects), 557 (291 subjects)- and 71 (21 subjects)- samples were CC and GG/GC genotype, respectively. Twelve samples (4 subjects) did not have genotype information. The analysis revealed that the frequency of plasma TILRR was higher in women with CC genotype than in women with GG/GC genotype, with 82.05% (457/557) was observed among women with CC genotype, and 54.93% (39/71) was observed among women with GG/GC genotype (**Figure 3.27A; Appendix Figure B7.10A)**.

The level of TILRR in blood plasma was correlated to the frequency of detection among women with FREM1 SNP rs1552896 genotypes (**Figure 3.27B; Appendix Figure B7.10B**). The level of plasma TILRR was significantly higher among CC genotype individuals than that of GG/GC genotype individuals (median [IQR]: 56.96 [26.58 - 108.44] ng/ml versus 21.36 [0.00-62.37] ng/ml, $p< 0.0001$). Taken together, these data showed that a higher level of plasma TILRR is present with higher frequencies in women with FREM1 SNP rs155289 major allele genotype (CC) than women with the minor allele genotype of FREM1 SNP rs1552896 (GG/GC).

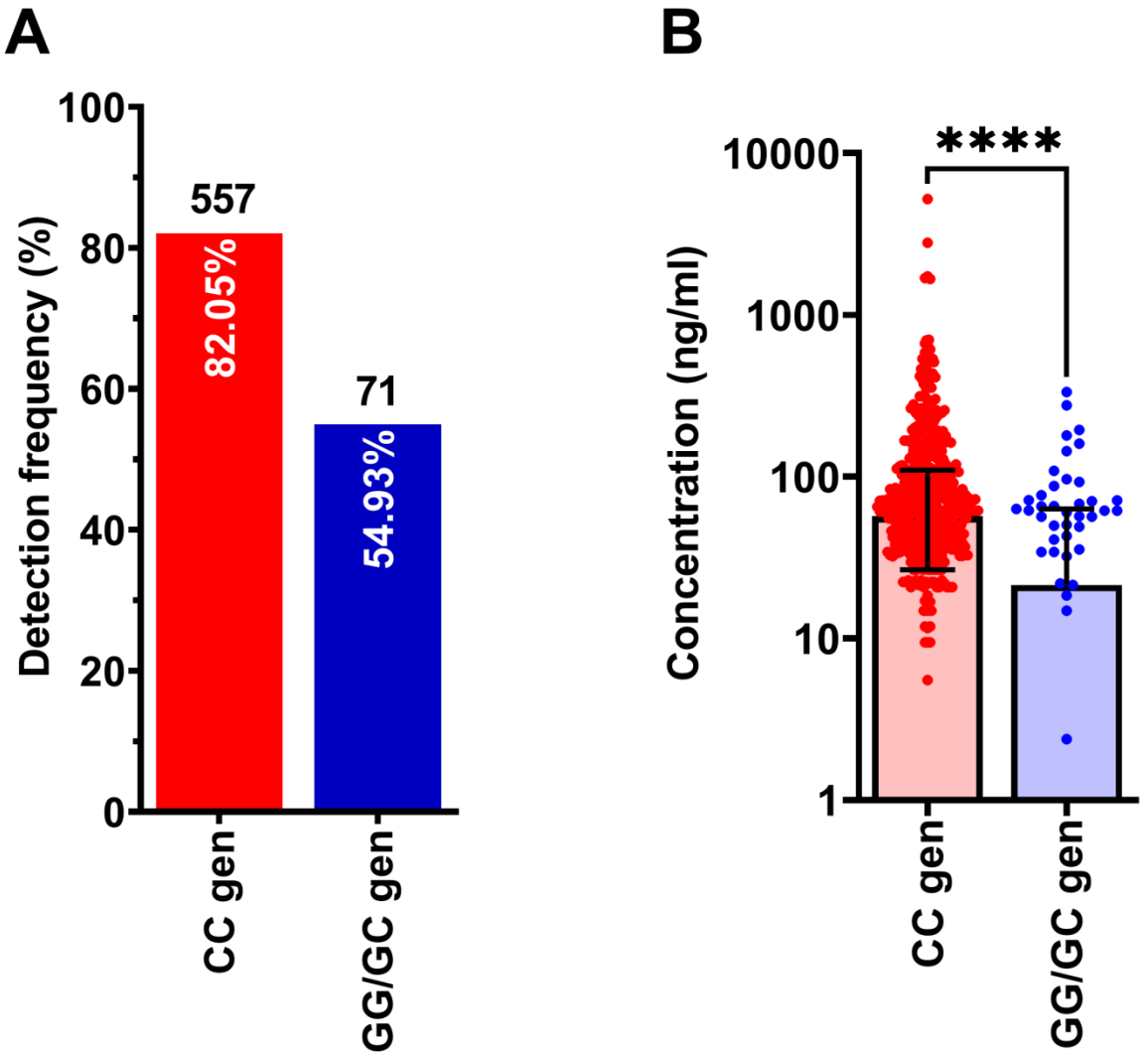

Figure 3.27: Frequency and the level of plasma TILRR in women with FREM1 SNP rs1552896 genotype quantified by Bio-Pex. A) Frequency of plasma TILRR detection between major allele (CC genotype) (plasma n=557) and minor allele (GG/GC genotype) (plasma n=71) of FREM1 SNP rs1552896 genotype women. The numbers on the top and the percentage within the bar show the total plasma sample (n) tested and frequency of TILRR detection, respectively; **B)** The level of plasma TILRR (median with IQR) between CC genotype and GG/GC genotype women (plasma n=628). The detailed breakdown of the data among patients' groups 1-4 as classified in **Table 3.2** is shown in **Appendix Figure B7.10.** Statistical comparisons were conducted using student t-test with 95% CI, all $p<0.05$ were reported and indicated using an asterisks' ****$p<0.0001$. gen, genotype.

3.4.2.3 A higher frequency of high-level plasma TILRR was observed in HIV seroconverters

To assess whether plasma TILRR protein expression is higher in HIV seroconverters (HIV SCON) than HIV resistant women (HESN), I next compared the frequencies and the level of median plasma TILRR level between HIV SCON and HIV resistant women. Among 449 samples (169 subjects), 171 samples (78 subjects) were from HIV SCON before seroconversion and 278 samples (91 subjects) were from HIV resistant women. The analysis showed that a higher frequency of plasma TILRR was detected in HIV SCON than that of HIV resistant women (99.42% [170/171] versus 60.43 % [168/278], respectively) (**Figure 3.28A; Appendix Figure B7.11A**).

The median level of plasma TILRR was also compared between HIV SCON and HIV resistant women (**Figure 3.28B; Appendix Figure B7.11B**). The result showed that the HIV SCON women had a significantly higher median level of plasma TILRR than the HIV resistant women (median [IQR]: 167.09 [107.05 - 257.37] ng/ml versus 35.44 [0.00 - 61.65] ng/ml, $p<0.0001$). Thus, the median plasma TILRR protein level is significantly higher in HIV seroconverters.

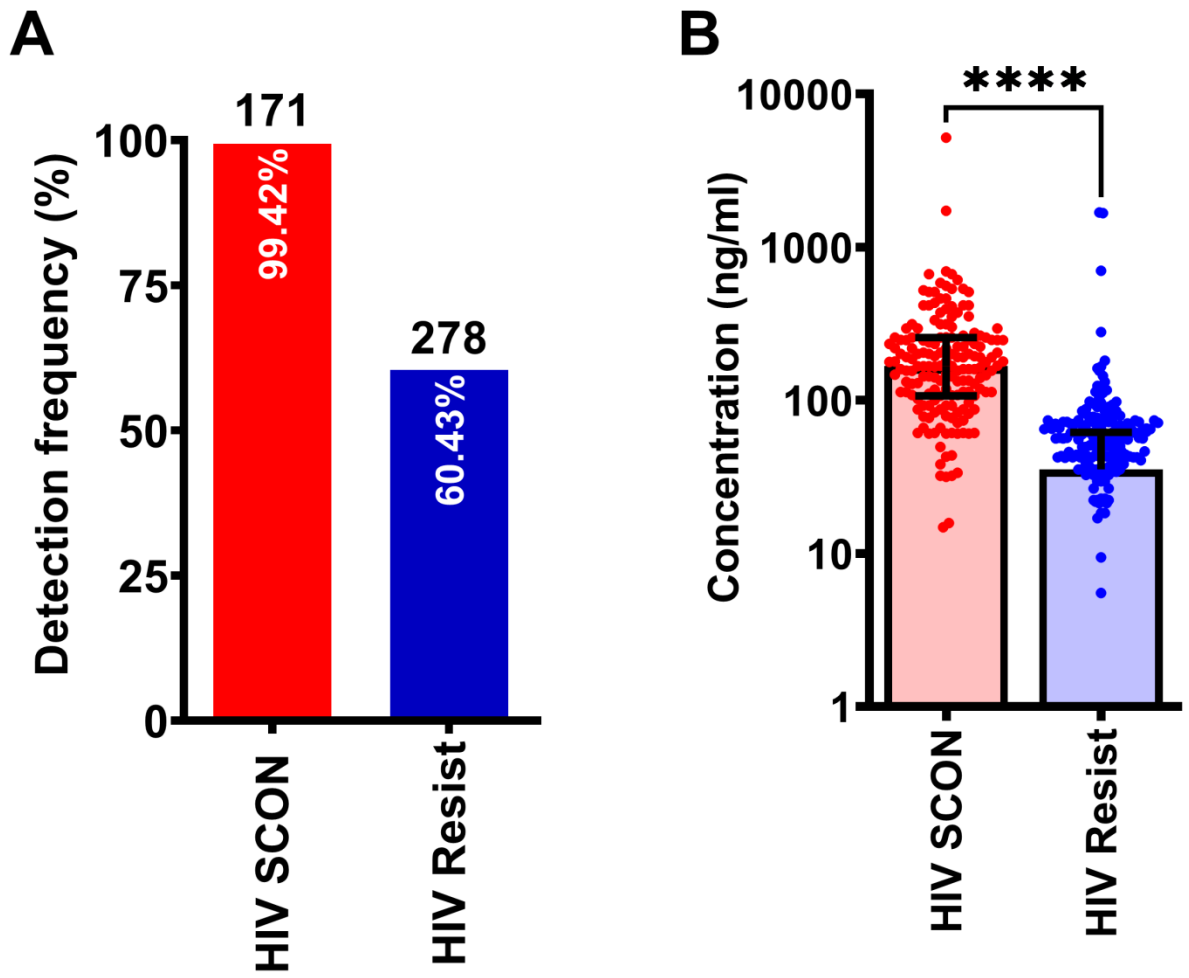

Figure 3.28: Frequency and the median level of plasma TILRR between HIV SCON and HIV resistant women of PSWC quantified by Bio-Plex. A) Frequency of plasma TILRR detection between HIV SCON (n=171) and HIV resistant (n=278) women. The numbers on the top and the percentage within the bar show the total sample (n) tested and frequency of TILRR detection, respectively; **B)** The median level of plasma TILRR (median with IQR) between HIV SCON and HIV resistant women (n=449). The detailed breakdown of the data among patients' groups 1-4 as classified in **Table 3.2** is presented in **Appendix Figure B7.11.** Statistical comparisons were conducted using student t-test with 95% CI, all $p<0.05$ were reported and indicated using asterisks' ****$p<0.0001$. HIV SCON, HIV seroconverters; Resist, resistant.

3.4.2.4 Plasma TILRR level is correlated with the levels of several plasma inflammatory cytokines/chemokines

Next, I examined the plasma TILRR and its relationship with the levels of 14 plasma inflammatory cytokines/chemokines in 352 patients. Spearman rank correlation analysis was conducted and showed that plasma TILRR level is positively correlated with the levels of several plasma pro-inflammatory cytokines/chemokines, including IL-1β (rho= 0.259, p<0.0001), MCP-1 (rho= 0.2377, p<0.0001), and IL-17A (rho= 0.1225, p=0.0220) (**Table 3.6**). There is also a trend of positive correlation of plasma TILRR with the levels of IFNγ, IL-6, GM-CSF, MIP-1α, MIP-1β, IL-10, and IP-10. Many of the pro-inflammatory cytokines/chemokines are positively correlated with each other (**Table 3.6**). For instance, IL-1β was positively correlated with IL-6 (rho= 0.3057, p<0.0001), GM-CSF (rho= 0.1063, p= 0.0464), MCP-1 (rho= 0.2805, p<0.0001), MIP-α (rho= 0.2312, p<0.0001), MIP-β (rho= 0.2782, p<0.0001), IL-10 (rho= 0.2529, p<0.0001), IP-10 (rho= 0.2893, p<0.0001), and IL-17A (rho= 0.2741, p<0.0001). Cytokine MCP-1 was also significantly correlated with IL-6 (rho= 0.1540, p=0.0038), GM-CSF (rho= 0.1197, p=0.0247), IL-1β (rho= 0.2805, p<0.0001), MIP-α (rho= 0.1693, p=0.0014), MIP-1β (rho= 0.4372, p<0.0001), IP-10 (rho= 0.2543, p<0.0001), and IL-17A (rho= 0.4072, p<0.0001).

Furthermore, IFNγ, IL-6, GM-CSF, MIP-1α, MIP-1β, IL-10, IP-10, and IL-17A were positively correlated with each other. Since overexpression of TILRR increased the secretion of several pro-inflammatory cytokine/chemokines, that the positive correlation of plasma TILRR with the proinflammatory cytokines/chemokines in the blood is consistent with the role of TILRR in modulating the level of circulating inflammatory cytokines/chemokines in human blood and may contribute to systemic inflammation and HIV acquisition.

Table 3.6: Spearman rank correlation of plasma TILRR with plasma inflammatory cytokines/chemokines.

	TILRR	**IFNγ**	**IL-6**	**GM-CSF**	**IL-1β**	**MCP-1**	**MIP-1α**	**MIP-1β**	**IL-10**	**IP-10**	**IL17A**
TILRR (rho)	1.0000	0.0972	0.0990	0.0152	0.2593	0.2377	0.0166	0.0658	0.0673	0.0425	0.1225
p-value	.	0.0685	0.0635	0.7765	**<0.0001**	**<0.0001**	0.7566	0.2179	0.2076	0.4266	**0.0216**
IFNγ (rho)	0.0972	1.0000	0.1993	0.0540	0.0880	-0.0717	-0.2116	0.1319	0.4395	-0.2009	0.2268
p-value	0.0685	.	**0.0002**	0.3121	0.0994	0.1793	**0.0001**	**0.0133**	**<0.0001**	**0.0001**	**<0.0001**
IL-6 (rho)	0.0990	0.1993	1.0000	0.4051	0.3057	0.1540	0.3282	0.3264	0.3076	0.3206	0.2038
p-value	0.0635	**0.0002**	.	**<0.0001**	**<0.0001**	**0.0038**	**<0.0001**	**<0.0001**	**<0.0001**	**<0.0001**	**0.0001**
GM-CSF (rho)	0.0152	0.0540	0.4051	1.0000	0.1063	0.1197	0.0363	0.0991	0.3114	0.2240	0.0769
p-value	0.7765	0.3121	**<0.0001**	.	**0.0464**	**0.0247**	0.4978	0.0633	**<0.0001**	**<0.0001**	0.1500
IL-1β (rho)	**0.2593**	0.0880	0.3057	0.1063	1.0000	0.2805	0.2312	0.2782	0.2529	0.2893	0.2741
p-value	**<0.0001**	0.0994	**<0.0001**	**0.0464**	.	**<0.0001**	**<0.0001**	**<0.0001**	**<0.0001**	**<0.0001**	**<0.0001**
MCP-1 (rho)	**0.2377**	-0.0717	0.1540	0.1197	0.2805	1.0000	0.1693	0.4372	-0.0356	0.2543	0.4072
p-value	**<0.0001**	0.1793	**0.0038**	**0.0247**	**<0.0001**	.	**0.0014**	**<0.0001**	0.5051	**<0.0001**	**<0.0001**
MIP-1α (rho)	0.0166	-0.2116	0.3282	0.0363	0.2312	0.1693	1.0000	0.6035	-0.0377	0.3864	0.3175
p-value	0.7566	**0.0001**	**<0.0001**	0.4978	**<0.0001**	**0.0014**	.	**<0.0001**	0.4804	**<0.0001**	**<0.0001**
MIP-1β (rho)	0.0658	0.1319	0.3264	0.0991	0.2782	0.4372	0.6035	1.0000	0.1307	0.2774	0.6468
p-value	0.2179	**0.0133**	**<0.0001**	0.0633	**<0.0001**	**<0.0001**	**<0.0001**	.	**0.0142**	**<0.0001**	**<0.0001**
IL-10 (rho)	0.0673	0.4395	0.3076	0.3114	0.2529	-0.0356	-0.0377	0.1307	1.0000	-0.0362	0.2042
p-value	0.2076	**<0.0001**	**<0.0001**	**<0.0001**	**<0.0001**	0.5051	0.4804	**0.0142**	.	0.4986	**0.0001**
IP-10 (rho)	0.0425	-0.2009	0.3206	0.2240	0.2893	0.2543	0.3864	0.2774	-0.0362	1.0000	0.0944
p-value	0.4266	**0.0001**	**<0.0001**	**<0.0001**	**<0.0001**	**<0.0001**	**<0.0001**	**<0.0001**	0.4986	.	0.0769
IL-17A (rho)	**0.1225**	0.2268	0.2038	0.0769	0.2741	0.4072	0.3175	0.6468	0.2042	0.0944	1.0000
p-value	**0.0216**	**<0.0001**	**0.0001**	0.1500	**<0.0001**	**<0.0001**	**<0.0001**	**<0.0001**	**0.0001**	0.0769	.

rho, Spearman's rank correlation coefficient or Spearman's ρ; Significant p-values showed as bold and underlined

3.4.3 SUMMARY

In this section of my thesis, I described the investigations to determine whether TILRR exists as a soluble protein in human plasma and if it is the case whether its levels in plasma are correlated with the FREM1 SNP rs1552896 genotypes, plasma inflammatory cytokines/chemokines, and HIV resistance/susceptibility. The existence of TILRR in human blood plasma has not been reported. The anti-FREM1 mAbs developed in our lab were used to develop a multiplex bead array method (Bio-Plex) to detect and quantify the plasma TILRR. The detected plasma TILRR is validated with affinity-purification and Western blot analysis. The data of my studies demonstrated that TILRR circulates in the human blood of all patients in this study and the level of TILRR in plasma varied greatly among the patients.

I also found that women who are homozygous of the major allele of FREM1 SNP rs1552896 (CC) are more likely to have a higher median level of TILRR in their blood plasma than those who have the minor allele (GG/GC) of the FREM1 SNP. HIV seroconverters (HIV SCON) are more likely to have a higher median level of plasma TILRR (before seroconversion) than HIV resistant (HESN) women in the Pumwani sex worker cohort. Furthermore, the median levels of plasma TILRR are significantly correlated with the levels of several plasma pro-inflammatory cytokines/chemokines, including IL-1β, MCP-1, and IL-17A. Thus, plasma TILRR may play an important role in modulating systemic inflammation, and a high median level of plasma TILRR is a risk factor or biomarker for susceptibility to HIV acquisition.

4 CHAPTER 4: DISCUSSION

4.1 TILRR increases the mRNA expression of many genes in the NF-κB signaling pathway and is an important modulator of inflammation responsive genes

Inflammation is an intricate host biological response to pathogenic stimuli in which immune system components are highly activated [325]. Host inflammatory response stimulates the transactivation of an array of genes involved in a wide range of physiological functions, including the induction of antimicrobial activity [326]. NF-κB activation is central to inflammation [327, 328] and critical in response to viral infections [299]. NF-κB signaling can be activated by binding of IL-1 with IL-1R1 transmembrane receptor [329]. Previous studies have identified TILRR, a variant of FREM1, as a co-receptor of IL-1R1, and its association with the IL-1R1 receptor enhances the recruitment of MYD88, controls the induction of Ras GTPase, and amplifies the activation of NF-κB and inflammatory responses [285, 293]. A subsequent study showed that TILRR is associated with the development of cardiovascular disease via aberrant activation of inflammatory genes [288]. Since TILRR is involved in modulating NF-κB activation and inflammatory responses [285], it may influence HIV susceptibility through its role in modulating inflammation. To understand the effect of TILRR on mRNA expression of genes in the NF-κB signaling pathway, I conducted a more extensive analysis of genes influenced by TILRR overexpression in two cell lines, human cervical epithelial (HeLa) cells, and human normal vaginal mucosal (VK2/E6E7) cells, using a PCR array system, RT^2 profiler qPCR array. The RT^2 profiler qPCR array allows to evaluate the expression of 84 genes in the NF-κB signal transduction pathway, and the RT^2 qPCR Primer assay was then used to further evaluate the selected immune and inflammation responsive genes. Real-time qPCR array analysis is a

convenient, sensitive, and time-efficient technique to analyze the mRNA expression of multiple genes [330].

The data from my study showed that TILRR overexpression significantly regulated the expression of immune and inflammation-responsive genes in a dose-dependent manner. My study also showed that overexpression of TILRR up-regulated the expression of many genes in the NF-κB signaling pathway, far more than previously reported. In addition to the expression of IL-1R1, MYD88, TRAF6 reported previously [285], among the 84 genes involved in the NF-κB signaling pathway, TILRR overexpression significantly up-regulated the expression of many genes in HeLa and VK2/E6E7 cells. Among the significantly up-regulated genes, some have critical roles in NF-κB activation, and innate and adaptive immune responses (**Appendix Table C7.9**). The effects of TILRR on these NF-κB signaling-related genes and inflammation-mediated genes demonstrated the importance of TILRR in immune regulation and inflammatory responses. A number of studies showed that the NF-κB pathway coordinates the expression of several hundred functionally diverse genes in many key cellular and physiological processes, such as immune regulation, cytokines/chemokines production, cell adhesion, survival, and proliferation [298, 331-333].

My study demonstrated that TILRR overexpression alone increased the expression of **1)** signaling ligands, such as CXCL8 (IL-8), IL-1α, IL-1β, and TNFα; **2)** cell surface receptor, such as TLR2, TLR3, TNFRSF10A, and TNFRSF10B, and many downstream signaling genes in NF-κB signal transduction pathway **(Figure 3.9, Figure 3.10 and Figure 3.11),** and significantly augmented the mRNA transcript expression of several immune responsive genes when together with IL-1β in serum-free media (**Figure 3.12)**. Thus, TILRR appears to not only be a co-receptor

of the IL-1R1 but also have a direct effect on genes in the NF-κB signal transduction and inflammation pathway.

In humans, cervical epithelial cells express higher amounts of FREM1 [260] and TILRR when compared to other tissues. Using HeLa and VK2/E6E7 cells as an *in vitro* system in this study may help to understand the influence of TILRR, a variant of FREM1, on the inflammatory responses in the epithelial mucosal barrier. Mucosal epithelial cells not only serve as a physical barrier but also act as the first line of defense against infection [334]. Breaches in the epithelial lining increase the risk of inflammation and infection [335].

Collectively, this study is the first to show that TILRR overexpression regulates the expression of many genes in the NF-κB signal transduction pathway. TILRR could be an important mediator of the NF-κB signaling pathway and plays a major role in regulating innate immune and inflammatory responses, and may play an important role in microbial infection and disease pathogenesis, including HIV vaginal infection and transmission.

4.2 TILRR induces the production of soluble cytokines/chemokines in cervicovaginal epithelial cells

Activation of NF-κB signal transduction leads to the production of pro-inflammatory cytokines/chemokines [181, 295]. An elevated level of pro-inflammatory cytokines/chemokines, including IL-1β, IL-6, IL-8/CXCL8, MCP-1/CCL2, MIP-1α/CCL3, MIP-1β/CCL4, and TNFα in cervicovaginal lavage (CVL) favors the vaginal HIV infection and transmission [218, 336]. Since TILRR augments the TIR-MYD88 dependent NF-κB activation and inflammatory responses [285, 293], TILRR overexpression could induce and increase the production of pro-inflammatory cytokines/chemokines in cervicovaginal epithelial cells. To test this, I analyzed 13-

inflammatory cytokines/chemokines in the cell culture supernatants of TILRR-transfected epithelial cells using an in-house developed multiplex magnetic bead assay (Bio-Plex). The multiplex magnetic bead assay can quantify 13-inflammatory cytokines/chemokines simultaneously and is a more sensitive, cost-efficient, and less time-consuming method [337], and required less volume of sample input than that of conventional ELISA, which can measure only one analyte at a time.

The data showed that TILRR overexpression increased the production of several inflammatory cytokines/chemokines, including IL-6, IL-8/CXCL8, IP-10/CXCL10, MCP-1/CCL2, MIP-1β/CCL4, and RANTES/CCL5 by HeLa cells and VK2/E6E7 cells. These inflammatory cytokines/chemokines were increased in a time-dependent manner within 24 hours. The increase in the protein level of these mediators is consistent with the increase in their mRNA transcripts. My study data also showed that the addition of IL-1β significantly increased the level of IL-6, IL-8/CXCL8, IP-10/CXCL10, MCP-1/CCL2, MIP-1β/CCL4, and RANTES/CCL5 in the supernatants of the TILRR-overexpressed HeLa and VK2/E6E7 cells. This observation is consistent with the TILRR's role in NF-κB activation and pro-inflammatory responses [285, 294].

This study, therefore, shows that TILRR influences the production of inflammatory mediators, although the mechanisms need to be explored in future studies. Pro-inflammatory cytokines/chemokines have been reported as the multifunctional regulator, the inducer of immune cell infiltration, a potent activator of nuclear localization of NF-κB, and an enhancer of inflammation [338-342]. Regulation of these pro-inflammatory cytokines/chemokines by TILRR suggests that TILRR may be a direct regulator in the NF-κB signal transduction, and inflammatory responses. Altogether, these data showed that TILRR, in the presence of IL-1β,

can modulate the production of pro-inflammatory cytokines/chemokines by cervicovaginal epithelial cells. Mucosal pro-inflammatory cytokines/chemokines are associated with the risk of genital inflammation and HIV acquisition [218]. The elevated level of soluble mediators in cervicovaginal lavage (CVL) positively correlates with increased genital HIV RNA shedding, and plasma viral load set point and is also inversely correlated with systemic CD4+T cell counts [218, 229, 230, 343, 344].

My study thus suggested that TILRR-promoted cytokines/chemokines production from cervicovaginal epithelial cells may function as a critical regulator in augmenting inflammation-mediated microbial infection, including vaginal HIV infection, transmission, and disease progression.

4.3 TILRR promotes the migration of immune cells through the induction of soluble inflammatory mediators

Inflammatory mediators activate the host defense mechanisms by infiltrating the immune cells, including monocytes/macrophages, lymphocytes, and neutrophils, to the site of infection [326]. The infiltrated immune cells become activated and release more cytokines/chemokines in the injured tissues, resulting in amplified inflammatory responses [345]. Several studies have shown that chemo-attractants, including IL-8/CXCL8, IP-10/CXCL10, MCP-1/CCL2, MIP-1α/CCL3, MIP-1β/CCL4, MIP-3α, and RANTES/CCL5 produced by female genital epithelium induced the infiltration of circulating immune cells, causing an increased risk of HIV/SIV acquisition [218, 219, 312, 346]. Because TILRR expression induced the production of several cytokines/chemokines in cervical epithelial cell lines, I investigated the effect of the supernatant of the TILRR-overexpressed HeLa cells on the migration of immune cells in this study using Transwell and microfluidic device assays. My study data showed that the supernatants of

TILRR-overexpressed HeLa cells attracted migration of THP-1 and MOLT-4 cells in Transwell assay. Besides, with a novel microfluidic assay, I demonstrated that the THP-1 and MOLT-4 cells migrated further towards the supernatants of the TILRR-overexpressed HeLa cells. THP-1 cells (monocytes) and MOLT-4 cells (T cells) are CD4-expressing cells, the targets of HIV [304, 305, 311]. Thus, the supernatant of TILRR overexpressed HeLa cells, containing multiple pro-inflammatory cytokines/chemokines [254], attracts HIV target cells.

The purpose of using two different cell migration techniques in this study was to confirm the study findings in parallel. The traditional Transwell assay was used to analyze the ability of the cells to migrate through a porous membrane accompanied by the relative percentage of total cell migration towards the gradients of HeLa cell culture supernatants. The traditional Transwell assay is convenient and compatible with all kinds of cell types, and the most widely used sensitive quantification of *in vitro* cell migration technique [347]. However, the Transwell assay does not provide how far a single cell can migrate towards the added chemo-attractants. Despite the popularity and advantages of Transwell for cell migration study, this assay only offers the endpoint readout of the entire number of cells without providing other important migratory aspects of the individual cell level. To fill the gap and exclude the possible effect on the gravitational force of loaded cells during the experiment, I applied a novel microfluidic device to confirm the attraction effect of the same supernatant on the migration of THP-1 and MOLT-4 cells. Specifically, this microfluidic device enables eight independent experiment groups conducted simultaneously, which dramatically increased the experimental throughput. Unlike other microfluidic devices that require external input, such as pumps to generate and maintain a stable chemical gradient, this device offers a stable chemical gradient generated by the pressure differences between the chemical inlets and waste outlets in a well-controlled manner [348]. In

addition, the advanced cell docking design provides the initial alignment of all the loaded cells in the cell-loading channel at the beginning, which increases the accuracy of displacement measurement on each individual migrated cell during the experiment. On the other hand, the presence of the docking barrier requires all loaded cells to transform the cell size to squeeze and horizontally migrate through the area when stimulated by the chemical gradient, which excludes the gravity issue that may exist in Transwell assay. Microfluidic devices have been widely applied for cell migration studies because of several advantages, including extremely low cell and reagent consumption, stable chemical gradient generation, and live-cell tracking. Due to the versatile features of the microfluidic device, many important properties of an individual migrated cell, such as speed and displacement can be extracted from the migration experiment [349]. Therefore, the combination of these two techniques in my experimental settings confirmed that immune cells, the HIV target cells, were successfully migrated to the TILRR-overexpressed HeLa cell culture supernatants.

Studies have shown that genital pro-inflammatory cytokines/chemokines induce a rapid influx of HIV target cells, leading to inflammation [59, 180, 222, 312, 313]. The elevated levels of cytokines/chemokines IL-8/CXCL8, MIP-1α/CCL3, and MIP-1β/CCL4 are strongly associated with the recruitment of monocytes/macrophages and neutrophils in female genital secretion [209]. My study showed that TILRR plays an important role in regulating this pro-inflammatory cytokine/chemokine environment and immune cell infiltration in cervical epithelial tissue. TILRR could promote the migration of immune cells, especially the HIV target cells, in the female genital epithelium through the modulation of pro-inflammatory cytokines/chemokines secretion, resulting in an increased risk of vaginal HIV infection and transmission. Thus, TILRR-promoted migration of immune cells warrants further studies.

Collectively, TILRR-modulated cytokines/chemokines from HeLa cells promote the migration of immune cells. My study is the first to show that TILRR can regulate the migration of HIV target cells into cervical epithelial tissues. Targeting TILRR may lead to new interventions in reducing vaginal HIV infection.

4.4 TILRR protein is detected in human plasma using in-house developed Bio-Plex and Western blot analysis

Using *in vitro* and *in vivo* models, I and others have previously shown that IL-1R1 co-receptor TILRR is an important modulator of the NF-κB signaling pathway and aberrant inflammatory responses [254, 285, 288, 294]. Despite the role of TILRR in the NF-κB signal transduction pathway, it is unknown whether TILRR exists as a soluble protein in human blood plasma. I used an in-house developed multiplexed bead array method and Western blot analysis and confirmed that TILRR indeed exists in patient plasma samples enrolled in the Pumwani sex worker cohort.

Although the amino acid sequence of TILRR is almost identical to FREM1, it can be differentiated from the full-length FREM1 protein using a combination of monoclonal antibodies recognizing epitopes on different protein domains of FREM1. The multiplexed bead array TILRR quantification method has been validated by affinity purification and Western blot analysis.

My study showed that TILRR protein is present in all blood plasma samples examined, but its quantities vary greatly among the patients, ranging from 2.38 ng/ml to 5196.79 ng/ml among 640 plasma samples from 316 patients. Thus, the multiplexed bead array method can detect and quantify plasma TILRR as low as 2.38 ng/ml. The plasma TILRR below this amount can only be detected by affinity purification and Western blot analysis.

My study demonstrated that TILRR exists as a soluble protein in human blood plasma and can be quantified by an in-house developed multiplexed bead array method using in-house developed anti-FREM1 mAbs with rFREM1 spD protein as a standard. I, for the first time, demonstrated that TILRR protein is circulating in the blood and may be an important mediator of systemic inflammatory responses.

Technical notes about plasma TILRR quantification

The following should be practiced to quantify plasma TILRR protein using the in-house developed methods.

1. There were no additional benefits of using a higher concentration (>20 µg) of anti-FREM1 mAbs to couple the magnetic beads. Among 3 different concentrations of primary anti-FREM1 mAbs I used, 20 µg of mAb coupled magnetic beads showed better detection efficiency in my experimental setting. The possible reason could be due to the available binding sites on magnetic beads that can only bind a certain amount of IgG mAbs. The amount of >20 µg of mAbs should saturate the 100 µl beads (1.25×10^6). Thus, more antibodies to couple the beads will not improve the detection efficiency.
2. The 1µg/ml biotinylated detection antibody worked better than the higher concentration (2µg/ml) of detection antibody.
3. Inter- and intra- assay variations: Specific attention should be paid to minimize inter- and intra-assay percentage coefficient of variation (% CV). I maintained Bio-Rad recommended % CV between inter- and intra-assay during the optimization of methods, which was <15%.
4. I observed plasma IgGs in the affinity-purified TILRR proteins. The possible reason for having plasma IgGs in affinity-purified protein could be due to the free binding sites on protein G agarose beads that were not completely cross-linked with the Fc region of added

anti-FREM1 IgG (0.2 mg/ml). Since the binding capacity of Pierce Protein G agarose beads ranges from 11 to 15 mg/ml of resin, the free binding sites on protein G agarose beads could bind plasma IgGs during the overnight incubation of the affinity purification process. I had to remove the plasma IgGs after affinity purification.

5. Cross-linked anti-FREM1 mAb with agarose beads could deteriorate over time. Thus, it is important to use freshly coupled beads during affinity purification of TILRR protein from plasma samples.
6. The container used for Coomassie blue staining should not be used, in any steps, for primary or secondary antibody incubations in Western blotting because Coomassie blue gives high background signals in the Odyssey imaging system (LI-COR). If needed, the containers must be cleaned with 100% Methanol/Methylene Chloride (Fisher Scientific, Catalog# D151-1) followed by 3X washes with ddH_2O.
7. After the acquisition of the image by the Odyssey imaging system, the image should be optimized to reduce the background effects for each channel (700 and 800 channels).
8. Other factors could influence detection sensitivity in Bio-Plex assays, such as 1) variations of assay buffers; 2) biotinylation efficiency of the detection antibody (should biotinylate the required amount of antibodies for all assays, instead of multiple batches); 3) minimizing freeze-thaw of antibodies, plasma, and purified proteins; 4) minimizing pipetting variations (should always use calibrated pipette), and 5) handling of samples (should always keep them on ice).

4.5 The level of plasma TILRR is associated with HIV seroconversion

A previous study from our lab has shown that major allele "C" (CC genotype) of FREM1 SNP rs1552896 is more frequently observed in HIV susceptible individuals, whereas minor allele "G"

(GG/GC genotype) is significantly associated with HIV resistant phenotype of women of PSWC [260]. A pilot study from our group also showed that TILRR mRNA expression was absent or very low in women with the protective allele (GG/GC genotype) of FREM1 SNP rs1552896 [350]. Because the major allele "C" (CC genotype) of FREM1 SNP is significantly higher in HIV susceptible individuals and FREM1 isoform TILRR has been demonstrated as a major modulator of inflammatory responses [254], I hypothesized that the level of TILRR in human plasma may correlate with FREM1 SNP rs1552896 genotypes, plasma pro-inflammatory cytokines/chemokines, and HIV seroconversion.

The data showed that the levels of plasma TILRR are variable among the women enrolled in the Pumwani cohort. Women with CC genotype of FREM1 SNP rs1552896 were more likely to have an elevated level of TILRR in blood plasma than women who were GG/GC genotype. It is possible that the SNP rs1552896 may influence the splicing event of FREM1 and the generation of TILRR mRNA and TILRR protein. These need to be confirmed in future studies.

My study also showed that HIV SCON were more likely to have higher plasma TILRR than HIV-resistant women. Because my study showed that TILRR is a major modulator of many inflammation-responsive genes in the IL-1-NF-κB signaling pathway [254], a higher level of plasma TILRR may promote systemic inflammatory responses. The RGD motif of TILRR binds integrins, which promote the migration of effector T cells into the interstitial inflamed tissues [266]. The binding of circulating TILRR with integrin may further promote the infiltration of immune cells from the circulation, resulting in aberrant systemic inflammatory responses and HIV susceptibility. These also need to be further studied and confirmed.

My study demonstrated that the level of plasma TILRR is positively correlated with the levels of plasma IL-1β, MCP-1, and IL-17A. Studies have shown that circulating inflammatory mediators regulate systemic immune activation, inflammatory responses, and inflammation during acute HIV infection and transmission [61, 65]. Pro-inflammatory cytokine IL-1β is a pleiotropic cytokine, which mediates the expression of diverse cytokines/chemokines during the immune response and inflammation [351]. At low concentration, IL-1β causes inflammatory responses followed by protective immunity, whereas at high-level IL-1β causes inflammation accompanied by aberrant tissue damage [351]. Pro-inflammatory chemokine MCP-1 is playing a critical role in recruiting CCR2 expressing memory CD4+ T cells, and monocytes/macrophages [352]. The recruitment of CD4+T cells and monocytes/macrophages by MCP-1 at the site of inflammation may fuel the HIV infection. Studies demonstrated that elevated plasma cytokines/chemokines (IL-1β, MCP-1, and IL-17A) are positively correlated with plasma viral load [65, 353-356], and inversely correlated with blood CD4+T cell count [357, 358]. Because of the significant positive correlation observed among several cytokines/chemokines, the positive association of high-level plasma TILRR and cytokines/chemokines may lead to systemic inflammation. These data suggested that a high level of plasma TILRR may associate with dysregulated plasma cytokines/chemokines production and high inflammatory status, which may increase the risk of HIV seroconversion.

My study focused on the women of the Pumwani sex worker cohort (PSWC), which was established in Nairobi, Kenya in 1985 [268-271]. This cohort has greatly contributed to HIV research in general and understanding natural immunity to HIV infection. A group of women enrolled in the cohort remain HIV uninfected (HESN) despite repeated high-risk exposure through sex work [271]. Many studies (host genetics [279-283], proteomics [273, 274], and

immune responses [275-278]) have been conducted to understand the natural immunity to HIV. A novel HIV vaccine strategy targeting protease cleavage sites (PCSs) has been developed based on studies of this natural immunity [88]. My thesis research on TILRR is a part of these studies. The next step of this project is to further investigate the roles of TILRR in regulating genital mucosal inflammation and HIV susceptibility using human specimens from this cohort (a detailed future work plan is described in limitations and future direction sections). Further studies on TILRR and its role in HIV acquisition may lead to developing novel therapeutic and prevention approaches.

Apart from HIV infection, studies have shown that cytokine storm plays a critical role in the severity and lethality of SARS-CoV-2 (Severe Acute Respiratory Syndrome Coronavirus-2), SARS-CoV, MERS-CoV (Middle East respiratory syndrome coronavirus), and H5N1 influenza A virus infection [359-362]. Specifically, the levels of plasma or serum inflammatory cytokines/chemokines (IL-1β, IL-6, IL-8/CXCL8, IP-10/CXCL10, MCP-1/CCL2, MIP-1α/CCL3, RANTES/CCL5, and TNF-α in SARS-CoV-2 and MARS-CoV [359, 361, 363, 364]; and IL-6, IL-8/CXCL8, IL-10, IP-10/CXCL10, MCP-1/CCL2, and MIG/CXCL9 in H5N1 influenza A virus [362]) were particularly increased in severely infected patients than that of healthy controls. As circulating inflammatory mediators are mostly produced by the immune cells (monocytes/macrophages, T-lymphocytes, and neutrophils) and TILRR is expressed in immune cells, it is also possible that plasma TILRR plays a critical role in the severity of SARS-CoV-2 and other viral infections. This can be investigated in future studies.

In conclusion, my study demonstrated that TILRR exists in blood plasma and its level is associated with FREM1 SNP rs1552896 genotypes, plasma inflammatory mediators, and HIV

seroconversion status. The plasma TILRR and its role in promoting systemic inflammation warrants further study.

If future studies demonstrate that plasma TILRR promotes systemic inflammation, it can be targeted using anti-TILRR monoclonal antibodies (mAbs) or other means (for example, blocking IL-1R1 binding sites of TILRR, two GAG attachment sites at C-terminus, using glycosaminoglycans, GAGs [365]) to reduce plasma TILRR level. Monoclonal antibodies to specific proinflammatory cytokines have been used to treat patients [366-369]. Anti-TILRR mAbs may block the binding of TILRR to the IL-1R1 receptor and thus block downstream signaling effects. Anti-TILRR mAbs may bind plasma TILRR so it will not be able to promote the secretion of pro-inflammatory cytokines/chemokines. If these are the case, targeting plasma TILRR may be more beneficial over the targeting single plasma pro-inflammatory cytokine/chemokine because the diminished level of TILRR may dampen the IL-1-NF-κB signaling pathway, resulting in the reduced production of an array of proinflammatory mediators, and decreased systemic inflammation.

Because host immune response and inflammation play an important role in the pathogenesis of infectious pathogens [370], including SARS-CoV-2, MERS-CoV, and H5N1 influenza A virus infection [359, 362, 364, 371], and further in the progression of cancer [372] and inflammatory diseases [327], studying the role of TILRR in inflammation-mediated pathogenesis of viral infection, cancer development, and inflammatory diseases could also be important. My study also opened more research questions about TILRR and its importance with inflammation-mediated diseases. These are important future studies.

5 CHAPTER 5: MAJOR FINDINGS, CONCLUSION, LIMITATION, AND FUTURE DIRECTIONS

5.1 MAJOR FINDINGS OF THE THESIS

Several major findings from my thesis research on TILRR. These findings are summarized as follows:

A. TILRR overexpression in cervicovaginal epithelial cells increased mRNA expression of many inflammation responsive genes in the NF-κB signal transduction pathway. TILRR potentiates the activation of NF-κB transcription factors and downstream signaling cascades. TILRR is a major modulator of inflammation-responsive genes [254].

B. Overexpression of TILRR in cervicovaginal epithelial cells increased the production of pro-inflammatory cytokines/chemokines [254]. The pro-inflammatory cytokines/chemokines are critical drivers in mucosal immune activation and inflammatory responses and the increase of inflammatory cytokines/chemokines could attract HIV target cells.

C. TILRR overexpression increased the secretion of cytokines/chemokines by HeLa cells and the increased cytokines/chemokines in HeLa cell culture supernatants significantly enhanced migration of CD4+ cells (monocytes and T-lymphocytes)- the HIV target cells [373].

D. TILRR not only exists in cells and tissue but also circulates in the blood.

E. The levels of plasma TILRR were higher in women with major allele "C" (CC genotype) of FREM1 SNP rs1552896 than women with minor allele "G" (GG/GC genotype) of FREM1 SNP rs1552896 in the Pumwani sex worker cohort. Women with the major allele genotype

(CC) of rs1552896 are more likely to have high and detectable TILRR in their blood. The major allele (CC genotype) of rs1552896 is associated with a higher risk of HIV infection.

F. The frequency and the level of plasma TILRR were higher in HIV seroconverters (HIV SCON) than in HIV resistant women (HESN). The high level of plasma TILRR may influence the level of plasma inflammatory cytokines/chemokines and play an important role in HIV seroconversion.

G. The level of plasma TILRR is positively correlated with the levels of multiple plasma inflammatory cytokines/chemokines, including IL-1β, MCP-1, and IL-17A.

Based on these major findings, I propose a model to describe how TILRR may enhance vaginal HIV acquisition in women **(Figure 5.1A-D**). The model is briefly described as follows:

In this model, I propose that the physiological level of TILRR expression in healthy female genital tissues maintains the epithelial integrity, which prevents the invasion of pathogens, including HIV into the genital tissues **(Figure 5.1B**). In HIV-susceptible female genital tissues, on the other hand, the high-level expression of TILRR increases the expression of different inflammation responsive genes through activation of NF-κB signaling pathway, and production of inflammatory cytokines/chemokines by epithelial cells **(Figure 5.1C**). The increased production of inflammatory cytokines/chemokines attracts the infiltration of immune cells, including CD4+T cells and monocytes/macrophages, the HIV target cells, from the periphery to the genital tissue. The increased HIV target cells will increase the chance for the HIV to establish infection. Additionally, cytokines/chemokines secreted by the infiltrated immune cells may further activate and attract more HIV target cells and resulted in cycles of inflammation and breakdown of epithelial barrier (**Figure 5.1C**).

Studies have shown that genital inflammation is a driving force of HIV acquisition [217, 218, 227], and the IL-1-NF-κB signaling pathway increases the risk of HIV susceptibility [209]. Since the NF-κB activation is potentiated by the association of TILRR with IL-1R1 receptor [285, 294], and TILRR-mediated NF-κB activation induces the production of inflammatory cytokines/chemokines, and migration of immune cells [242, 286, 373], the high-level expression of TILRR in genital tissues could be a risk factor in vaginal HIV infection. Thus, the proposed model showed that the elevated expression of TILRR promotes the increased production of inflammatory mediators, increased infiltration of HIV target cells, and profound inflammatory responses resulting in the breakdown of epithelial integrity and HIV susceptibility (**Figure 5.1D**).

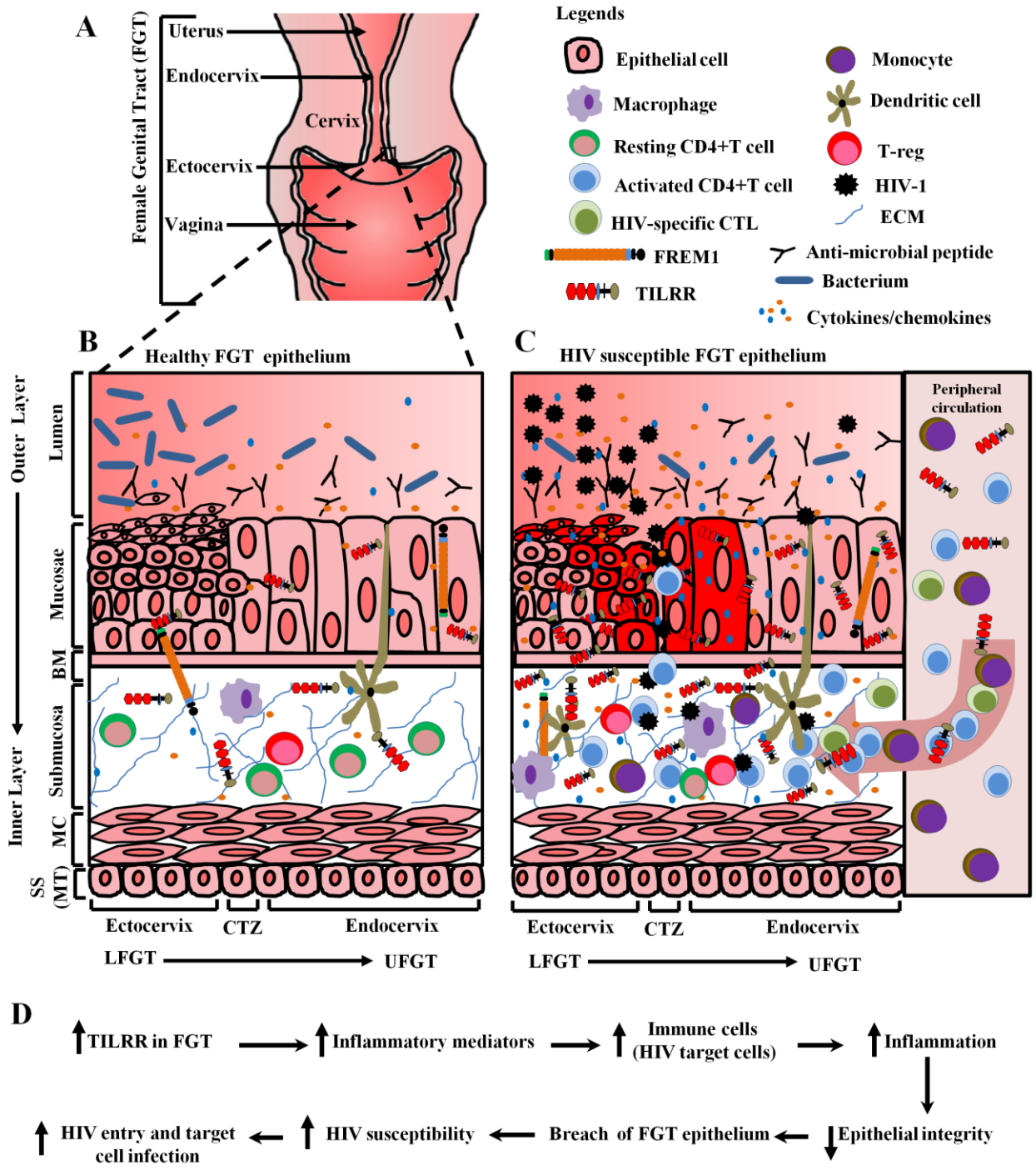

Figure 5.1: Proposed model on the potential role of TILRR in promoting vaginal HIV infection. A) A schematic view of the female genital tract (FGT). **B)** A close-up view of different layers of healthy cervical epithelial tissue. In figure B, the expression of TILRR in healthy cervical tissue maintains the epithelial integrity, which prevents the invasion of pathogens including HIV into the genital tissue. **C)** A close-up view of different layers of HIV-susceptible cervical epithelial tissue. In figure C, the high-level expression of TILRR increases

the production of proinflammatory cytokines/chemokines by epithelial cells. The increased production of pro-inflammatory cytokines/chemokines attracts the infiltration of immune cells from the periphery to the cervical tissues, including HIV target cells. The cytokines secreted by the infiltrated immune cells may further activate and attract more immune cells and resulted in cycles of inflammation and breakdown epithelial barrier. Studies showed that genital inflammation increases the risk of HIV acquisition [217, 218, 227]. The proposed model showed that TILRR promotes the production of cytokines/chemokines by epithelial cells and attracts infiltration of immune cells, including CD4+T-cells and macrophages [286], and it is a risk factor in HIV acquisition. **D)** A flow diagram shows the effect of TILRR in vaginal HIV acquisition through genital epithelium as illustrated in figure C. Legends on the upper right corner indicate the various immune components of the female genital tract. FGT, female genital tract; BM, basement membrane; MC, muscular; SS, serosae; MT, mesothelium; CTZ, cervical transformation zone; LFGT, lower female genital tract; UFGT, upper female genital tract; CTL, cytotoxic t-lymphocyte; T-REG, t-regulatory; FREM1, Fras-related extracellular matrix 1; and TILRR, toll-like interleukin-1 receptor regulator; ECM, extracellular matrix; HIV, human immunodeficiency virus. This figure was reprinted with permission from Kashem et al. [350] under the license of Creative Commons Attribution (CC BY 4.0)

5.2 CONCLUSION

The *in vitro* study with two cervicovaginal epithelial cell lines showed that TILRR is a major modulator of many genes in the NF-κB signaling pathway. It increases the production of many pro-inflammatory cytokines/chemokines. Although how TILRR influences the expression of these genes needs to be further studied, my study is the first to show that TILRR may directly influence gene expression and cytokines/chemokines secretion in addition to its role in enhancing NF-κB signal transduction pathway and inflammatory responses. My study demonstrated that cytokines/chemokines produced through TILRR-overexpressed epithelial cell lines attracted immune cells (HIV target cells) that could enhance cervicovaginal HIV acquisition. Because cervicovaginal inflammation accompanied by rapid infiltration of immune cells is extremely important in vaginal HIV acquisition, further study of the role of TILRR in modulating vaginal mucosal inflammation may identify a new target in preventing HIV acquisition.

My study is the first to identify TILRR in blood. The existence of TILRR in blood suggests that TILRR may also modulate systemic inflammation. My study also showed that the level of TILRR in plasma is variable, and its level is correlated with the FREM1 SNP rs1552896 genotype. A high level of plasma TILRR is correlated with high levels of plasma inflammatory cytokines/chemokines and the risk of HIV acquisition. The discovery of TILRR in blood opens a door to new research on its importance in modulating systemic inflammation, and plasma TILRR may be a target for modulating systemic inflammation and preventing HIV transmission. TILRR may also be an important target for respiratory viral infections (SARS-CoV-2, MERS-CoV, and H5N1 influenza A virus) or other inflammation-mediated inflammatory diseases (rheumatoid arthritis and inflammatory bowel diseases, etc.). Additionally, inflammation, inflammatory

mediators, and inflammatory immune cell migration are critical for cancer progression [374, 375]. Since TILRR promotes the migration of immune cells (monocytes/macrophages and T-lymphocytes) and augments the inflammatory responses, it can also be an important target for cancer progression. These all possibilities need to be examined in future studies.

5.3 LIMITATION OF THE STUDY

While the results described in chapter 3 of this thesis are the first to show the important role of TILRR in modulating mRNA expression of many genes in the NF-κB signaling pathway, production of cytokines/chemokines, and migration of immune cells, the results are based on *in vitro* systems with cell lines. A follow-up study with human cervicovaginal cytology specimens, CVL (cervicovaginal lavage) samples, and genital mucosal leukocytes (from both HIV susceptible and HESN women in the Pumwani cohort) will be needed to support these findings.

Cervicovaginal cytology specimens can be collected and processed to analyze RNA expression with the protocol described elsewhere [376]. The qRT-PCR analysis of mRNA expression of TILRR and inflammation responsive genes in the NF-κB signaling pathway can be conducted with the cervicovaginal specimens. Human cervicovaginal lavage (CVL) samples can also be analyzed in addition to the cervicovaginal cytology specimens to investigate the association of TILRR with pro-inflammatory mediators in the vaginal mucosa. Additionally, genital leukocytes from cervicovaginal cytobrush specimens can be analyzed by flow cytometry staining for CD4+T-, CD8+T- cells, and CD14+ macrophages as previously described [377]. The correlation between the level of TILRR (protein and mRNA) expression and amount of immune cells (HIV target cells), and their differences between HIV susceptible and HESN women, as well as FREM1 SNP rs1552896 genotypes, will help to understand the importance of the mucosal tissue TILRR level of expression in the attraction of HIV target cells. Collectively, these future studies may add more evidence to support the role of TILRR in vaginal HIV acquisition.

Furthermore, although *in vitro* studies provided consistent and reproducible results under a controlled physiochemical environment (pH, osmotic pressure, oxygen, temperature, and CO_2 tension, etc.), it could not capture the complexity of the multi-organ biological system, such as

genetic (altered genetic content), phenotypic and functional alteration of cells, as well as interactions between cells [378-381]. Thus, the findings of *in vitro* studies need to be validated in animal models *in vivo*. An *in vivo* animal model, such as a non-human primate model, could address many shortcomings of *in vitro* studies [381] because non-human primates are evolutionarily, genetically, and immunologically similar to humans and are susceptible to many of the same pathogens [382-385].

5.4 FUTURE DIRECTIONS

I would like to conduct further research to understand and validate the specifics and molecular process of the proposed model in **Figure 5.1**:

A. I would like to examine TILRR expression in cervicovaginal cytology specimens and CVL samples of the Pumwani cohort in future studies. I expect to see that higher TILRR expression in cervicovaginal specimens will enhance higher mRNA expression of many inflammation-responsive genes in HIV susceptible women compared to that of HESN. I also expect to see that TILRR protein is highly expressed in CVL samples of HIV susceptible women, and CVL TILRR is positively correlated with the levels of CVL pro-inflammatory cytokines/chemokines and genital mucosal immune cells (especially CD4+ HIV target cells). Because NF-κB regulates the transcriptional activity of HIV-LTR in infected cells [208], and HIV transmission can be enhanced by NF-κB pathway activation, pro-inflammatory responses, and HIV target cell recruitment [209], the examination of TILRR in cervical cytology and CVL specimens would provide valuable information relevant to the TILRR involvement in vaginal HIV infection. Confirming these would help to conclude that TILRR is a risk factor in vaginal HIV acquisition.

B. Because the plasma TILRR level is positively correlated with the levels of plasma inflammatory cytokines/chemokines, targeting plasma TILRR with anti-TILRR antibodies may help to reduce inflammatory cytokines/chemokines and systemic inflammation. I would like to conduct a pilot study using the Rhesus monkey (*Macaca mulatta*) model because TILRR was also detected in the Rhesus monkey plasma (**Figure 5.2**). As the level of plasma cytokines/chemokines is strongly associated with higher HIV seroconversion and acquisition risk in women [221, 226], the reduction of inflammatory cytokines/chemokines with anti-

TILRR antibodies could show that plasma TILRR could be a novel therapeutic target to treat inflammation and reduce the risk of HIV acquisition.

C. HIV-associated co-morbidities are associated with chronic inflammation and immune activation in People living with HIV (PLWH) despite under cART (combined antiretroviral therapy) [386-389]. It would be interesting to study whether the level of plasma TILRR plays a role in HIV infection-associated chronic inflammation.

D. Future studies can also be extended to investigate the role of TILRR in inflammation-related pathogenesis of respiratory viral infections, including SARS-CoV-2, MERS-CoV, and the H5N1 influenza A virus. Because NF-κB activation, cytokine storm, and immune cell infiltration potentiate the respiratory viral infection [359, 361-363, 390-393], and TILRR protein expresses in lung tissues, it is possible that TILRR may also be a therapeutic target for inflammation caused by respiratory viral infections. Additionally, TILRR can be a target for the reduction of cancer progression.

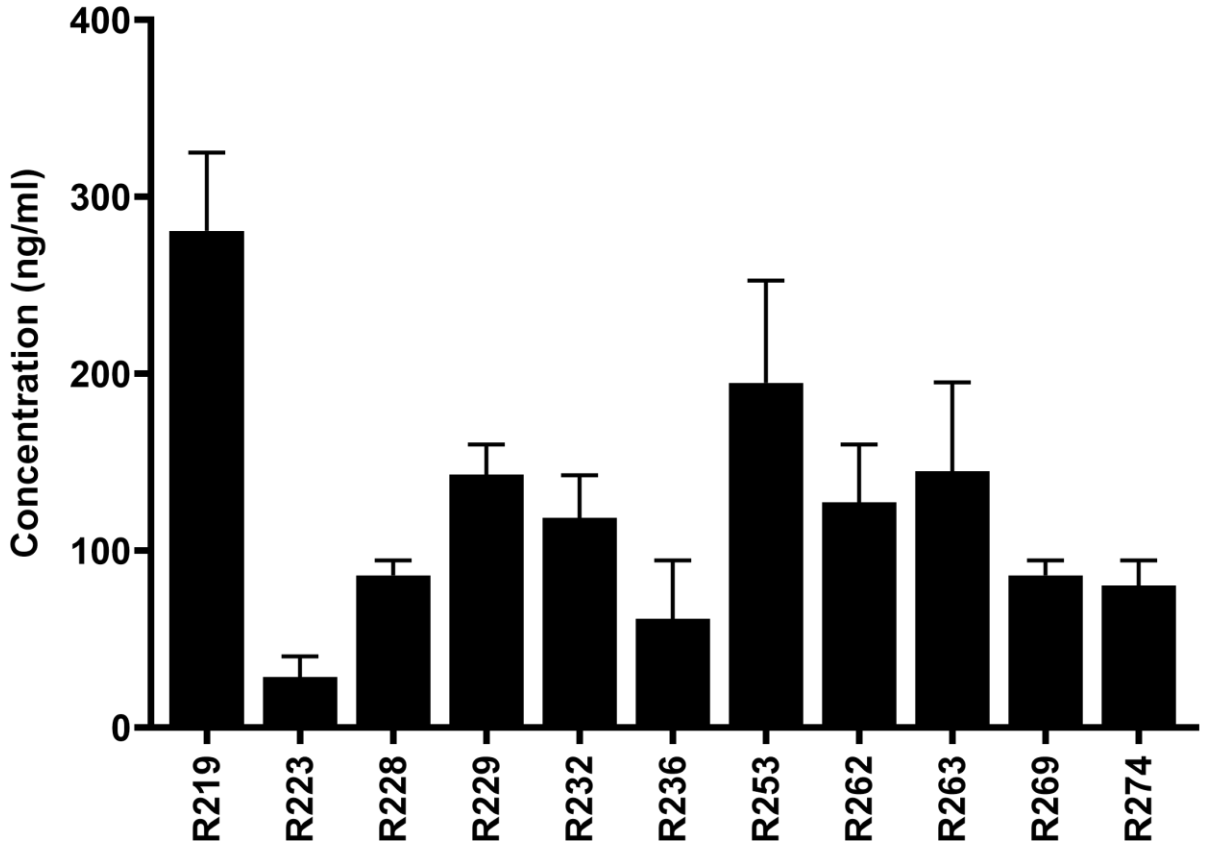

Figure 5.2: Blood plasma TILRR in Rhesus Monkeys. Plasma TILRR has been detected in all Rhesus Monkeys (n=11) using the Bio-Plex multiplex bead array system as described in the materials and methods chapter (**section 2.4.4.6)**. The concentration of TILRR in Monkeys' plasma ranges from 28.37 ng/ml to 279.32 ng/ml. The X-axis shows the monkey ID#.

6 CHAPTER 6: REFERENCES

1. Fauci, A.S., *Twenty-five years of HIV/AIDS.* Science, 2006. **313**(5786): p. 409.
2. CDC, *Kaposi's sarcoma and Pneumocystis pneumonia among homosexual men--New York City and California.* MMWR Morb Mortal Wkly Rep, 1981. **30**(25): p. 305-8.
3. Greene, W.C., *A history of AIDS: looking back to see ahead.* Eur J Immunol, 2007. **37 Suppl 1**: p. S94-102.
4. Sudharshan, S. and J. Biswas, *Introduction and immunopathogenesis of acquired immune deficiency syndrome.* Indian J Ophthalmol, 2008. **56**(5): p. 357-62.
5. CDC, *Current trends update on acquired immune deficiency syndrome (AIDS)--United States.* MMWR Morb Mortal Wkly Rep, 1982. **31**(37): p. 507-8, 513-4.
6. Barre-Sinoussi, F., J.C. Chermann, F. Rey, M.T. Nugeyre, S. Chamaret, J. Gruest, C. Dauguet, C. Axler-Blin, F. Vezinet-Brun, C. Rouzioux, W. Rozenbaum, and L. Montagnier, *Isolation of a T-lymphotropic retrovirus from a patient at risk for acquired immune deficiency syndrome (AIDS).* Science, 1983. **220**(4599): p. 868-71.
7. Gallo, R.C., S.Z. Salahuddin, M. Popovic, G.M. Shearer, M. Kaplan, B.F. Haynes, T.J. Palker, R. Redfield, J. Oleske, B. Safai, and et al., *Frequent detection and isolation of cytopathic retroviruses (HTLV-III) from patients with AIDS and at risk for AIDS.* Science, 1984. **224**(4648): p. 500-3.
8. Popovic, M., M.G. Sarngadharan, E. Read, and R.C. Gallo, *Detection, isolation, and continuous production of cytopathic retroviruses (HTLV-III) from patients with AIDS and pre-AIDS.* Science, 1984. **224**(4648): p. 497-500.
9. Coffin, J., A. Haase, J.A. Levy, L. Montagnier, S. Oroszlan, N. Teich, H. Temin, K. Toyoshima, H. Varmus, P. Vogt, and et al., *What to call the AIDS virus?* Nature, 1986. **321**(6065): p. 10.
10. UNAIDS. *Global HIV & AIDS statistics-2020 fact sheet*. 2020 (Accessed on March 13, 2021); Available from: https://www.unaids.org/en/resources/fact-sheet.
11. Seitz, R., *Human Immunodeficiency Virus (HIV).* Transfus Med Hemother, 2016. **43**(3): p. 203-22.
12. Nyamweya, S., A. Hegedus, A. Jaye, S. Rowland-Jones, K.L. Flanagan, and D.C. Macallan, *Comparing HIV-1 and HIV-2 infection: Lessons for viral immunopathogenesis.* Rev Med Virol, 2013. **23**(4): p. 221-40.

13. Korber, B., M. Muldoon, J. Theiler, F. Gao, R. Gupta, A. Lapedes, B.H. Hahn, S. Wolinsky, and T. Bhattacharya, *Timing the ancestor of the HIV-1 pandemic strains.* Science, 2000. **288**(5472): p. 1789-96.
14. Lemey, P., O.G. Pybus, B. Wang, N.K. Saksena, M. Salemi, and A.M. Vandamme, *Tracing the origin and history of the HIV-2 epidemic.* Proc Natl Acad Sci U S A, 2003. **100**(11): p. 6588-92.
15. Taylor, B.S., M.E. Sobieszczyk, F.E. McCutchan, and S.M. Hammer, *The challenge of HIV-1 subtype diversity.* N Engl J Med, 2008. **358**(15): p. 1590-602.
16. D'Arc, M., A. Ayouba, A. Esteban, G.H. Learn, V. Boue, F. Liegeois, L. Etienne, N. Tagg, F.H. Leendertz, C. Boesch, N.F. Madinda, M.M. Robbins, M. Gray, A. Cournil, M. Ooms, M. Letko, V.A. Simon, P.M. Sharp, B.H. Hahn, E. Delaporte, E. Mpoudi Ngole, and M. Peeters, *Origin of the HIV-1 group O epidemic in western lowland gorillas.* Proc Natl Acad Sci U S A, 2015. **112**(11): p. E1343-52.
17. Keele, B.F., F. Van Heuverswyn, Y. Li, E. Bailes, J. Takehisa, M.L. Santiago, F. Bibollet-Ruche, Y. Chen, L.V. Wain, F. Liegeois, S. Loul, E.M. Ngole, Y. Bienvenue, E. Delaporte, J.F. Brookfield, P.M. Sharp, G.M. Shaw, M. Peeters, and B.H. Hahn, *Chimpanzee reservoirs of pandemic and nonpandemic HIV-1.* Science, 2006. **313**(5786): p. 523-6.
18. Van Heuverswyn, F., Y. Li, C. Neel, E. Bailes, B.F. Keele, W. Liu, S. Loul, C. Butel, F. Liegeois, Y. Bienvenue, E.M. Ngolle, P.M. Sharp, G.M. Shaw, E. Delaporte, B.H. Hahn, and M. Peeters, *Human immunodeficiency viruses: SIV infection in wild gorillas.* Nature, 2006. **444**(7116): p. 164.
19. Plantier, J.C., M. Leoz, J.E. Dickerson, F. De Oliveira, F. Cordonnier, V. Lemee, F. Damond, D.L. Robertson, and F. Simon, *A new human immunodeficiency virus derived from gorillas.* Nat Med, 2009. **15**(8): p. 871-2.
20. Hemelaar, J., E. Gouws, P.D. Ghys, and S. Osmanov, *Global and regional distribution of HIV-1 genetic subtypes and recombinants in 2004.* AIDS, 2006. **20**(16): p. W13-23.
21. Bbosa, N., P. Kaleebu, and D. Ssemwanga, *HIV subtype diversity worldwide.* Curr Opin HIV AIDS, 2019. **14**(3): p. 153-160.

22. Esbjornsson, J., M. Jansson, S. Jespersen, F. Mansson, B.L. Honge, J. Lindman, C. Medina, Z.J. da Silva, H. Norrgren, P. Medstrand, S.L. Rowland-Jones, and C. Wejse, *HIV-2 as a model to identify a functional HIV cure.* AIDS Res Ther, 2019. **16**(1): p. 24.
23. Ayouba, A., C. Akoua-Koffi, S. Calvignac-Spencer, A. Esteban, S. Locatelli, H. Li, Y. Li, B.H. Hahn, E. Delaporte, F.H. Leendertz, and M. Peeters, *Evidence for continuing cross-species transmission of SIVsmm to humans: characterization of a new HIV-2 lineage in rural Cote d'Ivoire.* AIDS, 2013. **27**(15): p. 2488-91.
24. Fanales-Belasio, E., M. Raimondo, B. Suligoi, and S. Butto, *HIV virology and pathogenetic mechanisms of infection: a brief overview.* Ann Ist Super Sanita, 2010. **46**(1): p. 5-14.
25. Sierra, S., B. Kupfer, and R. Kaiser, *Basics of the virology of HIV-1 and its replication.* J Clin Virol, 2005. **34**(4): p. 233-44.
26. Musumeci, D., C. Riccardi, and D. Montesarchio, *G-Quadruplex Forming Oligonucleotides as Anti-HIV Agents.* Molecules, 2015. **20**(9): p. 17511-32.
27. Costin, J.M., *Cytopathic mechanisms of HIV-1.* Virol J, 2007. **4**: p. 100.
28. Xiao, Q., D. Guo, and S. Chen, *Application of CRISPR/Cas9-Based Gene Editing in HIV-1/AIDS Therapy.* Front Cell Infect Microbiol, 2019. **9**: p. 69.
29. Zulfiqar, H.F., A. Javed, Sumbal, B. Afroze, Q. Ali, K. Akbar, T. Nadeem, M.A. Rana, Z.A. Nazar, I.A. Nasir, and T. Husnain, *HIV Diagnosis and Treatment through Advanced Technologies.* Front Public Health, 2017. **5**: p. 32.
30. Tebit, D.M., N. Ndembi, A. Weinberg, and M.E. Quinones-Mateu, *Mucosal transmission of human immunodeficiency virus.* Curr HIV Res, 2012. **10**(1): p. 3-8.
31. Friedman, S.R., S. Lieb, B. Tempalski, H. Cooper, M. Keem, R. Friedman, and P.L. Flom, *HIV among injection drug users in large US metropolitan areas, 1998.* J Urban Health, 2005. **82**(3): p. 434-45.
32. Moore, A., G. Herrera, J. Nyamongo, E. Lackritz, T. Granade, B. Nahlen, A. Oloo, G. Opondo, R. Muga, and R. Janssen, *Estimated risk of HIV transmission by blood transfusion in Kenya.* Lancet, 2001. **358**(9282): p. 657-60.
33. CDC, *HIV transmission through transfusion --- Missouri and Colorado, 2008.* MMWR Morb Mortal Wkly Rep, 2010. **59**(41): p. 1335-9.

34. Gurtler, L.G., J. Eberle, and L. Bader, *HIV transmission by needle stick and eczematous lesion--three cases from Germany.* Infection, 1993. **21**(1): p. 40-1.
35. Landesman, S.H., L.A. Kalish, D.N. Burns, H. Minkoff, H.E. Fox, C. Zorrilla, P. Garcia, M.G. Fowler, L. Mofenson, and R. Tuomala, *Obstetrical factors and the transmission of human immunodeficiency virus type 1 from mother to child. The Women and Infants Transmission Study.* N Engl J Med, 1996. **334**(25): p. 1617-23.
36. Nduati, R., G. John, D. Mbori-Ngacha, B. Richardson, J. Overbaugh, A. Mwatha, J. Ndinya-Achola, J. Bwayo, F.E. Onyango, J. Hughes, and J. Kreiss, *Effect of breastfeeding and formula feeding on transmission of HIV-1: a randomized clinical trial.* JAMA, 2000. **283**(9): p. 1167-74.
37. Newell, M.L., *Mechanisms and timing of mother-to-child transmission of HIV-1.* AIDS, 1998. **12**(8): p. 831-7.
38. Cohen, M.S., *Preventing sexual transmission of HIV.* Clin Infect Dis, 2007. **45 Suppl 4**: p. S287-92.
39. Gouws, E., P.J. White, J. Stover, and T. Brown, *Short term estimates of adult HIV incidence by mode of transmission: Kenya and Thailand as examples.* Sex Transm Infect, 2006. **82 Suppl 3**: p. iii51-55.
40. Royce, R.A., A. Sena, W. Cates, Jr., and M.S. Cohen, *Sexual transmission of HIV.* N Engl J Med, 1997. **336**(15): p. 1072-8.
41. Kinloch-de Loes, S., P. de Saussure, J.H. Saurat, H. Stalder, B. Hirschel, and L.H. Perrin, *Symptomatic primary infection due to human immunodeficiency virus type 1: review of 31 cases.* Clin Infect Dis, 1993. **17**(1): p. 59-65.
42. Boily, M.C., R.F. Baggaley, L. Wang, B. Masse, R.G. White, R.J. Hayes, and M. Alary, *Heterosexual risk of HIV-1 infection per sexual act: systematic review and meta-analysis of observational studies.* Lancet Infect Dis, 2009. **9**(2): p. 118-29.
43. Hladik, F., P. Sakchalathorn, L. Ballweber, G. Lentz, M. Fialkow, D. Eschenbach, and M.J. McElrath, *Initial events in establishing vaginal entry and infection by human immunodeficiency virus type-1.* Immunity, 2007. **26**(2): p. 257-70.
44. Haase, A.T., *Perils at mucosal front lines for HIV and SIV and their hosts.* Nat Rev Immunol, 2005. **5**(10): p. 783-92.

45. Miller, C.J., Q. Li, K. Abel, E.Y. Kim, Z.M. Ma, S. Wietgrefe, L. La Franco-Scheuch, L. Compton, L. Duan, M.D. Shore, M. Zupancic, M. Busch, J. Carlis, S. Wolinsky, and A.T. Haase, *Propagation and dissemination of infection after vaginal transmission of simian immunodeficiency virus.* J Virol, 2005. **79**(14): p. 9217-27.
46. Kinlock, B.L., Y. Wang, T.M. Turner, C. Wang, and B. Liu, *Transcytosis of HIV-1 through vaginal epithelial cells is dependent on trafficking to the endocytic recycling pathway.* PLoS One, 2014. **9**(5): p. e96760.
47. Bomsel, M., *Transcytosis of infectious human immunodeficiency virus across a tight human epithelial cell line barrier.* Nat Med, 1997. **3**(1): p. 42-7.
48. Greene, W.C. and B.M. Peterlin, *Charting HIV's remarkable voyage through the cell: Basic science as a passport to future therapy.* Nat Med, 2002. **8**(7): p. 673-80.
49. Auewarakul, P., P. Wacharapornin, S. Srichatrapimuk, S. Chutipongtanate, and P. Puthavathana, *Uncoating of HIV-1 requires cellular activation.* Virology, 2005. **337**(1): p. 93-101.
50. Lusic, M. and R.F. Siliciano, *Nuclear landscape of HIV-1 infection and integration.* Nat Rev Microbiol, 2017. **15**(2): p. 69-82.
51. Dahabieh, M.S., E. Battivelli, and E. Verdin, *Understanding HIV latency: the road to an HIV cure.* Annu Rev Med, 2015. **66**: p. 407-21.
52. Roulston, A., R. Lin, P. Beauparlant, M.A. Wainberg, and J. Hiscott, *Regulation of human immunodeficiency virus type 1 and cytokine gene expression in myeloid cells by NF-kappa B/Rel transcription factors.* Microbiol Rev, 1995. **59**(3): p. 481-505.
53. Cullen, B.R., *Retroviruses as model systems for the study of nuclear RNA export pathways.* Virology, 1998. **249**(2): p. 203-10.
54. Checkley, M.A., B.G. Luttge, and E.O. Freed, *HIV-1 envelope glycoprotein biosynthesis, trafficking, and incorporation.* J Mol Biol, 2011. **410**(4): p. 582-608.
55. Sundquist, W.I. and H.G. Krausslich, *HIV-1 assembly, budding, and maturation.* Cold Spring Harb Perspect Med, 2012. **2**(7): p. a006924.
56. Shen, R., H.E. Richter, and P.D. Smith, *Interactions between HIV-1 and mucosal cells in the female reproductive tract.* Am J Reprod Immunol, 2014. **71**(6): p. 608-17.
57. Zhang, Z., T. Schuler, M. Zupancic, S. Wietgrefe, K.A. Staskus, K.A. Reimann, T.A. Reinhart, M. Rogan, W. Cavert, C.J. Miller, R.S. Veazey, D. Notermans, S. Little, S.A.

Danner, D.D. Richman, D. Havlir, J. Wong, H.L. Jordan, T.W. Schacker, P. Racz, K. Tenner-Racz, N.L. Letvin, S. Wolinsky, and A.T. Haase, *Sexual transmission and propagation of SIV and HIV in resting and activated CD4+ T cells.* Science, 1999. **286**(5443): p. 1353-7.

58. Zhang, Z.Q., S.W. Wietgrefe, Q. Li, M.D. Shore, L. Duan, C. Reilly, J.D. Lifson, and A.T. Haase, *Roles of substrate availability and infection of resting and activated CD4+ T cells in transmission and acute simian immunodeficiency virus infection.* Proc Natl Acad Sci U S A, 2004. **101**(15): p. 5640-5.
59. Haase, A.T., *Targeting early infection to prevent HIV-1 mucosal transmission.* Nature, 2010. **464**(7286): p. 217-23.
60. Haase, A.T., *Early events in sexual transmission of HIV and SIV and opportunities for interventions.* Annu Rev Med, 2011. **62**: p. 127-39.
61. McMichael, A.J., P. Borrow, G.D. Tomaras, N. Goonetilleke, and B.F. Haynes, *The immune response during acute HIV-1 infection: clues for vaccine development.* Nat Rev Immunol, 2010. **10**(1): p. 11-23.
62. Kahn, J.O. and B.D. Walker, *Acute human immunodeficiency virus type 1 infection.* N Engl J Med, 1998. **339**(1): p. 33-9.
63. Quinn, T.C., M.J. Wawer, N. Sewankambo, D. Serwadda, C. Li, F. Wabwire-Mangen, M.O. Meehan, T. Lutalo, and R.H. Gray, *Viral load and heterosexual transmission of human immunodeficiency virus type 1. Rakai Project Study Group.* N Engl J Med, 2000. **342**(13): p. 921-9.
64. Vidya Vijayan, K.K., K.P. Karthigeyan, S.P. Tripathi, and L.E. Hanna, *Pathophysiology of CD4+ T-Cell Depletion in HIV-1 and HIV-2 Infections.* Front Immunol, 2017. **8**: p. 580.
65. Stacey, A.R., P.J. Norris, L. Qin, E.A. Haygreen, E. Taylor, J. Heitman, M. Lebedeva, A. DeCamp, D. Li, D. Grove, S.G. Self, and P. Borrow, *Induction of a striking systemic cytokine cascade prior to peak viremia in acute human immunodeficiency virus type 1 infection, in contrast to more modest and delayed responses in acute hepatitis B and C virus infections.* J Virol, 2009. **83**(8): p. 3719-33.
66. Streeck, H. and D.F. Nixon, *T cell immunity in acute HIV-1 infection.* J Infect Dis, 2010. **202 Suppl 2**: p. S302-8.

67. Connick, E., D.G. Marr, X.Q. Zhang, S.J. Clark, M.S. Saag, R.T. Schooley, and T.J. Curiel, *HIV-specific cellular and humoral immune responses in primary HIV infection.* AIDS Res Hum Retroviruses, 1996. **12**(12): p. 1129-40.

68. Siliciano, J.D., J. Kajdas, D. Finzi, T.C. Quinn, K. Chadwick, J.B. Margolick, C. Kovacs, S.J. Gange, and R.F. Siliciano, *Long-term follow-up studies confirm the stability of the latent reservoir for HIV-1 in resting CD4+ T cells.* Nat Med, 2003. **9**(6): p. 727-8.

69. Okoye, A.A. and L.J. Picker, *CD4(+) T-cell depletion in HIV infection: mechanisms of immunological failure.* Immunol Rev, 2013. **254**(1): p. 54-64.

70. Vieira, J., E. Frank, T.J. Spira, and S.H. Landesman, *Acquired immune deficiency in Haitians: opportunistic infections in previously healthy Haitian immigrants.* N Engl J Med, 1983. **308**(3): p. 125-9.

71. Collier, A.C., R.W. Coombs, D.A. Schoenfeld, R.L. Bassett, J. Timpone, A. Baruch, M. Jones, K. Facey, C. Whitacre, V.J. McAuliffe, H.M. Friedman, T.C. Merigan, R.C. Reichman, C. Hooper, and L. Corey, *Treatment of human immunodeficiency virus infection with saquinavir, zidovudine, and zalcitabine. AIDS Clinical Trials Group.* N Engl J Med, 1996. **334**(16): p. 1011-7.

72. Arts, E.J. and D.J. Hazuda, *HIV-1 antiretroviral drug therapy.* Cold Spring Harb Perspect Med, 2012. **2**(4): p. a007161.

73. Autran, B., G. Carcelain, T.S. Li, C. Blanc, D. Mathez, R. Tubiana, C. Katlama, P. Debre, and J. Leibowitch, *Positive effects of combined antiretroviral therapy on CD4+ T cell homeostasis and function in advanced HIV disease.* Science, 1997. **277**(5322): p. 112-6.

74. Lederman, M.M., E. Connick, A. Landay, D.R. Kuritzkes, J. Spritzler, M. St Clair, B.L. Kotzin, L. Fox, M.H. Chiozzi, J.M. Leonard, F. Rousseau, M. Wade, J.D. Roe, A. Martinez, and H. Kessler, *Immunologic responses associated with 12 weeks of combination antiretroviral therapy consisting of zidovudine, lamivudine, and ritonavir: results of AIDS Clinical Trials Group Protocol 315.* J Infect Dis, 1998. **178**(1): p. 70-9.

75. Zagury, D., R. Leonard, M. Fouchard, B. Reveil, J. Bernard, D. Ittele, A. Cattan, L. Zirimwabagabo, M. Kalumbu, W. Justin, and et al., *Immunization against AIDS in humans.* Nature, 1987. **326**(6110): p. 249-50.

76. Safrit, J.T., P.E. Fast, L. Gieber, H. Kuipers, H.J. Dean, and W.C. Koff, *Status of vaccine research and development of vaccines for HIV-1.* Vaccine, 2016. **34**(26): p. 2921-2925.
77. Parikh, A. *The quest for the HIV Vaccine: are we closer than we think?* 2016 (Accessed on March 13, 2021); Available from: https://www.clinicalcorrelations.org/2016/01/20/the-quest-for-the-hiv-vaccine-are-we-closer-than-we-think/.
78. Wang, H.B., Q.H. Mo, and Z. Yang, *HIV vaccine research: the challenge and the way forward.* J Immunol Res, 2015. **2015**: p. 503978.
79. Cohen, J., *AIDS research. Promising AIDS vaccine's failure leaves field reeling.* Science, 2007. **318**(5847): p. 28-9.
80. Steinbrook, R., *One step forward, two steps back--will there ever be an AIDS vaccine?* N Engl J Med, 2007. **357**(26): p. 2653-5.
81. Rerks-Ngarm, S., P. Pitisuttithum, S. Nitayaphan, J. Kaewkungwal, J. Chiu, R. Paris, N. Premsri, C. Namwat, M. de Souza, E. Adams, M. Benenson, S. Gurunathan, J. Tartaglia, J.G. McNeil, D.P. Francis, D. Stablein, D.L. Birx, S. Chunsuttiwat, C. Khamboonruang, P. Thongcharoen, M.L. Robb, N.L. Michael, P. Kunasol, and J.H. Kim, *Vaccination with ALVAC and AIDSVAX to prevent HIV-1 infection in Thailand.* N Engl J Med, 2009. **361**(23): p. 2209-20.
82. AVAC. *Global Advocacy for HIV Prevention*. 2020 (Accessed on March 13, 2021); Available from: https://www.avac.org/trial/hvtn-702
83. Ng'uni, T., C. Chasara, and Z.M. Ndhlovu, *Major Scientific Hurdles in HIV Vaccine Development: Historical Perspective and Future Directions.* Front Immunol, 2020. **11**: p. 590780.
84. UNAIDS. *HVTN 702 clinical trial of an HIV vaccine stopped*. 2020 (Accessed on March 13, 2021); Available from: https://www.unaids.org/en/resources/presscentre/pressreleaseandstatementarchive/2020/february/20200204_vaccine.
85. NIH. *Experimental HIV Vaccine Regimen Ineffective in Preventing HIV*. 2020 (Accessed on March 13, 2021); Available from: https://www.niaid.nih.gov/news-events/experimental-hiv-vaccine-regimen-ineffective-preventing-hiv.

86. ClinicalTrials.gov. *A Study to Assess the Efficacy of a Heterologous Prime/Boost Vaccine Regimen of Ad26.Mos4.HIV and Aluminum Phosphate-Adjuvanted Clade C gp140 in Preventing Human Immunodeficiency Virus (HIV) -1 Infection in Women in Sub-Saharan Africa*. (Accessed on March 13, 2021); Available from: https://clinicaltrials.gov/ct2/show/NCT03060629?term=NCT03060629&draw=2.

87. ClinicalTrials.gov. *A Study of Heterologous Vaccine Regimen of Adenovirus Serotype 26 Mosaic4 Human Immunodeficiency Virus(Ad26.Mos4.HIV), Adjuvanted Clade C gp140 and Mosaic gp140 to Prevent HIV-1 Infection Among Cis-gender Men and Transgender Individuals Who Have Sex With Cis-gender Men and/or Transgender Individuals (MOSAICO)*. (Accessed on March 13, 2021); Available from: https://clinicaltrials.gov/ct2/show/NCT03964415?term=NCT03964415&draw=2.

88. Li, H., R.W. Omange, B. Liang, N. Toledo, Y. Hai, L. Liu, D. Schalk, J. Crecente-Campo, T.G. Dacoba, A.B. Lambe, S.Y. Lim, L. Li, M.A. Kashem, Y. Wan, J.F. Correia-Pinto, M.S. Seaman, X.Q. Liu, R.F. Balshaw, Q. Li, N. Schultz-Darken, M.J. Alonso, F.A. Plummer, J.B. Whitney, and M. Luo, *Vaccine targeting SIVmac251 protease cleavage sites protects macaques against vaginal infection.* Journal of Clinical Investigation, 2020.

89. Li, H., Y. Hai, S.Y. Lim, N. Toledo, J. Crecente-Campo, D. Schalk, L. Li, R.W. Omange, T.G. Dacoba, L.R. Liu, M.A. Kashem, Y. Wan, B. Liang, Q. Li, E. Rakasz, N. Schultz-Darken, M.J. Alonso, F.A. Plummer, J.B. Whitney, and M. Luo, *Mucosal antibody responses to vaccines targeting SIV protease cleavage sites or full-length Gag and Env proteins in Mauritian cynomolgus macaques.* PLoS One, 2018. **13**(8): p. e0202997.

90. Medzhitov, R. and C. Janeway, Jr., *Innate immunity.* N Engl J Med, 2000. **343**(5): p. 338-44.

91. Akira, S., S. Uematsu, and O. Takeuchi, *Pathogen recognition and innate immunity.* Cell, 2006. **124**(4): p. 783-801.

92. Pasupuleti, M., A. Schmidtchen, and M. Malmsten, *Antimicrobial peptides: key components of the innate immune system.* Crit Rev Biotechnol, 2012. **32**(2): p. 143-71.

93. Basset, C., J. Holton, R. O'Mahony, and I. Roitt, *Innate immunity and pathogen-host interaction.* Vaccine, 2003. **21 Suppl 2**: p. S12-23.

94. Dunkelberger, J.R. and W.C. Song, *Complement and its role in innate and adaptive immune responses.* Cell Res, 2010. **20**(1): p. 34-50.
95. Kambayashi, T. and T.M. Laufer, *Atypical MHC class II-expressing antigen-presenting cells: can anything replace a dendritic cell?* Nat Rev Immunol, 2014. **14**(11): p. 719-30.
96. Kumar, V., *Innate lymphoid cells: new paradigm in immunology of inflammation.* Immunol Lett, 2014. **157**(1-2): p. 23-37.
97. Auffray, C., M.H. Sieweke, and F. Geissmann, *Blood monocytes: development, heterogeneity, and relationship with dendritic cells.* Annu Rev Immunol, 2009. **27**: p. 669-92.
98. Fahy, R.J., A.I. Doseff, and M.D. Wewers, *Spontaneous human monocyte apoptosis utilizes a caspase-3-dependent pathway that is blocked by endotoxin and is independent of caspase-1.* J Immunol, 1999. **163**(4): p. 1755-62.
99. Patel, A.A., Y. Zhang, J.N. Fullerton, L. Boelen, A. Rongvaux, A.A. Maini, V. Bigley, R.A. Flavell, D.W. Gilroy, B. Asquith, D. Macallan, and S. Yona, *The fate and lifespan of human monocyte subsets in steady state and systemic inflammation.* J Exp Med, 2017. **214**(7): p. 1913-1923.
100. Mangan, D.F. and S.M. Wahl, *Differential regulation of human monocyte programmed cell death (apoptosis) by chemotactic factors and pro-inflammatory cytokines.* J Immunol, 1991. **147**(10): p. 3408-12.
101. Parihar, A., T.D. Eubank, and A.I. Doseff, *Monocytes and macrophages regulate immunity through dynamic networks of survival and cell death.* J Innate Immun, 2010. **2**(3): p. 204-15.
102. Mangan, D.F., G.R. Welch, and S.M. Wahl, *Lipopolysaccharide, tumor necrosis factor-alpha, and IL-1 beta prevent programmed cell death (apoptosis) in human peripheral blood monocytes.* J Immunol, 1991. **146**(5): p. 1541-6.
103. Goyal, A., Y. Wang, M.M. Graham, A.I. Doseff, N.Y. Bhatt, and C.B. Marsh, *Monocyte survival factors induce Akt activation and suppress caspase-3.* Am J Respir Cell Mol Biol, 2002. **26**(2): p. 224-30.
104. Herbein, G. and A. Varin, *The macrophage in HIV-1 infection: from activation to deactivation?* Retrovirology, 2010. **7**: p. 33.

105. Carter, C.A. and L.S. Ehrlich, *Cell biology of HIV-1 infection of macrophages.* Annu Rev Microbiol, 2008. **62**: p. 425-43.
106. Kedzierska, K., S.M. Crowe, S. Turville, and A.L. Cunningham, *The influence of cytokines, chemokines and their receptors on HIV-1 replication in monocytes and macrophages.* Rev Med Virol, 2003. **13**(1): p. 39-56.
107. Coakley, E., C.J. Petropoulos, and J.M. Whitcomb, *Assessing chemokine co-receptor usage in HIV.* Curr Opin Infect Dis, 2005. **18**(1): p. 9-15.
108. Deng, H., R. Liu, W. Ellmeier, S. Choe, D. Unutmaz, M. Burkhart, P. Di Marzio, S. Marmon, R.E. Sutton, C.M. Hill, C.B. Davis, S.C. Peiper, T.J. Schall, D.R. Littman, and N.R. Landau, *Identification of a major co-receptor for primary isolates of HIV-1.* Nature, 1996. **381**(6584): p. 661-6.
109. Doranz, B.J., S.S. Baik, and R.W. Doms, *Use of a gp120 binding assay to dissect the requirements and kinetics of human immunodeficiency virus fusion events.* J Virol, 1999. **73**(12): p. 10346-58.
110. Lee, C., Q.H. Liu, B. Tomkowicz, Y. Yi, B.D. Freedman, and R.G. Collman, *Macrophage activation through CCR5- and CXCR4-mediated gp120-elicited signaling pathways.* J Leukoc Biol, 2003. **74**(5): p. 676-82.
111. Swingler, S., A. Mann, J. Jacque, B. Brichacek, V.G. Sasseville, K. Williams, A.A. Lackner, E.N. Janoff, R. Wang, D. Fisher, and M. Stevenson, *HIV-1 Nef mediates lymphocyte chemotaxis and activation by infected macrophages.* Nat Med, 1999. **5**(9): p. 997-103.
112. Griffin, G.E., K. Leung, T.M. Folks, S. Kunkel, and G.J. Nabel, *Activation of HIV gene expression during monocyte differentiation by induction of NF-kappa B.* Nature, 1989. **339**(6219): p. 70-3.
113. Dieu-Nosjean, M.C., A. Vicari, S. Lebecque, and C. Caux, *Regulation of dendritic cell trafficking: a process that involves the participation of selective chemokines.* J Leukoc Biol, 1999. **66**(2): p. 252-62.
114. Patente, T.A., M.P. Pinho, A.A. Oliveira, G.C.M. Evangelista, P.C. Bergami-Santos, and J.A.M. Barbuto, *Human Dendritic Cells: Their Heterogeneity and Clinical Application Potential in Cancer Immunotherapy.* Front Immunol, 2018. **9**: p. 3176.

115. ten Broeke, T., R. Wubbolts, and W. Stoorvogel, *MHC class II antigen presentation by dendritic cells regulated through endosomal sorting.* Cold Spring Harb Perspect Biol, 2013. **5**(12): p. a016873.
116. Manches, O., D. Frleta, and N. Bhardwaj, *Dendritic cells in progression and pathology of HIV infection.* Trends Immunol, 2014. **35**(3): p. 114-22.
117. Altfeld, M., L. Fadda, D. Frleta, and N. Bhardwaj, *DCs and NK cells: critical effectors in the immune response to HIV-1.* Nat Rev Immunol, 2011. **11**(3): p. 176-86.
118. Ahmed, Z., T. Kawamura, S. Shimada, and V. Piguet, *The role of human dendritic cells in HIV-1 infection.* J Invest Dermatol, 2015. **135**(5): p. 1225-1233.
119. Sandgren, K.J., A. Smed-Sorensen, M.N. Forsell, M. Soldemo, W.C. Adams, F. Liang, L. Perbeck, R.A. Koup, R.T. Wyatt, G.B. Karlsson Hedestam, and K. Lore, *Human plasmacytoid dendritic cells efficiently capture HIV-1 envelope glycoproteins via CD4 for antigen presentation.* J Immunol, 2013. **191**(1): p. 60-9.
120. Chauveau, L., D.A. Donahue, B. Monel, F. Porrot, T. Bruel, L. Richard, N. Casartelli, and O. Schwartz, *HIV Fusion in Dendritic Cells Occurs Mainly at the Surface and Is Limited by Low CD4 Levels.* J Virol, 2017. **91**(21).
121. Takeuchi, O. and S. Akira, *Pattern recognition receptors and inflammation.* Cell, 2010. **140**(6): p. 805-20.
122. Mogensen, T.H., *Pathogen recognition and inflammatory signaling in innate immune defenses.* Clin Microbiol Rev, 2009. **22**(2): p. 240-73, Table of Contents.
123. Mahla, R.S., M.C. Reddy, D.V. Prasad, and H. Kumar, *Sweeten PAMPs: Role of Sugar Complexed PAMPs in Innate Immunity and Vaccine Biology.* Front Immunol, 2013. **4**: p. 248.
124. Vijay, K., *Toll-like receptors in immunity and inflammatory diseases: Past, present, and future.* Int Immunopharmacol, 2018. **59**: p. 391-412.
125. Kawai, T. and S. Akira, *Toll-like receptors and their crosstalk with other innate receptors in infection and immunity.* Immunity, 2011. **34**(5): p. 637-50.
126. Hasan, U., C. Chaffois, C. Gaillard, V. Saulnier, E. Merck, S. Tancredi, C. Guiet, F. Briere, J. Vlach, S. Lebecque, G. Trinchieri, and E.E. Bates, *Human TLR10 is a functional receptor, expressed by B cells and plasmacytoid dendritic cells, which activates gene transcription through MyD88.* J Immunol, 2005. **174**(5): p. 2942-50.

127. Kumar, H., T. Kawai, and S. Akira, *Toll-like receptors and innate immunity.* Biochem Biophys Res Commun, 2009. **388**(4): p. 621-5.

128. Blasius, A.L. and B. Beutler, *Intracellular toll-like receptors.* Immunity, 2010. **32**(3): p. 305-15.

129. Uronen-Hansson, H., J. Allen, M. Osman, G. Squires, N. Klein, and R.E. Callard, *Toll-like receptor 2 (TLR2) and TLR4 are present inside human dendritic cells, associated with microtubules and the Golgi apparatus but are not detectable on the cell surface: integrity of microtubules is required for interleukin-12 production in response to internalized bacteria.* Immunology, 2004. **111**(2): p. 173-8.

130. Hornef, M.W., B.H. Normark, A. Vandewalle, and S. Normark, *Intracellular recognition of lipopolysaccharide by toll-like receptor 4 in intestinal epithelial cells.* J Exp Med, 2003. **198**(8): p. 1225-35.

131. Shuang, C., M.H. Wong, D.J. Schulte, M. Arditi, and K.S. Michelsen, *Differential expression of Toll-like receptor 2 (TLR2) and responses to TLR2 ligands between human and murine vascular endothelial cells.* J Endotoxin Res, 2007. **13**(5): p. 281-96.

132. Funderburg, N., A.A. Luciano, W. Jiang, B. Rodriguez, S.F. Sieg, and M.M. Lederman, *Toll-like receptor ligands induce human T cell activation and death, a model for HIV pathogenesis.* PLoS One, 2008. **3**(4): p. e1915.

133. Equils, O., E. Faure, L. Thomas, Y. Bulut, S. Trushin, and M. Arditi, *Bacterial lipopolysaccharide activates HIV long terminal repeat through Toll-like receptor 4.* J Immunol, 2001. **166**(4): p. 2342-7.

134. Appay, V. and D. Sauce, *Immune activation and inflammation in HIV-1 infection: causes and consequences.* J Pathol, 2008. **214**(2): p. 231-41.

135. Brenchley, J.M., D.A. Price, T.W. Schacker, T.E. Asher, G. Silvestri, S. Rao, Z. Kazzaz, E. Bornstein, O. Lambotte, D. Altmann, B.R. Blazar, B. Rodriguez, L. Teixeira-Johnson, A. Landay, J.N. Martin, F.M. Hecht, L.J. Picker, M.M. Lederman, S.G. Deeks, and D.C. Douek, *Microbial translocation is a cause of systemic immune activation in chronic HIV infection.* Nat Med, 2006. **12**(12): p. 1365-71.

136. Shan, L. and R.F. Siliciano, *Unraveling the relationship between microbial translocation and systemic immune activation in HIV infection.* J Clin Invest, 2014. **124**(6): p. 2368-71.

137. Kristoff, J., G. Haret-Richter, D. Ma, R.M. Ribeiro, C. Xu, E. Cornell, J.L. Stock, T. He, A.D. Mobley, S. Ross, A. Trichel, C. Wilson, R. Tracy, A. Landay, C. Apetrei, and I. Pandrea, *Early microbial translocation blockade reduces SIV-mediated inflammation and viral replication.* J Clin Invest, 2014. **124**(6): p. 2802-6.

138. Tipping, P.G., *Toll-like receptors: the interface between innate and adaptive immunity.* J Am Soc Nephrol, 2006. **17**(7): p. 1769-71.

139. Neefjes, J., M.L. Jongsma, P. Paul, and O. Bakke, *Towards a systems understanding of MHC class I and MHC class II antigen presentation.* Nat Rev Immunol, 2011. **11**(12): p. 823-36.

140. Bonilla, F.A. and H.C. Oettgen, *Adaptive immunity.* J Allergy Clin Immunol, 2010. **125**(2 Suppl 2): p. S33-40.

141. Luckheeram, R.V., R. Zhou, A.D. Verma, and B. Xia, *CD4(+)T cells: differentiation and functions.* Clin Dev Immunol, 2012. **2012**: p. 925135.

142. Novy, P., M. Quigley, X. Huang, and Y. Yang, *CD4 T cells are required for CD8 T cell survival during both primary and memory recall responses.* J Immunol, 2007. **179**(12): p. 8243-51.

143. Ahrends, T., J. Busselaar, T.M. Severson, N. Babala, E. de Vries, A. Bovens, L. Wessels, F. van Leeuwen, and J. Borst, *CD4(+) T cell help creates memory CD8(+) T cells with innate and help-independent recall capacities.* Nat Commun, 2019. **10**(1): p. 5531.

144. Laidlaw, B.J., J.E. Craft, and S.M. Kaech, *The multifaceted role of CD4(+) T cells in CD8(+) T cell memory.* Nat Rev Immunol, 2016. **16**(2): p. 102-11.

145. Douek, D.C., J.M. Brenchley, M.R. Betts, D.R. Ambrozak, B.J. Hill, Y. Okamoto, J.P. Casazza, J. Kuruppu, K. Kunstman, S. Wolinsky, Z. Grossman, M. Dybul, A. Oxenius, D.A. Price, M. Connors, and R.A. Koup, *HIV preferentially infects HIV-specific CD4+ T cells.* Nature, 2002. **417**(6884): p. 95-8.

146. Pantaleo, G., C. Graziosi, L. Butini, P.A. Pizzo, S.M. Schnittman, D.P. Kotler, and A.S. Fauci, *Lymphoid organs function as major reservoirs for human immunodeficiency virus.* Proc Natl Acad Sci U S A, 1991. **88**(21): p. 9838-42.

147. Pantaleo, G., C. Graziosi, J.F. Demarest, O.J. Cohen, M. Vaccarezza, K. Gantt, C. Muro-Cacho, and A.S. Fauci, *Role of lymphoid organs in the pathogenesis of human immunodeficiency virus (HIV) infection.* Immunol Rev, 1994. **140**: p. 105-30.

148. Kaech, S.M. and W. Cui, *Transcriptional control of effector and memory CD8+ T cell differentiation.* Nat Rev Immunol, 2012. **12**(11): p. 749-61.

149. Kalia, V. and S. Sarkar, *Regulation of Effector and Memory CD8 T Cell Differentiation by IL-2-A Balancing Act.* Front Immunol, 2018. **9**: p. 2987.

150. Starbeck-Miller, G.R., H.H. Xue, and J.T. Harty, *IL-12 and type I interferon prolong the division of activated CD8 T cells by maintaining high-affinity IL-2 signaling in vivo.* J Exp Med, 2014. **211**(1): p. 105-20.

151. Whitmire, J.K., J.T. Tan, and J.L. Whitton, *Interferon-gamma acts directly on CD8+ T cells to increase their abundance during virus infection.* J Exp Med, 2005. **201**(7): p. 1053-9.

152. Pearce, E.L. and H. Shen, *Generation of CD8 T cell memory is regulated by IL-12.* J Immunol, 2007. **179**(4): p. 2074-81.

153. Musey, L., J. Hughes, T. Schacker, T. Shea, L. Corey, and M.J. McElrath, *Cytotoxic-T-cell responses, viral load, and disease progression in early human immunodeficiency virus type 1 infection.* N Engl J Med, 1997. **337**(18): p. 1267-74.

154. Koup, R.A., J.T. Safrit, Y. Cao, C.A. Andrews, G. McLeod, W. Borkowsky, C. Farthing, and D.D. Ho, *Temporal association of cellular immune responses with the initial control of viremia in primary human immunodeficiency virus type 1 syndrome.* J Virol, 1994. **68**(7): p. 4650-5.

155. Borrow, P., H. Lewicki, B.H. Hahn, G.M. Shaw, and M.B. Oldstone, *Virus-specific CD8+ cytotoxic T-lymphocyte activity associated with control of viremia in primary human immunodeficiency virus type 1 infection.* J Virol, 1994. **68**(9): p. 6103-10.

156. Jin, X., D.E. Bauer, S.E. Tuttleton, S. Lewin, A. Gettie, J. Blanchard, C.E. Irwin, J.T. Safrit, J. Mittler, L. Weinberger, L.G. Kostrikis, L. Zhang, A.S. Perelson, and D.D. Ho, *Dramatic rise in plasma viremia after CD8(+) T cell depletion in simian immunodeficiency virus-infected macaques.* J Exp Med, 1999. **189**(6): p. 991-8.

157. Schmitz, J.E., M.J. Kuroda, S. Santra, V.G. Sasseville, M.A. Simon, M.A. Lifton, P. Racz, K. Tenner-Racz, M. Dalesandro, B.J. Scallon, J. Ghrayeb, M.A. Forman, D.C. Montefiori, E.P. Rieber, N.L. Letvin, and K.A. Reimann, *Control of viremia in simian immunodeficiency virus infection by CD8+ lymphocytes.* Science, 1999. **283**(5403): p. 857-60.

158. Flamand, L., R.W. Crowley, P. Lusso, S. Colombini-Hatch, D.M. Margolis, and R.C. Gallo, *Activation of CD8+ T lymphocytes through the T cell receptor turns on CD4 gene expression: implications for HIV pathogenesis.* Proc Natl Acad Sci U S A, 1998. **95**(6): p. 3111-6.

159. LeBien, T.W. and T.F. Tedder, *B lymphocytes: how they develop and function.* Blood, 2008. **112**(5): p. 1570-80.

160. Su, T.T., B. Guo, B. Wei, J. Braun, and D.J. Rawlings, *Signaling in transitional type 2 B cells is critical for peripheral B-cell development.* Immunol Rev, 2004. **197**: p. 161-78.

161. Moir, S. and A.S. Fauci, *B-cell responses to HIV infection.* Immunol Rev, 2017. **275**(1): p. 33-48.

162. Boliar, S., M.K. Murphy, T.C. Tran, D.G. Carnathan, W.S. Armstrong, G. Silvestri, and C.A. Derdeyn, *B-lymphocyte dysfunction in chronic HIV-1 infection does not prevent cross-clade neutralization breadth.* J Virol, 2012. **86**(15): p. 8031-40.

163. De Milito, A., A. Nilsson, K. Titanji, R. Thorstensson, E. Reizenstein, M. Narita, S. Grutzmeier, A. Sonnerborg, and F. Chiodi, *Mechanisms of hypergammaglobulinemia and impaired antigen-specific humoral immunity in HIV-1 infection.* Blood, 2004. **103**(6): p. 2180-6.

164. Sanchez-Merino, V., A. Fabra-Garcia, N. Gonzalez, D. Nicolas, A. Merino-Mansilla, C. Manzardo, J. Ambrosioni, A. Schultz, A. Meyerhans, J.R. Mascola, J.M. Gatell, J. Alcami, J.M. Miro, and E. Yuste, *Detection of Broadly Neutralizing Activity within the First Months of HIV-1 Infection.* J Virol, 2016. **90**(11): p. 5231-5245.

165. Frost, S.D., A. Trkola, H.F. Gunthard, and D.D. Richman, *Antibody responses in primary HIV-1 infection.* Curr Opin HIV AIDS, 2008. **3**(1): p. 45-51.

166. Richman, D.D., T. Wrin, S.J. Little, and C.J. Petropoulos, *Rapid evolution of the neutralizing antibody response to HIV type 1 infection.* Proc Natl Acad Sci U S A, 2003. **100**(7): p. 4144-9.

167. Moore, J.P., Y. Cao, L. Qing, Q.J. Sattentau, J. Pyati, R. Koduri, J. Robinson, C.F. Barbas, 3rd, D.R. Burton, and D.D. Ho, *Primary isolates of human immunodeficiency virus type 1 are relatively resistant to neutralization by monoclonal antibodies to gp120, and their neutralization is not predicted by studies with monomeric gp120.* J Virol, 1995. **69**(1): p. 101-9.

168. Stamatatos, L., L. Morris, D.R. Burton, and J.R. Mascola, *Neutralizing antibodies generated during natural HIV-1 infection: good news for an HIV-1 vaccine?* Nat Med, 2009. **15**(8): p. 866-70.

169. Shen, X., R.J. Parks, D.C. Montefiori, J.L. Kirchherr, B.F. Keele, J.M. Decker, W.A. Blattner, F. Gao, K.J. Weinhold, C.B. Hicks, M.L. Greenberg, B.H. Hahn, G.M. Shaw, B.F. Haynes, and G.D. Tomaras, *In vivo gp41 antibodies targeting the 2F5 monoclonal antibody epitope mediate human immunodeficiency virus type 1 neutralization breadth.* J Virol, 2009. **83**(8): p. 3617-25.

170. Zhang, Y.J., C. Fracasso, J.R. Fiore, A. Bjorndal, G. Angarano, A. Gringeri, and E.M. Fenyo, *Augmented serum neutralizing activity against primary human immunodeficiency virus type 1 (HIV-1) isolates in two groups of HIV-1-infected long-term nonprogressors.* J Infect Dis, 1997. **176**(5): p. 1180-7.

171. ClinicalTrials.gov. *Evaluating the Safety and Efficacy of the VRC01 Antibody in Reducing Acquisition of HIV-1 Infection in Women*. (Accessed on March 13, 2021); Available from: https://clinicaltrials.gov/ct2/show/NCT02568215?term=NCT02568215&draw=2&rank=1.

172. ClinicalTrials.gov. *Evaluating the Safety and Efficacy of the VRC01 Antibody in Reducing Acquisition of HIV-1 Infection Among Men and Transgender Persons Who Have Sex With Men*. (Accessed on March 13, 2021); Available from: https://clinicaltrials.gov/ct2/show/NCT02716675?term=NCT02716675&draw=2&rank=1.

173. Iwasaki, A., *Antiviral immune responses in the genital tract: clues for vaccines.* Nat Rev Immunol, 2010. **10**(10): p. 699-711.

174. Saba, E., J.C. Grivel, C. Vanpouille, B. Brichacek, W. Fitzgerald, L. Margolis, and A. Lisco, *HIV-1 sexual transmission: early events of HIV-1 infection of human cervico-vaginal tissue in an optimized ex vivo model.* Mucosal Immunol, 2010. **3**(3): p. 280-90.

175. Pudney, J., A.J. Quayle, and D.J. Anderson, *Immunological microenvironments in the human vagina and cervix: mediators of cellular immunity are concentrated in the cervical transformation zone.* Biol Reprod, 2005. **73**(6): p. 1253-63.

176. Johansson, E.L., A. Rudin, L. Wassen, and J. Holmgren, *Distribution of lymphocytes and adhesion molecules in human cervix and vagina.* Immunology, 1999. **96**(2): p. 272-7.

177. Givan, A.L., H.D. White, J.E. Stern, E. Colby, E.J. Gosselin, P.M. Guyre, and C.R. Wira, *Flow cytometric analysis of leukocytes in the human female reproductive tract: comparison of fallopian tube, uterus, cervix, and vagina.* Am J Reprod Immunol, 1997. **38**(5): p. 350-9.

178. Trifonova, R.T., J. Lieberman, and D. van Baarle, *Distribution of immune cells in the human cervix and implications for HIV transmission.* Am J Reprod Immunol, 2014. **71**(3): p. 252-64.

179. Shen, R., H.E. Richter, and P.D. Smith, *Early HIV-1 target cells in human vaginal and ectocervical mucosa.* Am J Reprod Immunol, 2011. **65**(3): p. 261-7.

180. Kaul, R., J. Prodger, V. Joag, B. Shannon, S. Yegorov, R. Galiwango, and L. McKinnon, *Inflammation and HIV Transmission in Sub-Saharan Africa.* Curr HIV/AIDS Rep, 2015. **12**(2): p. 216-22.

181. Liu, T., L. Zhang, D. Joo, and S.C. Sun, *NF-kappaB signaling in inflammation.* Signal Transduct Target Ther, 2017. **2**.

182. Zhang, H. and S.C. Sun, *NF-kappaB in inflammation and renal diseases.* Cell Biosci, 2015. **5**: p. 63.

183. Sims, J.E. and D.E. Smith, *The IL-1 family: regulators of immunity.* Nat Rev Immunol, 2010. **10**(2): p. 89-102.

184. Sims, J.E., M.J. Nicklin, J.F. Bazan, J.L. Barton, S.J. Busfield, J.E. Ford, R.A. Kastelein, S. Kumar, H. Lin, J.J. Mulero, J. Pan, Y. Pan, D.E. Smith, and P.R. Young, *A new nomenclature for IL-1-family genes.* Trends Immunol, 2001. **22**(10): p. 536-7.

185. Dunn, E., J.E. Sims, M.J. Nicklin, and L.A. O'Neill, *Annotating genes with potential roles in the immune system: six new members of the IL-1 family.* Trends Immunol, 2001. **22**(10): p. 533-6.

186. Gunther, S., D. Deredge, A.L. Bowers, A. Luchini, D.A. Bonsor, R. Beadenkopf, L. Liotta, P.L. Wintrode, and E.J. Sundberg, *IL-1 Family Cytokines Use Distinct Molecular Mechanisms to Signal through Their Shared Co-receptor.* Immunity, 2017. **47**(3): p. 510-523 e4.

187. Thomas, C., J.F. Bazan, and K.C. Garcia, *Structure of the activating IL-1 receptor signaling complex.* Nat Struct Mol Biol, 2012. **19**(4): p. 455-7.

188. Wang, D., S. Zhang, L. Li, X. Liu, K. Mei, and X. Wang, *Structural insights into the assembly and activation of IL-1beta with its receptors.* Nat Immunol, 2010. **11**(10): p. 905-11.

189. Dunne, A. and L.A. O'Neill, *The interleukin-1 receptor/Toll-like receptor superfamily: signal transduction during inflammation and host defense.* Sci STKE, 2003. **2003**(171): p. re3.

190. Granowitz, E.V., B.M. Saget, M.Z. Wang, C.A. Dinarello, and P.R. Skolnik, *Interleukin 1 induces HIV-1 expression in chronically infected U1 cells: blockade by interleukin 1 receptor antagonist and tumor necrosis factor binding protein type 1.* Mol Med, 1995. **1**(6): p. 667-77.

191. Osborn, L., S. Kunkel, and G.J. Nabel, *Tumor necrosis factor alpha and interleukin 1 stimulate the human immunodeficiency virus enhancer by activation of the nuclear factor kappa B.* Proc Natl Acad Sci U S A, 1989. **86**(7): p. 2336-40.

192. Poli, G., A.L. Kinter, and A.S. Fauci, *Interleukin 1 induces expression of the human immunodeficiency virus alone and in synergy with interleukin 6 in chronically infected U1 cells: inhibition of inductive effects by the interleukin 1 receptor antagonist.* Proc Natl Acad Sci U S A, 1994. **91**(1): p. 108-12.

193. Kobayashi, N., Y. Hamamoto, Y. Koyanagi, I.S. Chen, and N. Yamamoto, *Effect of interleukin-1 on the augmentation of human immunodeficiency virus gene expression.* Biochem Biophys Res Commun, 1989. **165**(2): p. 715-21.

194. Ikejima, T., S. Okusawa, P. Ghezzi, J.W. van der Meer, and C.A. Dinarello, *Interleukin-1 induces tumor necrosis factor (TNF) in human peripheral blood mononuclear cells in vitro and a circulating TNF-like activity in rabbits.* J Infect Dis, 1990. **162**(1): p. 215-23.

195. Goletti, D., A.L. Kinter, E.C. Hardy, G. Poli, and A.S. Fauci, *Modulation of endogenous IL-1 beta and IL-1 receptor antagonist results in opposing effects on HIV expression in chronically infected monocytic cells.* J Immunol, 1996. **156**(9): p. 3501-8.

196. Zavala, F., A.C. Rimaniol, F. Boussin, D. Dormont, J.F. Bach, and B. Descamps-Latscha, *HIV predominantly induces IL-1 receptor antagonist over IL-1 synthesis in human primary monocytes.* J Immunol, 1995. **155**(5): p. 2784-93.

197. Oeckinghaus, A. and S. Ghosh, *The NF-kappaB family of transcription factors and its regulation.* Cold Spring Harb Perspect Biol, 2009. **1**(4): p. a000034.

198. Liang, Y., Y. Zhou, and P. Shen, *NF-kappaB and its regulation on the immune system.* Cell Mol Immunol, 2004. **1**(5): p. 343-50.

199. Israel, A., *The IKK complex, a central regulator of NF-kappaB activation.* Cold Spring Harb Perspect Biol, 2010. **2**(3): p. a000158.

200. Sun, S.C., *The noncanonical NF-kappaB pathway.* Immunol Rev, 2012. **246**(1): p. 125-40.

201. Sun, S.C., *The non-canonical NF-kappaB pathway in immunity and inflammation.* Nat Rev Immunol, 2017. **17**(9): p. 545-558.

202. Sun, S.C. and Z.G. Liu, *A special issue on NF-kappaB signaling and function.* Cell Res, 2011. **21**(1): p. 1-2.

203. Hayden, M.S. and S. Ghosh, *NF-kappaB, the first quarter-century: remarkable progress and outstanding questions.* Genes Dev, 2012. **26**(3): p. 203-34.

204. Pasquereau, S., A. Kumar, and G. Herbein, *Targeting TNF and TNF Receptor Pathway in HIV-1 Infection: from Immune Activation to Viral Reservoirs.* Viruses, 2017. **9**(4).

205. Hiscott, J., H. Kwon, and P. Genin, *Hostile takeovers: viral appropriation of the NF-kappaB pathway.* J Clin Invest, 2001. **107**(2): p. 143-51.

206. Nabel, G. and D. Baltimore, *An inducible transcription factor activates expression of human immunodeficiency virus in T cells.* Nature, 1987. **326**(6114): p. 711-3.

207. Mallardo, M., E. Dragonetti, F. Baldassarre, C. Ambrosino, G. Scala, and I. Quinto, *An NF-kappaB site in the 5'-untranslated leader region of the human immunodeficiency virus type 1 enhances the viral expression in response to NF-kappaB-activating stimuli.* J Biol Chem, 1996. **271**(34): p. 20820-7.

208. Stroud, J.C., A. Oltman, A. Han, D.L. Bates, and L. Chen, *Structural basis of HIV-1 activation by NF-kappaB--a higher-order complex of p50:RelA bound to the HIV-1 LTR.* J Mol Biol, 2009. **393**(1): p. 98-112.

209. Fichorova, R.N., L.D. Tucker, and D.J. Anderson, *The molecular basis of nonoxynol-9-induced vaginal inflammation and its possible relevance to human immunodeficiency virus type 1 transmission.* J Infect Dis, 2001. **184**(4): p. 418-28.

210. Duh, E.J., W.J. Maury, T.M. Folks, A.S. Fauci, and A.B. Rabson, *Tumor necrosis factor alpha activates human immunodeficiency virus type 1 through induction of nuclear factor binding to the NF-kappa B sites in the long terminal repeat.* Proc Natl Acad Sci U S A, 1989. **86**(15): p. 5974-8.

211. Duverger, A., J. Jones, J. May, F. Bibollet-Ruche, F.A. Wagner, R.Q. Cron, and O. Kutsch, *Determinants of the establishment of human immunodeficiency virus type 1 latency.* J Virol, 2009. **83**(7): p. 3078-93.

212. Barrios De Tomasi, J., M.M. Opata, and C.N. Mowa, *Immunity in the Cervix: Interphase between Immune and Cervical Epithelial Cells.* J Immunol Res, 2019. **2019**: p. 7693183.

213. Tugizov, S., *Human immunodeficiency virus-associated disruption of mucosal barriers and its role in HIV transmission and pathogenesis of HIV/AIDS disease.* Tissue Barriers, 2016. **4**(3): p. e1159276.

214. Nazli, A., J.K. Kafka, V.H. Ferreira, V. Anipindi, K. Mueller, B.J. Osborne, S. Dizzell, S. Chauvin, M.F. Mian, M. Ouellet, M.J. Tremblay, K.L. Mossman, A.A. Ashkar, C. Kovacs, D.M. Bowdish, D.P. Snider, R. Kaul, and C. Kaushic, *HIV-1 gp120 induces TLR2- and TLR4-mediated innate immune activation in human female genital epithelium.* J Immunol, 2013. **191**(8): p. 4246-58.

215. Fichorova, R.N., M. Bajpai, N. Chandra, J.G. Hsiu, M. Spangler, V. Ratnam, and G.F. Doncel, *Interleukin (IL)-1, IL-6, and IL-8 predict mucosal toxicity of vaginal microbicidal contraceptives.* Biol Reprod, 2004. **71**(3): p. 761-9.

216. Nazli, A., O. Chan, W.N. Dobson-Belaire, M. Ouellet, M.J. Tremblay, S.D. Gray-Owen, A.L. Arsenault, and C. Kaushic, *Exposure to HIV-1 directly impairs mucosal epithelial barrier integrity allowing microbial translocation.* PLoS Pathog, 2010. **6**(4): p. e1000852.

217. Passmore, J.A., H.B. Jaspan, and L. Masson, *Genital inflammation, immune activation and risk of sexual HIV acquisition.* Curr Opin HIV AIDS, 2016. **11**(2): p. 156-62.

218. Masson, L., J.A. Passmore, L.J. Liebenberg, L. Werner, C. Baxter, K.B. Arnold, C. Williamson, F. Little, L.E. Mansoor, V. Naranbhai, D.A. Lauffenburger, K. Ronacher, G. Walzl, N.J. Garrett, B.L. Williams, M. Couto-Rodriguez, M. Hornig, W.I. Lipkin, A. Grobler, Q. Abdool Karim, and S.S. Abdool Karim, *Genital inflammation and the risk of HIV acquisition in women.* Clin Infect Dis, 2015. **61**(2): p. 260-9.

219. Arnold, K.B., A. Burgener, K. Birse, L. Romas, L.J. Dunphy, K. Shahabi, M. Abou, G.R. Westmacott, S. McCorrister, J. Kwatampora, B. Nyanga, J. Kimani, L. Masson, L.J. Liebenberg, S.S. Abdool Karim, J.A. Passmore, D.A. Lauffenburger, R. Kaul, and L.R. McKinnon, *Increased levels of inflammatory cytokines in the female reproductive tract are associated with altered expression of proteases, mucosal barrier proteins, and an influx of HIV-susceptible target cells.* Mucosal Immunol, 2016. **9**(1): p. 194-205.

220. Francis, S.C., Y. Hou, K. Baisley, J. van de Wijgert, D. Watson-Jones, T.T. Ao, C. Herrera, K. Maganja, A. Andreasen, S. Kapiga, G.R. Coulton, R.J. Hayes, and R.J. Shattock, *Immune Activation in the Female Genital Tract: Expression Profiles of Soluble Proteins in Women at High Risk for HIV Infection.* PLoS One, 2016. **11**(1): p. e0143109.

221. Liebenberg, L.J., L. Masson, K.B. Arnold, L.R. McKinnon, L. Werner, E. Proctor, D. Archary, L.E. Mansoor, D.A. Lauffenburger, Q. Abdool Karim, S.S. Abdool Karim, and J.S. Passmore, *Genital-Systemic Chemokine Gradients and the Risk of HIV Acquisition in Women.* J Acquir Immune Defic Syndr, 2017. **74**(3): p. 318-325.

222. Kaul, R., A. Rebbapragada, T. Hirbod, C. Wachihi, T.B. Ball, F.A. Plummer, J. Kimani, and W. Jaoko, *Genital levels of soluble immune factors with anti-HIV activity may correlate with increased HIV susceptibility.* AIDS, 2008. **22**(15): p. 2049-51.

223. Morrison, C., R.N. Fichorova, C. Mauck, P.L. Chen, C. Kwok, T. Chipato, R. Salata, and G.F. Doncel, *Cervical inflammation and immunity associated with hormonal contraception, pregnancy, and HIV-1 seroconversion.* J Acquir Immune Defic Syndr, 2014. **66**(2): p. 109-17.

224. Dabee, S., S.L. Barnabas, K.S. Lennard, S.Z. Jaumdally, H. Gamieldien, C. Balle, A.U. Happel, B.D. Murugan, A.L. Williamson, N. Mkhize, J. Dietrich, D.A. Lewis, F. Chiodi, T.J. Hope, R. Shattock, G. Gray, L.G. Bekker, H.B. Jaspan, and J.S. Passmore, *Defining characteristics of genital health in South African adolescent girls and young women at high risk for HIV infection.* PLoS One, 2019. **14**(4): p. e0213975.

225. Naranbhai, V., S.S. Abdool Karim, M. Altfeld, N. Samsunder, R. Durgiah, S. Sibeko, Q. Abdool Karim, and W.H. Carr, *Innate immune activation enhances hiv acquisition in women, diminishing the effectiveness of tenofovir microbicide gel.* J Infect Dis, 2012. **206**(7): p. 993-1001.

226. Kahle, E.M., M. Bolton, J.P. Hughes, D. Donnell, C. Celum, J.R. Lingappa, A. Ronald, C.R. Cohen, G. de Bruyn, Y. Fong, E. Katabira, M.J. McElrath, and J.M. Baeten, *Plasma cytokine levels and risk of HIV type 1 (HIV-1) transmission and acquisition: a nested case-control study among HIV-1-serodiscordant couples.* J Infect Dis, 2015. **211**(9): p. 1451-60.

227. McKinnon, L.R., L.J. Liebenberg, N. Yende-Zuma, D. Archary, S. Ngcapu, A. Sivro, N. Nagelkerke, J.G. Garcia Lerma, A.D. Kashuba, L. Masson, L.E. Mansoor, Q.A. Karim, S.S.A. Karim, and J.S. Passmore, *Genital inflammation undermines the effectiveness of tenofovir gel in preventing HIV acquisition in women.* Nat Med, 2018. **24**(4): p. 491-496.

228. Cohen, C.R., A.B. Moscicki, M.E. Scott, Y. Ma, S. Shiboski, E. Bukusi, I. Daud, A. Rebbapragada, J. Brown, and R. Kaul, *Increased levels of immune activation in the genital tract of healthy young women from sub-Saharan Africa.* AIDS, 2010. **24**(13): p. 2069-74.

229. Bebell, L.M., J.A. Passmore, C. Williamson, K. Mlisana, I. Iriogbe, F. van Loggerenberg, Q.A. Karim, and S.A. Karim, *Relationship between levels of inflammatory cytokines in the genital tract and CD4+ cell counts in women with acute HIV-1 infection.* J Infect Dis, 2008. **198**(5): p. 710-4.

230. Roberts, L., J.A. Passmore, K. Mlisana, C. Williamson, F. Little, L.M. Bebell, G. Walzl, M.R. Abrahams, Z. Woodman, Q. Abdool Karim, and S.S. Abdool Karim, *Genital tract inflammation during early HIV-1 infection predicts higher plasma viral load set point in women.* J Infect Dis, 2012. **205**(2): p. 194-203.

231. Paiardini, M. and M. Muller-Trutwin, *HIV-associated chronic immune activation.* Immunol Rev, 2013. **254**(1): p. 78-101.

232. Giorgi, J.V., L.E. Hultin, J.A. McKeating, T.D. Johnson, B. Owens, L.P. Jacobson, R. Shih, J. Lewis, D.J. Wiley, J.P. Phair, S.M. Wolinsky, and R. Detels, *Shorter survival in advanced human immunodeficiency virus type 1 infection is more closely associated with T lymphocyte activation than with plasma virus burden or virus chemokine coreceptor usage.* J Infect Dis, 1999. **179**(4): p. 859-70.

233. Deeks, S.G., C.M. Kitchen, L. Liu, H. Guo, R. Gascon, A.B. Narvaez, P. Hunt, J.N. Martin, J.O. Kahn, J. Levy, M.S. McGrath, and F.M. Hecht, *Immune activation set point*

during early HIV infection predicts subsequent CD4+ T-cell changes independent of viral load. Blood, 2004. **104**(4): p. 942-7.

234. Card, C.M., T.B. Ball, and K.R. Fowke, *Immune quiescence: a model of protection against HIV infection.* Retrovirology, 2013. **10**: p. 141.

235. Card, C.M., P.J. McLaren, C. Wachihi, J. Kimani, F.A. Plummer, and K.R. Fowke, *Decreased immune activation in resistance to HIV-1 infection is associated with an elevated frequency of CD4(+)CD25(+)FOXP3(+) regulatory T cells.* J Infect Dis, 2009. **199**(9): p. 1318-22.

236. McLaren, P.J., T.B. Ball, C. Wachihi, W. Jaoko, D.J. Kelvin, A. Danesh, J. Kimani, F.A. Plummer, and K.R. Fowke, *HIV-exposed seronegative commercial sex workers show a quiescent phenotype in the CD4+ T cell compartment and reduced expression of HIV-dependent host factors.* J Infect Dis, 2010. **202 Suppl 3**: p. S339-44.

237. Lajoie, J., J. Juno, A. Burgener, S. Rahman, K. Mogk, C. Wachihi, J. Mwanjewe, F.A. Plummer, J. Kimani, T.B. Ball, and K.R. Fowke, *A distinct cytokine and chemokine profile at the genital mucosa is associated with HIV-1 protection among HIV-exposed seronegative commercial sex workers.* Mucosal Immunol, 2012. **5**(3): p. 277-87.

238. Begaud, E., L. Chartier, V. Marechal, J. Ipero, J. Leal, P. Versmisse, G. Breton, A. Fontanet, C. Capoulade-Metay, H. Fleury, F. Barre-Sinoussi, D. Scott-Algara, and G. Pancino, *Reduced CD4 T cell activation and in vitro susceptibility to HIV-1 infection in exposed uninfected Central Africans.* Retrovirology, 2006. **3**: p. 35.

239. Kiyozumi, D., A. Osada, N. Sugimoto, C.N. Weber, Y. Ono, T. Imai, A. Okada, and K. Sekiguchi, *Identification of a novel cell-adhesive protein spatiotemporally expressed in the basement membrane of mouse developing hair follicle.* Exp Cell Res, 2005. **306**(1): p. 9-23.

240. Staub, E., B. Hinzmann, and A. Rosenthal, *A novel repeat in the melanoma-associated chondroitin sulfate proteoglycan defines a new protein family.* FEBS Lett, 2002. **527**(1-3): p. 114-8.

241. Yuan, X.Y., L.R. Liu, A. Krawchenko, J. Sainsbury, L. Zhao, F. Plummer, X. Yang, and M. Luo, *Development of monoclonal antibodies to interrogate functional domains and isoforms of FREM1 protein.* Monoclon Antib Immunodiagn Immunother, 2014. **33**(2): p. 129-40.

242. Kashem, M.A., H. Li, N.P. Toledo, R.W. Omange, B. Liang, L.R. Liu, L. Li, X. Yang, X.-Y. Yuan, J. Kindrachuk, F.A. Plummer, and M. Luo, *Toll-like Interleukin 1 Receptor Regulator Is an Important Modulator of Inflammation Responsive Genes.* Frontiers in Immunology, 2019. **10**(272): p. 1-16.

243. Smyth, I., X. Du, M.S. Taylor, M.J. Justice, B. Beutler, and I.J. Jackson, *The extracellular matrix gene Frem1 is essential for the normal adhesion of the embryonic epidermis.* Proc Natl Acad Sci U S A, 2004. **101**(37): p. 13560-5.

244. Nishiyama, A., K.J. Dahlin, J.T. Prince, S.R. Johnstone, and W.B. Stallcup, *The primary structure of NG2, a novel membrane-spanning proteoglycan.* J Cell Biol, 1991. **114**(2): p. 359-71.

245. Burg, M.A., E. Tillet, R. Timpl, and W.B. Stallcup, *Binding of the NG2 proteoglycan to type VI collagen and other extracellular matrix molecules.* J Biol Chem, 1996. **271**(42): p. 26110-6.

246. Tillet, E., B. Gential, R. Garrone, and W.B. Stallcup, *NG2 proteoglycan mediates beta1 integrin-independent cell adhesion and spreading on collagen VI.* J Cell Biochem, 2002. **86**(4): p. 726-36.

247. Nishiyama, A. and W.B. Stallcup, *Expression of NG2 proteoglycan causes retention of type VI collagen on the cell surface.* Mol Biol Cell, 1993. **4**(11): p. 1097-108.

248. Goretzki, L., M.A. Burg, K.A. Grako, and W.B. Stallcup, *High-affinity binding of basic fibroblast growth factor and platelet-derived growth factor-AA to the core protein of the NG2 proteoglycan.* J Biol Chem, 1999. **274**(24): p. 16831-7.

249. Nathanson, J., D.T. Swarr, A. Singer, M. Liu, A. Chinn, W. Jones, J. Hurst, N. Khalek, E. Zackai, and A. Slavotinek, *Novel FREM1 mutations expand the phenotypic spectrum associated with Manitoba-oculo-tricho-anal (MOTA) syndrome and bifid nose renal agenesis anorectal malformations (BNAR) syndrome.* Am J Med Genet A, 2013. **161A**(3): p. 473-8.

250. Schwarz, E.M. and S. Benzer, *Calx, a Na-Ca exchanger gene of Drosophila melanogaster.* Proc Natl Acad Sci U S A, 1997. **94**(19): p. 10249-54.

251. Short, K., F. Wiradjaja, and I. Smyth, *Let's stick together: the role of the Fras1 and Frem proteins in epidermal adhesion.* IUBMB Life, 2007. **59**(7): p. 427-35.

252. Thierry-Mieg, D. and J. Thierry-Mieg, *AceView: a comprehensive cDNA-supported gene and transcripts annotation.* Genome Biol, 2006. **7 Suppl 1**: p. S12 1-14.

253. NCBI. *The AceView genes* 2012 (Accessed on April 20, 2020); Available from: https://www.ncbi.nlm.nih.gov/IEB/Research/Acembly/.

254. Kashem, M.A., H. Li, N.P. Toledo, R.W. Omange, B. Liang, L.R. Liu, L. Li, X. Yang, X.-Y. Yuan, J. Kindrachuk, F.A. Plummer, and M. Luo, *Toll-like Interleukin 1 Receptor Regulator Is an Important Modulator of Inflammation Responsive Genes.* Front Immunol, 2019. **10**(272): p. 1-16.

255. Beck, T.F., D. Veenma, O.A. Shchelochkov, Z. Yu, B.J. Kim, H.P. Zaveri, Y. van Bever, S. Choi, H. Douben, T.K. Bertin, P.I. Patel, B. Lee, D. Tibboel, A. de Klein, D.W. Stockton, M.J. Justice, and D.A. Scott, *Deficiency of FRAS1-related extracellular matrix 1 (FREM1) causes congenital diaphragmatic hernia in humans and mice.* Hum Mol Genet, 2013. **22**(5): p. 1026-38.

256. Petrou, P., R. Chiotaki, Y. Dalezios, and G. Chalepakis, *Overlapping and divergent localization of Frem1 and Fras1 and its functional implications during mouse embryonic development.* Exp Cell Res, 2007. **313**(5): p. 910-20.

257. Kiyozumi, D., N. Sugimoto, and K. Sekiguchi, *Breakdown of the reciprocal stabilization of QBRICK/Frem1, Fras1, and Frem2 at the basement membrane provokes Fraser syndrome-like defects.* Proc Natl Acad Sci U S A, 2006. **103**(32): p. 11981-6.

258. Vissers, L.E., T.C. Cox, A.M. Maga, K.M. Short, F. Wiradjaja, I.M. Janssen, F. Jehee, D. Bertola, J. Liu, G. Yagnik, K. Sekiguchi, D. Kiyozumi, H. van Bokhoven, C. Marcelis, M.L. Cunningham, P.J. Anderson, S.A. Boyadjiev, M.R. Passos-Bueno, J.A. Veltman, I. Smyth, M.F. Buckley, and T. Roscioli, *Heterozygous mutations of FREM1 are associated with an increased risk of isolated metopic craniosynostosis in humans and mice.* PLoS Genet, 2011. **7**(9): p. e1002278.

259. Alazami, A.M., R. Shaheen, F. Alzahrani, K. Snape, A. Saggar, B. Brinkmann, P. Bavi, L.I. Al-Gazali, and F.S. Alkuraya, *FREM1 mutations cause bifid nose, renal agenesis, and anorectal malformations syndrome.* Am J Hum Genet, 2009. **85**(3): p. 414-8.

260. Luo, M., J. Sainsbury, J. Tuff, P.A. Lacap, X.Y. Yuan, T. Hirbod, J. Kimani, C. Wachihi, S. Ramdahin, T. Bielawny, J. Embree, K. Broliden, T.B. Ball, and F.A. Plummer, *A*

genetic polymorphism of FREM1 is associated with resistance against HIV infection in the Pumwani sex worker cohort. J Virol, 2012. **86**(21): p. 11899-905.

261. Arroyo, A.G. and M.L. Iruela-Arispe, *Extracellular matrix, inflammation, and the angiogenic response.* Cardiovasc Res, 2010. **86**(2): p. 226-35.
262. Adair-Kirk, T.L. and R.M. Senior, *Fragments of extracellular matrix as mediators of inflammation.* Int J Biochem Cell Biol, 2008. **40**(6-7): p. 1101-10.
263. Gaudet, A.D. and P.G. Popovich, *Extracellular matrix regulation of inflammation in the healthy and injured spinal cord.* Exp Neurol, 2014. **258**: p. 24-34.
264. Gopal, S., *Syndecans in Inflammation at a Glance.* Front Immunol, 2020. **11**: p. 227.
265. Li, H.N., X.R. Li, Z.T. Lv, M.M. Cai, G. Wang, and Z.F. Yang, *Elevated expression of FREM1 in breast cancer indicates favorable prognosis and high-level immune infiltration status.* Cancer Med, 2020.
266. Kim, C.H., *Crawling of effector T cells on extracellular matrix: role of integrins in interstitial migration in inflamed tissues.* Cell Mol Immunol, 2014. **11**(1): p. 1-4.
267. Hernandez, J.C., M. Stevenson, E. Latz, and S. Urcuqui-Inchima, *HIV type 1 infection up-regulates TLR2 and TLR4 expression and function in vivo and in vitro.* AIDS Res Hum Retroviruses, 2012. **28**(10): p. 1313-28.
268. Simonsen, J.N., F.A. Plummer, E.N. Ngugi, C. Black, J.K. Kreiss, M.N. Gakinya, P. Waiyaki, L.J. D'Costa, J.O. Ndinya-Achola, P. Piot, and et al., *HIV infection among lower socioeconomic strata prostitutes in Nairobi.* AIDS, 1990. **4**(2): p. 139-44.
269. Kreiss, J.K., D. Koech, F.A. Plummer, K.K. Holmes, M. Lightfoote, P. Piot, A.R. Ronald, J.O. Ndinya-Achola, L.J. D'Costa, P. Roberts, and et al., *AIDS virus infection in Nairobi prostitutes. Spread of the epidemic to East Africa.* N Engl J Med, 1986. **314**(7): p. 414-8.
270. Plummer, F.A., J.N. Simonsen, D.W. Cameron, J.O. Ndinya-Achola, J.K. Kreiss, M.N. Gakinya, P. Waiyaki, M. Cheang, P. Piot, A.R. Ronald, and et al., *Cofactors in male-female sexual transmission of human immunodeficiency virus type 1.* J Infect Dis, 1991. **163**(2): p. 233-9.
271. Fowke, K.R., N.J. Nagelkerke, J. Kimani, J.N. Simonsen, A.O. Anzala, J.J. Bwayo, K.S. MacDonald, E.N. Ngugi, and F.A. Plummer, *Resistance to HIV-1 infection among*

persistently seronegative prostitutes in Nairobi, Kenya. Lancet, 1996. **348**(9038): p. 1347-51.

272. Iqbal, S.M., T.B. Ball, J. Kimani, P. Kiama, P. Thottingal, J.E. Embree, K.R. Fowke, and F.A. Plummer, *Elevated T cell counts and RANTES expression in the genital mucosa of HIV-1-resistant Kenyan commercial sex workers.* J Infect Dis, 2005. **192**(5): p. 728-38.
273. Burgener, A., J. Boutilier, C. Wachihi, J. Kimani, M. Carpenter, G. Westmacott, K. Cheng, T.B. Ball, and F. Plummer, *Identification of differentially expressed proteins in the cervical mucosa of HIV-1-resistant sex workers.* J Proteome Res, 2008. **7**(10): p. 4446-54.
274. Iqbal, S.M., T.B. Ball, P. Levinson, L. Maranan, W. Jaoko, C. Wachihi, B.J. Pak, V.N. Podust, K. Broliden, T. Hirbod, R. Kaul, and F.A. Plummer, *Elevated elafin/trappin-2 in the female genital tract is associated with protection against HIV acquisition.* AIDS, 2009. **23**(13): p. 1669-77.
275. Alimonti, J.B., J. Kimani, L. Matu, C. Wachihi, R. Kaul, F.A. Plummer, and K.R. Fowke, *Characterization of CD8 T-cell responses in HIV-1-exposed seronegative commercial sex workers from Nairobi, Kenya.* Immunol Cell Biol, 2006. **84**(5): p. 482-5.
276. Alimonti, J.B., S.A. Koesters, J. Kimani, L. Matu, C. Wachihi, F.A. Plummer, and K.R. Fowke, *CD4+ T cell responses in HIV-exposed seronegative women are qualitatively distinct from those in HIV-infected women.* J Infect Dis, 2005. **191**(1): p. 20-4.
277. Luo, M., C.A. Daniuk, T.O. Diallo, R.E. Capina, J. Kimani, C. Wachihi, M. Kimani, T. Bielawny, T. Peterson, M.G. Mendoza, S. Kiazyk, T.B. Ball, and F.A. Plummer, *For protection from HIV-1 infection, more might not be better: a systematic analysis of HIV Gag epitopes of two alleles associated with different outcomes of HIV-1 infection.* J Virol, 2012. **86**(2): p. 1166-80.
278. Rowland-Jones, S.L., T. Dong, K.R. Fowke, J. Kimani, P. Krausa, H. Newell, T. Blanchard, K. Ariyoshi, J. Oyugi, E. Ngugi, J. Bwayo, K.S. MacDonald, A.J. McMichael, and F.A. Plummer, *Cytotoxic T cell responses to multiple conserved HIV epitopes in HIV-resistant prostitutes in Nairobi.* J Clin Invest, 1998. **102**(9): p. 1758-65.
279. Lacap, P.A., J.D. Huntington, M. Luo, N.J. Nagelkerke, T. Bielawny, J. Kimani, C. Wachihi, E.N. Ngugi, and F.A. Plummer, *Associations of human leukocyte antigen DRB*

with resistance or susceptibility to HIV-1 infection in the Pumwani Sex Worker Cohort. AIDS, 2008. **22**(9): p. 1029-38.

280. Price, H., P. Lacap, J. Tuff, C. Wachihi, J. Kimani, T.B. Ball, M. Luo, and F.A. Plummer, *A TRIM5alpha exon 2 polymorphism is associated with protection from HIV-1 infection in the Pumwani sex worker cohort.* AIDS, 2010. **24**(12): p. 1813-21.
281. Ball, T.B., H. Ji, J. Kimani, P. McLaren, C. Marlin, A.V. Hill, and F.A. Plummer, *Polymorphisms in IRF-1 associated with resistance to HIV-1 infection in highly exposed uninfected Kenyan sex workers.* AIDS, 2007. **21**(9): p. 1091-101.
282. Hardie, R.A., E. Knight, B. Bruneau, C. Semeniuk, K. Gill, N. Nagelkerke, J. Kimani, C. Wachihi, E. Ngugi, M. Luo, and F.A. Plummer, *A common human leucocyte antigen-DP genotype is associated with resistance to HIV-1 infection in Kenyan sex workers.* AIDS, 2008. **22**(15): p. 2038-42.
283. Hardie, R.A., M. Luo, B. Bruneau, E. Knight, N.J. Nagelkerke, J. Kimani, C. Wachihi, E.N. Ngugi, and F.A. Plummer, *Human leukocyte antigen-DQ alleles and haplotypes and their associations with resistance and susceptibility to HIV-1 infection.* AIDS, 2008. **22**(7): p. 807-16.
284. Salazar, G., N. Zhang, T.M. Fu, and Z. An, *Antibody therapies for the prevention and treatment of viral infections.* NPJ Vaccines, 2017. **2**: p. 19.
285. Zhang, X., F. Shephard, H.B. Kim, I.R. Palmer, S. McHarg, G.J. Fowler, L.A. O'Neill, E. Kiss-Toth, and E.E. Qwarnstrom, *TILRR, a novel IL-1RI co-receptor, potentiates MyD88 recruitment to control Ras-dependent amplification of NF-kappaB.* J Biol Chem, 2010. **285**(10): p. 7222-32.
286. Xu, X.Y., W.J. Guo, S.H. Pan, Y. Zhang, F.L. Gao, J.T. Wang, S. Zhang, H.Y. Li, R. Wang, and X. Zhang, *TILRR (FREM1 isoform 2) is a prognostic biomarker correlated with immune infiltration in breast cancer.* Aging (Albany NY), 2020. **12**(19): p. 19335-19351.
287. Hudson, R.C., C. Gray, E. Kiss-Toth, T.J. Chico, and E.E. Qwarnstrom, *Bioinformatics Analysis of the FREM1 Gene-Evolutionary Development of the IL-1R1 Co-Receptor, TILRR.* Biology (Basel), 2012. **1**(3): p. 484-94.
288. Smith, S.A., A.O. Samokhin, M. Alfadi, E.C. Murphy, D. Rhodes, W.M.L. Holcombe, E. Kiss-Toth, R.F. Storey, S.P. Yee, S.E. Francis, and E.E. Qwarnstrom, *The IL-1RI Co-*

Receptor TILRR (FREM1 Isoform 2) Controls Aberrant Inflammatory Responses and Development of Vascular Disease. JACC Basic Transl Sci, 2017. **2**(4): p. 398-414.

289. Akira, S. and K. Takeda, *Toll-like receptor signalling.* Nat Rev Immunol, 2004. **4**(7): p. 499-511.
290. O'Neill, L.A. and A.G. Bowie, *The family of five: TIR-domain-containing adaptors in Toll-like receptor signalling.* Nat Rev Immunol, 2007. **7**(5): p. 353-64.
291. O'Neill, L.A., *How Toll-like receptors signal: what we know and what we don't know.* Curr Opin Immunol, 2006. **18**(1): p. 3-9.
292. Rhodes, D.M., S.A. Smith, M. Holcombe, and E.E. Qwarnstrom, *Computational Modelling of NF-kappaB Activation by IL-1RI and Its Co-Receptor TILRR, Predicts a Role for Cytoskeletal Sequestration of IkappaBalpha in Inflammatory Signalling.* PLoS One, 2015. **10**(6): p. e0129888.
293. Zhang, X., G.M. Pino, F. Shephard, E. Kiss-Toth, and E.E. Qwarnstrom, *Distinct control of MyD88 adapter-dependent and Akt kinase-regulated responses by the interleukin (IL)-1RI co-receptor, TILRR.* J Biol Chem, 2012. **287**(15): p. 12348-52.
294. Mac Gabhann, F., *TILRR Steers Interleukin-1 Signaling: Co-Receptor Provides Context and a Therapeutic Target.* JACC Basic Transl Sci, 2017. **2**(4): p. 415-417.
295. Lawrence, T., *The nuclear factor NF-kappaB pathway in inflammation.* Cold Spring Harb Perspect Biol, 2009. **1**(6): p. a001651.
296. Deshmane, S.L., S. Kremlev, S. Amini, and B.E. Sawaya, *Monocyte chemoattractant protein-1 (MCP-1): an overview.* J Interferon Cytokine Res, 2009. **29**(6): p. 313-26.
297. Caamano, J. and C.A. Hunter, *NF-kappaB family of transcription factors: central regulators of innate and adaptive immune functions.* Clin Microbiol Rev, 2002. **15**(3): p. 414-29.
298. Barnes, P.J. and M. Karin, *Nuclear factor-kappaB: a pivotal transcription factor in chronic inflammatory diseases.* N Engl J Med, 1997. **336**(15): p. 1066-71.
299. Santoro, M.G., A. Rossi, and C. Amici, *NF-kappaB and virus infection: who controls whom.* EMBO J, 2003. **22**(11): p. 2552-60.
300. Li, H., M. Nykoluk, L. Li, L.R. Liu, R.W. Omange, G. Soule, L.T. Schroeder, N. Toledo, M.A. Kashem, J.F. Correia-Pinto, B. Liang, N. Schultz-Darken, M.J. Alonso, J.B.

Whitney, F.A. Plummer, and M. Luo, *Natural and cross-inducible anti-SIV antibodies in Mauritian cynomolgus macaques.* PLoS One, 2017. **12**(10): p. e0186079.

301. Cadena-Herrera, D., J.E. Esparza-De Lara, N.D. Ramirez-Ibanez, C.A. Lopez-Morales, N.O. Perez, L.F. Flores-Ortiz, and E. Medina-Rivero, *Validation of three viable-cell counting methods: Manual, semi-automated, and automated.* Biotechnol Rep (Amst), 2015. **7**: p. 9-16.
302. Louis, K.S. and A.C. Siegel, *Cell viability analysis using trypan blue: manual and automated methods.* Methods Mol Biol, 2011. **740**: p. 7-12.
303. Dejucq, N., G. Simmons, and P.R. Clapham, *Expanded tropism of primary human immunodeficiency virus type 1 R5 strains to CD4(+) T-cell lines determined by the capacity to exploit low concentrations of CCR5.* J Virol, 1999. **73**(9): p. 7842-7.
304. Konopka, K. and N. Duzgunes, *Expression of CD4 controls the susceptibility of THP-1 cells to infection by R5 and X4 HIV type 1 isolates.* AIDS Res Hum Retroviruses, 2002. **18**(2): p. 123-31.
305. Dejucq, N., *HIV-1 replication in CD4+ T cell lines: the effects of adaptation on co-receptor use, tropism, and accessory gene function.* J Leukoc Biol, 2000. **68**(3): p. 331-7.
306. Miyake, H., Y. Iizawa, and M. Baba, *Novel reporter T-cell line highly susceptible to both CCR5- and CXCR4-using human immunodeficiency virus type 1 and its application to drug susceptibility tests.* J Clin Microbiol, 2003. **41**(6): p. 2515-21.
307. Blanco, J., B. Bosch, M.T. Fernandez-Figueras, J. Barretina, B. Clotet, and J.A. Este, *High level of coreceptor-independent HIV transfer induced by contacts between primary CD4 T cells.* J Biol Chem, 2004. **279**(49): p. 51305-14.
308. Guo, H., J. Gao, D.J. Taxman, J.P. Ting, and L. Su, *HIV-1 infection induces interleukin-1beta production via TLR8 protein-dependent and NLRP3 inflammasome mechanisms in human monocytes.* J Biol Chem, 2014. **289**(31): p. 21716-26.
309. Ushijima, H., M. Dairaku, H. Honma, K. Yamaguchi, H. Shimizu, H. Tsuchie, K. Abe, A. Yamamoto, H. Hoshino, and W.E. Muller, *Human immunodeficiency virus infection in cells of myeloid-monocytic lineage.* Microbiol Immunol, 1991. **35**(6): p. 487-92.
310. Cassol, E., M. Alfano, P. Biswas, and G. Poli, *Monocyte-derived macrophages and myeloid cell lines as targets of HIV-1 replication and persistence.* J Leukoc Biol, 2006. **80**(5): p. 1018-30.

311. Lodge, R., J.C. Gilmore, J.A. Ferreira Barbosa, F. Lombard-Vadnais, and E.A. Cohen, *Regulation of CD4 Receptor and HIV-1 Entry by MicroRNAs-221 and -222 during Differentiation of THP-1 Cells.* Viruses, 2017. **10**(1).

312. Li, Q., J.D. Estes, P.M. Schlievert, L. Duan, A.J. Brosnahan, P.J. Southern, C.S. Reilly, M.L. Peterson, N. Schultz-Darken, K.G. Brunner, K.R. Nephew, S. Pambuccian, J.D. Lifson, J.V. Carlis, and A.T. Haase, *Glycerol monolaurate prevents mucosal SIV transmission.* Nature, 2009. **458**(7241): p. 1034-8.

313. Kaul, R., C. Pettengell, P.M. Sheth, S. Sunderji, A. Biringer, K. MacDonald, S. Walmsley, and A. Rebbapragada, *The genital tract immune milieu: an important determinant of HIV susceptibility and secondary transmission.* J Reprod Immunol, 2008. **77**(1): p. 32-40.

314. Pioli, P.D. *Protocol: Hemocytometer cell counting*. 2019 (Accessed on March 13, 2021); Available from: med.wmich.edu/sites/default/files/Hemacytometer_Cell_Counting.pdf.

315. Wu, J., A. Kumar-Kanojia, S. Hombach-Klonisch, T. Klonisch, and F. Lin, *A radial microfluidic platform for higher throughput chemotaxis studies with individual gradient control.* Lab on a Chip, 2018. **18**(24): p. 3855-3864.

316. Ren, X., J. Wu, D. Levin, S. Santos, R.L. de Faria, M. Zhang, and F. Lin, *Sputum from chronic obstructive pulmonary disease patients inhibits T cell migration in a microfluidic device.* Annals of the New York Academy of Sciences, 2019. **1445**(1): p. 52-61.

317. Ren, X., A. Alamri, J. Hipolito, F. Lin, and S.K.P. Kung, *Applications of microfluidic devices in advancing NK-cell migration studies.* Methods Enzymol, 2020. **631**: p. 357-370.

318. Bio-Rad. *Bio-Plex Pro Magnetic COOH Beads Bio-Plex COOH Beads Amine Coupling kit*. (Accessed on March 13, 2021); Available from: https://www.bio-rad.com/webroot/web/pdf/lsr/literature/4110012C.pdf.

319. Invitrogen. *APEX Antibody Labeling protocol*. (Accessed on March 13, 2021); Available from: https://www.thermofisher.com/document-connect/document-connect.html?url=https%3A%2F%2Fassets.thermofisher.com%2FTFS-Assets%2FLSG%2Fmanuals%2Fmp10468.pdf&title=QVBFWCBBbnRpYm9keSBMYWJlbGluZyBLaXRz.

320. Bio-Rad. *Instructions for staining Polyacrylamide Gels*. (Accessed on March 13, 2021); Available from: https://www.bio-rad.com/webroot/web/pdf/lsr/literature/4307051.pdf.
321. Feldmann, A., N. Berndt, R. Bergmann, and M. Bachmann, *Gel Drying Methods.* Methods Mol Biol, 2018. **1853**: p. 269-271.
322. Invitrogen. *DryEase Mini-Gel Drying System*. 2012 (Accessed on March 13, 2021); Available from: https://www.thermofisher.com/document-connect/document-connect.html?url=https%3A%2F%2Fassets.thermofisher.com%2FTFS-Assets%2FLSG%2Fmanuals%2Fdryease_man.pdf&title=RHJ5RWFzZSBNaW5pLUdlbCBEcnlpbmcgU3lzdGVt.
323. Ottoson, N.C., J.T. Pribila, A.S. Chan, and Y. Shimizu, *Cutting edge: T cell migration regulated by CXCR4 chemokine receptor signaling to ZAP-70 tyrosine kinase.* J Immunol, 2001. **167**(4): p. 1857-61.
324. Okabe, S., S. Fukuda, Y.J. Kim, M. Niki, L.M. Pelus, K. Ohyashiki, P.P. Pandolfi, and H.E. Broxmeyer, *Stromal cell-derived factor-1alpha/CXCL12-induced chemotaxis of T cells involves activation of the RasGAP-associated docking protein p62Dok-1*. Blood, 2005. **105**(2): p. 474-80.
325. Chen, L., H. Deng, H. Cui, J. Fang, Z. Zuo, J. Deng, Y. Li, X. Wang, and L. Zhao, *Inflammatory responses and inflammation-associated diseases in organs.* Oncotarget, 2018. **9**(6): p. 7204-7218.
326. Ahmed, A.U., B.R. Williams, and G.E. Hannigan, *Transcriptional Activation of Inflammatory Genes: Mechanistic Insight into Selectivity and Diversity.* Biomolecules, 2015. **5**(4): p. 3087-111.
327. Tak, P.P. and G.S. Firestein, *NF-kappaB: a key role in inflammatory diseases.* J Clin Invest, 2001. **107**(1): p. 7-11.
328. Baldwin, A.S., Jr., *The NF-kappa B and I kappa B proteins: new discoveries and insights.* Annu Rev Immunol, 1996. **14**: p. 649-83.
329. Sha, Y. and S. Markovic-Plese, *A role of IL-1R1 signaling in the differentiation of Th17 cells and the development of autoimmune diseases.* Self Nonself, 2011. **2**(1): p. 35-42.
330. Smith, C.J. and A.M. Osborn, *Advantages and limitations of quantitative PCR (Q-PCR)-based approaches in microbial ecology.* FEMS Microbiol Ecol, 2009. **67**(1): p. 6-20.

331. Joyce, D., C. Albanese, J. Steer, M. Fu, B. Bouzahzah, and R.G. Pestell, *NF-kappaB and cell-cycle regulation: the cyclin connection.* Cytokine Growth Factor Rev, 2001. **12**(1): p. 73-90.

332. Beg, A.A. and D. Baltimore, *An essential role for NF-kappaB in preventing TNF-alpha-induced cell death.* Science, 1996. **274**(5288): p. 782-4.

333. DiDonato, J.A., F. Mercurio, and M. Karin, *NF-kappaB and the link between inflammation and cancer.* Immunol Rev, 2012. **246**(1): p. 379-400.

334. Blaskewicz, C.D., J. Pudney, and D.J. Anderson, *Structure and function of intercellular junctions in human cervical and vaginal mucosal epithelia.* Biol Reprod, 2011. **85**(1): p. 97-104.

335. Ghosh, M., M. Rodriguez-Garcia, and C.R. Wira, *Immunobiology of genital tract trauma: endocrine regulation of HIV acquisition in women following sexual assault or genital tract mutilation.* Am J Reprod Immunol, 2013. **69 Suppl 1**: p. 51-60.

336. Mlisana, K., N. Naicker, L. Werner, L. Roberts, F. van Loggerenberg, C. Baxter, J.A. Passmore, A.C. Grobler, A.W. Sturm, C. Williamson, K. Ronacher, G. Walzl, and S.S. Abdool Karim, *Symptomatic vaginal discharge is a poor predictor of sexually transmitted infections and genital tract inflammation in high-risk women in South Africa.* J Infect Dis, 2012. **206**(1): p. 6-14.

337. Tighe, P.J., R.R. Ryder, I. Todd, and L.C. Fairclough, *ELISA in the multiplex era: potentials and pitfalls.* Proteomics Clin Appl, 2015. **9**(3-4): p. 406-22.

338. Liu, M., S. Guo, J.M. Hibbert, V. Jain, N. Singh, N.O. Wilson, and J.K. Stiles, *CXCL10/IP-10 in infectious diseases pathogenesis and potential therapeutic implications.* Cytokine Growth Factor Rev, 2011. **22**(3): p. 121-30.

339. Marques, R.E., R. Guabiraba, R.C. Russo, and M.M. Teixeira, *Targeting CCL5 in inflammation.* Expert Opin Ther Targets, 2013. **17**(12): p. 1439-60.

340. Choy, E. and S. Rose-John, *Interleukin-6 as a Multifunctional Regulator: Inflammation, Immune Response, and Fibrosis.* Journal of Scleroderma and Related Disorders, 2017. **2**(Suppl 2): p. S1-S5.

341. Sprague, A.H. and R.A. Khalil, *Inflammatory cytokines in vascular dysfunction and vascular disease.* Biochem Pharmacol, 2009. **78**(6): p. 539-52.

342. Manna, S.K. and G.T. Ramesh, *Interleukin-8 induces nuclear transcription factor-kappaB through a TRAF6-dependent pathway.* J Biol Chem, 2005. **280**(8): p. 7010-21.

343. Gumbi, P.P., N.N. Nkwanyana, A. Bere, W.A. Burgers, C.M. Gray, A.L. Williamson, M. Hoffman, D. Coetzee, L. Denny, and J.A. Passmore, *Impact of mucosal inflammation on cervical human immunodeficiency virus (HIV-1)-specific CD8 T-cell responses in the female genital tract during chronic HIV infection.* J Virol, 2008. **82**(17): p. 8529-36.

344. Cummins, J.E., L. Christensen, J.L. Lennox, T.J. Bush, Z. Wu, D. Malamud, T. Evans-Strickfaden, A. Siddig, A.M. Caliendo, C.E. Hart, and C.S. Dezzutti, *Mucosal innate immune factors in the female genital tract are associated with vaginal HIV-1 shedding independent of plasma viral load.* AIDS Res Hum Retroviruses, 2006. **22**(8): p. 788-95.

345. Sokol, C.L. and A.D. Luster, *The chemokine system in innate immunity.* Cold Spring Harb Perspect Biol, 2015. **7**(5).

346. Wira, C.R., J.V. Fahey, C.L. Sentman, P.A. Pioli, and L. Shen, *Innate and adaptive immunity in female genital tract: cellular responses and interactions.* Immunol Rev, 2005. **206**: p. 306-35.

347. Boyden, S., *The chemotactic effect of mixtures of antibody and antigen on polymorphonuclear leucocytes.* J Exp Med, 1962. **115**: p. 453-66.

348. Wu, J., A. Kumar-Kanojia, S. Hombach-Klonisch, T. Klonisch, and F. Lin, *A radial microfluidic platform for higher throughput chemotaxis studies with individual gradient control.* Lab Chip, 2018. **18**(24): p. 3855-3864.

349. Ren, X., D. Levin, and F. Lin, *Cell Migration Research Based on Organ-on-Chip-Related Approaches.* Micromachines (Basel), 2017. **8**(11).

350. Kashem, M.A., H. Li, L.R. Liu, B. Liang, R.W. Omange, F.A. Plummer, and M. Luo, *The Potential Role of FREM1 and Its Isoform TILRR in HIV-1 Acquisition through Mediating Inflammation.* International Journal of Molecular Sciences, 2021. **22**(15): p. 7825.

351. Apte, R.N. and E. Voronov, *Interleukin-1--a major pleiotropic cytokine in tumor-host interactions.* Semin Cancer Biol, 2002. **12**(4): p. 277-90.

352. Ansari, A.W., H. Heiken, D. Meyer-Olson, and R.E. Schmidt, *CCL2: a potential prognostic marker and target of anti-inflammatory strategy in HIV/AIDS pathogenesis.* Eur J Immunol, 2011. **41**(12): p. 3412-8.

353. Barqasho, B., P. Nowak, A. Tjernlund, S. Kinloch, L.E. Goh, F. Lampe, M. Fisher, J. Andersson, and A. Sonnerborg, *Kinetics of plasma cytokines and chemokines during primary HIV-1 infection and after analytical treatment interruption.* HIV Med, 2009. **10**(2): p. 94-102.

354. Weiss, L., A. Si-Mohamed, P. Giral, P. Castiel, A. Ledur, C. Blondin, M.D. Kazatchkine, and N. Haeffner-Cavaillon, *Plasma levels of monocyte chemoattractant protein-1 but not those of macrophage inhibitory protein-1alpha and RANTES correlate with virus load in human immunodeficiency virus infection.* J Infect Dis, 1997. **176**(6): p. 1621-4.

355. Mlambo, T., M. Tshabalala, T. Bandason, K. Mhandire, B. Mudenge, and L.S. Zijenah, *Correlation of High Interleukin 17A and Interleukin 6 Levels with High Virus Load Among Subtype C HIV-infected, Antiretroviral Therapy-naive Zimbabwean Patients: A Cross-sectional Study.* The Open AIDS Journal, 2019. **13**: p. 59-64.

356. Ansari, A.W., N. Bhatnagar, O. Dittrich-Breiholz, M. Kracht, R.E. Schmidt, and H. Heiken, *Host chemokine (C-C motif) ligand-2 (CCL2) is differentially regulated in HIV type 1 (HIV-1)-infected individuals.* Int Immunol, 2006. **18**(10): p. 1443-51.

357. Shebl, F.M., K. Yu, O. Landgren, J.J. Goedert, and C.S. Rabkin, *Increased levels of circulating cytokines with HIV-related immunosuppression.* AIDS Res Hum Retroviruses, 2012. **28**(8): p. 809-15.

358. Malherbe, G., H.C. Steel, S. Cassol, T. de Oliveira, C.J. Seebregts, R. Anderson, E. Cassol, and T.M. Rossouw, *Circulating biomarkers of immune activation distinguish viral suppression from nonsuppression in HAART-treated patients with advanced HIV-1 subtype C infection.* Mediators Inflamm, 2014. **2014**: p. 198413.

359. Del Valle, D.M., S. Kim-Schulze, H.H. Huang, N.D. Beckmann, S. Nirenberg, B. Wang, Y. Lavin, T.H. Swartz, D. Madduri, A. Stock, T.U. Marron, H. Xie, M. Patel, K. Tuballes, O. Van Oekelen, A. Rahman, P. Kovatch, J.A. Aberg, E. Schadt, S. Jagannath, M. Mazumdar, A.W. Charney, A. Firpo-Betancourt, D.R. Mendu, J. Jhang, D. Reich, K. Sigel, C. Cordon-Cardo, M. Feldmann, S. Parekh, M. Merad, and S. Gnjatic, *An inflammatory cytokine signature predicts COVID-19 severity and survival.* Nat Med, 2020. **26**(10): p. 1636-1643.

360. Wong, C.K., C.W. Lam, A.K. Wu, W.K. Ip, N.L. Lee, I.H. Chan, L.C. Lit, D.S. Hui, M.H. Chan, S.S. Chung, and J.J. Sung, *Plasma inflammatory cytokines and chemokines in severe acute respiratory syndrome.* Clin Exp Immunol, 2004. **136**(1): p. 95-103.

361. Mahallawi, W.H., O.F. Khabour, Q. Zhang, H.M. Makhdoum, and B.A. Suliman, *MERS-CoV infection in humans is associated with a pro-inflammatory Th1 and Th17 cytokine profile.* Cytokine, 2018. **104**: p. 8-13.

362. de Jong, M.D., C.P. Simmons, T.T. Thanh, V.M. Hien, G.J. Smith, T.N. Chau, D.M. Hoang, N.V. Chau, T.H. Khanh, V.C. Dong, P.T. Qui, B.V. Cam, Q. Ha do, Y. Guan, J.S. Peiris, N.T. Chinh, T.T. Hien, and J. Farrar, *Fatal outcome of human influenza A (H5N1) is associated with high viral load and hypercytokinemia.* Nat Med, 2006. **12**(10): p. 1203-7.

363. Huang, C., Y. Wang, X. Li, L. Ren, J. Zhao, Y. Hu, L. Zhang, G. Fan, J. Xu, X. Gu, Z. Cheng, T. Yu, J. Xia, Y. Wei, W. Wu, X. Xie, W. Yin, H. Li, M. Liu, Y. Xiao, H. Gao, L. Guo, J. Xie, G. Wang, R. Jiang, Z. Gao, Q. Jin, J. Wang, and B. Cao, *Clinical features of patients infected with 2019 novel coronavirus in Wuhan, China.* Lancet, 2020. **395**(10223): p. 497-506.

364. Min, C.K., S. Cheon, N.Y. Ha, K.M. Sohn, Y. Kim, A. Aigerim, H.M. Shin, J.Y. Choi, K.S. Inn, J.H. Kim, J.Y. Moon, M.S. Choi, N.H. Cho, and Y.S. Kim, *Comparative and kinetic analysis of viral shedding and immunological responses in MERS patients representing a broad spectrum of disease severity.* Sci Rep, 2016. **6**: p. 25359.

365. Voynow, J.A., S. Zheng, and A.B. Kummarapurugu, *Glycosaminoglycans as Multifunctional Anti-Elastase and Anti-Inflammatory Drugs in Cystic Fibrosis Lung Disease.* Front Pharmacol, 2020. **11**: p. 1011.

366. Lundh, A., *Tocilizumab in Patients Hospitalized with Covid-19 Pneumonia.* N Engl J Med, 2021. **384**(15): p. 1473.

367. Castelnovo, L., A. Tamburello, A. Lurati, E. Zaccara, M.G. Marrazza, M. Olivetti, N. Mumoli, D. Mastroiacovo, D. Colombo, E. Ricchiuti, P. Vigano, F. Paola, and A. Mazzone, *Anti-IL6 treatment of serious COVID-19 disease: A monocentric retrospective experience.* Medicine (Baltimore), 2021. **100**(1): p. e23582.

368. Buckley, L.F., G.F. Wohlford, C. Ting, A. Alahmed, B.W. Van Tassell, A. Abbate, J.W. Devlin, and P. Libby, *Role for Anti-Cytokine Therapies in Severe Coronavirus Disease 2019.* Crit Care Explor, 2020. **2**(8): p. e0178.

369. Deb, P., M.M.A. Molla, and K.M.S. Rahman, *An update to monoclonal antibody as therapeutic option against COVID-19.* Biosaf Health, 2021.

370. Bhattacharyya, S., *Inflammation During Virus Infection: Swings and Roundabouts*, in *Dynamics of Immune Activation in Viral Diseases*, P.V. Bramhachari, Editor. 2020, Springer: Singapore. p. 43-59.

371. Garcia, L.F., *Immune Response, Inflammation, and the Clinical Spectrum of COVID-19.* Front Immunol, 2020. **11**: p. 1441.

372. Di Caro, G., M. Carvello, S. Pesce, M. Erreni, F. Marchesi, J. Todoric, M. Sacchi, M. Montorsi, P. Allavena, and A. Spinelli, *Circulating Inflammatory Mediators as Potential Prognostic Markers of Human Colorectal Cancer.* PLoS One, 2016. **11**(2): p. e0148186.

373. Kashem, M.A., X. Ren, H. Li, B. Liang, L. Li, F. Lin, F. Plummer, and M. Luo, *TILRR Promotes Migration of Immune Cells Through Induction of Soluble Inflammatory Mediators.* Frontiers in Cell and Developmental Biology, 2020. **8**(563): p. 1-13.

374. Gonzalez, H., C. Hagerling, and Z. Werb, *Roles of the immune system in cancer: from tumor initiation to metastatic progression.* Genes Dev, 2018. **32**(19-20): p. 1267-1284.

375. Savant, S.S., S. Sriramkumar, and H.M. O'Hagan, *The Role of Inflammation and Inflammatory Mediators in the Development, Progression, Metastasis, and Chemoresistance of Epithelial Ovarian Cancer.* Cancers (Basel), 2018. **10**(8).

376. Chong, G.O., H.S. Han, S.D. Lee, and Y.H. Lee, *Improvement in RNA quantity and quality in cervico-vaginal cytology.* Virol J, 2020. **17**(1): p. 8.

377. McKinnon, L.R., S.M. Hughes, S.C. De Rosa, J.A. Martinson, J. Plants, K.E. Brady, P.P. Gumbi, D.J. Adams, L. Vojtech, C.G. Galloway, M. Fialkow, G. Lentz, D. Gao, Z. Shu, B. Nyanga, P. Izulla, J. Kimani, S. Kimwaki, A. Bere, Z. Moodie, A.L. Landay, J.A. Passmore, R. Kaul, R.M. Novak, M.J. McElrath, and F. Hladik, *Optimizing viable leukocyte sampling from the female genital tract for clinical trials: an international multi-site study.* PLoS One, 2014. **9**(1): p. e85675.

378. Arango, M.-T., P. Quintero-Ronderos, J. Castiblanco, and G. Montoya-Ortiz, *Cell culture and cell analysis*, in *Autoimmunity: From Bench to Bedside*, J.M. Anaya, et al., Editors. 2013: Bogota (Colombia). p. 741-754.
379. Arantes-Rodrigues, R., A. Colaco, R. Pinto-Leite, and P.A. Oliveira, *In vitro and in vivo experimental models as tools to investigate the efficacy of antineoplastic drugs on urinary bladder cancer.* Anticancer Res, 2013. **33**(4): p. 1273-96.
380. PromoCell. *Human primary cells and immortal cell lines: differences and advantages*. 2019 (Accessed on April 28, 2021); Available from: https://promocell.com/in-the-lab/human-primary-cells-and-immortal-cell-lines/.
381. Tang, C. *In vitro vs. In vivo: Is One Better?* (Accessed on April 28, 2021); Available from: https://www.uhnresearch.ca/news/vitro-vs-vivo-one-better.
382. Zhang, X.L., W. Pang, X.T. Hu, J.L. Li, Y.G. Yao, and Y.T. Zheng, *Experimental primates and non-human primate (NHP) models of human diseases in China: current status and progress.* Dongwuxue Yanjiu, 2014. **35**(6): p. 447-64.
383. Heijmans, C.M.C., N.G. de Groot, and R.E. Bontrop, *Comparative genetics of the major histocompatibility complex in humans and nonhuman primates.* Int J Immunogenet, 2020. **47**(3): p. 243-260.
384. Estes, J.D., S.W. Wong, and J.M. Brenchley, *Nonhuman primate models of human viral infections.* Nat Rev Immunol, 2018. **18**(6): p. 390-404.
385. Messaoudi, I., R. Estep, B. Robinson, and S.W. Wong, *Nonhuman primate models of human immunology.* Antioxid Redox Signal, 2011. **14**(2): p. 261-73.
386. Bloch, M., M. John, D. Smith, T.A. Rasmussen, and E. Wright, *Managing HIV-associated inflammation and ageing in the era of modern ART.* HIV Med, 2020. **21 Suppl 3**: p. 2-16.
387. Peterson, T.E. and J.V. Baker, *Assessing inflammation and its role in comorbidities among persons living with HIV.* Curr Opin Infect Dis, 2019. **32**(1): p. 8-15.
388. Sokoya, T., H.C. Steel, M. Nieuwoudt, and T.M. Rossouw, *HIV as a Cause of Immune Activation and Immunosenescence.* Mediators Inflamm, 2017. **2017**: p. 6825493.
389. Zicari, S., L. Sessa, N. Cotugno, A. Ruggiero, E. Morrocchi, C. Concato, S. Rocca, P. Zangari, E.C. Manno, and P. Palma, *Immune Activation, Inflammation, and Non-AIDS Co-Morbidities in HIV-Infected Patients under Long-Term ART.* Viruses, 2019. **11**(3).

390. Chan, M.C., C.Y. Cheung, W.H. Chui, S.W. Tsao, J.M. Nicholls, Y.O. Chan, R.W. Chan, H.T. Long, L.L. Poon, Y. Guan, and J.S. Peiris, *Proinflammatory cytokine responses induced by influenza A (H5N1) viruses in primary human alveolar and bronchial epithelial cells.* Respir Res, 2005. **6**: p. 135.

391. Smits, S.L., A. de Lang, J.M. van den Brand, L.M. Leijten, I.W.F. van, M.J. Eijkemans, G. van Amerongen, T. Kuiken, A.C. Andeweg, A.D. Osterhaus, and B.L. Haagmans, *Exacerbated innate host response to SARS-CoV in aged non-human primates.* PLoS Pathog, 2010. **6**(2): p. e1000756.

392. Tisoncik, J.R., M.J. Korth, C.P. Simmons, J. Farrar, T.R. Martin, and M.G. Katze, *Into the eye of the cytokine storm.* Microbiol Mol Biol Rev, 2012. **76**(1): p. 16-32.

393. Kircheis, R., E. Haasbach, D. Lueftenegger, W.T. Heyken, M. Ocker, and O. Planz, *NF-kappaB Pathway as a Potential Target for Treatment of Critical Stage COVID-19 Patients.* Front Immunol, 2020. **11**: p. 598444.

394. Ruland, J., G.S. Duncan, A. Elia, I. del Barco Barrantes, L. Nguyen, S. Plyte, D.G. Millar, D. Bouchard, A. Wakeham, P.S. Ohashi, and T.W. Mak, *Bcl10 is a positive regulator of antigen receptor-induced activation of NF-kappaB and neural tube closure.* Cell, 2001. **104**(1): p. 33-42.

395. Bertin, J., L. Wang, Y. Guo, M.D. Jacobson, J.L. Poyet, S.M. Srinivasula, S. Merriam, P.S. DiStefano, and E.S. Alnemri, *CARD11 and CARD14 are novel caspase recruitment domain (CARD)/membrane-associated guanylate kinase (MAGUK) family members that interact with BCL10 and activate NF-kappa B.* J Biol Chem, 2001. **276**(15): p. 11877-82.

396. Donadelli, R., M. Abbate, C. Zanchi, D. Corna, S. Tomasoni, A. Benigni, G. Remuzzi, and C. Zoja, *Protein traffic activates NF-kB gene signaling and promotes MCP-1-dependent interstitial inflammation.* Am J Kidney Dis, 2000. **36**(6): p. 1226-41.

397. Huang, C.Y., Y.C. Fong, C.Y. Lee, M.Y. Chen, H.C. Tsai, H.C. Hsu, and C.H. Tang, *CCL5 increases lung cancer migration via PI3K, Akt and NF-kappaB pathways.* Biochem Pharmacol, 2009. **77**(5): p. 794-803.

398. Adli, M., E. Merkhofer, P. Cogswell, and A.S. Baldwin, *IKKalpha and IKKbeta each function to regulate NF-kappaB activation in the TNF-induced/canonical pathway.* PLoS One, 2010. **5**(2): p. e9428.

399. Hacker, H. and M. Karin, *Regulation and function of IKK and IKK-related kinases.* Sci STKE, 2006. **2006**(357): p. re13.

400. Stanley, E.R., K.L. Berg, D.B. Einstein, P.S. Lee, F.J. Pixley, Y. Wang, and Y.G. Yeung, *Biology and action of colony--stimulating factor-1.* Mol Reprod Dev, 1997. **46**(1): p. 4-10.

401. Ushach, I. and A. Zlotnik, *Biological role of granulocyte macrophage colony-stimulating factor (GM-CSF) and macrophage colony-stimulating factor (M-CSF) on cells of the myeloid lineage.* J Leukoc Biol, 2016. **100**(3): p. 481-9.

402. Shi, Y., C.H. Liu, A.I. Roberts, J. Das, G. Xu, G. Ren, Y. Zhang, L. Zhang, Z.R. Yuan, H.S. Tan, G. Das, and S. Devadas, *Granulocyte-macrophage colony-stimulating factor (GM-CSF) and T-cell responses: what we do and don't know.* Cell Res, 2006. **16**(2): p. 126-33.

403. Mehta, H.M., M. Malandra, and S.J. Corey, *G-CSF and GM-CSF in Neutropenia.* J Immunol, 2015. **195**(4): p. 1341-9.

404. Xu, S., M. Hoglund, L. Hakansson, and P. Venge, *Granulocyte colony-stimulating factor (G-CSF) induces the production of cytokines in vivo.* Br J Haematol, 2000. **108**(4): p. 848-53.

405. Harada, A., N. Sekido, T. Akahoshi, T. Wada, N. Mukaida, and K. Matsushima, *Essential involvement of interleukin-8 (IL-8) in acute inflammation.* J Leukoc Biol, 1994. **56**(5): p. 559-64.

406. Di Paolo, N.C. and D.M. Shayakhmetov, *Interleukin 1alpha and the inflammatory process.* Nat Immunol, 2016. **17**(8): p. 906-13.

407. Borthwick, L.A., *The IL-1 cytokine family and its role in inflammation and fibrosis in the lung.* Semin Immunopathol, 2016. **38**(4): p. 517-34.

408. Liu, G., Y.J. Park, and E. Abraham, *Interleukin-1 receptor-associated kinase (IRAK) -1-mediated NF-kappaB activation requires cytosolic and nuclear activity.* FASEB J, 2008. **22**(7): p. 2285-96.

409. Keating, S.E., G.M. Maloney, E.M. Moran, and A.G. Bowie, *IRAK-2 participates in multiple toll-like receptor signaling pathways to NFkappaB via activation of TRAF6 ubiquitination.* J Biol Chem, 2007. **282**(46): p. 33435-43.

410. Kingeter, L.M. and B.C. Schaefer, *Malt1 and cIAP2-Malt1 as effectors of NF-kappaB activation: kissing cousins or distant relatives?* Cell Signal, 2010. **22**(1): p. 9-22.

411. Warner, N. and G. Nunez, *MyD88: a critical adaptor protein in innate immunity signal transduction.* J Immunol, 2013. **190**(1): p. 3-4.

412. Sun, S.C., *Non-canonical NF-kappaB signaling pathway.* Cell Res, 2011. **21**(1): p. 71-85.

413. Verma, I.M., J.K. Stevenson, E.M. Schwarz, D. Van Antwerp, and S. Miyamoto, *Rel/NF-kappa B/I kappa B family: intimate tales of association and dissociation.* Genes Dev, 1995. **9**(22): p. 2723-35.

414. Jacobs, M.D. and S.C. Harrison, *Structure of an IkappaBalpha/NF-kappaB complex.* Cell, 1998. **95**(6): p. 749-58.

415. Li, S. and J.M. Sedivy, *Raf-1 protein kinase activates the NF-kappa B transcription factor by dissociating the cytoplasmic NF-kappa B-I kappa B complex.* Proc Natl Acad Sci U S A, 1993. **90**(20): p. 9247-51.

416. Pomerantz, J.L. and D. Baltimore, *NF-kappaB activation by a signaling complex containing TRAF2, TANK and TBK1, a novel IKK-related kinase.* EMBO J, 1999. **18**(23): p. 6694-704.

417. Funami, K., M. Sasai, H. Oshiumi, T. Seya, and M. Matsumoto, *Homo-oligomerization is essential for Toll/interleukin-1 receptor domain-containing adaptor molecule-1-mediated NF-kappaB and interferon regulatory factor-3 activation.* J Biol Chem, 2008. **283**(26): p. 18283-91.

418. Alexopoulou, L., A.C. Holt, R. Medzhitov, and R.A. Flavell, *Recognition of double-stranded RNA and activation of NF-kappaB by Toll-like receptor 3.* Nature, 2001. **413**(6857): p. 732-8.

419. Yu, M. and S.J. Levine, *Toll-like receptor, RIG-I-like receptors and the NLRP3 inflammasome: key modulators of innate immune responses to double-stranded RNA viruses.* Cytokine Growth Factor Rev, 2011. **22**(2): p. 63-72.

420. Barton, G.M. and J.C. Kagan, *A cell biological view of Toll-like receptor function: regulation through compartmentalization.* Nat Rev Immunol, 2009. **9**(8): p. 535-42.

421. O'Neill, L.A., D. Golenbock, and A.G. Bowie, *The history of Toll-like receptors - redefining innate immunity.* Nat Rev Immunol, 2013. **13**(6): p. 453-60.

422. Schutze, S., K. Wiegmann, T. Machleidt, and M. Kronke, *TNF-induced activation of NF-kappa B.* Immunobiology, 1995. **193**(2-4): p. 193-203.

423. Zhou, A., S. Scoggin, R.B. Gaynor, and N.S. Williams, *Identification of NF-kappa B-regulated genes induced by TNFalpha utilizing expression profiling and RNA interference.* Oncogene, 2003. **22**(13): p. 2054-64.

424. Gupta, S., R. Bi, C. Kim, S. Chiplunkar, L. Yel, and S. Gollapudi, *Role of NF-kappaB signaling pathway in increased tumor necrosis factor-alpha-induced apoptosis of lymphocytes in aged humans.* Cell Death Differ, 2005. **12**(2): p. 177-83.

425. Zhang, L., K. Blackwell, A. Altaeva, Z. Shi, and H. Habelhah, *TRAF2 phosphorylation promotes NF-kappaB-dependent gene expression and inhibits oxidative stress-induced cell death.* Mol Biol Cell, 2011. **22**(1): p. 128-40.

426. Ni, C.Z., K. Welsh, E. Leo, C.K. Chiou, H. Wu, J.C. Reed, and K.R. Ely, *Molecular basis for CD40 signaling mediated by TRAF3.* Proc Natl Acad Sci U S A, 2000. **97**(19): p. 10395-9.

427. Konno, H., T. Yamamoto, K. Yamazaki, J. Gohda, T. Akiyama, K. Semba, H. Goto, A. Kato, T. Yujiri, T. Imai, Y. Kawaguchi, B. Su, O. Takeuchi, S. Akira, Y. Tsunetsugu-Yokota, and J. Inoue, *TRAF6 establishes innate immune responses by activating NF-kappaB and IRF7 upon sensing cytosolic viral RNA and DNA.* PLoS One, 2009. **4**(5): p. e5674.

7 CHAPTER 7: APPENDICES

7.1 APPENDIX A: GENERAL MATERIALS/REAGENTS

A. Cell lines and transfection reagents

Cell lines: HeLa (National Institute of Health AIDS [NIH AIDS] reagent program, USA; Catalog# 153) and VK2 E6/E7 (ATCC, Catalog# CRL2616) cells. These cell lines were used to overexpress TILRR.

Complete growth medium for HeLa cells: Dulbecco's Modified Eagle's Medium (DMEM) (Sigma-Aldrich, D5796) supplemented with 10% FBS (fetal bovine serum; Gibco, Catalog# 12483-020), 1 mM sodium pyruvate (Gibco, Catalog# 11360070), and 1% Antibiotic-Antimycotic (Gibco, Catalog# 15240062).

Complete growth medium for VK2/E6E7 cells: Keratinocyte-SFM (1X) growth medium (Gibco, Catalog# 10724-011) supplemented with human recombinant EGF (Epidermal Growth factor, 0.1 ng/ml), and BPE (Bovine Pituitary Extracts, 50 µg/ml) (Gibco, Catalog# 37000-015), 0.4 mM $CaCl_2$ (Sigma Aldrich, Catalog# C5670) and 1% Penicillin-Streptomycin solution (Gibco, Catalog# 15140-122).

Neutralization medium for VK2/E6E7 cells: DMEM Nutrient mixture F-12 Ham (Sigma-Aldrich, Catalog# D8437) supplemented with 10% FBS (Gibco, Catalog# 12483-020), and 1% Penicillin-Streptomycin solution (Gibco, Catalog# 15140-122). This medium was used to neutralize the cell dissociation reagents (0.25% Trypsin-EDTA).

Cell-dissociation reagents: Both HeLa and VK2/E6E7 adherent cells were dissociated from culture flasks/plates using 0.25% Trypsin-EDTA solution (Gibco, Catalog# 25200056).

Phosphate Buffered Saline (PBS): To prepare 1L of 1X PBS, added 8 g of NaCl, 0.2 g of KCl, 1.44 g of Na_2HPO_4, and 0.24 g of KH_2PO_4 to 800 ml of distilled water. Adjusted pH to 7.2 with HCl, and then added distilled water to a total volume of 1 L. Heat sterilized.

Freezing media: Complete growth medium supplemented with 5% (v/v) dimethyl sulfoxide (DMSO) (Sigma-Aldrich; Catalog# D2650).

Live/Dead cell counting reagent: Trypan Blue solution, 0.4% (Gibco, Catalog# 15250061) was used for counting cells by hemocytometer and automated cell counter (Invitrogen).

Plasmid purification: EndoFree Plasmid Maxi kit (Qiagen; Catalog# 12362) was used to purify TILRR-tagged plasmid and empty-vector plasmid DNA from bacterial culture.

Transfection reagents: HeLa and VK2/E6E7 cells were transfected using Opti-MEM^{TM} I Reduced Serum Medium (Gibco; Catalog# 31985070) and EndofectinMax transfection reagent (GeneCopoeia; Catalog# EFM1004-01).

B. mRNA expression analysis reagents

RNA isolation: Kits used for RNA isolations included QIAshredder (Qiagen, Catalog# 79654), RNeasy Mini Kit (Qiagen, Catalog# 74104), RNase-Free DNase Set (Qiagen, Catalog# 79254), RNeasy MinElute Cleanup kit (Qiagen, Catalog# 74204), and RNase-Free water (Qiagen, Catalog# 129112).

RNA quality analysis: RNA 6000 Nano LabChip$^{(R)}$ kit (Agilent Technologies, Catalog# 5067-1511).

Complementary DNA (cDNA) synthesis: Purified RNA was converted to cDNA using RT^2 first strand kit (Qiagen, Catalog# 330404).

RT^2-qPCR primer assay: mRNA expression of genes was analyzed using several primers, including TILRR (Qiagen, Catalog# PPH11469A-200), CCL5/RANTES (Qiagen, Catalog# PPH00703B-200), CXCL8/IL-8 (Qiagen, Catalog# PPH00568A-200), IL-6 (Qiagen, Catalog# PPH00560C-200), and TNFα (Qiagen, Catalog# PPH00341F-200), accompanied by RT^2 SYBR$^{(R)}$ Green ROX qPCR Mastermix (Qiagen, Catalog# 330523).

RT^2 Profiler PCR array: mRNA expression of 84 genes in NF-κB signal transduction pathway was evaluated with human RT^2 profiler qPCR array (Qiagen, Catalog# PAHS-025Z).

Other materials: Applied Biosystems^{TM} MicroAmp^{TM} Optical 96-well Reaction Plate with Barcode (ThermoFisher Scientific, Catalog# 4306737) and Applied Biosystems^{TM} MicroAmp^{TM} Optical Adhesive Film (ThermoFisher Scientific, Catalog# 4360954).

C. Confocal microscopy staining reagents and buffers

Cell fixation reagent: 4% paraformaldehyde. 2.8 ml of 20X Paraformaldehyde (Electron Microscopy Services, Catalog# 15713-S) in 11.2 ml of 1X PBS (pH 7.2) to prepare for 14 ml, 4% solution.

Permeabilization solution: 0.1% TritonX-100 in 1X PBS (pH 7.2). Ten microliter of TritonX-100 (Sigma-Aldrich, Catalog# X100) was added to 9.99 ml of 1X PBS (pH 7.2) to make 10 ml solution.

Wash buffer: 1X PBS (pH 7.2) used as wash buffer and prepared as **section 7.1 (A).**

3% BSA: 0.38 g of BSA powder (Sigma-Aldrich, Catalog# A9418) in 12.5 ml 1X PBS (pH 7.2) for 12.5 ml solution.

0.1 % BSA: 0.33 ml of 3% BSA solution was added to 9.67 ml of 1X PBS (pH 7.2) for 10 ml solution.

Blocking buffer: 3% BSA in 1X PBS containing 0.1% TritonX-100 was used as blocking buffer.

0.1% BSA in 1X PBS+0.1% TritonX-100 for antibody dilution: 8µl of TritonX-100 was added to 7.992 ml of 0.1% BSA to make 8 ml solution.

1 X PBS-T blocking buffer (1X PBS+0.05% TritonX-100+1.5% BSA) for wash: 25 µl of TritonX-100 was added to 49.975 ml of 1.5% BSA in PBS to make 50 ml solution.

D. Flow Cytometry staining reagents and kits

FACS Wash buffer: 2% FBS (heat-inactivated) in 1X PBS (pH 7.2). This buffer was used to wash the cells before and after staining for flow cytometry analysis.

3% BSA solution: Prepared as described **in section 7.1 (C).**

Perm/Wash^{TM} buffer: The working solution (1X) was made from a commercial 10X stock solution (BD Biosciences, Catalog# 554714). For 10 ml, added 1 ml of 10X perm/wash buffer to 9 ml of MilliQ water.

Cell Fixation buffer: Prepared 1X cell fixation buffer using 20X paraformaldehyde solution (Electron Microscopy Services, Catalog# 15713-S). For 10 ml 1X buffer, added 1 ml of 20X paraformaldehyde solution to 9 ml of 1X PBS (pH 7.2).

E. Western Blot analysis reagents, buffers, and kits

Sample lysis and extraction buffer: RIPA lysis buffer (1X) (ThermoFisher Scientific, Catalog# 89900) containing 25 mM Tris-HCl (pH 7.6), 150 mM NaCl, 1% sodium deoxycholate, and 0.1% SDS was used to prepare human cell lysates.

LDS sample loading buffer and Reducing agent: NuPAGE LDS sample buffer (4X) (ThermoFisher Scientific, Catalog# NP0008) containing lithium dodecyl sulfate (pH 8.4), Coomassie G250, and Phenol Red, and NuPAGE Reducing agent (10X) (ThermoFisher Scientific, Catalog# NP0009) containing 500 mM dithiothreitol (DTT) were used to prepare the sample. For a 10µl sample, added 2.5 µl of 4X LDS buffer and 1 µl of 10X reducing agent.

PBS (pH 7.2): The buffer was prepared as described in **section 7.1 (A).**

Wash buffer (PBS-T): Prepared by adding 1X PBS (pH 7.2) and 0.1% Tween 20 (Sigma-Aldrich, Catalog# P9416). One milliliter of Tween 20 was added to 999 ml of 1X PBS to make 1 L PBS-T.

Blocking buffer: 1X PBS-T with 5% w/v non-fat dry milk (Difco^{TM} Skim Milk, BD Biosciences, Catalog# 232100). For 100 ml buffer, added 5 g Difco Skim milk powder to 100 ml 1X PBS-T and mixed well.

Antibody diluents: 1X PBS-T containing 0.5% skim milk as a primary antibody diluent, and 1X PBS-T containing 0.25% skim milk as a secondary antibody diluent.

Running buffer: 20X NuPAGE MES SDS buffer (ThermoFisher Scientific, Catalog# NP0002) containing 50 mM MES, 50 mM Tris Base, 0.1% SDS, and 1 mM EDTA, pH 7.3, and NuPAGE Antioxidant (ThermoFisher Scientific, Catalog# NP0005). 50 ml of 20x MES SDS buffer in 950

ml of MilliQ water for 1L, 1X MES SDS buffer for an outer tank of Mini-cell gel tank (Invitrogen). 1X MES SDS buffer (400ml) containing 1 ml of NuPAGE antioxidant for inner gel tank.

Infrared dye-labeled secondary antibody: IRDye(R) 800CW goat anti-mouse IgG secondary antibody (Li-COR, Catalog# P/N: 926-32210). Reconstituted with 500 µl double distilled water (ddH_2O), and set aside for 30 min at room temperature before being used.

Protein marker: Spectra™ Multicolor Broad Range Protein Ladder (ThermoFisher Scientific, Catalog# 26634), and Odyssey(R) One-color protein molecular weight marker (LI-COR, P/N: 928-40000).

Other materials and reagents: NuPAGE 4-12% Bis-Tris 1.0 mm x 10 well gel (ThermoFisher Scientific, Catalog# NP0321BOX), iBlot gel transfer nitrocellulose mini stacks (ThermoFisher Scientific, Catalog# IB301002), Pierce ECL Western blotting substrate (ThermoFisher Scientific, Catalog# 32209), Restore™ PLUS Western blot stripping buffer (ThermoFisher Scientific, Catalog# 46428), ultrapure water, 50% isopropanol (Fisher Scientific, Catalog# A464-4), and 100% Methylene Chloride (Fisher Scientific, Catalog# D151-1).

F. Bio-Plex Magnetic multiplex bead array reagents

Bead coupling kit: Primary/capture antibodies were used to analyze selected cytokines/chemokines. The antibodies were coupled with magnetic beads using a Bio-Plex™ Amine Coupling kit (BioRad, Catalog# 171406001). This kit provided sufficient components to perform 30 coupling reactions including bead wash buffer, bead activation buffer, PBS buffer, blocking buffer, storage buffer, and staining buffer.

Magnetic beads: Multiple Bio-Plex Pro magnetic COOH beads were used to couple primary antibodies for the development of custom multiplex assay. Each magnetic COOH bead has unique fluorescent spectrum to distinguish from others. Thirteen beads are: 26 (catalog# MC10026-01), 28 (catalog# MC10028-01), 29 (catalog# MC10029-01), 34 (catalog# MC10034-01), 37 (catalog# MC10037-01), 43 (catalog# MC10043-01), 46 (catalog# MC10046-01), 52 (catalog# MC10052-01), 53 (catalog# MC10053-01), 55 (catalog# MC10055-01), 62 (catalog# MC10062-01), 64 (catalog# MC10064-01) and 65 (catalog# MC10065-01) for soluble cytokines/chemokines measurement. In addition, magnetic COOH beads, including 34 (catalog# MC10034-01), 36 (catalog# MC10036-01), and 64 (catalog# MC10064-01) were used for the plasma TILRR detection assay. One milliliter of each supplied vial contains 1.25×10^7 beads that were good to perform 10 coupling reactions. All beads were purchased from BioRad (Ontario, Canada).

Other reagents used for amine coupling: EDAC (1-ethyl-3-[3-dimethylaminopropyl] carbodiimide hydrochloride) (Invitrogen, Catalog# E2247) and Sulfo-NHS (N-hydroxysulfosuccinimide) (Thermo Scientific, Catalog# 24510).

Bio-Plex assay kit: Assays for cytokines/chemokines measurement were done using Bio-Plex Pro™ Reagent kit III with Flat Bottom Plate (Bio-Rad, Catalog# 171-304070M). The kit was provided assay buffer, standard diluent, sample diluent, detection antibody diluent, wash buffer, streptavidin-PE, flat bottom plate, and sealing tape.

Standards for the cytokines/chemokines assay: Bio-Plex Pro™ Human Cytokine Standards Group I 27-plex (BioRad, Catalog# 171D50001) used for cytokines/chemokines assay.

Primary/capture antibody for TILRR: In-house developed mouse monoclonal anti-FREM1 IgG abs (F237G1, F237G3, and F218G4).

Detection antibody and biotinylation used for plasma TILRR detection: In-house developed mouse monoclonal anti-FREM1 IgG ab (F237G12). Biotinylation of detection antibody was conducted by using an Apex antibody labeling kit (Invitrogen, Catalog# A10495).

Standards for the TILRR detection assay: In-house developed custom recombinant FREM1 spD protein (Lab ID# F-5) was used as standard.

Standard and sample diluents for TILRR assay: PBS pH 7.2 containing 2 mM EDTA, 150 mM NaCl, and 1% IGEPAL$^{(R)}$ CA-630 (Sigma-Aldrich, Catalog# I8896).

Other accessories used: Bio-Plex Pro^{TM} Flat bottom plate (BioRad, Catalog# 171025001), and streptavidin-PE conjugate (100x) (BioRad, Catalog# 171304501).

G. Transwell cell migration assay reagents

Cells and culture medium: THP-1 (ATCC) (NIH, Catalog# 9942), and MOLT-4 (NIH, Catalog# 175) were used for *in vitro* migration assay. RPMI 1640 growth medium (Sigma-Aldrich, Catalog# R0883) supplemented with 10% fetal bovine serum (FBS) (Giboco, Catalog# 12483), 2 mM GlutaMax-I (Gibco, Catalog# 35050-061), 10 mM HEPES (Gibco, Catalog# 15630-080), 1 mM sodium pyruvate (Gibco, Catalog# 11360070), and 1% Pen-Strep (Gibco, Catalog# 15140-122) was used. For THP-1 cells, 0.05 mM 2-Mercaptoethanol (Sigma-Aldrich, Catalog# M3148) was also added.

Medium used for migration assay: RPMI 1640 (Sigma-Aldrich, Catalog# R0883) supplemented with 2 mM GlutaMax-I (Gibco, Catalog# 35050-061), 10 mM HEPES (Gibco,

Catalog# 15630-080), 1 mM sodium pyruvate (Gibco, Catalog# 11360070) and 1% BSA (Sigma-Aldrich, Catalog# A9418-10G).

Chemoattractants diluents: Dulbecco's Modified Eagle's Medium (DMEM) (Sigma-Aldrich, D5796) supplemented with 1 mM sodium pyruvate (Gibco, Catalog# 11360070).

Stromal dermal factor 1 alpha (SDF-1α) or CXCL12: Used as a positive control for MOLT-4 T-cells. CXCL12 commercially available as a lyophilized powder (Sigma-Aldrich; Catalog# SRP3276-10UG) which was reconstituted by adding 50 µl molecular biology grade water and further diluted with 950 µl of 1X PBS (pH 7.2) containing 0.1% BSA to obtain 10 µg/ml stock solution. The working solution of desired concentration was made by diluting with DMEM media without FBS and Antibiotic-Antimycotic.

Monocyte chemoattractant protein 1 (MCP-1) or CCL2: Used as a positive control for THP-1 cells. CCL2 commercially available as a lyophilized powder (Sigma-Aldrich; Catalog# SRP3109-20UG) which was reconstituted by adding 50 µl molecular biology grade water as described for SDF-1α above (final conc., obtained 20 µg/ml stock solution). The working solution was prepared by a similar protocol as described for SDF-1α.

Other accessories: 24-well polycarbonated membrane 5µm pore size transwell plate (Corning, Catalog# CLS3421).

H. Microfluidic device cell migration assay reagents

Polydimethylsiloxane (PDMS) (Sylgard 184, Dow Corning, Manufacturer SKU# 2065622)

Rat-tail collagen type I (Corning, Catalog# 354236)

Fluorescein isothiocyanate (FITC)-dextran (Sigma-Aldrich, Catalog# FD10S)

Silicone oil (Alfa Aesar, Tewksbury, USA, Catalog# A12728-22)

I. Antibody cross-linking reagents and buffers

PBS (pH 7.2): This buffer was prepared as described in **section 7.1 (A).**

Cross-linking buffer: 0.2 M Triethanolamine (Sigma-Aldrich, Catalog# 90279). For a 100 ml buffer, added 3.04 ml Triethanolamine to 96.96 ml PBS (pH 7.2) and then adjusted pH to 8.2.

Cross-linking reagent: Dimethyl pimelimidate dihydrochloride (DMP; Sigma-Aldrich, Catalog# D8388) was used at 25 mM concentration in 0.2 M triethanolamine pH 8.2 (cross-linking buffer). Added 6.5 mg DMP powder into 1ml of 0.2 M triethanolamine.

Blocking buffer: 0.1 M Ethanolamine (Sigma-Aldrich, Catalog# E9508). To prepare 100 ml buffer, added 602.41µl Ethanolamine to 99.40 ml PBS (pH 7.2) and then adjusted pH to 8.2.

Binding buffer: 0.1 M Sodium phosphate buffer (pH 8.0).

Antibody diluents: Desired concentration of anti-FREM1 IgG mAb was diluted in binding buffer.

Elution buffer: 0.1 M Glycine-HCl (pH 2.5) was applied to elute unlinked antibodies.

J. Affinity purification reagents and buffers

Sample diluent: PBS (pH 7.2) supplemented with 1 mM EDTA and 10 µl/ml protease inhibitor cocktail (Halt protease inhibitor single-use cocktail-100x; ThermoFisher Scientific, Catalog# 78430) was added to the buffer just before the use.

Wash buffer: Prepared by mixing 10mM Tris HCl (pH 8.0), 1mM EDTA, 150mM NaCl, 1% TritonX-100, and Nuclease free water. Adjusted pH 7.4 by HCl. A protease inhibitor cocktail (10

µl in 1 ml buffer) (Halt protease inhibitor single-use cocktail-100x; ThermoFisher Scientific, Catalog# 78430) was added to the buffer just before the use.

Elution buffer: 0.1 M Glycine-HCl (pH 2.5) was applied to elute target protein from bead-antibody-protein complex. A protease inhibitor cocktail (10 µl in 1 ml buffer) was added to the elution buffer.

Neutralization buffer: 1M Tris HCl (pH 8.0).

Bead regeneration buffer: PBS (pH 7.2) containing 5 mM EDTA, and 0.02% Sodium azide. A protease inhibitor cocktail (10 µl in 1 ml buffer) was added to the buffer just before the use.

K. Protein concentration and buffer exchange

Protein centrifugal filter: Amicon$^{(R)}$ Ultra-2 Centrifugal filter with nominal molecular weight limit (NMWL) of 10 K (Millipore, Catalog# UFC201024) used for concentrating eluted protein volume.

Exchange buffer: PBS (pH 7.2) containing 1 mM EDTA, 154 mM NaCl, and protease inhibitor cocktail (10 µl in 1 ml buffer) (ThermoFisher Scientific, Catalog# 78430).

L. Bicinchoninic Acid (BCA) protein assay reagents

Protein standard: Bovine serum albumin (BSA) ampoule provided in Pierce BCA assay kit.

Standard and sample diluents: PBS (pH 7.2) containing 1 mM EDTA, 154 mM NaCl, and protease inhibitor cocktail (10 µl in 1 ml buffer).

Pierce^{TM} BCA protein assay kit (ThermoFisher Scientific, Catalog# 23227).

M. Coomassie staining and Gel drying

Coomassie stain: BioSafe™ Coomassie stain (Bio-Rad, Catalog# 1610786) used for staining NuPAGE Bis-Tris 4-12% gel.

Gel drying kit: DryEase™ Mini-Gel Drying system (Invitrogen, Catalog# NI2387).

7.2 APPENDIX B: SUPPLEMENTARY FIGURES

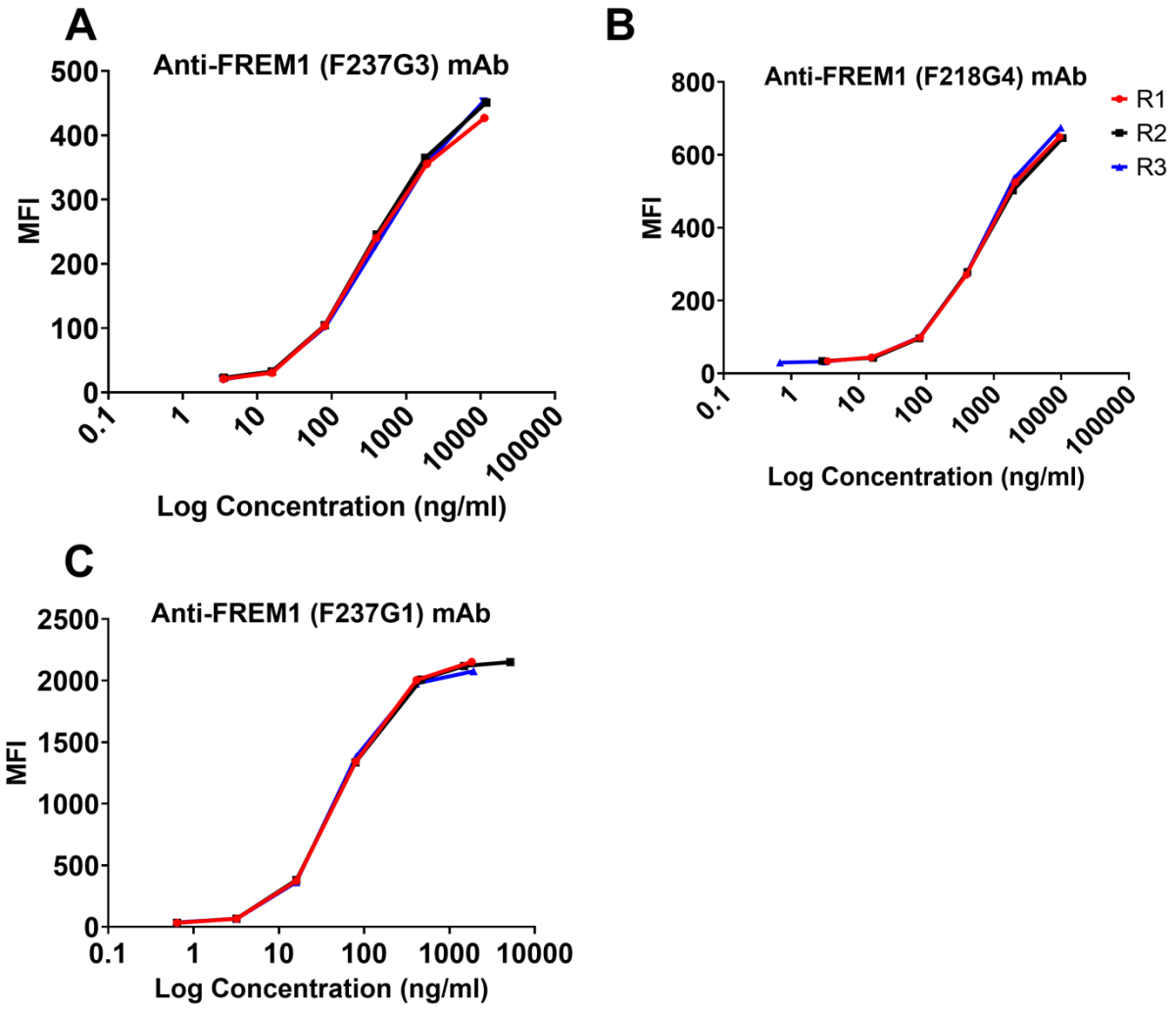

Appendix Figure B7.1: Standard curves generated by Bio-Plex multiplex magnetic bead array using recombinant FREM1 protein and anti-FREM1 mAbs. rFREM1 spD protein was diluted into 5-fold with concentration ranges from 10000ng/ml (S1) to 0.64 ng/ml (S7). Standard curves were generated with three anti-FREM1 mAbs, such as F237G3 (A), F218G4 (B), and F237G1 (C) that coupled with three different fluorescent spectrum beads. As a detection antibody, custom biotinylated anti-FREM1 (F237G12) mAb was used. MFI value for each antibody was graphed against the corresponding observed concentration of each point of rFREM1 spD protein (S1 to S7) where bead recovery ranges were maintained 70-130. Each line represents one replicate. A total of three independent experiments were conducted for each antibody (all three antibodies were tested together as a 3-plex). MFI, mean fluorescent intensity; R, replicate; mAb, monoclonal antibody.

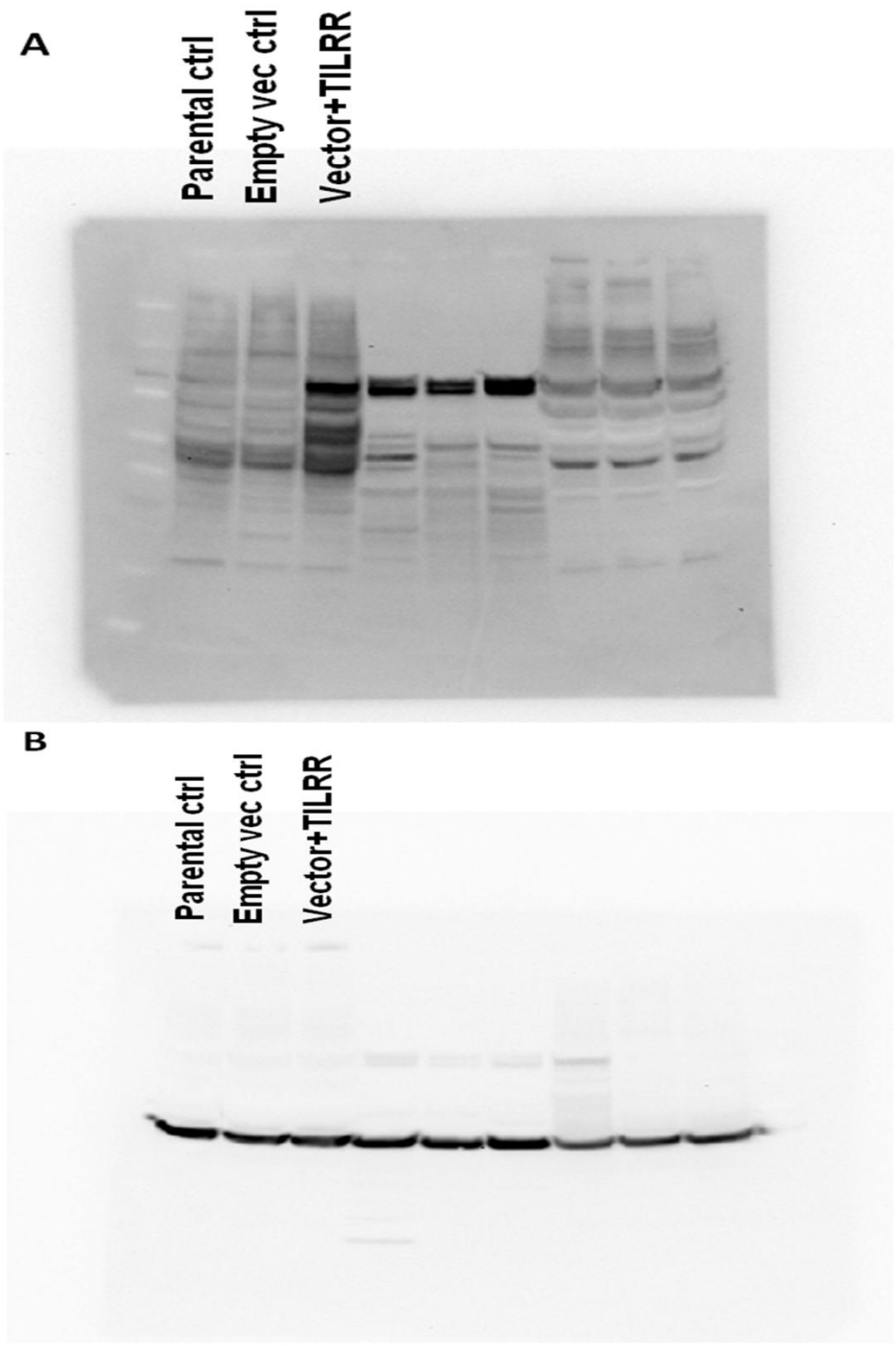

Appendix Figure B7.2: Full-length original Western blot image of TILRR protein confirmation. (A) Western blots confirmation of TILRR overexpression in HeLa cells compared to empty vector and parental controls. (**B**) GAPDH control expression for the same HeLa samples mentioned in figure A. Unlabelled columns are not related in this study.

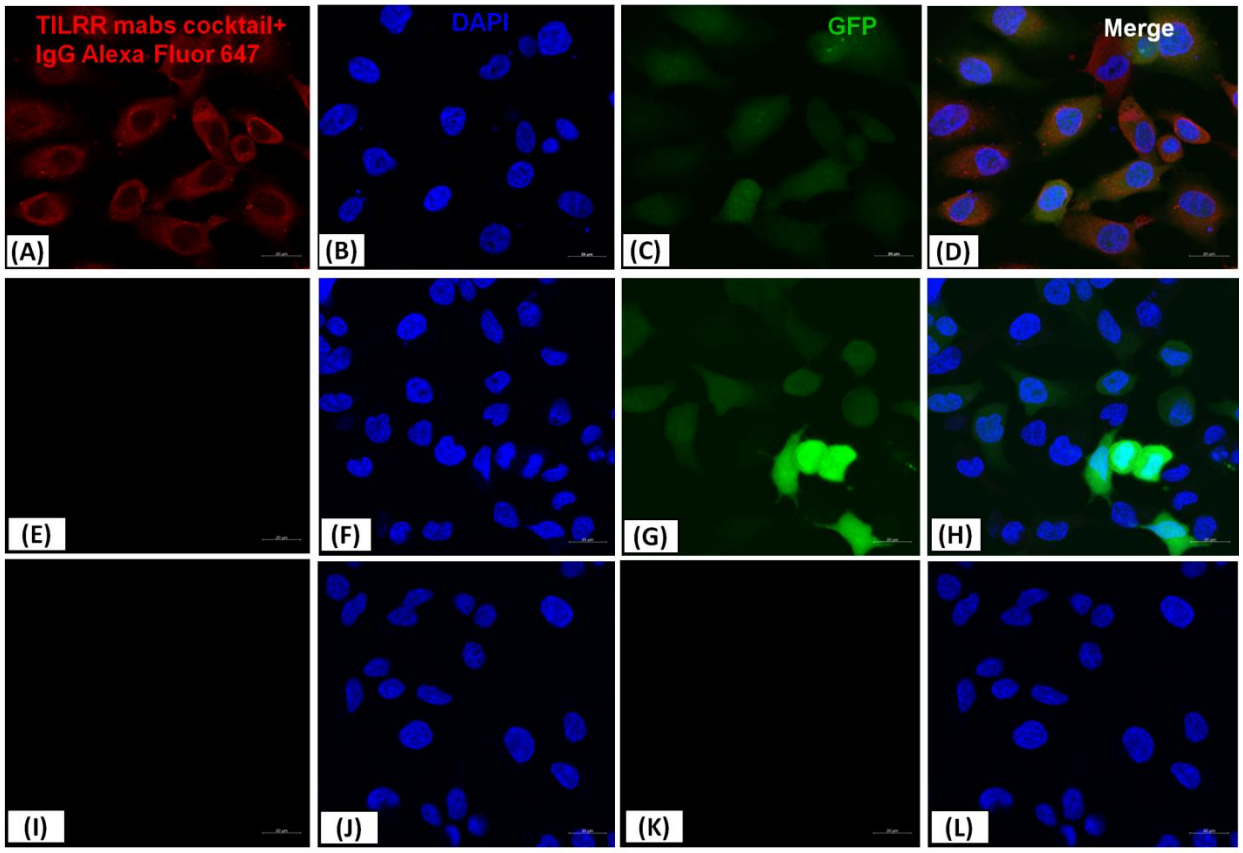

Appendix Figure B7.3: Overexpressed TILRR protein in transfected cells under confocal microscopy. HeLa cells were prepared and stained for confocal imaging as described in the materials and methods chapter (**section 2.1.13**). (**A-D)** TILRR protein expression in TILRR overexpressed cells, (**E-H)** Empty vector-transfected control cells **(I-L)** Parental non-transfected cells. Color code: red, TILRR protein (Alexa Fluor 647 channel); blue, nuclear DNA (DAPI channel); and green, eGFP (FITC channel). Image captured using 20x objectives with a 20µm scale.

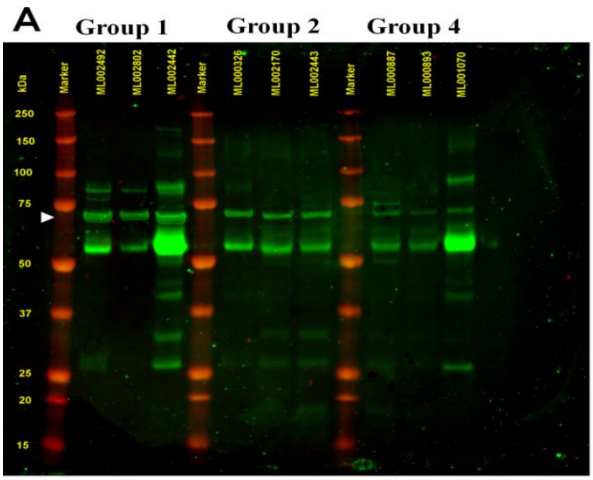

Full-length un-cropped blot 1 (probed with F237G3 mAb)

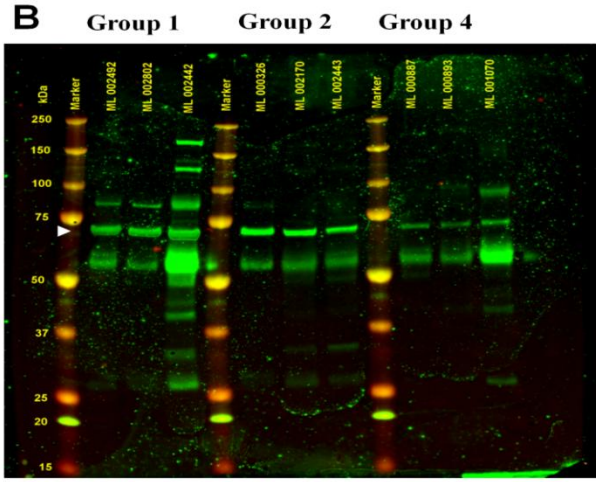

Full-length un-cropped blot 2 (probed with F218G4 mAb)

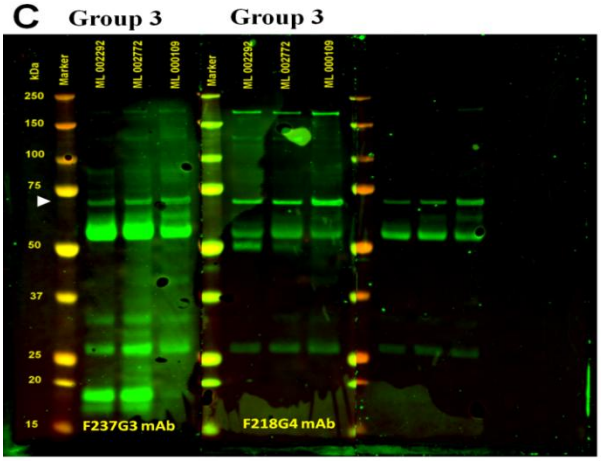

Full-length un-cropped blot 3 (Lanes 1-8 probed with F237G3 and F218G4 mAbs as indicated in the blot). This membrane was cut into three pieces and lanes 1-8 was incubated with two antibodies separately. Lanes 9-12 used for other purposes.

Appendix Figure B7.4: Full-length un-cropped blots of Western blot analysis. TILRR protein was confirmed by Western blot analysis in plasma of patients' group-1, -2, -3, and 4 (patient -1[ML002492], -2[ML002802], -3[ML002442], -4[ML000326], -5[ML002170], -6[ML002443], -7[ML2292], -8[ML2772], -9[ML000109], -10[ML000887], -11[ML000893], and -12[ML001070]) using affinity-purified protein (n=12; each group shows 3 patients data). The images show the bands in the blot for TILRR protein detected by two different anti-FREM1 IgG mAbs, such as F237G3 mAb **(A)**, F218G4 mAb **(B)**, whereas blot 3 **(C)** was cut in three slices and then probed with F237G3 mAb and F218G4 mAb separately as indicated. Western blot images were acquired by Odyssey CLx imaging system (LI-COR, USA) with auto channels (both 700 and 800), 42 µm resolution, high image quality, and 0mm focal offset. A white-colored arrowhead indicates the 70kDa sized TILRR protein band. Other observed bands (<70kDa or >70 kDa) in the blot could be the additional variants of FREM1 (yet uncharacterized). Patients' ID# and groups are mentioned on the top of the blots. kDa, kiloDalton.

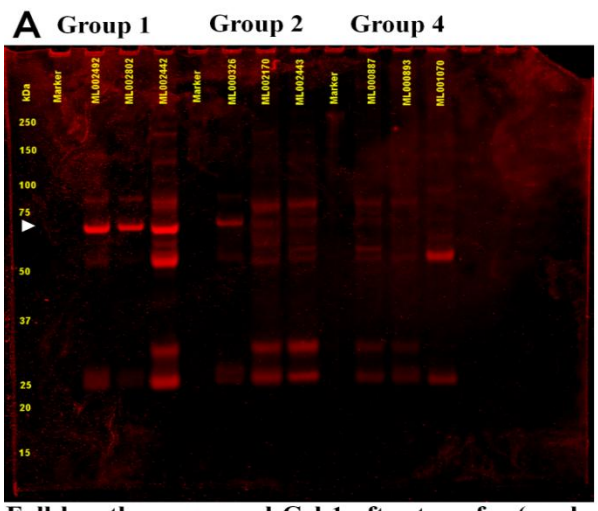

Full-length un-cropped Gel 1 after transfer (used for F237G3 mAb)

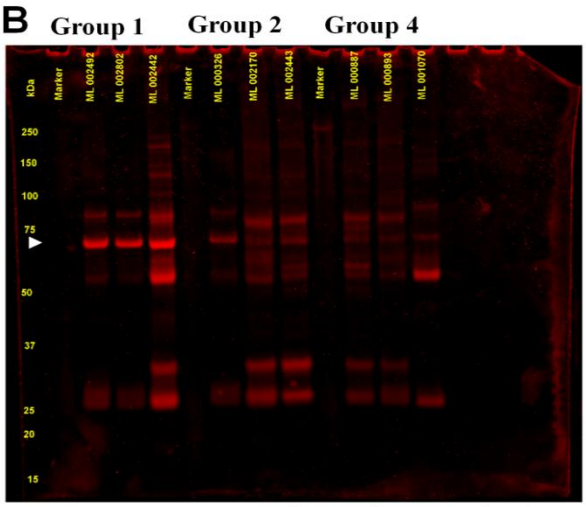

Full-length un-cropped Gel 2 after transfer (used for F218G4 mAb)

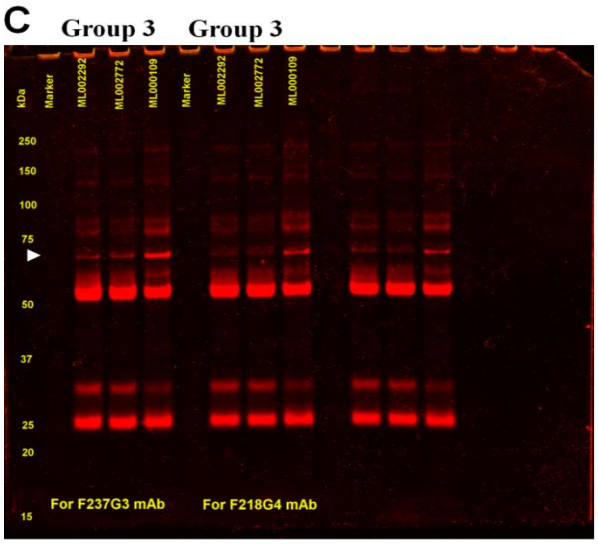

Full-length un-cropped Gel 3 after transfer (Lanes 1-8 used for F237G3 and F218G4 mAbs as indicated in the gel). Lanes 9-12 used for other purposes.

Appendix Figure B7.5: Full-length un-cropped gels of Coomassie blue staining. Non-transferred proteins in the gel after iBlot transfer in plasma of patients' group-1, -2, -3, and 4 (patient -1[ML002492], -2[ML002802], -3[ML002442], -4[ML000326], -5[ML002170], -6[ML002443], -7[ML2292], -8[ML2772], -9[ML000109], -10[ML000887], -11[ML000893], and -12[ML001070]) (n=12; each group shows 3 patients data). Gels were used to transfer proteins onto Nitrocellulose membranes that probed by F237G3 mAb **(A)**, and F218G4 mAb **(B)**, except Gel3 **(D)**, which was used for both F237G3 and F218G4 mAbs. The images show the bands in the gel for the different proteins including a 70 kDa TILRR protein (White-colored arrowhead). Coomassie blue staining gel images were acquired by Odyssey CLx imaging system (LI-COR, USA) with auto channel (700 channel), 42 µm resolution, high image quality, and 0.5mm focal offset. Patients' ID# and groups are mentioned on the top of the blots. kDa, kiloDalton.

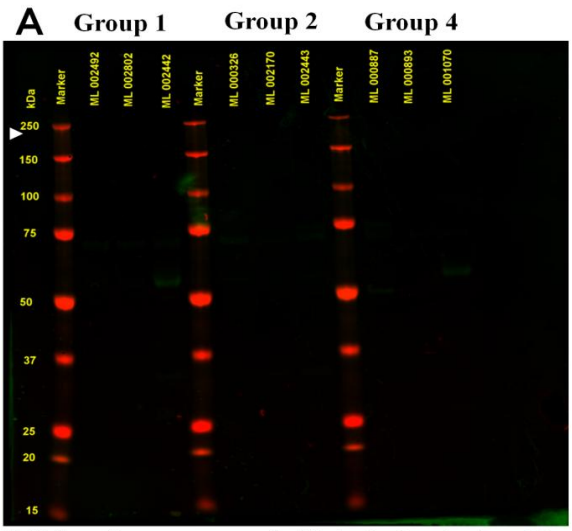

Full-length un-cropped blot 1 (probed with F237G1 mAb)

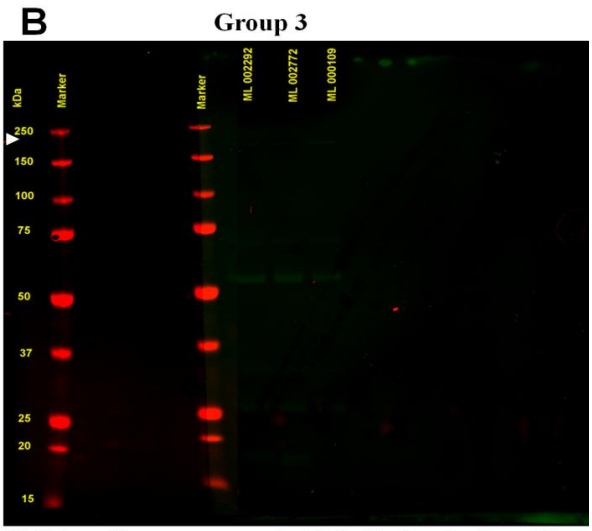

Full-length un-cropped blot 2 (probed with F237G1 mAb). Lanes 1-4 used for other purposes.

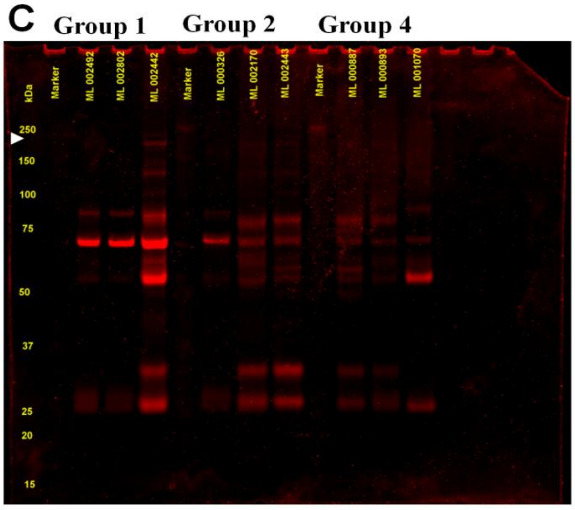

Full-length un-cropped Gel 1 after transfer (used for F237G1 mAb)

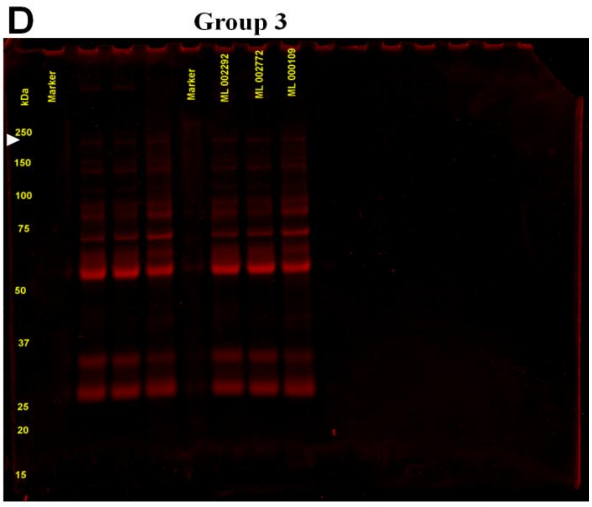

Full-length un-cropped Gel 2 after transfer (used for F237G1 mAb). Lanes 1-4 used for other purposes.

Appendix Figure B7.6: Western blot verification of full-length FREM1 protein after affinity purification. The blot was separately probed with primary antibody (anti-FREM1 mAb F237G1 targeting CSPG9 domain of FREM1) to identify the full-length FREM1 protein from affinity-purified protein of patients' plasma (patient -1[ML002492], -2[ML002802], -3[ML002442], -4[ML000326], -5[ML002170], -6[ML002443], -7[ML2292], -8[ML2772], -9[ML000109], -10[ML000887], -11[ML000893], and -12[ML001070]). **A-B)** Figure A shows the blot for group-1, -2, and -4 and Figure B for group-3. No band of ~235 kDa was detected (indicated by a white-colored arrowhead). **C-D)** Corresponding gels were used to transfer proteins onto the nitrocellulose membrane. Western blot and Coomassie blue staining images were acquired by Odyssey CLx imaging system (LI-COR, USA) with auto channels (both 700 and 800), 42 µm resolution, high image quality, and 0mm focal offset for blots and 0.5mm focal offset for gels. Patients' ID# and groups are mentioned on the top of the blots. kDa, kiloDalton.

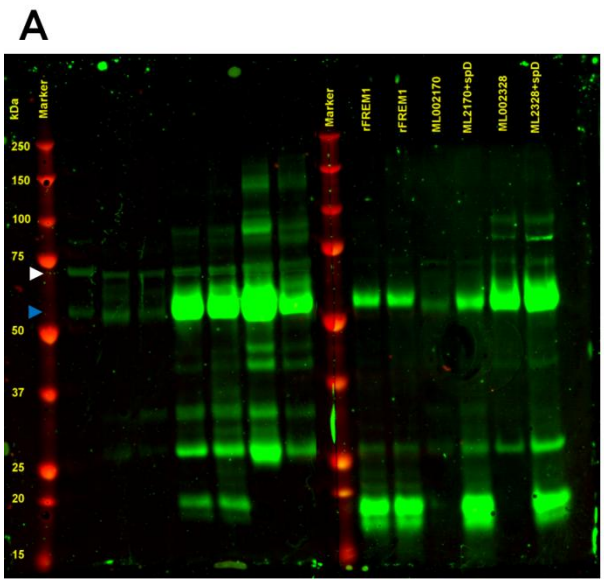

Full-length un-cropped blot (Lanes 9-15 probed with F237G3 mAb). Lanes 1-8 used for other purposes. This membrane was cut into two pieces and lanes 9-15 were incubated with F237G3 mAb.

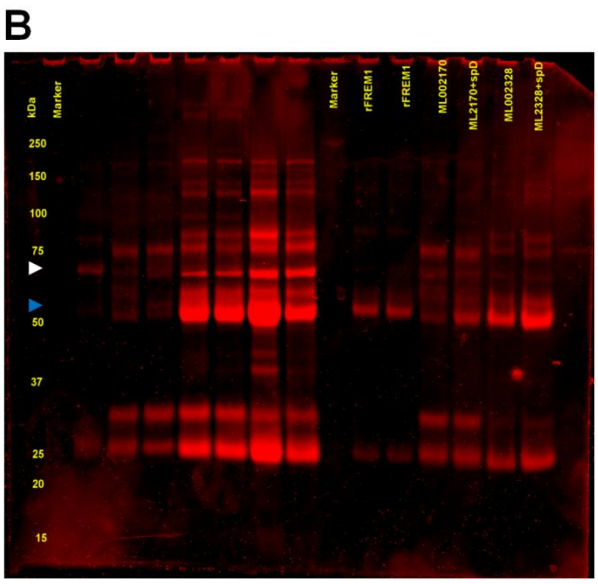

Full-length un-cropped Gel after transfer (Lanes 9-15 used for F237G3 mAb). Lanes 1-8 used for other purposes.

Appendix Figure B7.7: Full-length un-cropped blot and gel. A) The blot was cut into two pieces and the second piece was incubated with anti-FREM1 F237G3 mAb. A clear band of ~57 kDa (blue-colored arrowhead) rFREM1 spD was observed in all samples. A 70 kDa band (white-colored arrowhead) of TILRR protein is also observed in plasma alone and plasma with spiked rFREM1 spD protein. **B)** Corresponding gel following iBlot transfer onto Nitrocellulose membrane stained with Coomassie blue. The white arrowhead indicates 70kDa and the blue arrowhead represents ~57kDa. Western blot and Coomassie blue staining images were acquired by Odyssey CLx imaging system (LI-COR, USA) with auto channels (both 700 and 800), 42 µm resolution, high image quality, and 0mm focal offset for blot and 0.5mm focal offset for gel. Patients' ID# and groups are mentioned on the top of the blots. kDa, kiloDalton.

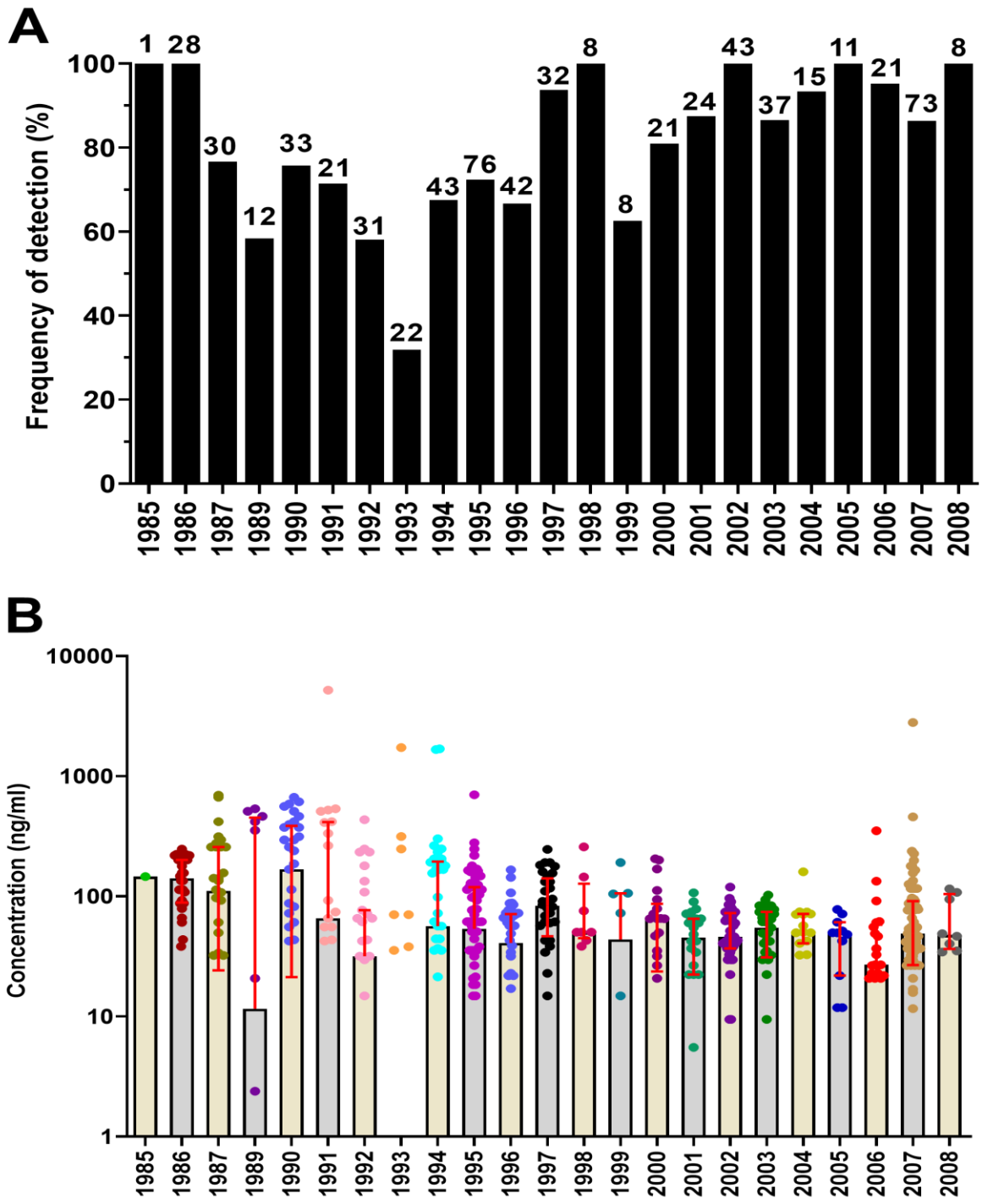

Appendix Figure B7.8: Detection frequency of plasma TILRR in archived samples of all patients' (groups 1-4) collected between 1985 and 2008. A) The detection frequency of plasma TILRR in archived samples in different years between 1985 and 2008 (n=640). Value on the top of each bar represents the number of the sample (n) tested; **B)** The level of plasma TILRR (median with IQR) in archived samples collected between 1985 and 2008 (n=640). The X-axis indicates the collection year of the plasma samples.

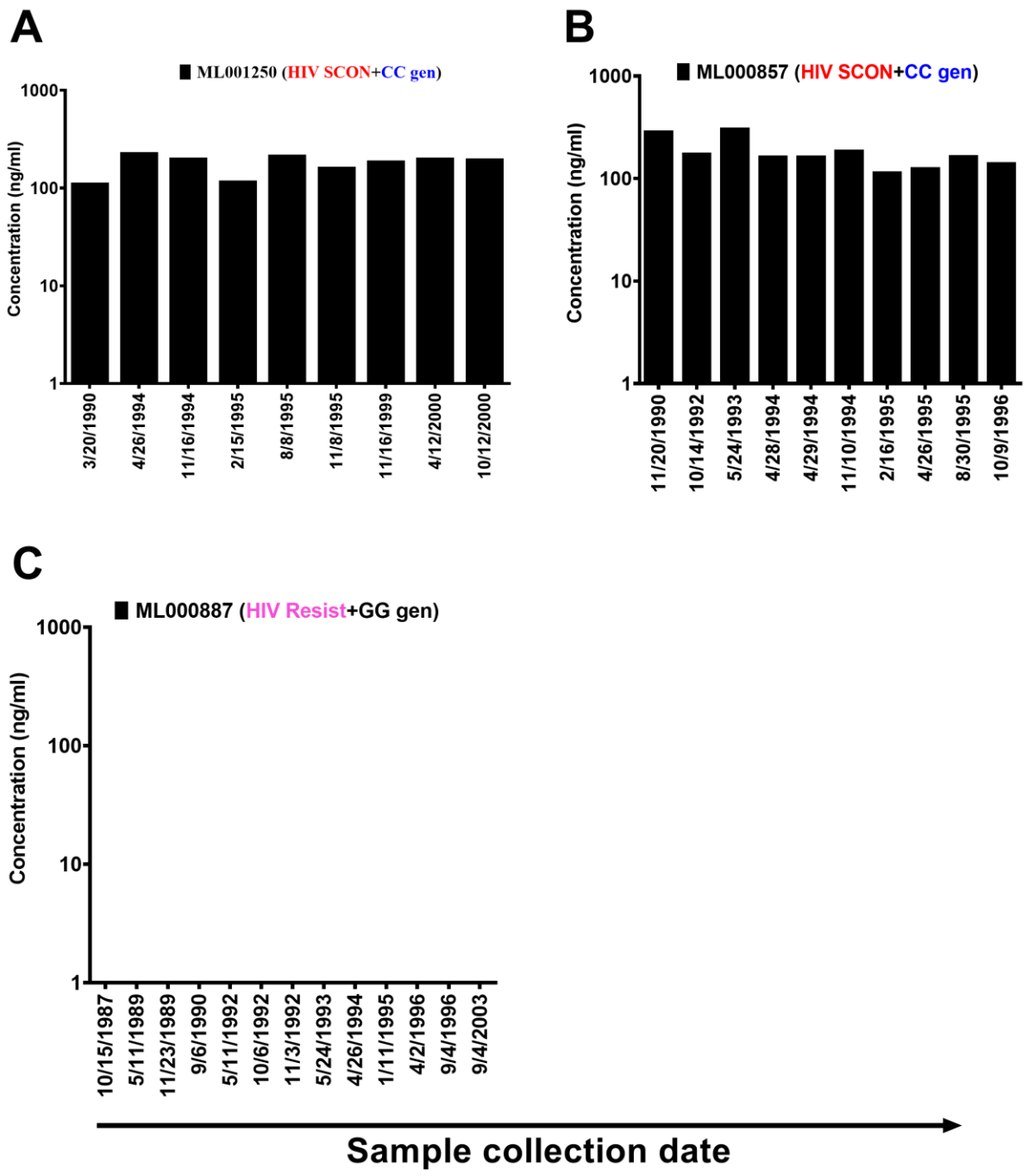

Appendix Figure B7.9: Level of plasmaTILRR in archived samples collected from the same patient with multiple time points between 1985 and 2008. A-C) The level of plasma TILRR observed in HIV SCON with FREM1 SNP rs1552896 CC genotype patients **(A-B)**, and HIV resistant (HESN) with GG genotype **(C)**. The X-axis indicates the sample collection date. Color-coded texts indicate the HIV status and FREM1 SNP rs1552896 genotypes. HIV SCON, HIV seroconverters; HIV Resist, HIV resistant.

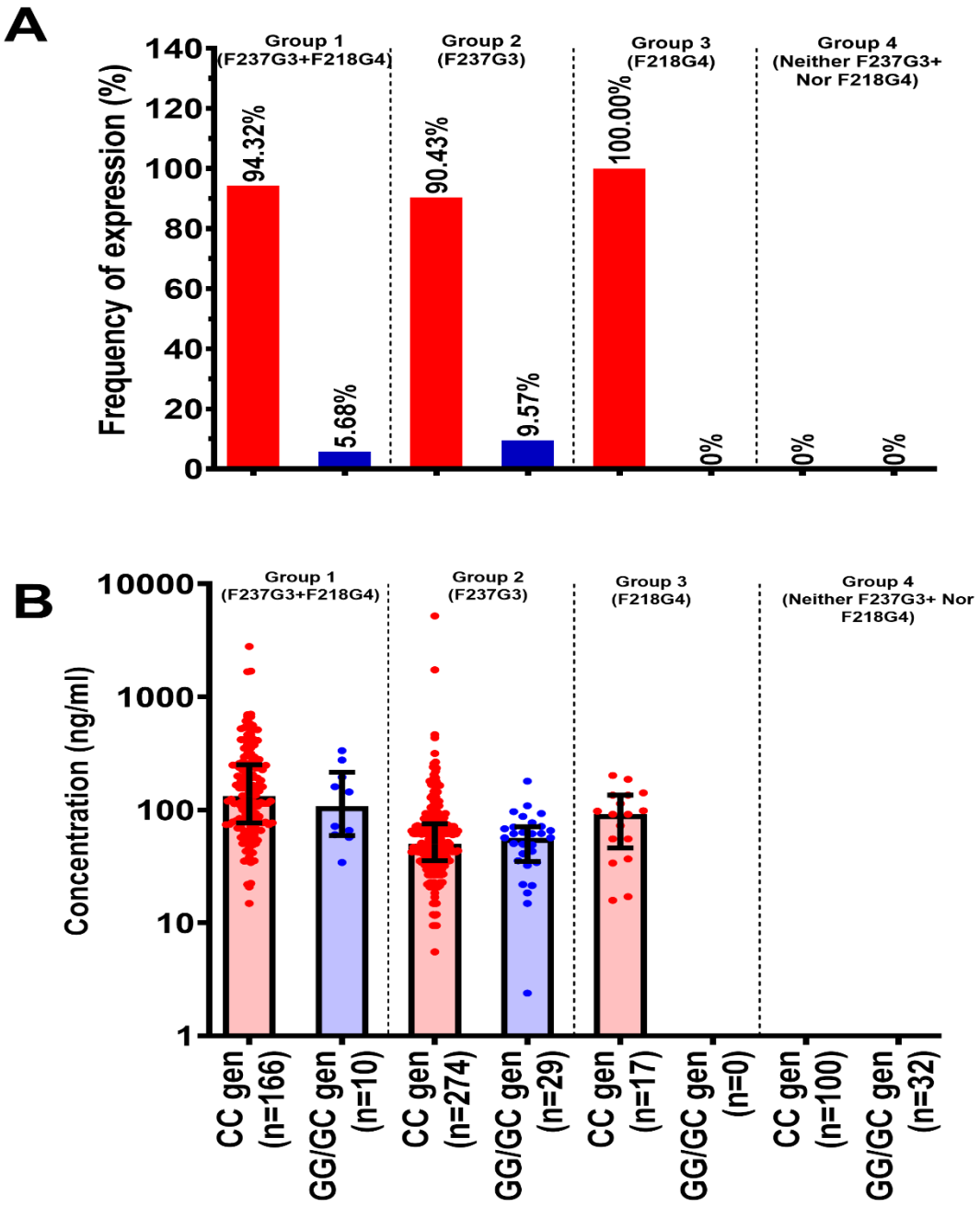

Appendix Figure B7.10: Expression frequency and the level of plasma TILRR in women with FREM1 SNP rs1552896 genotypes among patients' groups 1-4. A) The frequency of plasma TILRR expression in women with FREM1 SNP rs1552896 among groups 1-4 as classified in **Table 3.2** (n=628). Value on the top of each bar represents the frequency of expression; **B)** The level of plasma TILRR (median with IQR) in women with FREM1 SNP rs1552896 among groups 1-4 (n=628). The X-axis indicates the FREM1 SNP rs1552896 genotypes and the number of samples detected as TILRR positive (parenthesis). Groups 1-4 represent the quantification of plasma TILRR by two anti-FREM1 mAbs. Group 1 was detected by both mAbs (F237G3 and F218G4), group 2 by F237G3 mAb, and group 3 by F218G4 mAb. Group 4 did not detect by either F237G3 mAb or F218G4 mAb. gen, genotype

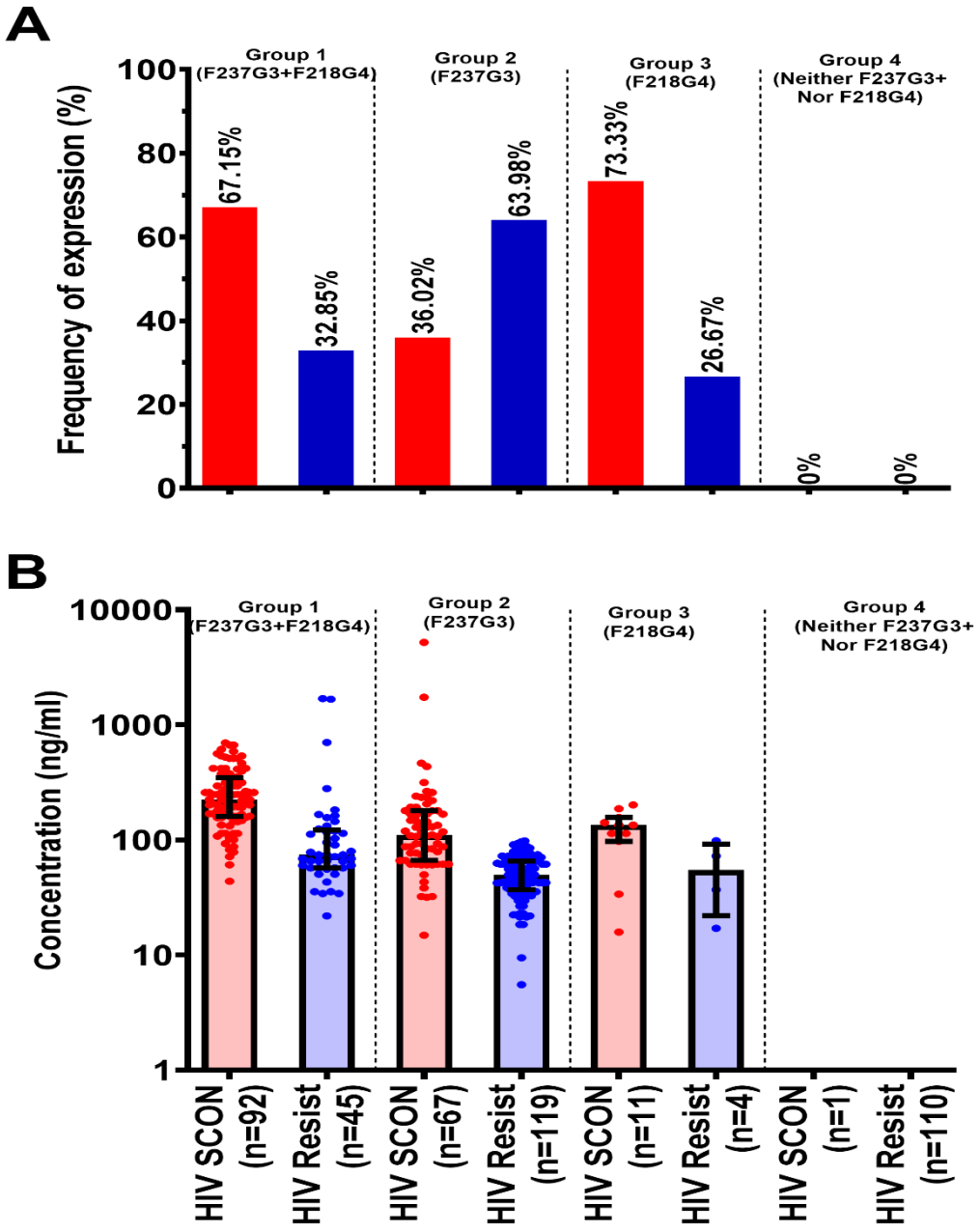

Appendix Figure B7.11: Expression frequency and the level of plasma TILRR in women with different HIV status among patients' groups 1-4. A) The frequency of plasma TILRR expression in HIV seroconverters (SCON) and HIV resistant (HESN) women among groups 1-4 as classified in **Table 3.2** (n=449). Value on the top of each bar represents the frequency of expression; **B)** The level of plasma TILRR (median with IQR) in HIV SCON and HIV resistant women with classified groups 1-4 (n=449). The X-axis indicates the HIV status and the number of samples detected as TILRR positive (parenthesis). Groups 1-4 represent the quantification of plasma TILRR by two anti-FREM1 mAbs. Group 1 was detected by both mAbs (F237G3 and F218G4), group 2 by F237G3 mAb, and group 3 by F218G4 mAb. Group 4 did not detect by either F237G3 mAb or F218G4 mAb. HIV SCON, HIV seroconverters; HIV Resist, HIV resistant.

7.3 APPENDIX C: SUPPLEMENTARY TABLES

Appendix Table C7.1: List of genes included in human NF-κB signaling pathway PCR array.
(PAHS-025Z, Qiagen).

Gene Symbol	Descriptions
AGT	Angiotensinogen (serpin peptidase inhibitor, clade A, member 8)
AKT1	V-akt murine thymoma viral oncogene homolog 1
ATF1	Activating transcription factor 1
BCL10	B-cell CLL/lymphoma 10
BCL2A1	BCL2-related protein A1
BCL2L1	BCL2-like 1
BCL3	B-cell CLL/lymphoma 3
BIRC2	Baculoviral IAP repeat containing 2
BIRC3	Baculoviral IAP repeat containing 3
CARD11	Caspase recruitment domain family, member 11
CASP1	Caspase 1, apoptosis-related cysteine peptidase (interleukin 1, beta, convertase)
CASP8	Caspase 8, apoptosis-related cysteine peptidase
CCL2	Chemokine (C-C motif) ligand 2
CCL5	Chemokine (C-C motif) ligand 5
CD27	CD27 molecule
CD40	CD40 molecule, TNF receptor superfamily member 5
CFLAR	CASP8 and FADD-like apoptosis regulator
CHUK	Conserved helix-loop-helix ubiquitous kinase
CSF1	Colony-stimulating factor 1 (macrophage)
CSF2	Colony-stimulating factor 2 (granulocyte-macrophage)
CSF3	Colony-stimulating factor 3 (granulocyte)
EGFR	Epidermal growth factor receptor
EGR1	Early growth response 1
ELK1	ELK1, member of ETS oncogene family
F2R	Coagulation factor II (thrombin) receptor
FADD	Fas (TNFRSF6)-associated via death domain
FASLG	Fas ligand (TNF superfamily, member 6)
FOS	FBJ murine osteosarcoma viral oncogene homolog
HMOX1	Heme oxygenase (decycling) 1
ICAM1	Intercellular adhesion molecule 1
IFNA1	Interferon, alpha 1
IFNG	Interferon, gamma
IKBKB	Inhibitor of kappa light polypeptide gene enhancer in B-cells, kinase beta
IKBKE	Inhibitor of kappa light polypeptide gene enhancer in B-cells, kinase epsilon
IKBKG	Inhibitor of kappa light polypeptide gene enhancer in B-cells, kinase gamma
IL10	Interleukin 10
IL1A	Interleukin 1, alpha
IL1B	Interleukin 1, beta
IL1R1	Interleukin 1 receptor, type I
CXCL8	Interleukin 8
IRAK1	Interleukin-1 receptor-associated kinase 1
IRAK2	Interleukin-1 receptor-associated kinase 2

IRF1	Interferon regulatory factor 1
JUN	Jun proto-oncogene
LTA	Lymphotoxin alpha (TNF superfamily, member 1)
LTBR	Lymphotoxin beta receptor (TNFR superfamily, member 3)
MALT1	Mucosa-associated lymphoid tissue lymphoma translocation gene 1
MAP3K1	Mitogen-activated protein kinase kinase kinase 1
MYD88	Myeloid differentiation primary response gene (88)
NFKB1	Nuclear factor of kappa light polypeptide gene enhancer in B-cells 1
NFKB2	Nuclear factor of kappa light polypeptide gene enhancer in B-cells 2 (p49/p100)
NFKBIA	Nuclear factor of kappa light polypeptide gene enhancer in B-cells inhibitor, alpha
NFKBIB	Nuclear factor of kappa light polypeptide gene enhancer in B-cells inhibitor, beta
NFKBIE	Nuclear factor of kappa light polypeptide gene enhancer in B-cells inhibitor, epsilon
NOD1	Nucleotide-binding oligomerization domain containing 1
PSIP1	PC4 and SFRS1 interacting protein 1
RAF1	V-raf-1 murine leukemia viral oncogene homolog 1
REL	V-rel reticuloendotheliosis viral oncogene homolog (avian)
RELA	V-rel reticuloendotheliosis viral oncogene homolog A (avian)
RELB	V-rel reticuloendotheliosis viral oncogene homolog B
RHOA	Ras homolog gene family, member A
RIPK1	Receptor (TNFRSF)-interacting serine-threonine kinase 1
STAT1	Signal transducer and activator of transcription 1, 91kDa
TBK1	TANK-binding kinase 1
TICAM1	Toll-like receptor adaptor molecule 1
TICAM2	Toll-like receptor adaptor molecule 2
TIMP1	TIMP metallopeptidase inhibitor 1
TLR1	Toll-like receptor 1
TLR2	Toll-like receptor 2
TLR3	Toll-like receptor 3
TLR4	Toll-like receptor 4
TLR6	Toll-like receptor 6
TLR9	Toll-like receptor 9
TNF	Tumor necrosis factor
TNFAIP3	Tumor necrosis factor, alpha-induced protein 3
TNFRSF10A	Tumor necrosis factor receptor superfamily, member 10a
TNFRSF10B	Tumor necrosis factor receptor superfamily, member 10b
TNFRSF1A	Tumor necrosis factor receptor superfamily, member 1A
TNFSF10	Tumor necrosis factor (ligand) superfamily, member 10
TNFSF14	Tumor necrosis factor (ligand) superfamily, member 14
TRADD	TNFRSF1A-associated via death domain
TRAF2	TNF receptor-associated factor 2
TRAF3	TNF receptor-associated factor 3
TRAF6	TNF receptor-associated factor 6
ACTB	Actin, beta
B2M	Beta-2-microglobulin
GAPDH	Glyceraldehyde-3-phosphate dehydrogenase
HPRT1	Hypoxanthine phosphoribosyltransferase 1
RPLP0	Ribosomal protein, large, P0

Appendix Table C7.2: Overall demographic characteristics of the study subjects

Characteristics (at sample collection)	**Study subjects (n=640)** Median (IQR)
Age, in years	35 (30-40) (n=624[a])
Duration of sex work, in years	10 (5-17) (n=632[b])
	% (n)
Sexually transmitted infection (STIs)	27.00 (172/637[c])
Vaginal discharge	18.37 (117/637[d])
Genital ulcer	6.12 (39/637[d])
Oral contraceptive used	22.45 (143/637[d])

[a]Samples with known age at the time of collection. Age was unknown for 16-samples. [b]Samples with known duration of sex work. The duration of sex work was unknown for 8-samples.
[c]Samples with a history of known STIs (Gonorrhea, Syphilis, Chlamydial infection, and Bacterial vaginosis). 3-samples do not have a history of STIs.
[d]Samples with a history of vaginal discharge, genital ulcer, and use of oral contraceptives. History was unknown for 3-samples.
IQR, interquartile range; n, sample#

Appendix Table C7.3: Dose-response effect of TILRR on immune responsive genes in HeLa cells.

Gene name	0.25 µg DNA		0.5 µg DNA		1.0 µg DNA		2.0 µg DNA	
	FI (mean±SEM)	p-value	FI (mean±SEM)	p-value	FI (mean±SEM)	p-value	FI (mean±SEM)	p-value
CCL5(RANTES)	3.66±0.72	0.0013	3.66±0.58	0.0006	7.76±0.90	0.0031	6.26±1.20	0.0009
CXCL8 (IL-8)	2.16±0.61	0.0122	10.39±2.00	0.0012	11.28±2.69	0.0121	6.98±1.71	0.0001
IL-6	1.52±0.16	0.0091	5.35±0.14	0.0017	5.52±1.30	0.0005	4.75±0.64	0.0003
TNFα	2.08±1.12	0.1651	3.21±0.24	0.0010	5.63±3.69	0.0100	3.63±2.50	0.0171
FI, fold increase								

Appendix Table C7.4: Dose-response effect of TILRR on immune responsive genes in VK2/E6E7 cells.

Gene name	0.25 µg DNA		0.5 µg DNA		1.0 µg DNA		2.0 µg DNA	
	FI (mean±SEM)	p-value	FI (mean±SEM)	p-value	FI (mean±SEM)	p-value	FI (mean±SEM)	p-value
CCL5(RANTES)	1.05±0.05	0.1857	1.18±0.22	0.1536	1.07±0.30	0.6925	1.01±0.17	0.9736
CXCL8 (IL-8)	0.93±0.13	0.6583	1.86±0.05	0.0020	1.88±0.90	0.0286	1.27±0.10	0.0066
IL-6	1.03±0.11	0.4043	1.59±0.31	0.0238	2.47±0.40	0.0031	0.98±0.23	0.8544
TNFα	0.89±0.16	0.2945	1.42±0.37	0.0775	2.40±1.39	0.0919	1.32±0.55	0.2911
FI, fold increase								

Appendix Table C7.5: Concentration of pro-inflammatory cytokine/chemokine proteins in HeLa cell culture supernatants.

Time	IL-6				IL-8/CXCL8			
	TILRR (Mean±SEM) (pg/ml)	Empty Ctrl (Mean±SEM) (pg/ml)	Fold change (Mean±SEM)	p-value	TILRR (Mean±SEM) (pg/ml)	Empty Ctrl (Mean±SEM) (pg/ml)	Fold change (Mean±SEM)	p-value
1H	121.64±23.97	12.44±0.59	9.75±1.72	0.0014	106.45±10.51	9.46±2.08	11.59±2.63	<0.0001
3H	294.75±34.30	70.95±6.53	4.15±0.15	0.0004	185.70±22.19	42.83±1.72	4.34±0.50	0.0004
6H	380.16±24.54	75.13±7.23	5.08±0.39	<0.0001	296.03±42.90	43.55±5.96	6.81±0.59	0.0005
15H	2707.57±262.46	579.48±266.03	5.97±4.24	0.0011	3165.10±169.81	856.21±77.63	3.72±0.45	<0.0001
24H	7426.33±335.91	1352.23±58.19	5.51±0.48	<0.0001	5670.27±359.71	951.53±91.13	6.01±0.78	0.0002

Time	IP-10/CXCL10				RANTES/CCL5			
	TILRR (Mean±SEM) (pg/ml)	Empty Ctrl (Mean±SEM) (pg/ml)	Fold change (Mean±SEM)	p-value	TILRR (Mean±SEM) (pg/ml)	Empty Ctrl (Mean±SEM) (pg/ml)	Fold change (Mean±SEM)	p-value
1H	47.19±4.79	0.87±1.51	18.07±1.83	<0.0001	13.33±1.71	0.00±0.00	-	0.0002
3H	64.01±10.32	14.88±0.69	4.31±0.73	0.0012	14.53±3.01	0.00±0.00	-	0.0011
6H	96.63±8.40	12.72±2.32	7.70±0.83	<0.0001	17.40±1.81	5.68±1.26	3.15±0.68	0.0008
15H	1425.13±88.25	413.80±36.16	3.45±0.10	<0.0001	1345.17±253.32	290.82±86.78	4.73±0.52	0.0024
24H	3081.38±71.55	540.93±14.60	5.70±0.18	<0.0001	2418.46±223.66	459.81±39.78	5.28±0.54	0.0001

Time	MCP-1/CCL2							
	TILRR (Mean±SEM) (pg/ml)	Empty Ctrl (Mean±SEM) (pg/ml)	Fold change (Mean±SEM)	p-value				
1H	32.65±9.22	4.71±0.76	6.89±1.15	0.0064				
3H	57.45±11.60	14.77±3.12	4.12±1.64	0.0035				
6H	61.00±9.68	15.23±2.14	4.01±0.33	0.0013				
15H	834.32±57.99	288.75±25.41	2.91±0.44	0.0001				
24H	1391.33±47.19	673.15±51.73	2.08±0.23	<0.0001				

Appendix Table C7.6: Concentration of pro-inflammatory cytokine/chemokine proteins in VK2/E6E7 cell culture supernatants.

Time	IL-6				IL-8/CXCL8			
	TILRR (Mean±SEM) (pg/ml)	Empty Ctrl (Mean±SEM) (pg/ml)	Fold change (Mean±SEM)	p-value	TILRR (Mean±SEM) (pg/ml)	Empty Ctrl (Mean±SEM) (pg/ml)	Fold change (Mean±SEM)	p-value
1H	19.03±2.81	16.02±2.35	1.22±0.35	0.2276	2.86±0.26	4.20±1.48	0.74±0.27	0.1954
3H	41.11±1.59	26.79±4.41	1.56±0.23	0.0061	19.85±0.26	6.20±2.44	3.51±1.21	0.0007
6H	55.22±3.87	35.28±1.95	1.57±0.17	0.0013	24.69±4.36	13.46±3.37	1.86±0.15	0.0243
15H	391.91±77.37	169.25±8.23	2.33±0.50	0.0077	252.37±20.20	180.58±9.23	1.40±0.07	0.0050
24H	529.26±90.37	275.72±6.59	1.93±0.37	0.0084	764.82±50.15	616.13±61.91	1.25±0.08	0.0319

Time	IP-10/CXCL10				RANTES/CCL5			
	TILRR (Mean±SEM) (pg/ml)	Empty Ctrl (Mean±SEM) (pg/ml)	Fold change (Mean±SEM)	p-value	TILRR (Mean±SEM) (pg/ml)	Empty Ctrl (Mean±SEM) (pg/ml)	Fold change (Mean±SEM)	p-value
1H	984.07±39.80	761.57±76.04	1.30±0.08	0.0109	110.49±13.85	69.89±23.59	1.72±0.68	0.0619
3H	1856.17±292.88	934.13±72.05	2.01±0.44	0.0061	125.66±31.22	62.91±8.47	2.05±0.74	0.0283
6H	2852.98±338.50	1939.18±99.64	1.47±0.15	0.0109	116.47±8.26	63.81±30.20	2.06±0.74	0.0435
15H	3739.30±102.09	2548.25±58.47	1.47±0.06	<0.0001	149.32±11.20	99.80±1.16	1.50±0.12	0.0016
24H	5367.07±254.08	3977.25±82.10	1.35±0.09	0.0301	434.49±25.38	241.24±23.77	1.81±0.07	0.0007

Time	MIP-1β/CCL4							
	TILRR (Mean±SEM) (pg/ml)	Empty Ctrl (Mean±SEM) (pg/ml)	Fold change (Mean±SEM)	p-value				
1H	4.08±7.07	1.61±2.79	-	0.6039				
3H	4.95±1.37	5.00±0.90	1.05±0.50	0.9578				
6H	12.63±3.76	7.09±1.26	1.89±0.88	0.0727				
15H	50.70±4.55	26.81±4.08	1.94±0.47	0.0025				
24H	59.20±3.50	38.41±1.56	1.54±0.14	0.0007				

Appendix Table C7.7: Concentration of pro-inflammatory cytokine/chemokine proteins in HeLa cell culture supernatants along with IL-1β stimulation.

Time	IL-6				IL-8/CXCL8			
	TILRR (Mean±SEM) (pg/ml)	Empty Ctrl (Mean±SEM) (pg/ml)	Fold change (Mean±SEM)	p-value	TILRR (Mean±SEM) (pg/ml)	Empty Ctrl (Mean±SEM) (pg/ml)	Fold change (Mean±SEM)	p-value
1H	88.83±9.06	9.11±5.50	15.26±14.17	0.0002	99.43±10.27	8.99±3.19	12.16±4.67	0.0001
3H	258.42±16.47	66.25±28.66	4.69±2.76	0.0005	237.47±13.30	58.23±2.48	4.08±0.21	<0.0001
6H	269.61±48.69	87.41±3.37	3.08±0.51	0.0029	232.95±49.69	62.51±6.56	3.77±1.02	0.0042
15H	2736.44±251.74	897.47±30.37	3.05±0.34	0.0002	3326.87±181.08	1010.87±49.24	3.29±0.09	<0.0001
24H	7653.85±343.17	1913.16±62.20	4.01±0.30	<0.0001	6052.45±801.13	1690.31±194.70	3.58±0.07	0.0008

Time	IP-10/CXCL10				RANTES/CCL5			
	TILRR (Mean±SEM) (pg/ml)	Empty Ctrl (Mean±SEM) (pg/ml)	Fold change (Mean±SEM)	p-value	TILRR (Mean±SEM) (pg/ml)	Empty Ctrl (Mean±SEM) (pg/ml)	Fold change (Mean±SEM)	p-value
1H	49.86±5.38	4.80±2.81	13.05±7.31	0.0002	12.27±14.32	9.02±4.19	1.94±2.36	0.7253
3H	94.55±1.50	18.11±1.06	5.23±0.28	<0.0001	12.64±11.04	4.19±0.45	3.21±2.79	0.2564
6H	131.43±25.87	13.05±2.28	10.36±2.99	0.0014	17.61±6.17	3.85±1.52	5.78±4.78	0.0199
15H	1398.63±71.33	467.10±23.33	3.00±0.20	<0.0001	1162.68±104.60	281.95±58.53	4.28±1.18	0.0002
24H	3121.19±130.12	733.19±24.52	4.26±0.23	<0.0001	3154.27±47.57	488.65±86.81	6.59±1.17	<0.0001

Time	MCP-1/CCL2							
	TILRR (Mean±SEM) (pg/ml)	Empty Ctrl (Mean±SEM) (pg/ml)	Fold change (Mean±SEM)	p-value				
1H	24.26±10.49	5.20±0.39	-	0.0368				
3H	62.69±5.95	10.70±2.12	6.06±1.54	0.0001				
6H	57.68±11.19	22.12±6.40	2.67±0.51	0.0088				
15H	1015.90±44.04	327.07±20.59	3.11±0.12	<0.0001				
24H	1551.77±75.27	675.26±44.36	2.31±0.27	<0.0001				

Appendix Table C7.8: Concentration of pro-inflammatory cytokine/chemokine proteins in VK2/E6E7 cell culture supernatants along with IL-1β stimulation.

Time	IL-6				IL-8/CXCL8			
	TILRR (Mean±SEM) (pg/ml)	Empty Ctrl (Mean±SEM) (pg/ml)	Fold change (Mean±SEM)	p-value	TILRR (Mean±SEM) (pg/ml)	Empty Ctrl (Mean±SEM) (pg/ml)	Fold change (Mean±SEM)	p-value
1H	20.05±5.10	15.92±3.34	1.33±0.52	0.3053	4.38±0.56	3.81±0.99	1.21±0.34	0.4334
3H	36.36±1.78	20.87±4.66	1.81±0.48	0.0058	13.20±0.93	8.31±0.38	1.59±0.18	0.0011
6H	46.44±6.10	34.21±7.58	1.44±0.53	0.0951	24.41±2.40	15.55±1.29	1.57±0.02	0.0049
15H	237.51±12.22	129.08±23.86	1.87±0.28	0.0022	238.96±57.33	164.40±5.26	1.45±0.32	0.0883
24H	626.95±102.33	452.75±17.58	1.38±0.19	0.0439	844.23±28.98	655.91±48.64	1.29±0.08	0.0045

Time	IP-10/CXCL10				RANTES/CCL5			
	TILRR (Mean±SEM) (pg/ml)	Empty Ctrl (Mean±SEM) (pg/ml)	Fold change (Mean±SEM)	p-value	TILRR (Mean±SEM) (pg/ml)	Empty Ctrl (Mean±SEM) (pg/ml)	Fold change (Mean±SEM)	p-value
1H	2070.51±95.58	1320.58±74.53	1.57±0.14	0.0004	107.22±8.21	73.92±20.76	1.53±0.43	0.0611
3H	3046.86±198.70	2206.86±425.20	1.43±0.36	0.0362	107.44±20.11	64.12±9.58	1.68±0.19	0.0281
6H	2960.62±166.51	2652.28±56.24	1.12±0.04	0.0384	175.96±8.40	121.20±10.52	1.46±0.11	0.0021
15H	4535.43±146.75	3514.91±74.44	1.29±0.02	0.0004	236.36±15.86	156.77±6.04	1.51±0.16	0.0012
24H	5609.92±224.33	4157.52±75.04	1.35±0.08	0.0004	450.47±45.16	329.32±47.54	1.40±0.33	0.0329

Time	MIP-1β/CCL4							
	TILRR (Mean±SEM) (pg/ml)	Empty Ctrl (Mean±SEM) (pg/ml)	Fold change (Mean±SEM)	p-value				
1H	4.93±8.54	2.11±3.66	-	0.6271				
3H	3.13±2.86	4.97±5.78	-	0.6470				
6H	15.11±8.61	12.53±7.30	2.05±2.37	0.7119				
15H	46.91±10.87	26.76±1.18	1.76±0.46	0.0332				
24H	57.77±11.11	39.76±3.42	1.47±0.40	0.0550				

Appendix Table C7.9: Functions of the gene associated with innate immunity and inflammatory responses.

Gene name	Function(s)
BCL10	Positive regulator to activate NF-κB [394]
CARD11	When expressed in cells, this protein activated NF-κB [395]
CCL2 (MCP-1)	Overexpressed by NF-κB activation and involved in immunoregulatory and inflammatory processes [396]
CCL5 (RANTES)	Activator of NF-kB [397]
CHUK/IKKα	Activator of transcription factor NF-κB [199, 398, 399]
CSF1 (M-CSF)	Controls the survival, differentiation, and function of monocytes and macrophages [400, 401]
CSF2 (GM-CSF)	Activates monocytes/macrophages, and acts as an important hematopoietic growth factor and immune modulator [401, 402]
CSF3 (G-CSF)	Promotes production, proliferation, and differentiation of granulocytes [403, 404]
CXCL8 (IL-8)	Associates in acute inflammation and plays a key role in neutrophil recruitment and activation [405]
IL-1α	Pleiotropic cytokine involved in various immune responses and inflammatory processes [351, 406, 407]
IL-1β	Pleiotropic mediator of the inflammatory response [351, 406, 407]
IL-1R1	An important receptor of the IL-1-NF-κB signaling pathway [189]
IKBKB (IKKβ)	Phosphorylates the inhibitor in the inhibitor/NF-κB complex, causing dissociation of the inhibitor and activation of NF-κB [199, 398, 399]
IRAK1	Participates in nuclear translocation and activation of NF-κB [408]
IRAK2	Plays a critical role in TLR-mediated NF-κB activation pathway [409]
MALT1	Activates NF-κB [410]
MYD88	Functions as a critical adaptor protein in innate immunity signal transduction [411]
NFKB1 (p50)	Involves in the canonical pathway of NF-κB activation [295]
NFKB2 (p52)	Involves in non-canonical activation of the NF-κB pathway [200, 295, 412]
NFKBIA/IkBα	Inhibits NF-κB/REL complexes, which are involved in inflammatory responses [413, 414]
NFKBIB/IkBβ	Inhibits NF-κB by complexing with and trapping it in the cytoplasm [413, 414]
RAF1	Activates NF-κB transcription factor [415]
REL	Regulates NF-κB activation [181, 197]
TBK1	Mediates NF-κB activation in a kinase-dependent manner [416]
TICAM1 (TRIF)	Activates interferon regulatory factor -3 (IRF-3) and NF-κB leading to induction of IFN-β production [417]
TLR1, TLR2, TLR3, TLR4, and TLR6	Plays a fundamental role in pathogen recognition and activation of innate immunity, Activation of TLRs leads to the up-regulation of signaling pathways to modulate the host's inflammatory response [291, 418-421]
TNF	Induces NF-κB activation and regulates a wide spectrum of the biological process including cell proliferation, differentiation, and apoptosis [422-424]
TRAF2	Involves in the activation of NF-κB and inhibits oxidative stress-induced cell death. [416, 425]
TRAF3	Participates in the signal transduction of CD40 and is important for the activation of the immune response [426]
TRAF6	Involves in innate and antigen-specific immune responses by activating NF-κB and Interferon regulatory factor 7 (IRF7) [427]